UNIVERSITY OF SOUTHAMPTON

STUDIES ON RECOMBINANT HUMAN 5-AMINOLAEVULINIC ACID DEHYDRATASE AND RECOMBINANT HUMAN PORPHOBILINOGEN DEAMINASE

By
Danica Simone Butler

Thesis submitted for the degree of Doctor of Philosophy

FACULTY OF SCIENCE

Division of Biochemistry and Molecular Biology

School of Biological Sciences

May, 2003

UNIVERSITY OF SOUTHAMPTON

ABSTRACT

FACULTY OF SCIENCE

DIVISION OF BIOCHEMISTRY AND MOLECULAR BIOLOGY

Doctor of Philosophy

STUDIES ON RECOMBINANT HUMAN 5-AMINOLAEVULINIC ACID DEHYDRATASE AND RECOMBINANT HUMAN PORPHOBILINOGEN DEAMINASE

By Danica Simone Butler

5-Aminolaevulinic acid dehydratase (ALAD) catalyses the condensation between two molecules of 5-aminolaevulinic acid to form porphobilinogen (PBG). Recombinant human ALAD, encoded by a synthetic gene, has been over-expressed and purified to yield milligram amounts of enzyme for characterisation. The recombinant enzyme was crystallised and the structure revealed a ligand resembling the product, PBG, at the active sites. Experiments described in this thesis indicate the bound ligand is not porphobilinogen but a putative intermediate, which has provided clues to the enzymes mechanism.

The human ALAD mutant, Phe12Leu, has been characterised. Phenylalanine 12 is located on the *N*-terminal arm and is thought to be involved in subunit interactions. Hybrid octamers of the mutant and the normal ALAD were formed, identifying residues that may be important in communication between subunits.

Porphobilinogen deaminase (PBGD) polymerises PBG to form the tetrapyrrole preuroporphyrinogen in the third step of the haem biosynthesis pathway. Recombinant erythroid and ubiquitous human PBGD were purified from an engineered strain of *E. coli*. The purified PBGD appeared homogenous when analysed by SDS-PAGE but existed in the form of a distinct double band when analysed by non-denaturing PAGE. Proteolytic digestion and peptide analysis of the two separated deaminase species was carried out to identify differences between the two protein forms.

A number of PBGD mutants were studied and some were found to accumulate enzyme substrate (ES) complexes. This thesis describes the purification of these complexes and their attempted crystallisation as the structure of an enzyme substrate complex would provide a wealth of information on the enzyme mechanism.

Acknowledgements

I would like to thank my supervisor Professor Peter Shoolingin-Jordan for his guidance and discussions throughout my time in his research group.

I am indebted to the following people for their help:

Julie Mosely and Abeer Al-Dbass for their help with the crystallisation of the human deaminases. Darren Thompson and Fiyaz Mohammed for solving the crystal structure of the human recombinant erythroid PBGD and the ubiquitous Arg-167-Gln PBGD mutant, respectively.

Dr. Peter Erskine, Dr. John Cooper and Nicky Mills-Davis who carried out crystallographic studies on human ALAD.

Neville Wright, Paul Skipp and Dr Iain Campuzano for invaluable help and advice.

Everyone in and associated with the Jordan group past and present: Abeer, Sooad, Ipsita, Shufen, Jack, Neil, Julie, Mark, Nicky, Will, Rob, Jed, Katy and Stuart. Special thanks to Dr Sarwar who provided invaluable help with molecular biology and to Donald and James who have been great fun to work with.

Thanks are also due to all members of my family, especially my brothers Chris and Matt and my parents, for all their support (emotional and financial) and encouragement.

And finally, although they will never know, I am very grateful to Queen for their music, which accompanied the writing of this thesis.

Abbreviations

A	Acetate
5-ALA	5-Aminolaevulinic acid
ALAD	Aminolaevulinic acid dehydratase
ALAS	Aminolaevulinic acid synthase
Å	Ångström (10^{-10}m)
Abs	Absorbance
AIP	Acute intermittent porphyria
amu	Atomic mass unit
CCP4	Collaborative Computational Project Number 4
CoA	Coenzyme A
CRIM	Cross reacting immunoreactive material
Da	Dalton
DEAE	Diethylaminoethyl
DNA	Deoxyribonucleic acid
DTT	Dithiothreitol
E.coli	Escherichia coli
EDTA	Ethylenediaminetetra-acetic acid
E_M	Molar extinction coefficient
f.p.l.c	Fast protein liquid chromatography
GABA	Gamma aminobutyric acid
hrALAD	Human recombinant ALAD
hrePBGD	Human recombinant erythroid PBGD
hruPBGD	Human recombinant ubiquitous PBGD
IPTG	Isopropyl-thiolgalactoside
K_m	Dissociation constant
Kb	Kilobase
Mes	2-[N-Morpholino]ethanesulphonic acid
M_r	Relative molecular mass
MRNA	Messenger ribonucleic acid
NMR	Nuclear Magnetic Resonance (spectroscopy)

P	Propionate
PBG	Porphobilinogen
PBGD	Porphobilinogen deaminase
PCR	Polymerase chain reaction
pI	Isoelectric point
PLP	Pyridoxal 5'-phosphate
SDS	Sodium dodecylsulphate
TEMED	N,N,N',N'-Tetramethylenediamine
Tris	Tris (hydroxymethyl)aminomethane
UPBGG	Ubiquitous PBGD
u.v	Ultraviolet

Amino acids and their abbreviations

Amino acid	Three letter abbreviation	Single letter abbreviation
Alanine	Ala	A
Arginine	Arg	R
Asparagine	Asn	N
Aspartate	Asp	D
Cysteine	Cys	C
Glutamate	Glu	E
Glutamine	Gln	Q
Glycine	Gly	G
Histidine	His	H
Isoleucine	Ile	I
Leucine	Leu	L
Lysine	Lys	K
Methionine	Met	M
Phenylalanine	Phe	F
Proline	Pro	P
Serine	Ser	S
Threonine	Thr	T
Tryptophan	Trp	W
Tyrosine	Tyr	Y
Valine	Val	V

Table of Contents

List of Figures

CHAPTER 1

CHAPTER 2

CHAPTER 3

CHAPTER 4

CHAPTER 5

CHAPTER 6

List of Tables

Chapter 1. Introduction.

1.1 Tetrapyrroles

Tetrapyrroles are natural molecules essential for processes such as respiration and photosynthesis. The tetrapyrrole biosynthetic pathway is similar in all living organisms, utilising 5-aminolaevulinic acid, an essential precursor, eight molecules of which form uroporphyrinogen III from which all other tetrapyrroles are derived.

Tetrapyrroles are only synthesised in small quantities and pathways are tightly regulated. In the past, the study of the enzymes in the tetrapyrrole pathway and their intermediates has been difficult, however, molecular biology techniques and the availability of encoded genes or cDNAs now allows the production of milligram amounts of the enzymes enabling detailed structural investigations, using techniques such as NMR and X-ray crystallography.

1.2 Haem

Haem is an essential molecule, produced in all mammalian tissues. Haem is involved in the binding and storage of oxygen, as the prosthetic group of haemoglobin and myoglobin. Haem is also a constituent of cytochromes involved in electron transfer and is found in catalases and peroxidases.

Most of the haem in the human body is derived from endogenous synthesis, with each tissue producing haem according to its own needs. The bone marrow accounts for more than 70% of total haem synthesis within the body. In the bone marrow haem is incorporated into haemoglobin for erythrocyte precursors. The liver is the second most important site accounting for approximately 15% of the total haem synthesised. In the liver there is a high requirement for haem to be incorporated into mitochondrial cytochromes as well as into cytochrome P_{450}, catalase and cytochrome b_5.

Chemically, haem consists of a ferrous ion chelated in the centre of a porphyrin macrocycle, protoporphyrin IX. Protoporphyrin IX is made up of four pyrrole rings

linked by single carbon bridges. Since the conjugated double bonds absorb visible light, haem containing proteins are coloured.

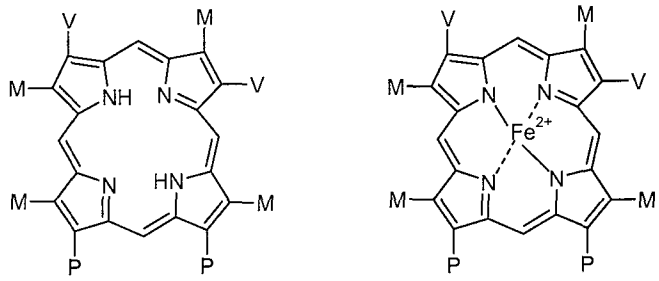

Figure 1.1 The macrocycle rings of protoporphyrin IX and haem.
M= CH_3; V= $CH{=}CH_2$; P= CH_2COOH.

Eight molecules each of glycine and succinyl CoA are required to form the organic part of haem. The formation of haem from glycine and succinyl CoA requires eight enzyme-catalysed steps. The first and last three reactions take place in the mitochondria and the other reactions occur in the cytosol.

1.3 The production of uroporphyrinogen III

Figure 1.2 depicts the early reactions in the haem biosynthesis pathway, up to the synthesis of uroporphyrinogen III. This early part of the pathway is common to many organisms. The uroporphyrinogen III molecule is often referred to as the common precursor molecule for tetrapyrroles, as uroporphyrinogen III can have several possible fates due the to branching of the tetrapyrrole biosynthetic pathway (figure 1.3). It can be converted into protoporphyrin IX for the production of haem, chlorophylls and bacteriochlorophylls, or methylated on route to sirohaem, vitamin B_{12} and factor F_{430}. Sirohaem is the prosthetic group of sulphite and nitrite reductases. Factor F_{430} is the coenzyme of the enzyme methyl CoM reductase. Cobalamin (vitamin B_{12}) is the cofactor of several enzymes that catalyse rearrangement and methylation. Chlorophylls are involved in photosynthesis. All these pathways have been extensively studied and detailed reviews published, [1, 2] [3] [4, 5] [6].

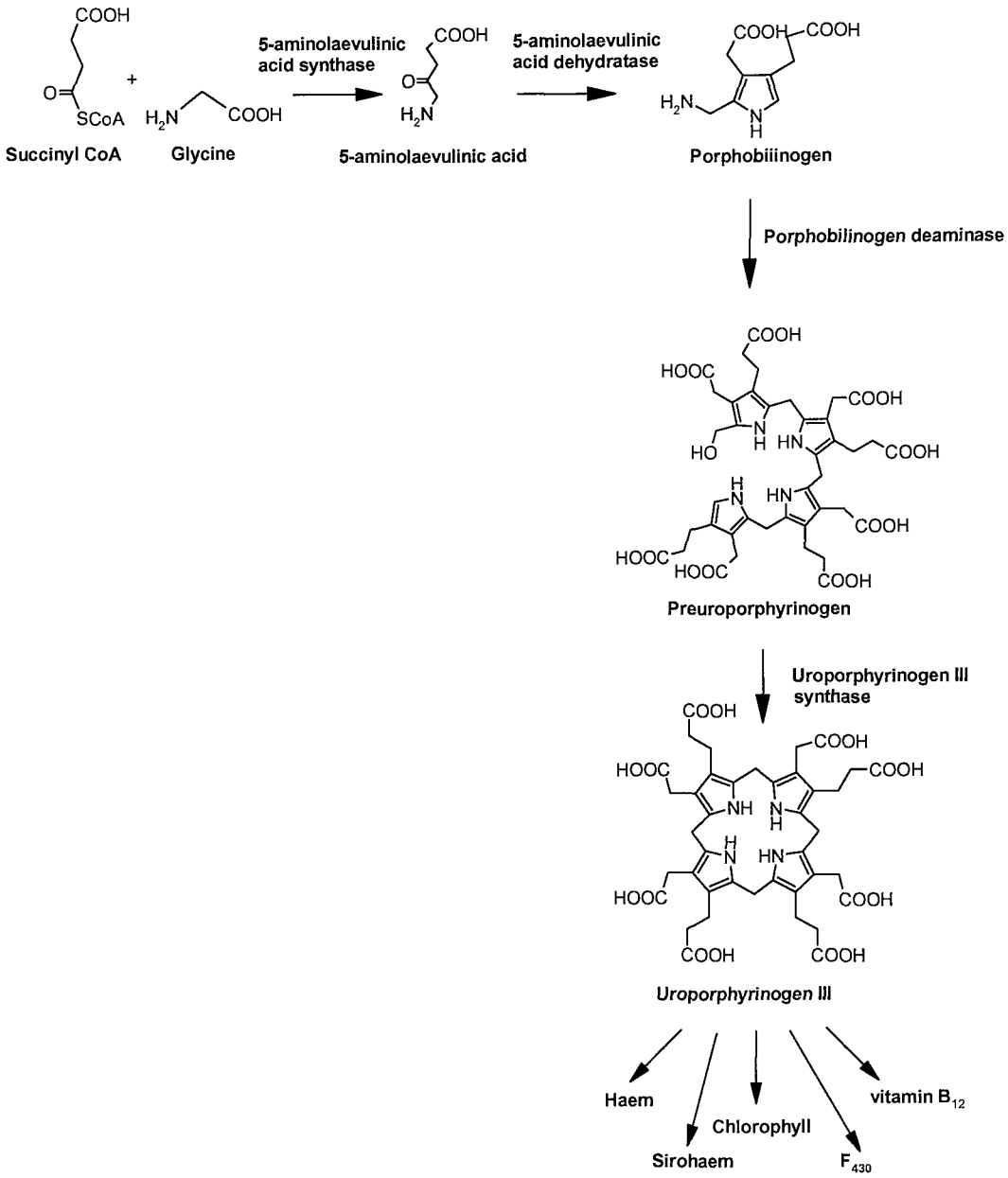

Figure 1.2. The biosynthesis of uroporphyrinogen III
In mammals 5-aminolaevulinic acid (ALA) is synthesised from succinyl CoA and glycine by the enzyme 5-aminolaevulinic acid synthase. Two molecules of ALA are condensed to form one molecule of PBG, by the enzyme 5-aminolaevulinic acid dehydratase. Four molecules of porphobilinogen (PBG) are taken up by the next enzyme in the pathway, porphobilinogen deaminase (PBGD), to form preuroporphyrinogen. Preuroporphyrinogen is converted to uroporphyrinogen III, by uroporphyrinogen III synthase. After the formation of uroporphyrinogen III the pathway branches converting uroporphyrinogen III into a variety of tetrapyrroles such as haem, chlorophyll and vitamin B_{12}.

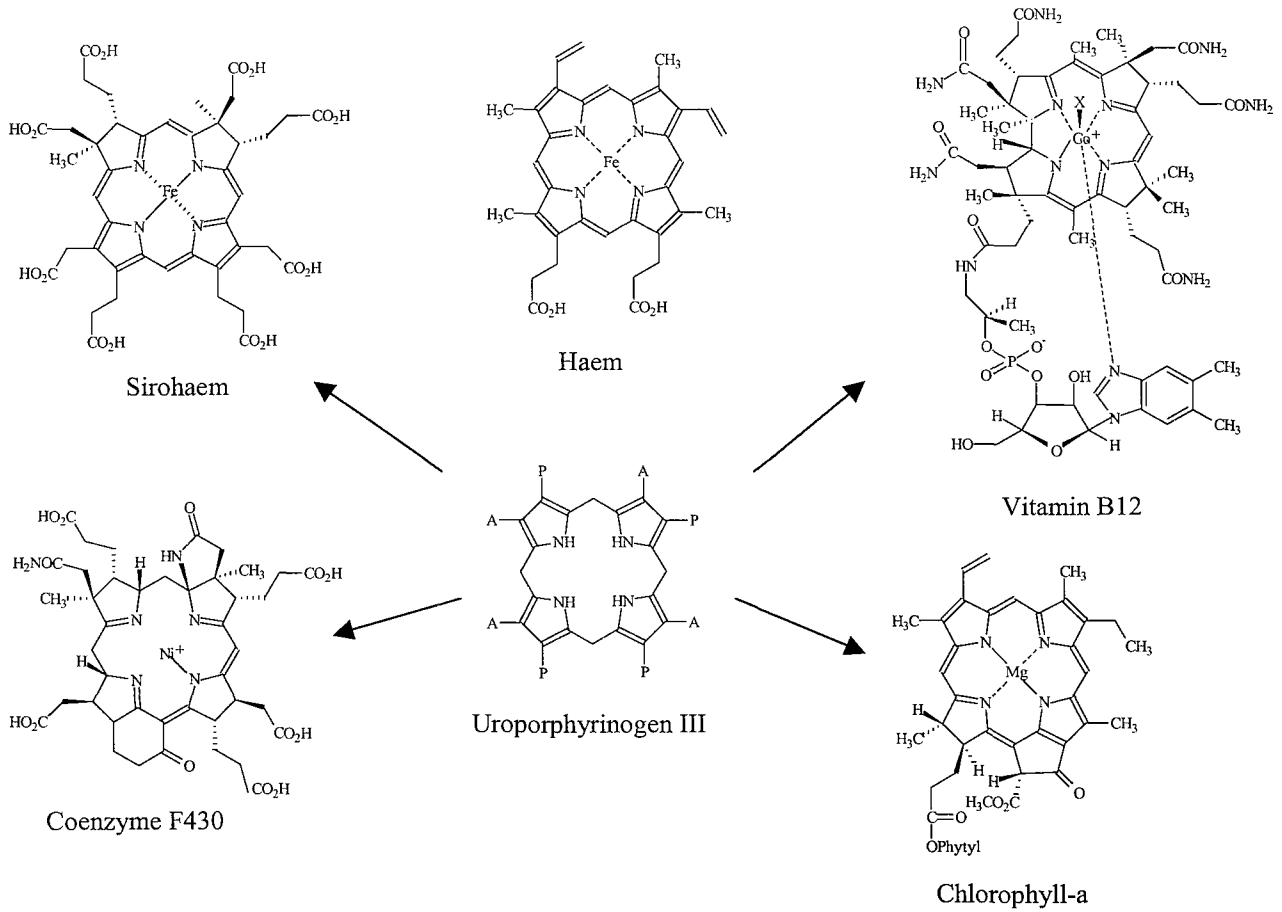

Figure 1.3 Structures of the modified tetrapyrroles haem, chlorophyll-a, vitamin B_{12} and Factor F_{430}.

Uroporphyrinogen III is the basic unit of these modified tetrapyrroles. The versatile nature of the tetrapyrroles is attributed to the modifications of the side chains and their metal ligands.

1.4 The C5 pathway

The first step in haem synthesis is the formation of 5-aminolaevulinic acid (ALA). There are two routes organisms utilise to synthesise ALA. In animals, yeast and photosynthetic bacteria, ALA is derived from succinyl-CoA and glycine, via the Shemin pathway, a reaction catalysed by 5-aminolaevulinic acid synthase (ALAS). Plants and most prokaryotes use the C-5 pathway, also known as the glutamate pathway, which synthesises ALA from glutamate via three enzyme-catalysed steps (figure 1.4).

The C-5 pathway, or glutamate pathway, discovered in the 1970s [7], involves at least three enzymes: glutamyl-tRNA ligase, glutamyl-tRNA reductase and glutamate 1-semialdehyde aminotransferase. Glutamyl-tRNA ligase catalyses the ligation of glutamate to $tRNA^{glu}$ in a reaction requiring magnesium ions and ATP. The α-carboxyl-activated glutamyl-$tRNA^{glu}$ is then reduced to glutamate 1-semialdehyde by the enzyme glutamyl-$tRNA^{glu}$ reductase in a NADPH dependent reaction. Finally, the enzyme glutamate 1-semialdehyde aminotransferase, which is pyridoxal 5'-phosphate dependent, transfers the amino group to produce ALA [1].

1.5 5-Aminolaevulinic acid synthase

In mammals, eukaryotes and photosynthetic bacteria ALA is synthesised from glycine and succinyl-CoA via the 'Shemin' pathway [8] ALA synthase (ALAS) converts glycine and succinyl-CoA into 5-aminolaevulinic acid, carbon dioxide and Co-A (figure 1.4).

ALAS is a pyridoxal 5'-phosphate dependent enzyme and lack of this cofactor causes a marked decrease in enzyme activity. The pyridoxal 5'-phosphate is bound to the enzyme through a Schiff base with an invariant lysine residue. In murine ALAS this invariant residue has been identified as lysine 313. Mutation of lysine 313 drastically reduces the activity of the enzyme, although the cofactor remains non-covalently bound [9].

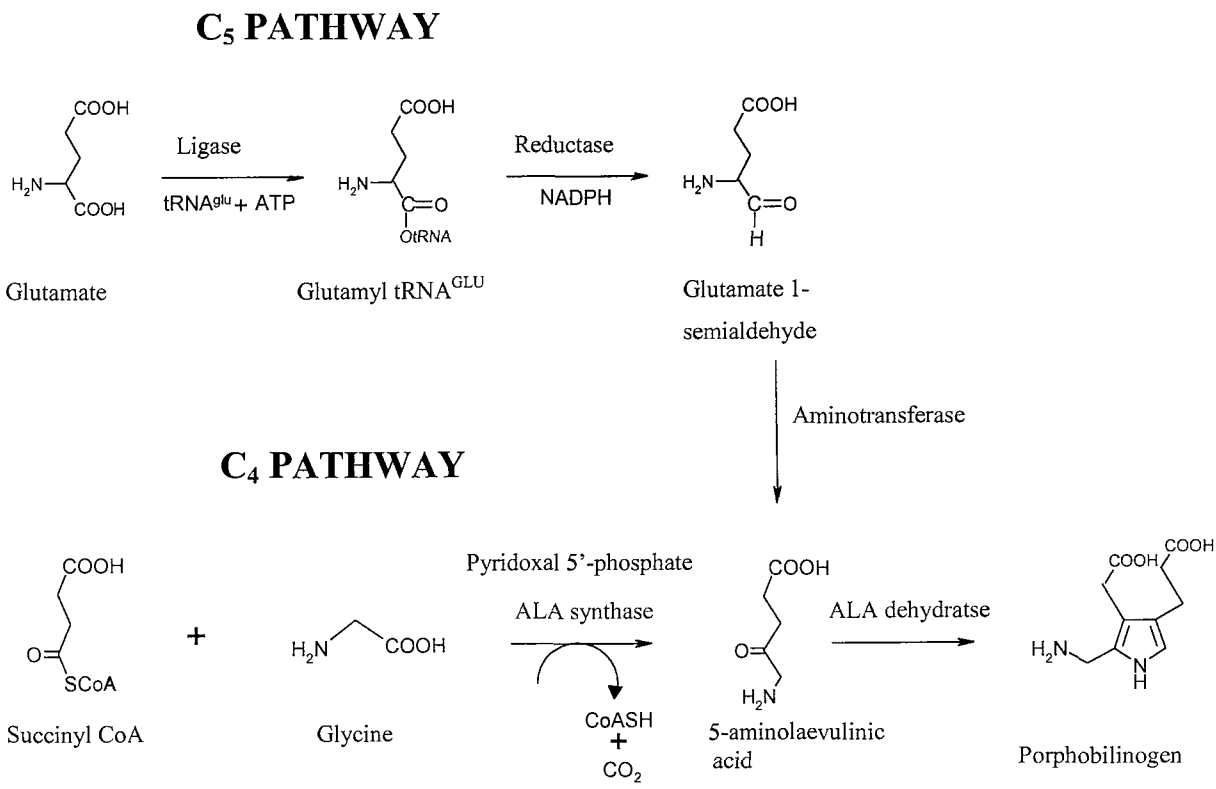

Figure 1.4 The alternative pathways used for 5-aminolaevulinic acid synthesis. Higher plants and many prokaryotic systems synthesise ALA by the C5 pathway, which utilises the carbon skeleton of glutamate. The C4 or Shemin pathway occurs in mammals and eukaryotes and synthesises ALA from succinyl-CoA and glycine.

In eukaryotes the fully functional enzyme is found in mitochondria. ALAS is first synthesised as a cytosolic protein that contains a *N*-terminal sequence thought to direct the enzyme to the mitochondria. A chaperone protein maintains the cytosolic ALAS in an unfolded state so that it can pass through the mitochondrial membrane. Once inside the mitochondrion, the *N*-terminal signal sequence is cleaved by a protease and the final folding is catalysed in an ATP dependent process.

ALASs are thought to exist as homodimers in all species. There are two ALAS genes in mammals, one is expressed in erythrocytes (ALAS2), figure 1.4, and the other, encoding a housekeeping enzyme (ALAS1), is expressed in all tissues [10]. Nucleotide sequences are similar for the two isoenzymes although there is no homology in the *N*-terminal region.

ALAS is the rate-limiting step of haem biosynthesis as it determines the quantity of substrates shunted into the pathway. Haem is thought to regulate ALAS1 production and activity in a number of ways, including inhibiting the enzyme itself by feedback inhibition and as a regulator at the nucleic acid level [11]. Mechanisms of regulation in the erythropoietic system and the liver are different. This regulation is essential not only for controlling the cellular haem levels, but also for preventing the build-up of pathway intermediates, several of which have cytotoxic, photodynamic properties in their oxidised forms.

The synthesis of ALAS1 mRNA can be suppressed in the presence of high intracellular concentrations of haem. Messenger RNA encoding ALAS has a short half-life, allowing a quick response to high haem levels [12]. Translation of ALAS1 can also be effected by haem. It has been postulated that haem may react with a specific regulatory protein, which can inhibit translation [11]. Haem is also proposed to have a role in determining the rate of ALAS transport through the mitochondrial membrane [11, 13].

Certain drugs can induce ALAS1 and therefore increase the flux through the pathway. In patients with porphyria, these drugs can precipitate an acute attack as the defective enzyme interrupts the flux through the pathway and can cause early intermediates such as ALA and PBG to accumulate to dangerous levels. Other porphyrinogenic drugs may

precipitate attacks by lowering the intracellular haem pool, usually caused by the demand for the formation of cytochrome P_{450} holoenzymes [14].

Genetic defects in the ALAS2 gene can cause X-linked sideroblastic anaemias [15, 16]. Mutations have been described which affect PLP binding at the active site explaining the response of certain patients to dietary pyridoxine treatment.

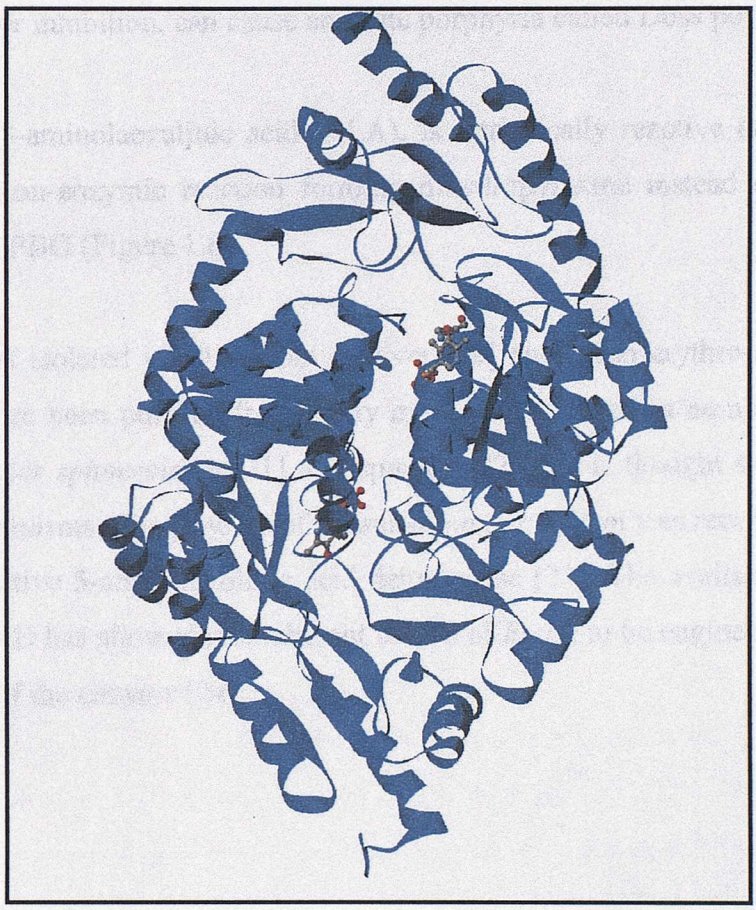

Figure 1.5 Model of human 5-aminolaevulinic acid synthase (ALAS).
ALAS has not been crystallised although a model of the human enzyme has been constructed (I. Roy, S. Wang, D. Kahari and P. Shoolingin-Jordan, unpublished results). The structure of 8-amino, 9-oxononanoate synthase (AONS), an enzyme which has many similarities with ALAS and whose crystal structure has been solved, was used to model the human ALAS. The enzyme exists as a dimer and pyridoxal 5-phosphate molecules can be seen at the active site.

1.6 5-Aminolaevulinic acid dehydratase

5-Aminolaevulinic acid dehydratase (ALAD), also known as porphobilinogen synthase (PBGS), is a cytosolic enzyme that catalyses the condensation between two molecules of ALA to form the monopyrrole PBG. This is the first reaction common in the formation of all tetrapyrroles. ALADs are highly conserved and are usually octameric enzymes with eight active sites per octamer. A reduced level of ALAD, caused by either genetic factors or inhibition, can cause an acute porphyria called Doss porphyria [17].

The substrate, 5-aminolaevulinic acid (ALA), is intrinsically reactive and can readily dimerise in a non-enzymic reaction forming dihydropyrazine instead of the desired pyrrole product PBG (Figure 1.6).

ALAD was first isolated in 1955 from ox liver [18] and avian erythrocytes [19]. The enzyme has since been purified from many more sources such as human erythrocytes [20], *Rhodobacter sphaeroidies* [21] and spinach [22] and is thought to be present in virtually all organisms. The genome of *Plasmodium falciparum* was recently discovered to encode an active 5-aminolevulinic acid dehydratase [23]. The availability of cDNA coding for ALAD has allowed recombinant strains of *E.coli* to be engineered to produce large amounts of the enzyme [24].

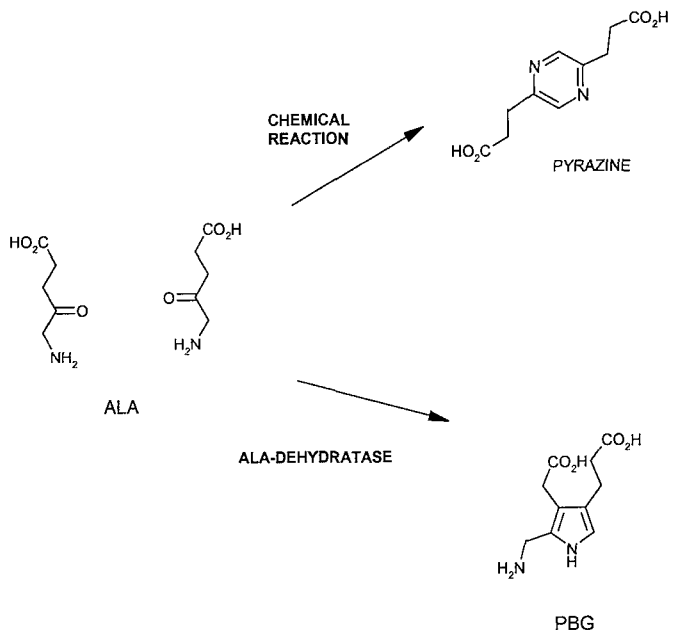

Figure 1.6 The dimerisation of 5-aminolaevulinic acid.
ALAD condenses the two molecules of ALA to form one molecule of PBG. The A-side and P-side ALA refer to the acetate and propionate side chains of PBG, respectively. Dihydropyrazine is formed from the non-enzymic reaction between two molecules of ALA and is converted to pyrazine.

1.6.1 Structure of ALAD

The first high-resolution structure of an ALAD was the yeast structure published in 1997 [25], followed by the structure of the *E. coli* enzyme [26]. The *P.aeruginosa* [27] and the human enzyme, both the recombinant human enzyme (unpublished results) and the human enzyme purified from human erythrocytes [28], have since been crystallised and the structures solved.

ALADs crystallise as octamers. The octameric structure is consistent with measurements made using electron microscopy on the bovine liver ALAD over 30 years ago [29]. The enzyme is regarded as a tetramer of dimers as interactions within the dimer are much stronger than those between the four dimers. The octamer has a solvent channel of 15-20 angstroms passing through the centre (figure 1.7) [25].

Each ALAD monomer adopts a TIM barrel or $(\alpha/\beta)_8$ fold, which is formed by an eight membered cylindrical β-sheet with eight surrounding α helices. The active site of each monomer is located in an opening formed by the loops connecting the C-terminal ends of the parallel β-strands and their alternating α-helices [25]. The structures of ALADs are remarkably conserved and a comparison of the monomers of yeast, *E.coli*, human and *P.aeruginosa* ALADs can be seen in figure 1.8.

In the human structure of human ALAD purified from erythrocytes [28] a loop covering the active site (residues 197-220) was seen in four monomers of the octamer. The loop of the second monomer in the dimer was disordered and could not be modelled.

Dimers are formed by each monomer wrapping an *N*-terminal arm around the TIM barrel of the neighbouring monomer. Many non-covalent interactions are formed between the *N*-terminal arm of each monomer and the barrel of the other, including several salt bridges, non-polar associations, hydrogen bonds and helix-helix interactions. When the four dimers come together, the resulting octamer is stabilised mainly by the interactions of the *N*-terminal arm with the other subunits. The arm caps one end of the β-barrel, interacting with two conserved phenylalanine residues at the base of the barrel [28].

The length of the *N*-terminal arm varies between species, but a α-helix and a 3-10 helix are found in nearly all of them. The yeast enzyme has a longer *N*-terminal arm than the human enzyme but the overall tertiary structures of the enzymes are strikingly similar since they have 53% sequence identity.

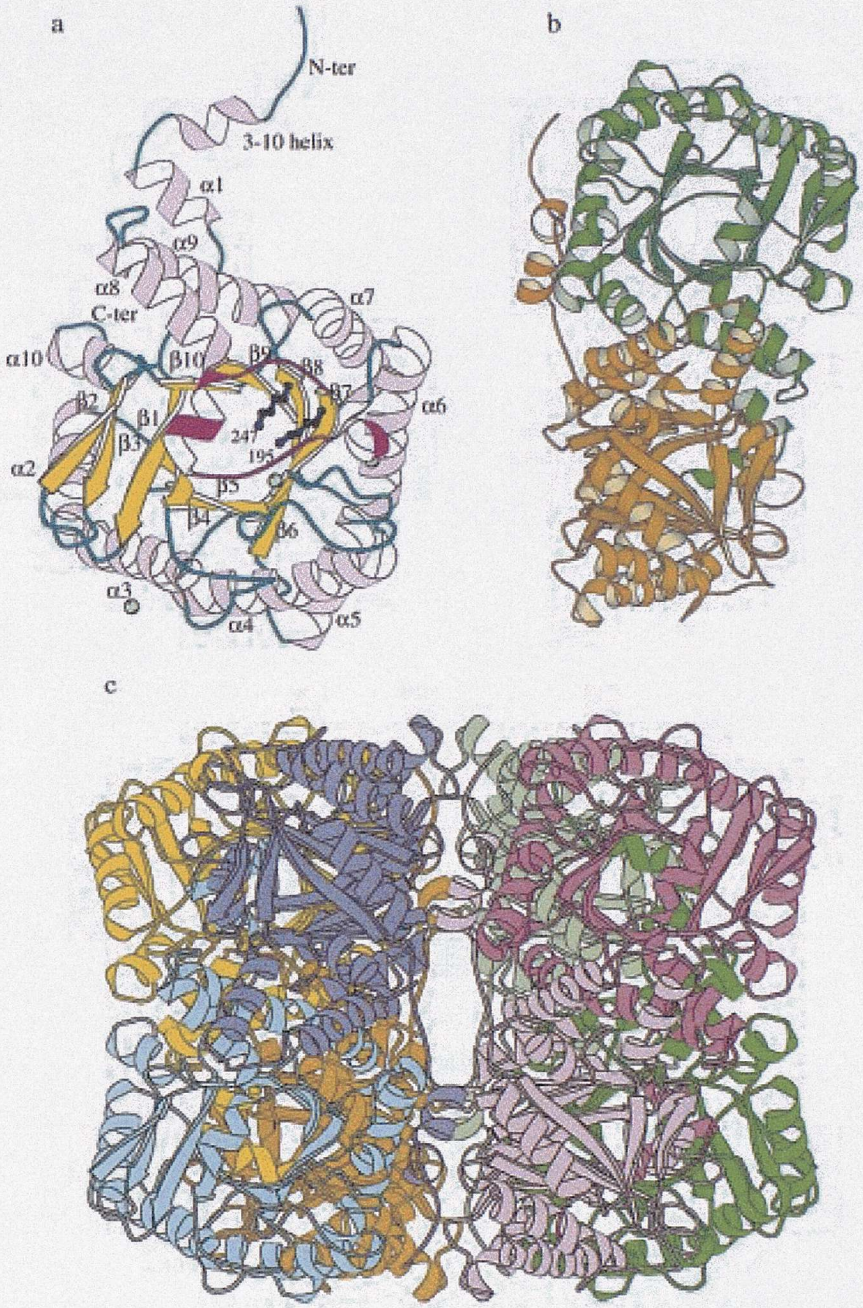

Figure 1.7 Structure of *E.coli* 5-aminolaevulinic acid dehydratase.

A) *E.coli* ALAD monomer displays the TIM barrel fold, with an extended *N*-terminal arm.

B) Two monomers combine to form the dimer, which displays the characteristic "69" formation, with the *N*-terminal arm of the monomers wrapped around its neighbour.

C) *E. coli* ALAD octamer forms a tetramer of dimers with all active sites directed outwards towards the solvent.

This figure was taken from Erskine *et al* 1999 [26].

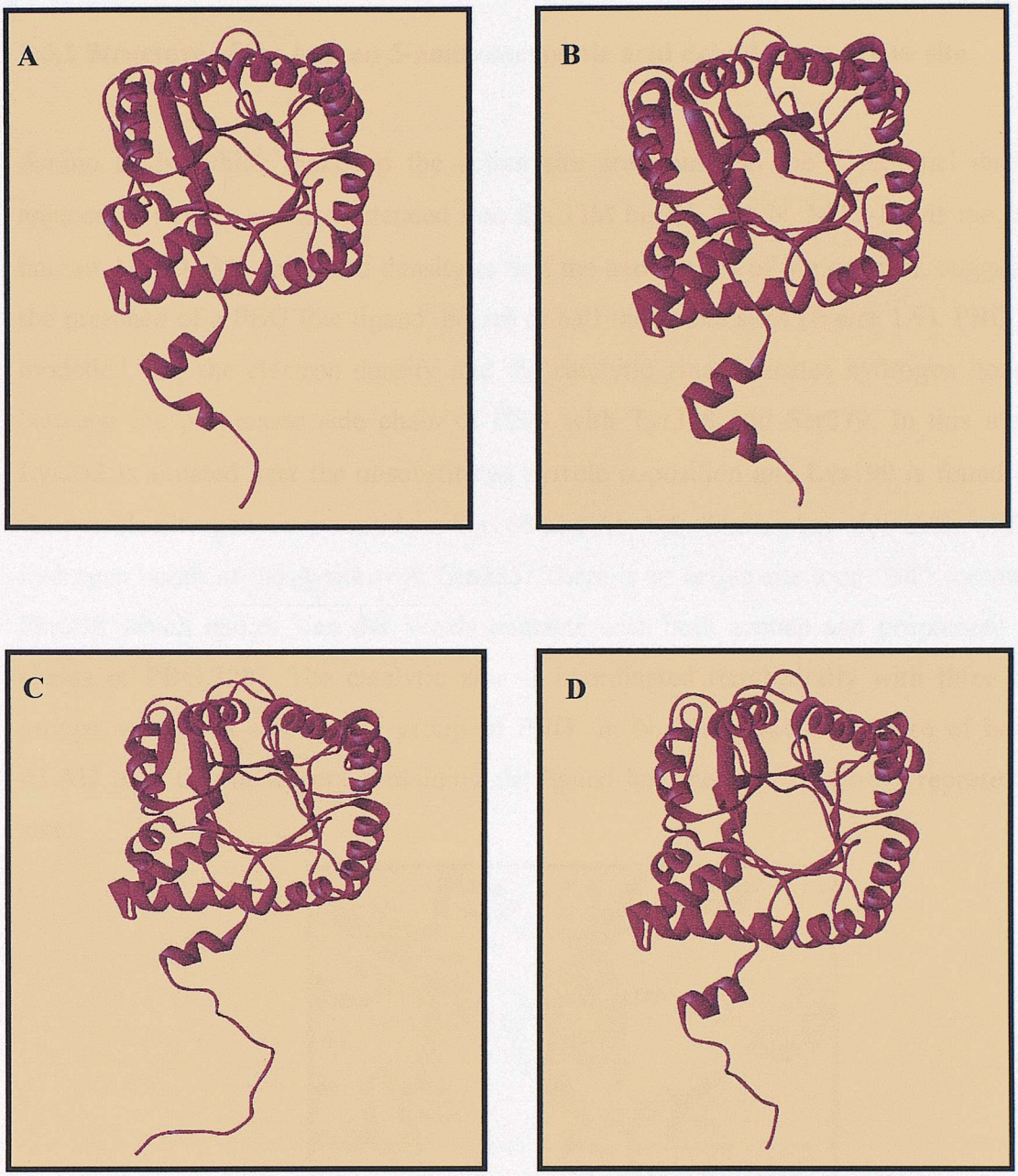

Figure 1.8 Comparison of 5-aminolaevulinic acid dehydratase monomers from four different species.

A. *E.coli* ALAD monomer.
B. *Pseudomonas aeruginosa* ALAD monomer.
C. Yeast ALAD monomer.
D. Human ALAD monomer.

The structures of ALAD monomers are remarkably conserved. The TIM barrel is present in all known ALADs. The most notable difference is the variation in the *N*-terminal arm, which varies in length and secondary structure.

This figure was prepared using the program WebLab Viewer Lite[30] and the following pdb files: A) 1B4E; B) 1B4K; C) 1H79 and D) 1E51 [31]

1.6.2 Structure of the human 5-aminolaevulinic acid dehydratase active site.

Amino acids, which make up the active site are found on the *C*-terminal ends of adjacent β-strands and are extended into the TIM barrel. The N. Mills-Davis model of human ALAD [32] contained density at half the active sites of the octamer, suggesting the presence of a PBG like ligand, bound at half the active sites (figure 1.9). PBG was modelled into the electron density and the catalytic zinc indicates hydrogen bonding between the propionate side chain of PBG with Tyr318 and Ser279. In this model, Lys252 is situated near the unsubstituted pyrrole α-position and Lys199 is found near the pyrrole nitrogen, as are residues Ser168 and Asp120. The acetate side chain of PBG hydrogen bonds at the A-site with Gln225. There is an active site loop "lid" containing Phe208 which makes Van der Waals contacts with both acetate and propionate side chains of PBG [28]. The catalytic zinc is coordinated tetrahedrally with three thiol groups and the A-side amino group of PBG. In N. Mills-Davis structure of human ALAD only the monomers containing the ligand had the intense density representing zinc.

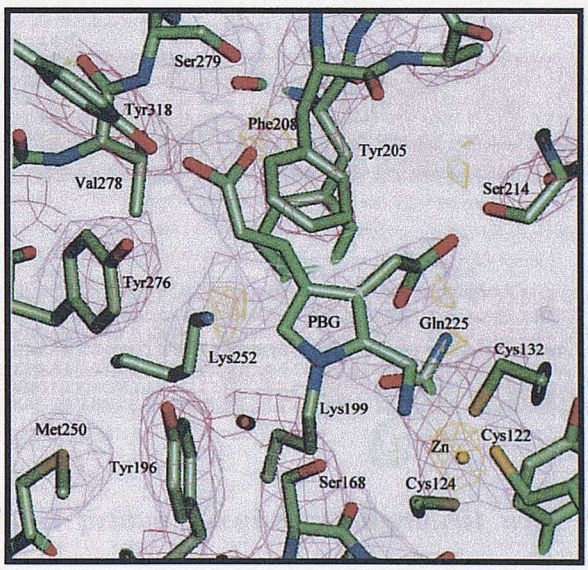

Figure 1.9 Model for the catalytic site of human ALAD monomer A with the catalytic zinc, and the product PBG modelled into the electron density at the active site.
The propionate side chain of PBG makes hydrogen bonds at the P-site with Tyr318 and Ser 279. Lys252 is located near the unsubstituted pyrrole α position and Lys199 close to the pyrrole nitrogen. The active site lid contains Phe208 that makes van der Waals contacts with the acetate and propionate side chains of PBG. The amino group of PBG is coordinated to the catalytic zinc that is ligated by Cys122, Cys124 and Cys132 [28].

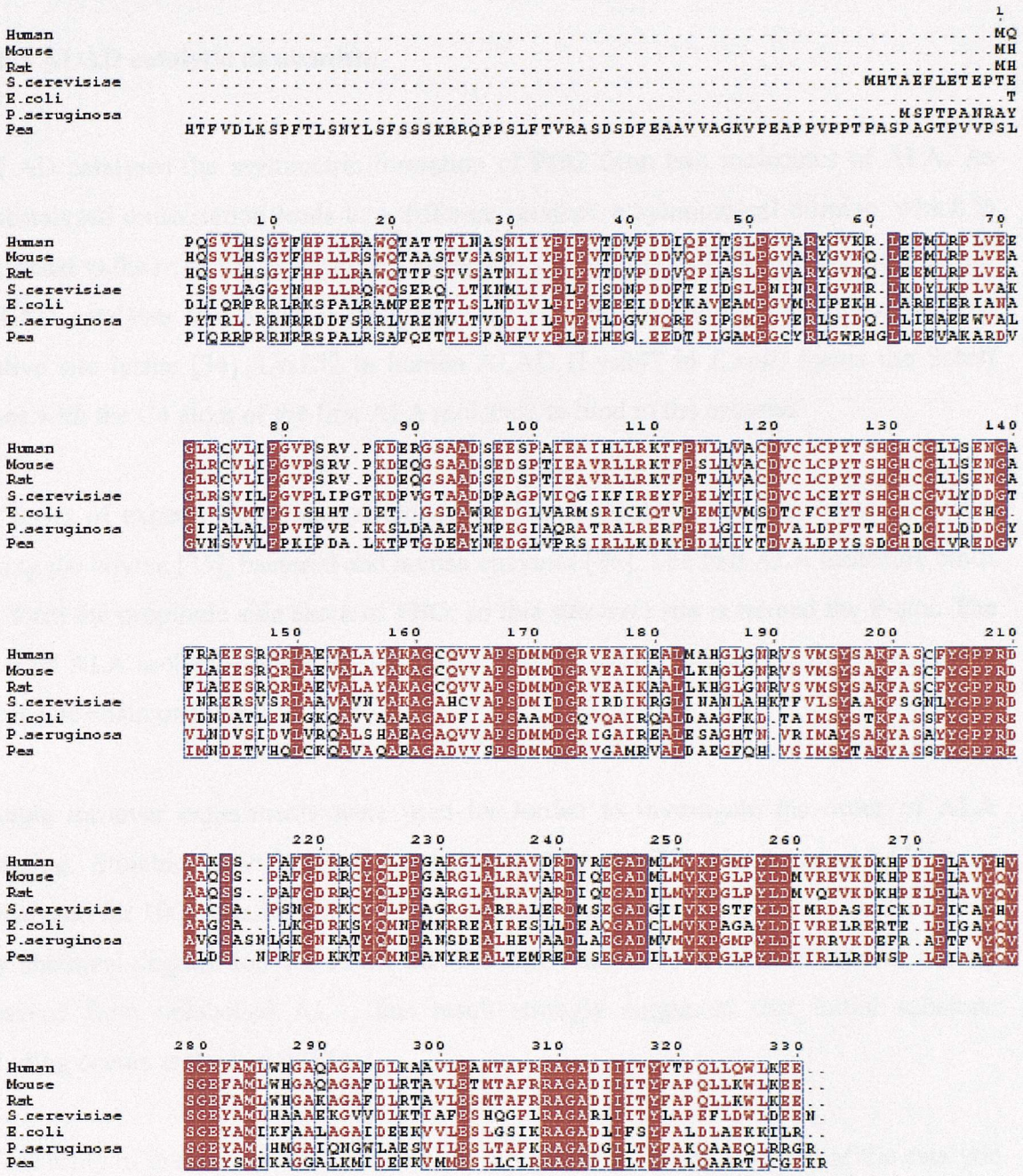

Figure 1.10 Human ALAD primary sequence alignment with ALADs from six other species.

This figure was prepared using the sequence alignment program Multalign [33]. Residues that are totally conserved in these ALADs are shown with white text with a red background and outlined in blue. Residues that are partially conserved are shown with red text and outlined in blue. Residues that are not conserved are shown in black text. Note the active site residues Lys199 and Lys252, and the catalytic zinc binding residues, Cys122, Cys124 and Cys132.

1.6.3 ALAD catalytic mechanism

ALAD catalyses the asymmetric formation of PBG from two molecules of ALA. As uncatalysed dimerisation leads to a different product, a symmetrical diimine, which is oxidised to the pyrazine, it is of great interest to understand the biosynthetic mechanism. ALAD catalyses this Knorr condensation reaction via a Schiff base formed with an active site lysine [34]. Lys252 in human ALAD (Lys247 in *E.coli*) forms the Schiff base with the C4 atom of the first ALA molecule to bind to the enzyme.

A series of experiments were carried out to determine the order of substrate binding, using the bovine [35], bacterial and human enzymes [36]. The first ALA molecule binds to form the propionic side chain of PBG, so this substrate site is termed the P-site. The second ALA molecule binds to a region referred to as the A-site as it forms the acetic acid side chain of PBG.

Single turnover experiments were used by Jordan to investigate the order of ALA binding. Stoichiometric amounts of labelled ALA (5-^{14}C ALA) and ALAD were incubated for 100ms before the addition of excess unlabelled ALA. It was demonstrated by chemical degradation and NMR that the acetic acid side chain of PBG was mainly derived from unlabelled ALA; this result strongly suggested that initial substrate binding occurs at the P-site [36].

The ability of the second ALA molecule to bind depends on the presence of the catalytic zinc and the first ALA bound to the P-site [37]. ALA binding at the A-site is prevented after removal of the metal ion, but the Schiff base was still able to form.

The identification of a Schiff base as an intermediate in the reaction strongly influenced views on the enzyme mechanism. An active site lysine was identified using labelled ALA, which was reduced onto the enzyme with $NaBH_4$ [38]. Although high-resolution structures of ALADs have been published the exact mechanism of PBG formation is not certain.

After the formation of the Schiff base, the next step could proceed by one of two mechanisms. There are two bonds formed: the C-C bond between the C4 of the P-site ALA and the C3 of the A-site ALA, and the C=N bond between the nitrogen of the P-site ALA and the C4 of the A side ALA.

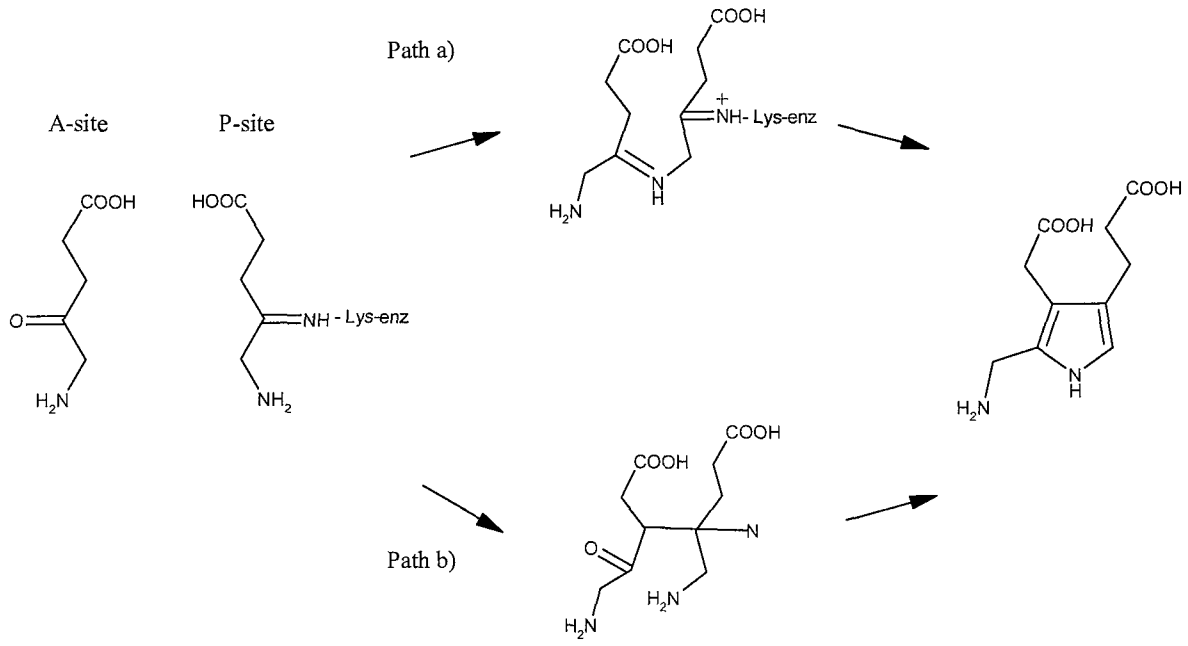

Figure 1.11 Two possible routes for the formation of porphobilinogen from 5-aminolaevulinic acid.
Path a) represents the initial formation of Schiff base (C=N bond) between the two substrates. Path b) represents a mechanism where aldol condensation (C-C bond formation) has occurred initially.

A second lysine residue in ALAD (Lys199 in the human ALAD, Lys195 in *E.* coli ALAD) has been implicated in catalysis. This second lysine is thought to increase the nucleophilicity of Lys252 (Lys247 in *E. coli* ALAD) responsible for Schiff base formation in human ALAD. Site directed mutagenesis in *E.coli* ALAD demonstrated the importance of this second lysine (Lys195 in *E.coli*) [39].

Two different mechanisms have been proposed. The first mechanism is based on the C=N bond forming first and the second mechanism is based on the formation of the C-C bond first (figure 1.11).

ALAD from *P. aeruginosa*, *E. coli*, yeast and human have all been co-crystallized with the inhibitor laevulinic acid (LA). These structures revealed an unoccupied A-site with the inhibitor LA covalently bound to the P-site by a Schiff base between its 4-keto-group and an active-site lysine residue (Lys260 in *P. aeruginosa*; Lys246 in *E. coli;* Lys263 in yeast and Lys252 in human). Recently, the structures of *E. coli* and yeast ALAD in complex with the irreversible inhibitor 4,7-dioxosebacic acid (DOSA), a diacid-based mimic of a possible reaction intermediate, first revealed simultaneous A and P-site occupancy [40] [41]. The inhibitor is covalently bound to the two active-site lysine residues. Although the inhibitor resembles one of two possible reaction intermediates, the enzymatic mechanism requires further investigation.

A 1.9Å crystal structure of the inactive *P. aeruginosa* ALAD mutant Asp139Asn in complex with the inhibitor 5-fluoro-laevulinic acid (5F-LA) was recently published [42]. The structure reveals the binding of two individual ALA-analogues, to both the A and P-sites. Both molecules are covalently linked to the two active-site lysine residues through Schiff bases using their 4-oxo-groups.

These recent crystal structures show the inhibitors DOSA and 4-oxosebacic acid bind at both the P-site and the A-site, both inhibitors bind in a similar conformation. These findings have prompted the proposal that the mechanism proceeds by the formation of two Schiff base bonds between the two ALA and the two lysine residues in the active site. DOSA mimics one of two possible reaction intermediates in which the C-N bond formation has occurred first. However, the additional free amino group of the true reaction intermediate is lacking.

Based on the *P.aeruginosa* structure complexed with F-LA, Frere *et al* 2002 [42] propose the first step of the reaction is the aldol-like C-C bond formation. The next step would then be the formation of the intersubstrate Schiff base, followed by the *trans*-elimination of the C-N bond between the P-side substrate and Lys260. It is only at this late stage that the bond between the substrate and the enzyme is broken. The last step is the deprotonation aromatisation step, which should be extremely fast and which would be the thermodynamic driving force for the reaction. However, the structure differs from a native ALAD-substrate complex in two important details. Asp139 was mutated to asparagine, and the ALA amino group was replaced by fluorine.

Although providing much information about the ALA binding sites the structure of ALADs complexed with these inhibitors has not been able to unequivocally resolve the question of whether the C-C bond or C-N bond formation occurs first.

1.6.4 Metal ion requirements of ALADs.

All ALADs require a divalent metal ion for activity although they differ in the type of metal ion they use [43]. Mammalian, yeast and some bacterial ALADs require zinc for activity, whereas plant and some bacterial ALADs require magnesium. Jordan and co-workers had shown mutations that introduced zinc-binding ligands into a magnesium-dependent enzyme conferred an absolute requirement for zinc [39]. Recently, experiments carried out by Jaffe's group in Philadelphia have "switched" metal binding regions in ALADs. They have been able to create chimeric ALADs, which possess the aspartate rich metal binding region of pea ALAD in the human ALAD and *vice versa* [44].

The *E.coli* enzyme is an interesting case as it is dependent on zinc for activity but is activated by magnesium [45]. The *Rhodobacter sphaeroides* ALAD is stimulated by potassium, which acts as an allosteric activator [46].

Zinc dependent ALADs have three cysteines known to be important in interacting with the zinc ion. Oxidation of these cysteine residues, forming disulphide bridges, results in

the loss of the zinc ion and inactivation of the enzyme. Incubation of the human erythrocyte ALAD enzyme with DTNB was found to decrease catalytic activity and prevent the enzyme binding zinc [47]. This suggested that the reactive cysteines were involved in zinc coordination.

The zinc ion may act to promote nucleophilic catalysis via water ionisation, it is possible that a zinc hydroxide acts as the nucleophile base causing deprotonation at the C-3 position of the A-site ALA. As in the yeast and *E.coli* crystal structures a water molecule is the fourth ligand for zinc [26], and as this tetrahedral coordination is favoured, the hydroxide mechanism is a strong possibility.

ALADs that require magnesium have alanine and aspartate residues in place of these cysteines, which are more suitable for binding magnesium. ALADs from plants (Mg^{2+} dependent) are not as sensitive to O_2 as they do not have the zinc binding cysteines.

Lead is a potent inhibitor of mammalian ALADs. The activity of human ALAD is inhibited by lead both *in vivo* and *in vitro* [48]. The lead is thought to displace zinc and either inhibit catalysis as it is either unable to perform the catalytic role in the reaction, or by steric hindrance. Patients with lead poisoning excrete high levels of ALA in their urine and have symptoms similar to those seen in acute porphyria.

1.6.5 The human ALAD gene

The human ALAD gene is situated on the 9q 34 chromosome [49] with two common alleles termed $ALAD^1$ and $ALAD^2$, that generate three electrophoretically distinguishable isozymes $ALAD^{1-1}$, $ALAD^{1-2}$ and $ALAD^{2-2}$ with distribution in the Caucasian population of 79%, 20% and 1% respectively [50] [51]. The $ALAD^1$ allele codes for a lysine at position 59, whereas $ALAD^2$ codes for an asparagine at that position (figure 1.12)

Lys59 is at the base of a hairpin loop, an elaboration of the α/β fold, which extends into the *C*-terminus of the active site. In the $ALAD^1$ monomer Lys59 forms an intramolecular salt bridge with an adjacent Asp 42 and fulfils a structural role.

Mutations in the ALAD gene can cause the inherited disease Doss porphyria (section 1.10). There are another four well-documented mutations: Gly133Arg, Arg240Trp, Ala274Thr and Val275Met which cause a severe decrease in ALAD activity [52-54].

Gly133 is adjacent to one of the conserved cysteines of the catalytic zinc-binding site and a mutation to an arginine would cause a steric clash that could affect metal binding. Arg240 forms an intramolecular salt bridge with Asp172, an invariant residue in ALADs. This is adjacent to the arm region of the neighboring monomer, but also forms an ionic interaction with a histidine at position 8 (an alanine in the yeast enzyme). Therefore, it can be predicted that this mutation could disrupt dimer conformation.

Ala274 and Val275 are positioned on β-strand 9, and form part of the hydrophobic core of the barrel. Many hydrophobic residues including Ile314, lle316, Met194 and Met250 surround Ala274. The Ala274Thr mutation would cause disruption in this hydrophobic environment and, as it has a branched polar side chain, it may also disrupt the environment due to its increased side chain size compared to alanine and may stop the correct folding of the protein. If the mutant protein does fold correctly, as the active site is close this alteration is likely to affect catalysis. Val275 (an alanine in the yeast structure) interacts with a loop region that coordinates intramolecular interactions at the

dimer interface. A change to methionine at this position would disrupt the loop and could inhibit dimer formation and protein stability.

Details on three further mutations have recently been published. Phe12Leu substitution was found in a healthy infant with normal ALAD levels, but with only 12% ALAD activity, despite only being a heterozygote [55]. Two mutations were described from one patient who had inherited one mutation from his mother and another from his father. The mutations were Val153Met as well as a premature stop codon after residue 294. Val153 is in the fourth α-helix, which interacts with residues in the third α-helix and this mutation causes structural problems leading to a protein with 10% activity. The stop codon inherited from the father resulted in a truncated unstable protein [56].

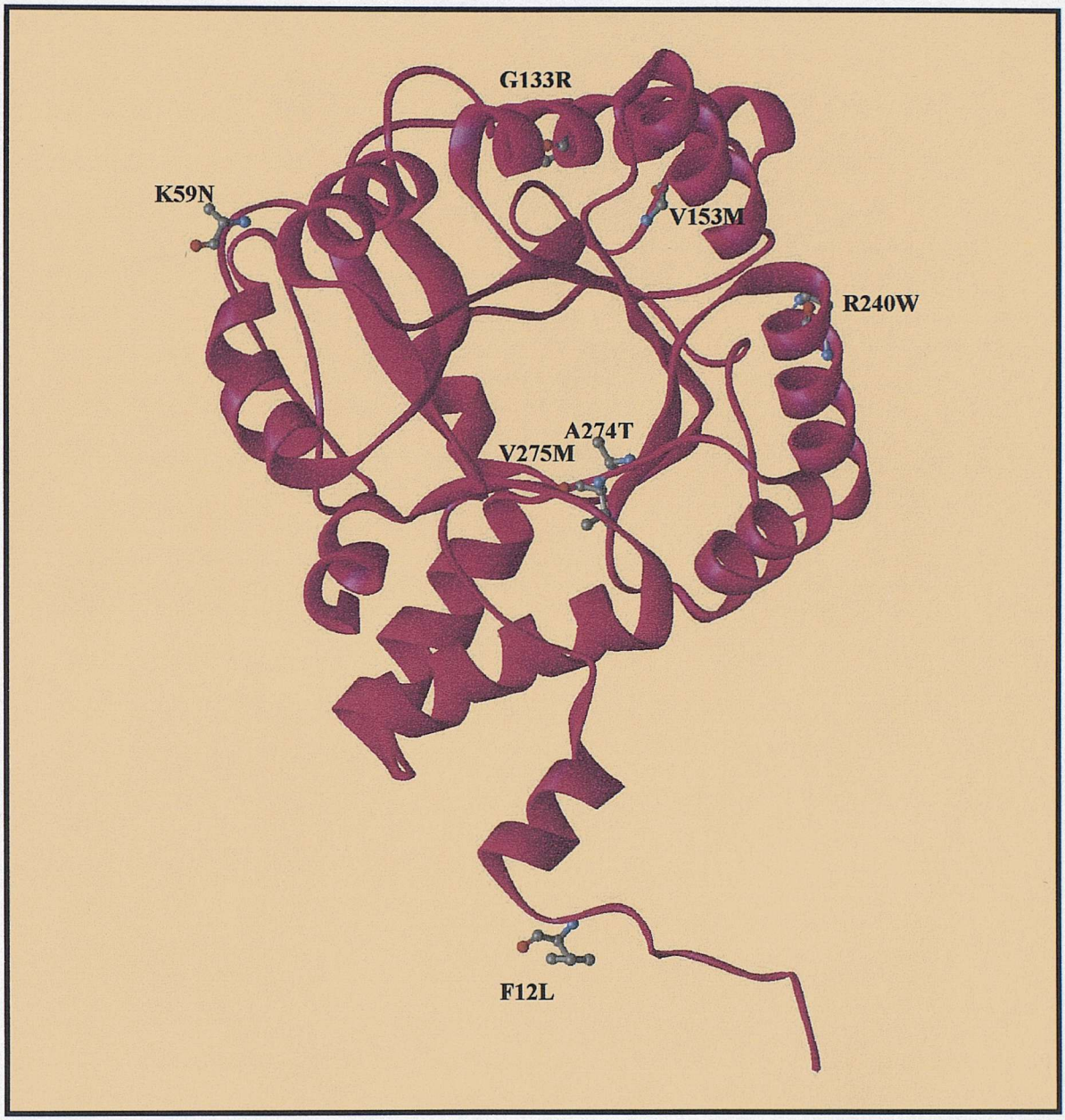

Figure 1.12 The positions of a polymorphism and mutations found in human ALAD.

The Lys59Asn polymorphism, is present in 20% of the Caucasian population. There are only a few well-documented mutations (Gly133Arg, Arg240Trp, Ala274Thr and Val275Met), which cause severe decrease in ALAD activity. Due to the naturally high abundance of ALAD, individuals with low levels of the active enzyme may never suffer from porphyria. For example, the proband with the Phe12Leu (F12L) mutation had ALAD activity levels of 12%, yet suffered no ill effects. This figure was prepared using the program WebLab Viewer Lite [30]

1.6.6 Proteosomes

ALAD is present in abundant levels in cells and has recently been suggested to also function as an accessory protein in the ubiquitin-ATP-dependent protein degradation machinery of mammalian cells. Proteins are degraded by their binding to ubiquitin (a 72 residue protein) marking them for hydrolysis by a 26S proteosome complex of around 2000kDa. The 26S proteosome complex is made up of three factors: CF1, CF2 and CF3. The CF1 component is a multimeric proteosome activator. The CF3 is also known as the 20S proteosome; [57] it is through a narrow opening in the center of the CF3 that the unfolded protein enters. The CF2 component is an ATP-stabilized inhibitor of the proteosome complex.

The CF2 component has many of the same properties as ALAD. It was found to be impossible to distinguish the two proteins with respect to their size, charge and cross reactivity with antibodies. Most interestingly, the CF-2 was found to have ALAD activity, that is, they were able to catalyse the conversion of ALA to PBG [58]. Such a dual role for ALAD would represent an interesting adaptation by nature to utilize a single protein for two such diverse processes.

1.7 Porphobilinogen deaminase (PBGD)

Porphobilinogen deaminase (PBGD) is also known as hydroxymethylbilane synthase (HMBS) and as uroporphyrinogen I synthase. PBGD catalyses the condensation of four molecules of PBG in a stepwise fashion to yield an unstable linear tetrapyrrole called preuroporphyrinogen (or 1-hydroxymethylbilane) (figure 1.13). PBGD has been isolated from many sources including *Rhodobacter sphaeroides* [59], human erythrocytes [60, 61], recombinant *E. coli* [62], rat liver [63] and pea [64].

There are two isoforms of PBGD, the erythroid specific enzyme and the housekeeping enzyme. Both originate from a single PBGD gene on chromosome 11 and arise by alternate splicing of the primary transcript [65]. The human erythroid PBGD contains 344 amino acids, whilst the ubiquitous PBGD contains 361 amino acids, due to an additional 17 amino acids at the *N*-terminus.

Deaminases from most sources show stability when heated, which has aided greatly in their purification. Recombinant strains of *E. coli* have been used to express the deaminases in sufficient amounts for crystallization [62]. From X-ray crystallography it has been shown that the enzyme is composed of three domains, which are linked by hinge regions [66].

All PBGDs are monomeric enzymes with Mr values ranging from 34,000 to 44,000 and contain a prosthetic group, the dipyrromethane cofactor, which is bound to the catalytic site. The cofactor consists of two molecules of linked PBG and acts as a primer for the reaction. PBG units bind sequentially to the cofactor until there are six bound together. The product is then cleaved from the cofactor.

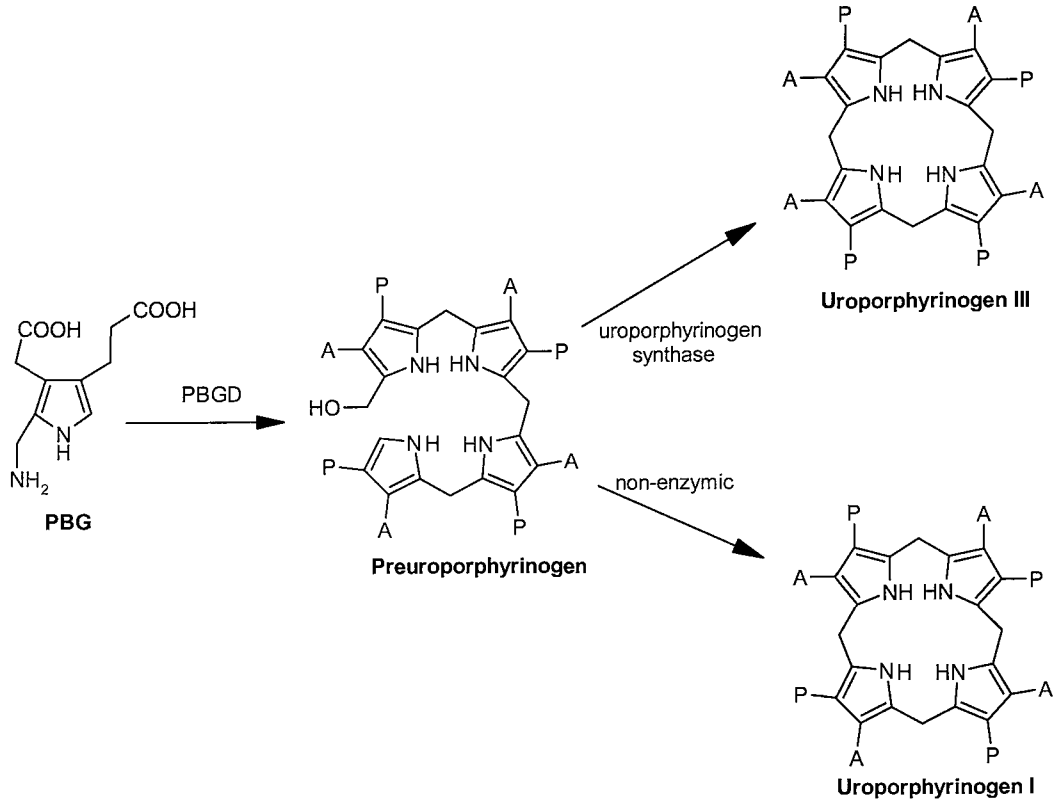

Figure 1.13 Formation of uroporphyrinogen I and uroporphyrinogen III from PBG.

PBG is polymerised by porphobilinogen deaminase forming preuroporphyrinogen, which is converted into uroporphyrinogen III by the next enzyme in the pathway uroporphyrinogen synthase. If uroporphyrinogen synthase is absent preuroporphyrinogen will non-enzymatically cyclize forming the biologically redundant uroporphyrinogen I.

1.7.1 Structure of PBGD

E.coli PBGD was the first enzyme in the tetrapyrrole pathway to have its structure determined by X-ray crystallography [66]. The enzyme is made up of three domains. Domains 1 and 2 are related, both having a doubly wound, parallel β-sheet of five strands (figure 1.14).

One of the α-helices ($\alpha 3_2$) found in domain 2 is replaced by a loop in domain 1. In this loop, two conserved prolines prevent the formation of secondary structure, the catalytic residue, Asp 84 in *E. coli*, is situated in this loop. Domain 3 is an open faced 3-stranded β-sheet with 3 α-helices packed on one face. There appear to be few interactions between domains 1 and 2 but both interact with the dipyrromethane cofactor by hydrogen bonds and ionic interactions.

The cleft between domains 1 and 2 is approximately 15 x 13 x 12 angstroms, and is filled by the dipyrromethane cofactor and the substrate molecules as they join the growing polypyrrole chain. The dipyrromethane cofactor is attached to the enzyme via Cys242 (in *E.coli* PBGD), which is situated in a β-turn of domain 3. The acidic side chains of the cofactor interact with the basic side chains of arginine residues lining the cleft and the presence of the cofactor in the cleft is thought partially to neutralise the considerable electropositivity in the cleft. In this way the cofactor is thought to contribute to the final 3-D structure of the enzyme and to stabilise it as well as acting as a primer for the reaction [67].

The X-ray structure showed that only one catalytic site exists in the enzyme and this means a large conformational change must occur during the reaction to make room for the growing polypyrrole chain [66].

The catalytic base, Asp84, has been identified in *E.coli* PBGD, as a critical catalytic residue both by its proximity to the cofactor pyrrole ring nitrogen and by structural [68] and kinetic studies [69] of the Asp84Glu mutant protein in *E. coli*. As positive charge builds up on the pyrrole nitrogens during catalysis it is possible Asp84 provides a stabilising influence.

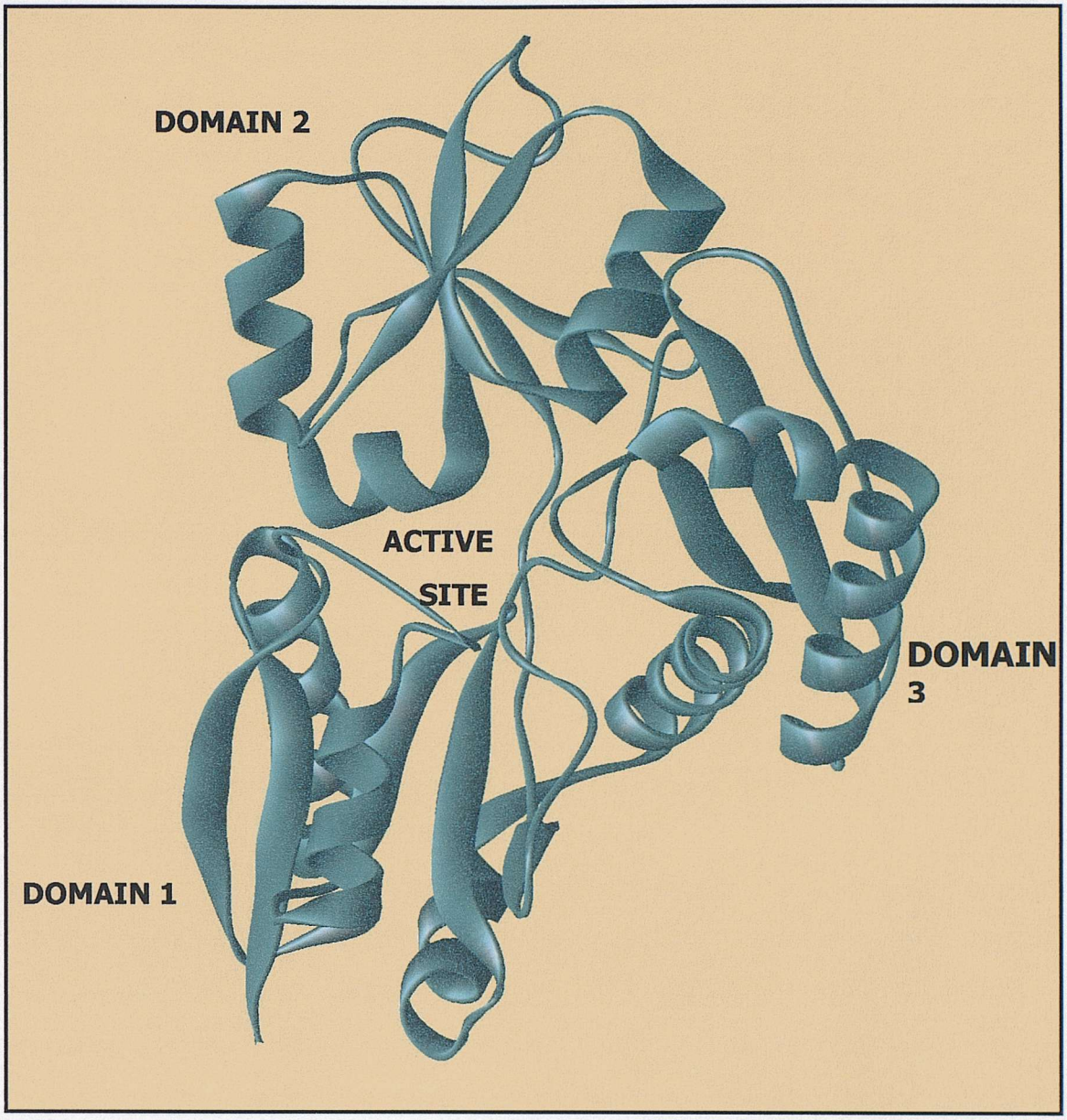

Figure 1.14 The three dimensional structure of *E.coli* porphobilinogen deaminase.

Domains 1 and 2 have a similar overall topology consisting of five stranded beta-sheet with intervening alpha-helices packed against each face. The dipyrromethane cofactor is attached to a loop that projects from domain 3 into the active site. This figure was prepared using the computer program WebLab Viewer Lite [30] using the IPDA pdb file [31].

Evidence for conformational changes in *E. coli* PBGD during stepwise pyrrole chain elongation was shown by increased reactivity of Cys134 to alkylation by *N*-ethylmaleimide [70]. Two suggestions have been put forward to explain how PBGD accommodates the polypyrrole chain during catalysis. Domain 3 may move away from domains 1 and 2 pulling the pyrrole chain with it so that the terminal pyrrole is next to the catalytic residues ready for the addition of another pyrrole or, alternatively, it has been proposed that the active site moves along the polypyrrole chain attaching PBG units one by one [71].

1.7.2 The dipyrromethane cofactor

The dipyrromethane cofactor is made up of two molecules of porphobilinogen and is essential for the catalytic process. The treatment of purified recombinant *E. coli* deaminase with Ehrlich's reagent gives a reaction typical of a dipyrromethane [72]. It was concluded from radiochemical studies, that the dipyrromethane is resident at the active site and provides the attachment site for the covalent binding of the substrate. This linked dipyrromethane was therefore termed the dipyrromethane cofactor [73].

After the discovery of the cofactor, the nature of the linkage between the enzyme and cofactor was examined. One group of researchers treated the *E. coli* deaminase with the thiol reagent DTNB under denaturing conditions and found three reactive thiol groups. However, a study of the *E. coli* gene derived amino acid sequence showed that four thiol groups are present, suggesting that the fourth was binding the dipyrromethane cofactor [74]. Further evidence came from site-directed mutagenesis studies where each of the conserved cysteine residues were separately mutated to serine, [75] showing that the Cys242Ser mutant had a much-reduced activity. From the X-ray structure it is clear the dipyrromethane cofactor is linked to domain 3 of the enzyme via a thioether bond to Cys242. The two pyrrole rings are designate C1 and C2, with C1 being covalently attached to the enzyme. The acetate and propionate side chains of the cofactor form salt bridges and hydrogen bonds with the basic side chains of the protein, such as arginines 131, 132, 149, 155 and lysine 83 (*E. coli* numbering). The two pyrrole nitrogens of the

cofactor are hydrogen bonded to the carboxyl side chain of aspartate 84 (aspartate 99 in human). The C2 ring of the cofactor is stacked against Phe62 [71].

The cofactor conformation in the cleft varies according to its oxidation state. The position of ring C1 of the cofactor (directly attached to the enzyme) alters very little between the two states but, when oxidised, the second pyrrole ring, C2, seems to occupy a space thought to be used by the incoming PBG substrate during catalysis. In the reduced and functional form of the enzyme, the cofactor adopts a conformation where the C2 ring occupies a more internal position in the cleft [71].

Cofactor assembly is initiated by the binding of preuroporphyrinogen to the apoenzyme followed by reaction with Cys242 to form an ES_2 "nascent" holoenzyme. The ES_2 complex is able to complete the catalytic cycle by reacting with two more porphobilinogen molecules [76]. After release of the product preuroporphyrinogen, the dipyrromethane cofactor remains at the active site.

The dipyrromethane cofactor is not subjected to catalytic turnover and assumes the role of primer during catalysis. This has been shown by ^{14}C labelling experiments. In these experiments a *hemA*$^-$ *E.coli* strain was grown in medium containing 5-amino 5-[^{14}C] laevulinic acid. The enzyme, containing the labelled cofactor, was then isolated and incubated with unlabelled PBG. As the final product of this reaction had no labelled compounds this indicated the dipyrromethane cofactor was not subjected to catalytic turnover but remains permanently linked to the enzyme [77].

1.7.3 Catalytic mechanism of PBGD

Catalysis begins with the binding of one PBG molecule that is deaminated to form at azafulvene. The azafulvene is then subjected to nucleophilic attack by the α-position of the C2 ring of the cofactor (or the free α position of an ES complex) resulting in the formation of a new carbon-carbon bond. The reaction is completed by deprotonation probably promoted by either Asp99 or the propionic side chain of PBG itself (figure1.15). The remaining three PBG molecules are added sequentially in the same way resulting in the hexapyrrole intermediate ES_4 [4] (figure 1.16).

Single turnover reactions were undertaken using two approaches: a radiochemical approach and a ^{13}C-NMR approach. The radiochemical approach produced labelled ^{14}C-preuroporphyrinogen using ^{14}C-porphobilinogen. The labelled product was converted to protoporphyrin IX that could be degraded into two compounds: ethylmethylmalemide (from rings A and B) and haematinic acid (from rings C and D). The radiolabel was found associated mainly with the ethylmethlymalemide, suggesting that the mechanism proceeded by the addition of the rings in the order a, b, c and d (Figure 1.6) [78]. These findings were confirmed by the ^{13}C-NMR approach [75].

The release of preuroporphyrinogen occurs by the reverse of synthesis in which the carbon at the α-position of the cofactor ring C2 is protonated and then the carbon-carbon bond between the C2 ring and ring a of the tetrapyrrolic intermediate (a tetrapyrrolic methylene pyrrolenine) is cleaved. The reaction of the methylene pyrrolenine with water yields preuroporphyrinogen and leaves the dipyrromethane cofactor attached to the enzyme ready for another catalytic cycle.

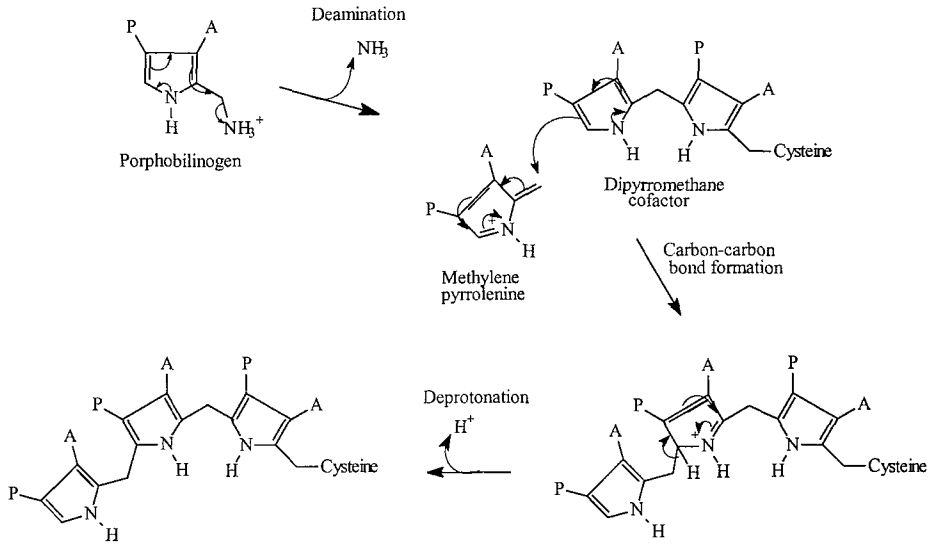

Figure 1.15 The chemistry of a porphobilinogen ring-coupling reaction.
Carbon-carbon bond formation proceeds through (1) deamination of the substrate PBG to produce the methylene pyrrolinene (azafulvene); (2) nucleophilic attack by the methylene carbon atom at the free α-position of the terminal enzyme bound ring; and (3) deprotonation at this same carbon atom. The acetate and propionate side-groups of PBG are denoted by A and P, respectively (adapted from Louie *et al* 1996 [71]).

1.7.4 Intermediate complexes of porphobilinogen deaminase

The porphobilinogen deaminase-catalysed reaction proceeds through enzyme intermediate complexes (ES, ES_2, ES_3, ES_4). These enzyme intermediate complexes were first demonstrated by incubating the human erythroid enzyme deaminase with [^{3}H]-PBG when four labelled species representing ES, ES_2, ES_3, ES_4 were produced. These complexes were more negatively charged than the original enzyme and could be separated using ion exchange chromatography or electrophoresis [61].

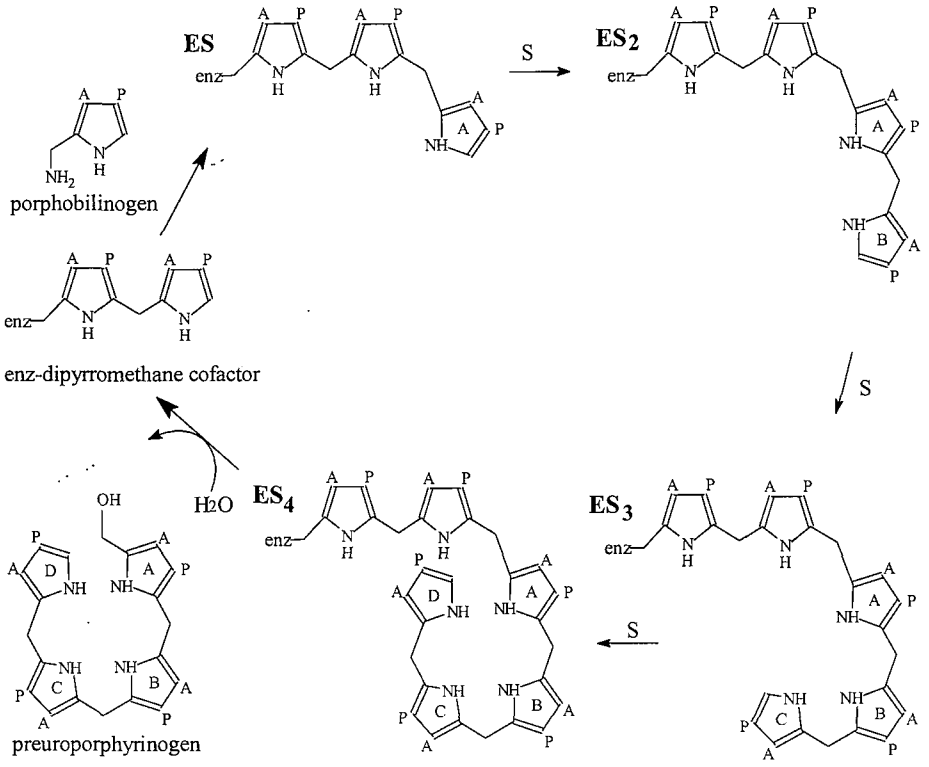

Figure 1.16 The sequential assembly of four PBG molecules by porphobilinogen deaminase to form the unstable product preuroporphyrinogen.
The pyrrole rings are labelled A, B, C and D in order of assembly. The acetate and propionate side chains are represented as A and P, respectively. The dipyrromethane cofactor (dpm) serves as a primer, to which the first substrate molecule binds. The intermediate steps, each with a different number of PBG units are termed ES, ES_2, ES_3 and ES_4, can be visualised by native PAGE. The final hexapyrrole intermediate ES_4 is subsequently cleaved with water to yield preuroporphyrinogen and the dpm remains bound to the enzyme for further rounds of catalysis.

1.7.5 Porphobilinogen deaminase genes and mutations

The porphobilinogen deaminase gene (*hemC*) was first identified and sequenced in *E.coli* [79]. The comparison of nucleotide sequences of PBGD genes from a number of species has revealed many invariant amino acids within the protein.

The gene encoding human PBGD is located on the long arm of chromosome 11. The coding sequence of 15 exons extends over 10kb of DNA. Two isoforms, arising from different promoters, are transcribed [65] [80]. The mRNA of the ubiquitous (housekeeping) isoform contains exons 1 and 3 to 15 coding for an enzyme of 361 amino acids, whereas the erythroid isoform is encoded by exons 2 to 15 and consists of 344 amino acids (figure 5.1, chapter 5). The translation initiation codon for the housekeeping isoform is located in exon 1 and for the erythroid-specific isoform in exon 3. The erythroid isoform, thus, lacks the first 17 amino acids of the amino terminus. As its name suggests the erythroid enzyme is only expressed in erythroid tissues whilst the ubiquitous form is expressed in all tissues.

Conserved arginines within the active site have been well studied and are known to be important in interactions with the cofactor and for substrate binding. Site-directed mutagenesis of these conserved residues has helped reveal the importance of certain amino acids in the catalytic mechanism[81]. Mutations of arginine 131 and 132 in *E.coli* PBGD result in mutant enzymes, which lack the dipyrromethane cofactor and are inactive. Mutation of arginines 149 and 176 in *E.coli* PBGD leads to mutant enzymes, which have reduced enzyme activity and show the accumulation of intermediates. Mutations of arginines 11 and 155 produce mutant enzymes that can assemble the cofactor, but cannot bind the substrate [81].

In addition to these invariant arginines Cys261 (Cys242 in *E.coli*), Lys98 (Lys83 in *E.coli*) and Asp99 (Asp84 in *E.*coli) are also invariant. An Asp84Glu mutant *E.coli* deaminase possesses less than one percent of the wild-type activity with a cofactor that is more sensitive to oxidation [69]. The reasons for this are evident from the X-ray structure, which shows the loss of a hydrogen bond, normally found between aspartate 84 and the NH group of the C2 pyrrole ring [68].

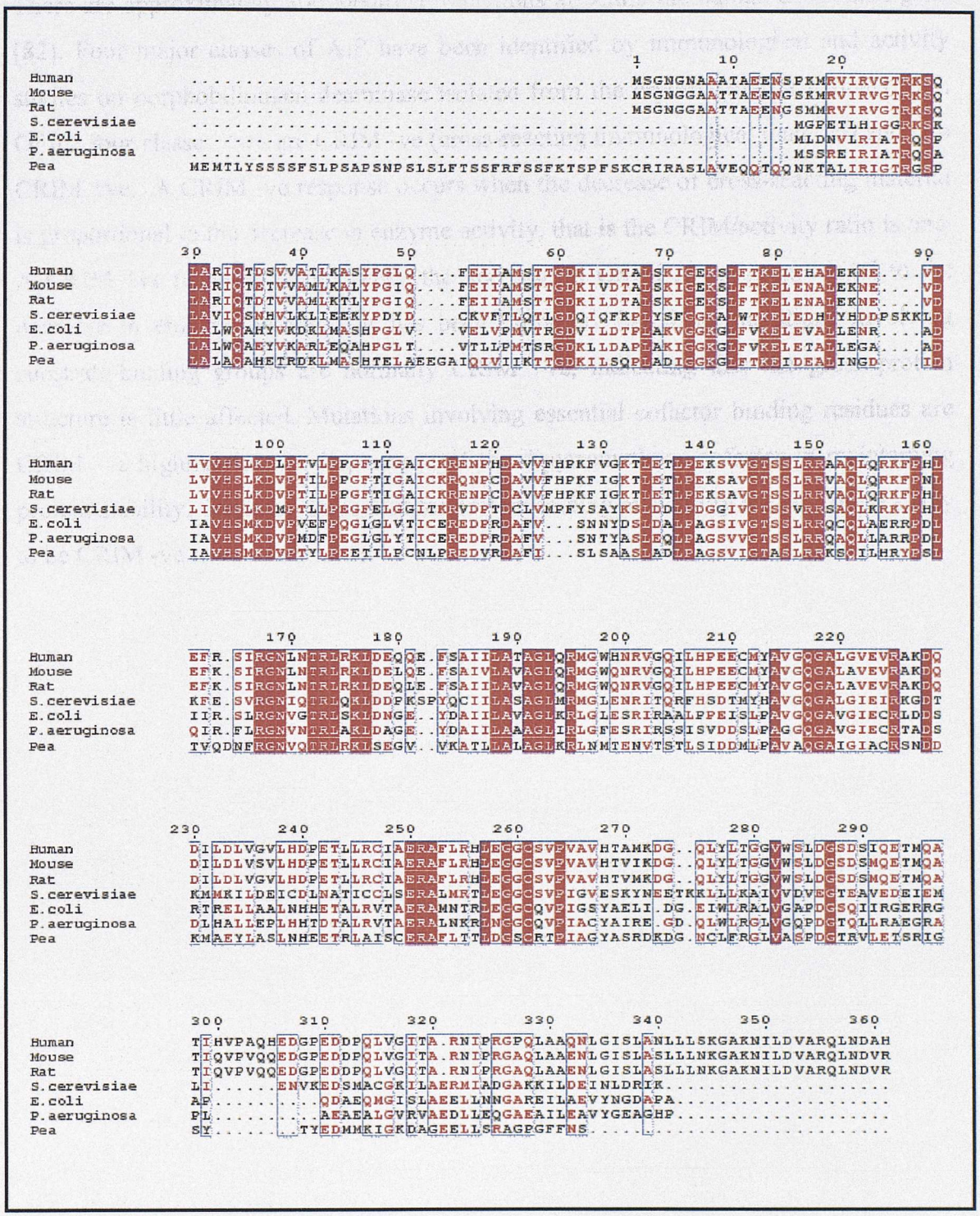

Figure 1.17 Human PBGD primary sequence alignment with PBGDs from six other species.

The alignment was performed using Multalign [33]. Residues that are totally conserved in these PBGDs are shown with white text with a red background and outlined in blue. Residues that are partially conserved are shown with red text and outlined in blue. Residues that are not conserved are shown in black text. Note the conserved cysteine at position 261, which is covalently bound to the cofactor and the active site aspartate-99.

There are approximately 300 identified mutations affecting the human deaminase gene [82]. Four major classes of AIP have been identified by immunological and activity studies on porphobilinogen deaminase isolated from the erythrocytes of patients [83]. Of the four classes, two are CRIM -ve (cross-reacting immunological material) and two CRIM +ve. A CRIM -ve response occurs when the decrease of cross-reacting material is proportional to the decrease in enzyme activity, that is the CRIM/activity ratio is one. A CRIM +ve response occurs when the decrease of CRIM is not proportional to the decrease in enzyme activity. It has been proposed that those mutations involving substrate-binding groups are normally CRIM +ve, indicating that the gross protein structure is little affected. Mutations involving essential cofactor binding residues are CRIM -ve highlighting the importance of the dipyrromethane cofactor in maintaining protein stability. Residues important for protein folding or stability are also more likely to be CRIM -ve.

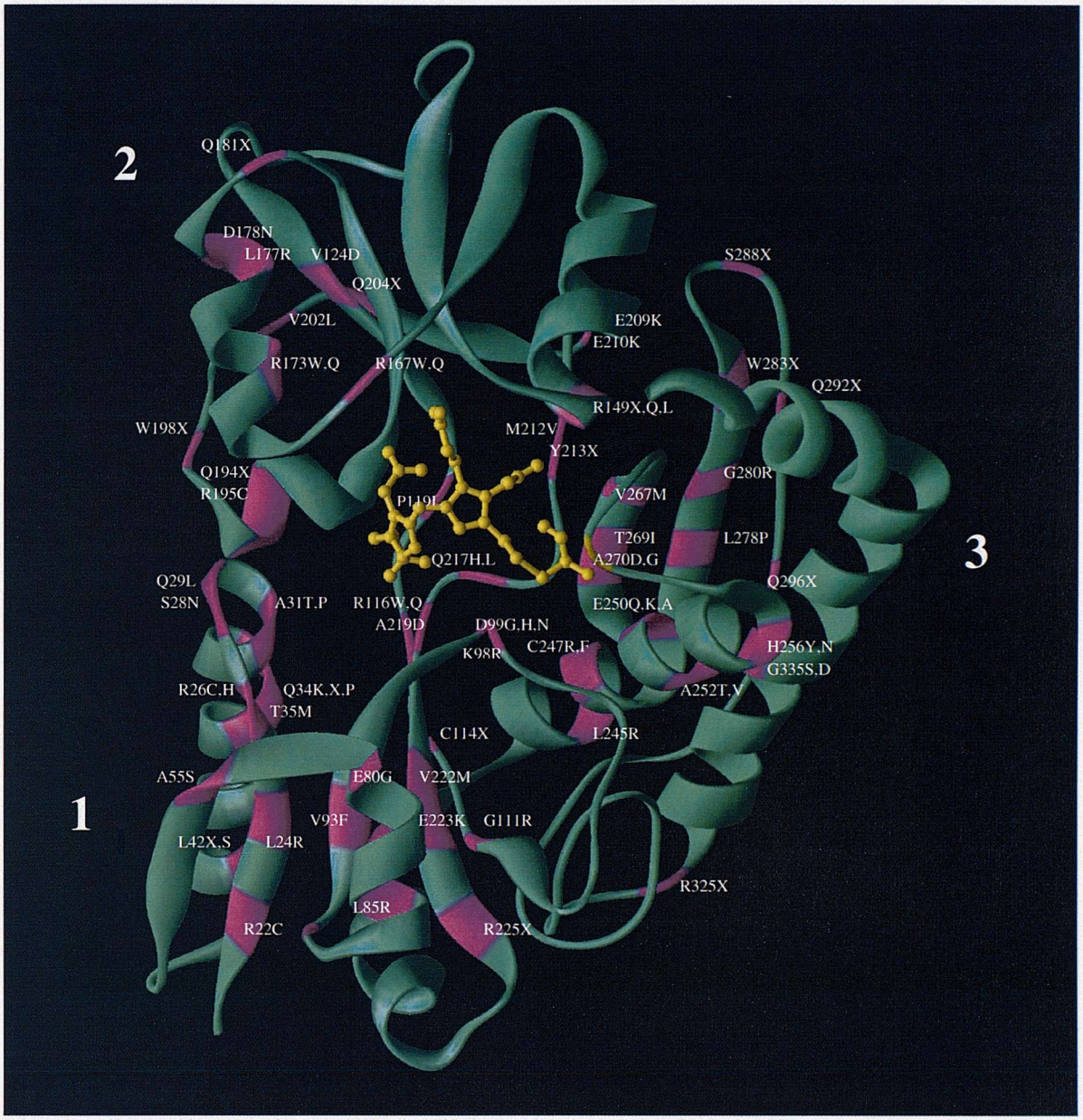

Figure 1.18 Three-dimensional structure of human ubiquitous porphobilinogen deaminase showing the positions of a number of mutations reported to cause acute intermittent porphyria.

The three domains are labelled, the dipyrromethane cofactor is highlighted in yellow and the positions of the mutations are highlighted in purple. This figure was prepared using the structure of the human ubiquitous Arg167Gln mutant [84], using the computer program WebLab Viewer Lite [30].

1.8 Uroporphyrinogen III synthase.

Uroporphyrinogen III synthase (formerly cosynthase) catalyses the rearrangement of the terminal, D, ring of preuroporphyrinogen and the closure of the macrocycle to form uroporphyrinogen III. If the enzyme is absent, or if only a small amount is present, the preuroporphyrinogen formed by PBGD will cyclize non-enzymatically to uroporphyrinogen I (figure 1.13).

In a disease state where there is a deficiency of uroporphyrinogen III synthase, the levels of uroporphyrinogen I will build up. This rare recessive disease is known as congenital erythropoietic porphyria (CEP). In this disease the uroporphyrinogen I accumulates in the erythrocytes and the spleen. When oxidized, the uroporphyrinogen I is converted to uroporphyrin I, which causes acute photosensitivity, leading to skin blistering [85].

Uroporphyrinogen III synthases are more difficult to purify than other enzymes of the pathway and the enzyme has only been purified from a limited number of sources, including *B. subtilis* [86] and human erythrocytes [87]. All uroporphyrinogen III synthases are monomeric enzymes with Mr values ranging from 26,000 to 31,000.

The first uroporphyrinogen III synthase gene (*hemD)* was characterized from *E. coli* [88]. Comparison of primary sequences of uroporphyrinogen III synthase from different species only displayed five invariant residues, with little evidence for a conserved substrate-binding site.

The mechanism of the uroporphyrinogen synthase is not well understood, mainly because both the enzyme and the substrate are unstable, making investigations difficult. Recently the X-ray structure (figure 1.19) has been published [89], however this has done little to help mechanistic predictions.

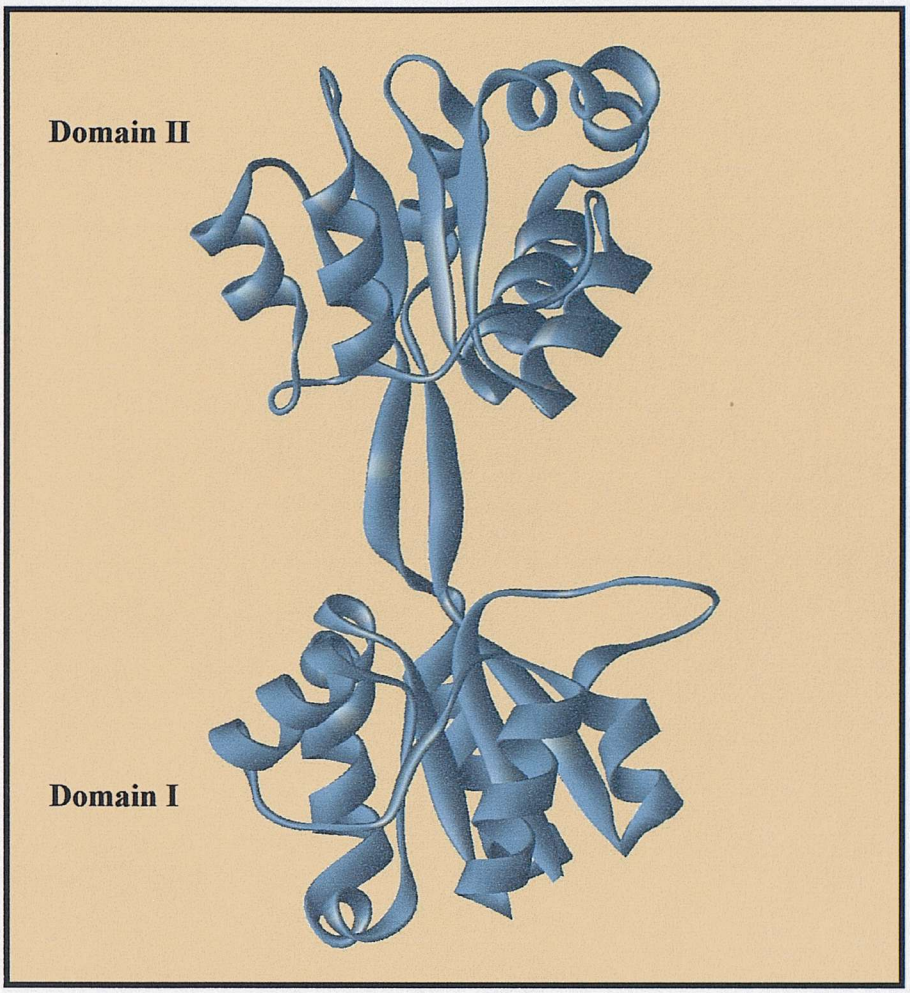

Figure 1.19 Schematic model of human uroporphyrinogen III synthase.
The protein folds into two domains, which are connected by a two strand anti-parallel beta-ladder. The active site is proposed to lie in the cleft between the two domains [89]. This figure was prepared using the computer program WebLab Viewer Lite [30] and the pdb file (1JR2) from the protein database [31].

1.9 Haem biosynthesis from uroporphyrinogen III

The tetrapyrrole pathway branches after the formation of uroporphyrinogen III. The branch of the pathway forming haem subjects the tetrapyrrole to a number of alterations involving decarboxylation and oxidation. The acetate side chains of uroporphyrinogen III are first decarboxylated to methyl groups, catalysed by uroporphyrinogen III decarboxylase, forming coproporphyrinogen III. The coproporphyrinogen III is then oxidatively decarboxylated, converting the propionate side chains of rings A and B to vinyl groups, to form protoporphyrinogen IX. The ring system of protoporphyrinogen IX is next aromatised to form protoporphyrin IX, by the removal of six hydrogen atoms catalysed by protoporphyrinogen oxidase. Finally iron is inserted into protoporphyrin IX by ferrochelatase, forming haem. These last steps in the haem biosynthesis pathway will not be discussed further in this thesis, but reviews are available [90].

1.10 The porphyrias

A strong incentive for research into haem biosynthesis has been the medical significance of this pathway. Genetic or chemically induced defects in the enzymes after the first enzyme in the pathway, 5-aminolevulinate synthase (ALAS), in mammals results in a disease state known as porphyria. There are biochemically and clinically distinct porphyrias for each enzymatic step. A defect in the first step results in X-linked sideroblastic anaemia rather than a porphyria. A complete deficiency of any of the enzymes in the pathway would be fatal, however, lowered levels of certain enzymes can cause intermediates of the pathway such as ALA and PBG to accumulate to dangerous levels causing distinct symptoms. King George III of England who has widely been portrayed as mad, may have suffered from porphyria [91, 92]

The porphyrias have been grouped into those causing acute neurological episodes and those that are non-acute and lead to cutaneous manifestations (Table 1.1). Acute symptoms include abdominal pain and neurological abnormalities whereas the non-acute porphyria symptoms include photosensitivity and porphyrin excretion with the exclusion of the acute symptoms [93].

Porphyria	Affected enzyme	Clinical symptoms
Acute porphyrias		
Acute intermittent porphyria (AIP)	PBG deaminase	No cutaneous involvement. Highly variable degree of clinical expression.
Variegate porphyria (VP)	Protoporphyrinogen oxidase	Cutaneous involvement and acute attacks
Hereditary Coproporphyria (HCP)	Coproporphyrinogen oxidase	Photocutaneous lesions occur but rarely in the absence of acute attacks.
Doss porphyria	ALA dehydratase	No cutaneous involvement, acute symptoms only. Similar presentation to lead poisoning.
Non-acute porphyrias		
Porphyria cutanea tarda (PCT)	Uroporphyrinogen decarboxylase	No acute attacks, only cutaneous involvement.
Erythropoietic protoporphyria (EPP)	Ferrochelatase	Only cutaneous involvement. Highly variable degree of clinical expression.
Congenital erythropoietic porphyria	Uroporphyrinogen III synthase	Severely photomutilation.

Table 1.1 The classification of porphyrias resulting from deficiencies in haem biosynthesis

Waldenström proposed that porphyrias could result from enzyme defects in the haem pathway and was the first to use the term 'acute intermittent porphyria' [94]. A screening test for porphobilinogen was introduced in 1941 by Watson [95], who also introduced haematin for treatment of acute porphyrias [96, 97]. In the 1960's Granick discovered that ALAS1, the first enzyme in haem biosynthesis, is induced by chemicals that cause acute porphyria [98]. This observation led to the proposal that overproduction of ALA may represent the primary genetic defect in all acute porphyrias [98], but this hypothesis proved false because it could not account for the distinct patterns of pathway intermediates and porphyrin excretion. In fact there are seven different types of porphyria, one for each enzyme in the pathway after ALAS.

Doss porphyria is a very rare acute porphyria caused by a deficiency of ALAD and is inherited in an autosomal recessive fashion [99] [100]. Other conditions such as lead poisoning and tyrosinaemia I may present symptoms similar to that of ALAD deficiency [101]. The symptoms of Doss porphyria are similar to those of acute intermittent porphyria, characterised by neuropathy, abdominal pain and vomiting. Due to the deficiency of ALAD, high levels of ALA can accumulate. Elevated plasma and urinary concentrations of ALA are diagnostic indicators of the disease. Levels become particularly high immediately proceeding and during an attack. It has been suggested that neurological symptoms maybe due to the structural similarities between ALA and the neurotransmitter GABA [102]. It has also been suggested that haem deficiency may be important in causing neurological symptoms [103].

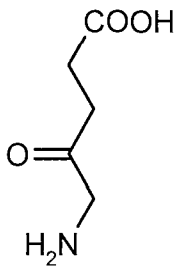

5-aminolaevulinic acid

4-aminobutyric acid

Figure 1.20 Chemical structures of 5-aminolaevlinic acid (ALA) and 4-amino butyric acid (GABA).

Acute intermittent porphyria (AIP) is caused by a deficiency of PBGD [104] [82] and is inherited as an autosomal dominant trait [105]. It is the most common hepatic porphyria and is notably more common in Sweden [106]. The characterization of the human porphobilinogen deaminase gene [48, 65, 107, 108], initiated investigations into the molecular genetic background of AIP, and today almost 300 mutations responsible for AIP have been identified (figure 1.18).

Symptoms include abdominal pain, vomiting and neuropathy and, during severe attacks, paralysis and respiratory failure can occur. Some agents are known to trigger attacks of AIP; fasting is known to precipitate attacks of AIP, as is the use of drugs such as barbiturates and sulphonamides [14].

Determination of the mutations causing the disease may help if it can identify pre-symptomatic heterozygotes. Counselling would help these individuals as they can be instructed to avoid certain drugs.

CEP is also known as Günther's disease and is caused by a deficiency of uroporphyrinogen III synthase. This is very rare disorder inherited as autosomal recessive fashion. Symptoms include severe photosensitivity and the disease can lead to severe disfigurement [109]. Despite its rarity it is one of the more famous porphyrias in the popular press, due to suggestions that individuals suffering from this disorder were the basis of the werewolf legend and there has been recent popularity in advertising porphyria as the basis for the vampire legend, due to photosensitivity of the sufferers of this disease. However, as porphyric patients do not crave blood, and quite plainly cannot turn into wolves, this myth is both inaccurate and hurtful to individuals suffering from the disease.

Hereditary coproporphyria is inherited in an autosomal dominant fashion and is caused by a deficiency in coproporphyrinogen oxidase [110]. Variegate porphyria is inherited in an autosomal dominant fashion and is caused by the deficiency of protoporphyrinogen oxidase [111]. Both of these porphyrias can cause acute attacks as well as photosensitivity.

Erythropoietic protoporphyria is caused by a deficiency of ferrochelatase. Protoporphyrin accumulates and is excreted in the faeces. Symptoms of the disease include photosensitivity [112] and a minority of patients suffer from acute liver disease and liver failure.

Management of acute porphyrias is usually to treat the symptoms of the disease and make the patient more comfortable as there are currently no absolute cures. In the management of AIP, for example, specific drugs are used to treat the symptoms; pain is relieved by pethidine and morphine, psychological disturbances can be treated with promazine. A high carbohydrate diet is also prescribed as low calorific intake can precipitate an attack. The most effective treatment is to administer haem arginate, which results in a dramatic cessation of symptoms, lowering of ALA and PBG levels and a reduction in ALAS, which is elevated during an acute attack [113].

Future treatment of porphyrias may involve enzyme [114] or gene therapy [115]. The erythropoietic porphyrias appear to be good candidates for gene therapy as the gene could be transferred to haematopoietic stem cells. Experiments in gene transfer using a mouse model of the disease erythropoietic protoporphyria have caused the long-term correction of the symptoms of the disease [116].

Chapter 2. Materials and methods.

2.1 Materials

Tryptone and yeast extract were from Difco Laboratories, Detroit, USA. Agar was from Lab M, Bury, UK. Iodine and 4-dimethylaminobenzaldehyde were from BDH, Poole, UK. IPTG was from Melford Laboratories Ltd., Suffolk, UK. All other chemicals were obtained from Sigma Chemical Company.

Electrophoresis equipment and Bio-Rad reagent were purchased from Bio-Rad laboratories limited. All columns for chromatography were purchased from Amersham-Pharmacia Biotech. Ltd., St Albans, UK. Membrane filters (0.2μm) were from Whatman International, Kent, UK. Ultra-filtration cells were from Amicon, Ltd., Stonehouse, UK.

2.1.1 Media and solutions for bacterial growth

Luria Broth (LB) media

Bactotryptone (10g), Bactoyeast extract (5g) and sodium chloride (5g) were made up to a volume of 1L and autoclaved, immediately. Ampicillin, if required, was added at a final concentration of 100μg/ml once the medium was sufficiently cooled.

Luria Broth plates

Bactoagar (15g) was added to 1 L of the above media before autoclaving. Ampicillin, if required, was added at a final concentration of 100μg/ml once the media were sufficiently cooled. After pouring the plates were stored inverted at 4°C.

Ampicillin stock solution

Ampicillin sodium salt was dissolved in AnalaR water to a concentration of 100mg/ml, and filtered through a 0.2μm filter. This solution was stored at -20°C, until needed, when it was thawed at room temperature and used at a final concentration of 100μg/ml.

2.1.2 Bacterial strains and plasmids used in this study

Strain	Genotype	Reference
BL21 (DE3)	F- *ompT gal* [*dcm*] [*lon*] *hsd*S_B (r_B-m_B-; an *E.coli* B strain) with DE3, a prophage carrying the T7 RNA polymerase gene.	[117]

Table 2.1 Bacterial strains used in this study

Plasmid	Properties
pT7-7	T7 promotor system [118, 119]
pUHD1	pT7-7 carrying *hemC* (1.14Kb fragment of a human deaminase gene)
pUHD2	pUHD1 with arginine 167 mutated to glutamine
pUHD5	pUHD1 with arginine 167 mutated to tryptophan
pUHD7	pUHD1 with lysine 210 mutated to glutamate
pUHD8	pUHD1 with aspartate 99 mutated to glutamate
pUHD9	pUHD1 with aspartate 99 mutated to glycine
pEHD1	pT7-7 carrying *hemC* (fragment of human deaminase gene)
pHALAD1	pT7-7 carrying *hemB* (fragment of human deaminase gene)
pHALAD2	pHALAD1 with phenylalanine 12 mutated to leucine

Table 2.2 Vectors and recombinant plasmids used in this study.

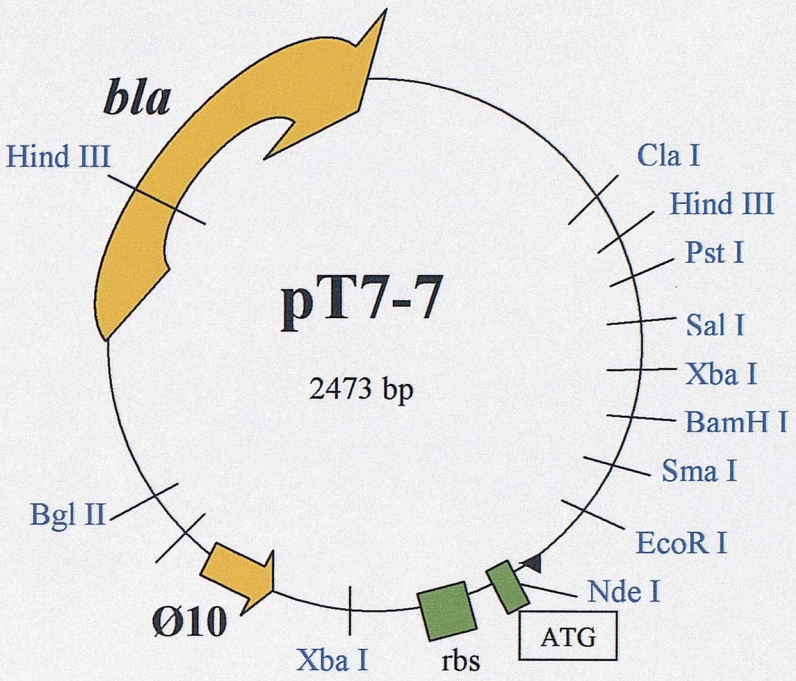

Figure 2.1. Map of the plasmid pT7-7, which contains the T7 RNA polymerase promoter Ø10.
The human PBGD cDNA was ligated between the sites *Nde*I/*Bam*HI in the 5' to 3' orientation. The inserted cDNA is in frame with the ATG start codon of the vector DNA and the optimal distance from the ribosome binding site (rbs), both being critical for efficient transformation of the transcribed mRNA. The *bla* gene confers ampicillin resistance, allowing selection of recombinant plasmids.

2.1.3 Buffers and solutions

Polyacrylamide gel electrophoresis

Acrylamide stock:

29g acrylamide

1g *N*, *N*-methylenebisacrylamide

Water was added to a final volume of 100ml and the solution was stirred gently for 30 minutes. The solution was then filtered through a Whatman 0.2μm nylon membrane filter.

10 x SDS-PAGE running buffer

For 1 litre: -

144g Glycine

30.3g Tris-HCl

10g Sodium dodecylsulphate

The components were dissolved in distilled water and stored at room temperature. For use, 100ml was mixed with 900mL of distilled water.

Non-denaturing PAGE running buffer was made as described above with the omission of SDS.

5 x Loading buffer (disruption buffer)

For 200ml: -

6.1g Trizma base

0.2g SDS

0.1g Bromophenol blue

100ml 50% Glycerol

Before use, 982.5μl was mixed with 17.5μl of 2-mercaptoethanol.

For non-denaturing PAGE the SDS and 2-mercaptoethanol were omitted.

Destain and stain solutions for SDS-PAGE and non-denaturing PAGE

100ml Glacial acetic acid

500ml Methanol

400ml Distilled H_2O

(1.5g of Coomassie brilliant blue was added to make stain solution.)

Modified Ehrlich's reagent

1g 4-Dimethylaminobenzaldehyde

42ml Glacial acetic acid

8ml Perchloric acid (70%)

The mixture was stored in the absence of light in a foil-covered bottle, at 4°C, and was used within one week.

Stop solution

10% Trichloroacetic acid

0.1M Mercuric chloride

The mixture was stored in the absence of light in a foil-covered bottle, at 4°C.

2.2 Methods.

2.2.1 Preparation of competent cells for transformation with recombinant plasmids.

LB media (10ml) was inoculated with a colony of BL21 (DE3) *E.coli* and incubated at overnight at 37°C. An aliquot (200µl) of the overnight culture was added to 20ml of LB media and was incubated at 37°C until the $OD_{600nm} \cong 0.3$. The cells were then harvested by centrifugation at 5,000rpm for 10 minutes and the supernatant was discarded. The cells were resuspended in 10ml of 50mM cold $CaCl_2$ and left on ice for 1hour followed by centrifugation for 10 mins at 5,000rpm. The pellet was resuspended with 1-2ml of cold 50mM $CaCl_2$ before transformation.

2.2.2 Transformation of competent cells

An aliquot (200µl) of competent cells was added to 1µl of the required plasmid DNA in a sterile Eppendorf tube and left on ice for 25 minutes. The mixture was then heat shocked for 2 minutes at 42°C followed by incubation on ice for 5 minutes. LB media (600µl) was added to the cell and DNA mixture and incubated at 37°C for 1hr, without shaking.

A 100 µl aliquot of transformed cells was spread on a LB agar plate containing ampicillin (100µg/ml) and incubated at 37°C.

2.2.3 Expression studies

For recombinant plasmids containing the T7-promoter, a single colony was inoculated in 10ml of LB media supplemented with ampicillin (100µg/ml) and grown to an $O.D_{600nm}$ of 1.0. Next, IPTG was added to a final concentration of 1mM and the cultures were grown for a further 3 hours at 37°C. Cells were harvested by

centrifugation for 25 minutes at 4,650 x g (5000rpm), using a Beckman centrifuge (JA-21) fitted with a JLA-10.500 rotor, at 4°C. The pellets were used immediately, or were frozen at -20°. The bacterial cell pellet was resuspended in 0.5mL of 20mM Tris-HCl buffer, pH8.2, containing 1mM DTT in an Eppendorf. The extract was sonicated at an amplitude of 10 microns in five bursts (30 seconds on / 60 seconds off). The crude sonicates were centrifuged at 4°C for 10 minutes, before transferring the supernatant to a separate tube. The pellets were centrifuged again and any remaining supernatant was removed by aspiration. The supernatant was then assayed for protein and PBGD activity and analysed by SDS-PAGE.

2.3.4 Purification of human recombinant ubiquitous and erythroid PBGD.

Growth of *E.coli* overexpressing the erythroid PBGD cDNA.

Individual colonies of ampicillin-resistant *E.coli* expressing the erythroid isoform of PBGD were grown in 10ml of LB media containing ampicillin (100μg/ml) at 37°C overnight. The overnight cultures were each used to inoculate 800mL of LB media containing ampicillin (100μg/ml) in 2L baffled flasks. The flasks were incubated at 37°C, with shaking at 120rpm, until the OD_{600nm} was approximately 1. IPTG was then added to a final concentration of 1mM and the cultures were incubated for a further 3 hours. Cells were harvested by centrifugation for 25 minutes at 4,650 x g (5000rpm), using a Beckman centrifuge (JA-21) fitted with a JLA-10.500 rotor, at 4°C. The pellets were used immediately, or were frozen at -20°C.

Sonication

The bacterial pellet from 1.6L of media was resuspended in approximately 40ml of 20mM Tris-HCl buffer, pH 8.2, containing 5mM DTT and 200μM PMSF (sonication buffer). The resuspended cells were then sonicated on ice for a total of twenty cycles, each cycle consisted of 30 seconds sonication with a 90 second cooling period.

Heat treatment

The sonicated cells were placed in a round-bottomed flask filled with nitrogen gas and rapidly heated to 60°C in a water-bath with constant swirling. The temperature was

maintained for 10 minutes, after which time the solution was rapidly cooled by placing the flask in an ice-water slurry. The heat-treated sample was then ultracentrifuged, using Beckman ultracentrifuge (L7-65), fitted with a TFT-45.94 rotor at 193,750 x g (40,000rpm) for 1 hour, at 4°C. The pellet was discarded and the supernatant was retained.

Ion exchange chromatography

The supernatant was loaded onto a DEAE Sephacel ion exchange column, which had previously been equilibrated in 20mM Tris-HCl buffer, pH 8.2, containing 5mM DTT and 100μM PMSF. After loading the sample, the column was washed using the same Tris-HCl buffer as above.

Contaminating protein was eluted from the column by applying a linear KCl gradient (0-70mM KCl; 500mL total volume) in 20mM Tris-HCl buffer, pH 8.2, containing 5mM DTT and 100μM PMSF. After the gradient, an isocratic procedure was performed using 70mM KCl to elute the enzyme. Fractions were collected and assayed for activity (section 2.2.8) and analysed by SDS-PAGE. The active fractions were pooled according to appearance on the SDS-PAGE and concentrated using an Amicon Diaflo Ultra Filter fitted with a PM10 membrane.

Gel filtration using a Superdex G75 (preparation grade) column.

The concentrated sample from the DEAE Sephacel ion exchange column was loaded onto a Hiload^{TM} 16/60 G75 Superdex preparation grade gel filtration column which had been pre-equilibrated with 100mM Tris-HCl buffer, pH 7.5, containing 5mM DTT and 100μM PMSF. The protein was eluted with the same buffer and fractions were collected at a flow rate of 0.5ml/min. Active fractions were pooled and concentrated using an Amicon ultra-filtration cell fitted with a PM10 membrane.

2.2.5 Purification of human recombinant ALAD

The purification for this enzyme is described in Chapter 3, section 3.2.1

2.2.6 Determination of protein concentration

Protein concentration was determined using the Bio-Rad protein assay. A 1ml assay consisted of 10µl of protein solution, 790µl of distilled water and 200µl of Bio-Rad reagent. Bio-Rad reagent is based on the Bradford assay [120]. The protein binds to the dye Coomassie brilliant blue G-250 in a concentration dependant manner. This assay was routinely used for protein samples between 200 and 1,400 µg/ml. The colour was allowed to develop for 5 minutes at room temperature and the absorbance was measured at 595nm. The concentration was calculated using the conversion Abs 0.1=1.95µg of protein.

2.2.7 Assay for ALAD activity.

An aliquot (10µl) of enzyme solution was added to 50mM potassium phosphate buffer, pH 6.8, containing 10mM DTT and 100µM $ZnCl_2$ and pre-warmed for 15 minutes at 37°C. ALA was added to a final assay concentration of 5mM, before mixing followed by incubation at 37°C for 10 minutes. Total assay volume was typically 250µl. The reaction was terminated with an equal volume of stop solution (10%TCA with 0.1M mercury chloride). Ehrlich's reagent was added in a volume equal to the total volume of the assay with the stop solution. Samples were centrifuged in a bench centrifuge and absorbance of the supernatant was measured at 555nm. Specific activity was calculated as µmoles PBG formed / mg of protein / hour, using the extinction co-efficient for the coloured complex formed by Ehrlich's reagent reacting with PBG at 555nm of 6.02×10^4 $M^{-1}cm^{-1}$ [121] (figure 2.2).

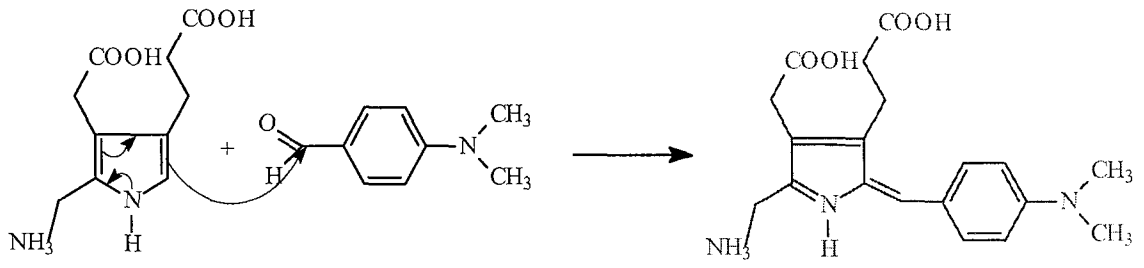

Figure 2.2. Reaction of Ehrlich's reagent with PBG.

2.2.8 Assay for PBGD activity.

Enzyme samples were added to 20mM Tris-HCl buffer, pH 8.2, to make a final volume of 400µl and were pre-warmed to 37°C for five minutes. Pre-warmed PBG was added to the samples at a final assay concentration of 200µM and the assay was incubated for 5 minutes. After incubation, the reaction was stopped by adding 125µl of 5M HCl, followed by the addition of 50µl benzoquinone (0.1% w/v in methanol). Samples were covered in foil and kept on ice for 20 minutes to allow the oxidation of uroporphyrinogen I to uroporphyrin I. Tubes were centrifuged using a bench centrifuge for 2 minutes and 100µl of supernatant was removed and diluted with 900µl of IM HCl. The absorbance of this solution at 405.5nm was measured (figure 2.3). Specific activity was calculated as µmoles uroporphyrin formed / mg of protein / hour, using the extinction co-efficient for uroporphyrins at 405.5nm of 5.48×10^5 $M^{-1}cm^{-1}$ [62].

2.2.9 Identification of the dipyrromethane cofactor

An aliquot (500µl) of a 1mg/ml enzyme solution (12.5nmoles) was mixed with an equal volume of modified Ehrlich's reagent at room temperature the resulting protein precipitant was remove by centrifugation. The absorption of the supernatant was measured by scanning between 380 and 600 nm after 1 and 15 minutes. Observation of a peak with λ_{max} of 565 nm and subsequent shift to a λ_{max} of 495 nm confirmed the presence of the cofactor. The reaction was blanked using buffer and Ehrlich's reagent. Figure 2.4 shows the reaction between the enzyme containing the dipyrromethane cofactor and Ehrlich's reagent.

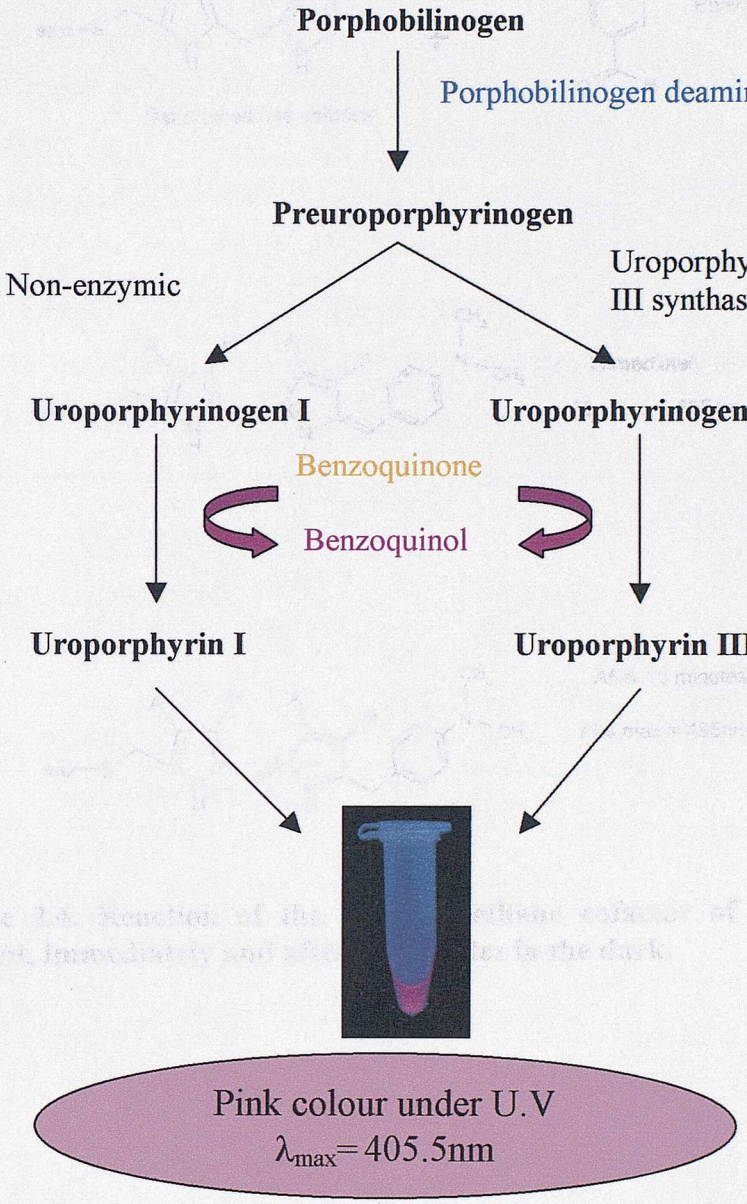

Figure 2.3. The oxidation of uroporphyrinogen I using benzoquinone, which is used to determine PBGD activity.

PBG, in the presence of PBGD, will be converted to preuroporphyrinogen. The preuroporphyrinogen is highly unstable, especially in acidic conditions and will rapidly cyclise to for uroporphyrinogen I. Benzoquinone is able to oxidise the uroporphyrinogens formed to uroporphyrin which has a λ_{max} at 405.5nm and produces a pink fluorescence under U.V light.

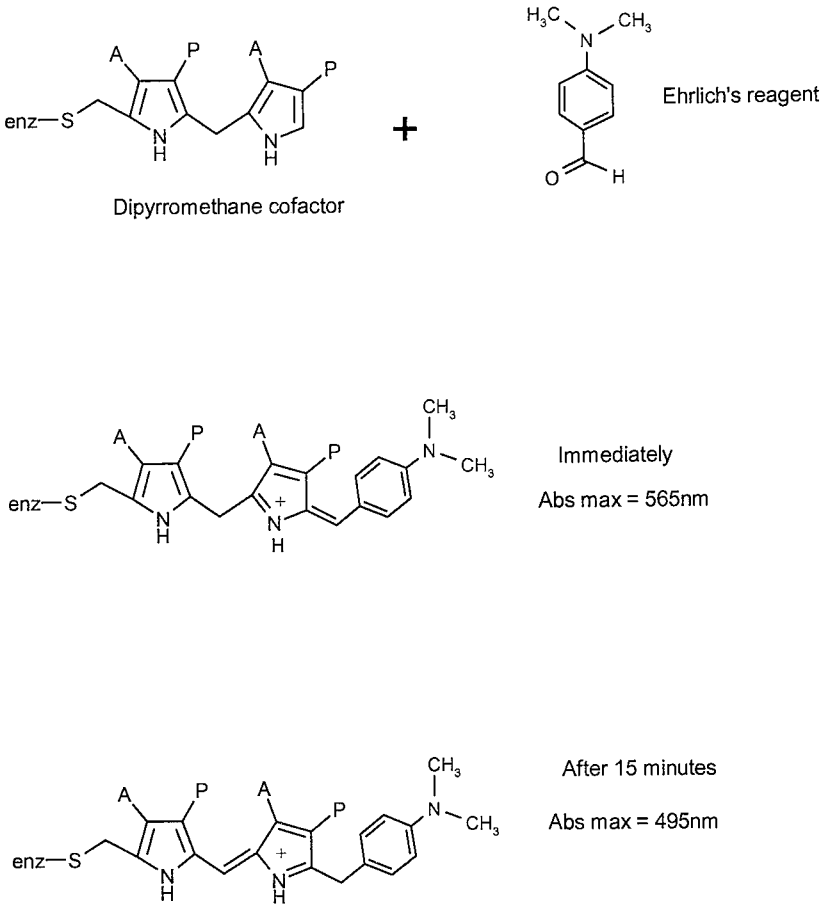

Figure 2.4. Reaction of the dipyrromethane cofactor of PBGD with Ehrlich's reagent, immediately and after 15 minutes in the dark.

2.2.10 Polyacrylamide gel electrophoresis (PAGE)

All denaturing polyacrylamide gel electrophoresis (PAGE) was carried out according to the Laemlli method [122]. The composition of the resolving and stacking gels are shown in Table 2.3. Where A) is for the resolving gel and B) is for the stacking gel. Protein samples were prepared by the addition of the appropriate amount of disruption buffer followed by boiling for 2 minutes. After the samples were loaded, electrophoresis was carried out at 150 volts until the bromophenol blue dye front had reached the bottom of the gel. Coomassie brilliant blue stain was used to visualise the protein samples, which were compared with various standard protein markers (Table 2.4).

A	12% SDS - PAGE	10% Non-denaturing PAGE
Acrylamide	3.2ml	3ml
1.5M Tris-HCl pH 8.8	2ml	2.8ml
dH_2O	2.8ml	3.0ml
10% SDS	80µl	—
10% APS	100µl	100µl
TEMED	20µl	40µl

B	12% SDS-PAGE	10% Non-denaturing PAGE
Acrylamide	1ml	1ml
0.5M Tris-HCl pH 6.8	1ml	2ml
dH_2O	3ml	2ml
10% SDS	80µl	—
10% APS	100µl	100µl
TEMED	20µl	40µl

Table 2.3 Compositions of polyacrylamide gels used for protein analysis.
A) Compositions of the resolving polyacrylamide gels used for protein analysis
B) Compositions of stacking polyacrylamide gels used for protein analysis.

Polyacrylamide gel electrophoresis under non-denaturing conditions was carried out as above using the same gel composition but in the absence of SDS and 2-mercaptoethanol. Enzyme activity on the gel was determined by incubating the gel in porphobilinogen solution (0.5mM in 0.1M Tris-HCl, pH 8.2) at 37°C for 20 minutes. This was visualised by placing the gel in iodine solution (0.01% in 0.1M HCl) for 5 minutes. The fluorescence due to the porphyrin product was seen by placing the gel on the uv-transilluminator.

Molecular weight markers used for SDS-PAGE

	Protein	Mw (Da)
1	Bovine serum albumin	66,000
2	Egg albumin	45,000
3	Glyceraldehyde-3-phosphate dehydrogenase	36,000
4	Carbonic anhydrase	29,000
5	Trypsinogen	24,000
6	Soybean trypsin inhibitor	20,100
7	α-Lactalbumin	14,200

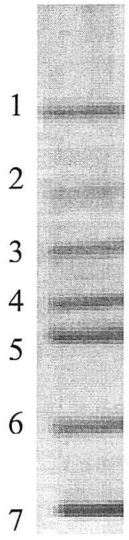

Table 2.4 Dalton VII marker protein Mr standards

Protein	Mw (KDa)
Myosin	208
Phosphorylase B	105
Glutamic dehydrogenase	53
Carbonic anhydrase	34
Myoglobin blue	23
Myoglobin red	17
Lyozyme	13
Aprotinin	7
Insulin	4

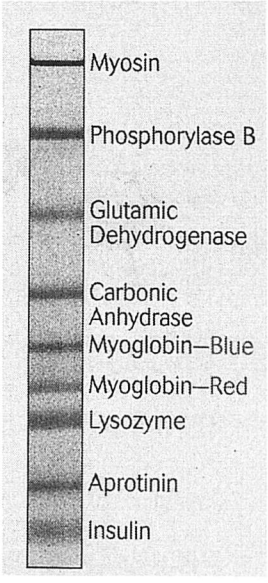

Table 2.5 Multimark molecular weight marker for SDS PAGE.

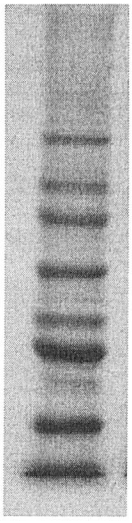

	Protein	Mw (Da)
1	Beta-galactosidase	116,250
2	Phosphorylase	97,400
3	Serum albumin	66,200
4	Ovalbumin	45,000
5	Carbonic anhydrase	31,000
6	Trypsin inhibitor	21,500
7	Lysozyme	14,000
8	Aprotinin	6,500

Table 2.6 Bio Rad markers for SDS PAGE

2.2.11 Formation and purification of enzyme-substrate intermediate complexes

The enzyme substrate intermediate complexes were generated by mixing stoichiometric amounts of PBGD (100nmoles) and substrate (100-400nmoles) rapidly, at 4°C. The individual complexes were isolated and purified using a high-resolution anion exchange Mono Q HR5/5 column attached to a Pharmacia f.p.l.c. system, which had been pre-equilibrated in 20mM Tris-HCl, pH 7.5. The enzyme and complexes were eluted using a linear gradient of sodium chloride (0-400mM, 60ml) at a flow rate of 1ml/minute. The enzyme complexes were stored at 4°C.

2.2.12 Formation of ALAD hybrids

Native and mutant human recombinant ALAD (1.5mg/ml) were unfolded separately, at room temperature in 100mM Tris-HCl, pH 7.0, containing 4.5M urea, 5mM DTT and 50μM $ZnCl_2$ for 60 minutes. The pattern of unfolding was monitored by non-denaturing PAGE. The unfolded hrALAD and the unfolded Phe12Leu mutant hrALAD were mixed in equal amounts and refolded by dialysis against 100mM Tris-HCl buffer, pH 7.0, containing 5mM DTT and 50μM $ZnCl_2$, overnight, in an attempt to generate hybrid octamers. Hybrid octamers were visualised by non-denaturing PAGE.

2.2.13 Electrospray mass spectrometry (ESMS) of proteins

Unless otherwise stated, samples of protein were prepared by diluting the enzyme to 0.1 mg/ml in 50:50:1 acetonitrile:water:formic acid. Samples were analysed on a Micromass VG Quattro II mass spectrometer. All data was processed using Mass Lynx and Maximum Entropy programs.

2.2.14 Protein crystallisation.

The hanging drop method [123] was used to crystallise purified protein (figure 2.5). This relies on the vapour diffusion technique where the droplet containing the protein, buffer, precipitating agent and additives, is equilibrated against a reservoir containing a solution of precipitating agent at a higher concentration. Water vapour slowly diffuses from the hanging drop to the more concentrated solution in the reservoir below, until equilibrium is reached. Consequently, the concentration of all the constituents in the protein drop will increase resulting in precipitation or protein crystallisation .

To set up the crystallisation screens, 1ml of crystallising solution was pipetted into each well of a 24 well Linbro tissue culture plate. BDH 22 x 22 mm glass coverslips, thickness no.1, were washed in methanol, dipped in silane solution, then washed in methanol again and dried in an oven. On a glass coverslip, 2μl of protein solution was mixed with 2μl of well solution before placing over the well, the edges of which had been previously coated with vacuum grease.

Details on crystallisation conditions are described in the relevant chapters, ALAD crystallisation is described in chapter 4 and PBGD crystallisation is described in chapter 5.

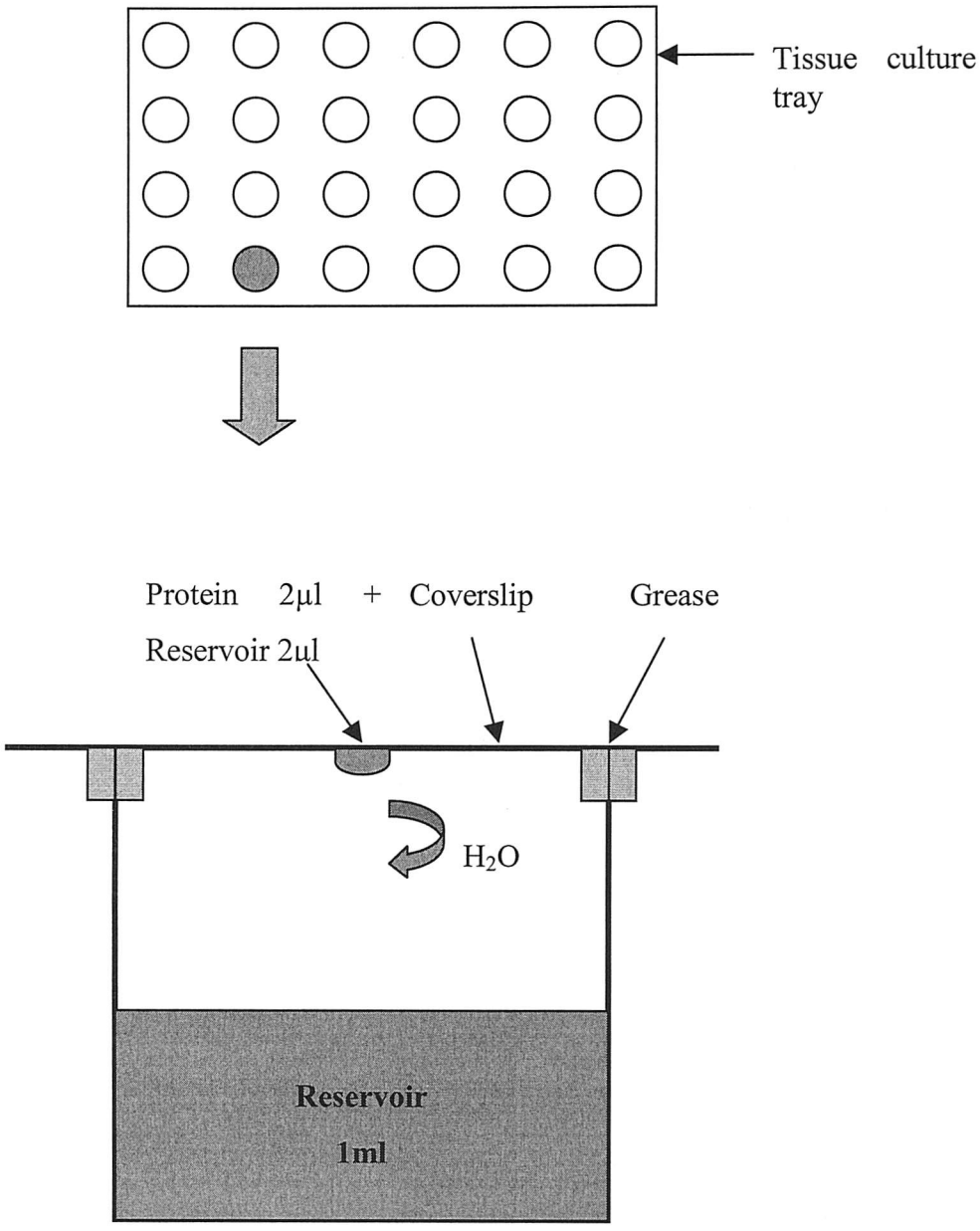

Figure 2.5. The hanging drop method used to crystallise purified protein.
The well contains precipitating agent at the desired final concentration. The coverslip is sealed onto the well of a multiwell plate with vacuum grease, with the droplet of protein hanging below. As time elapses, water vapor slowly diffuses from the hanging drop to the more concentrated solution below, until both solutions are at equal concentration of precipitating agent. A complete crystallisation trial explores several variables, including protein concentration, type of precipitant, precipitant concentration, pH, and concentrations of desired ligands, divalent cations etc.

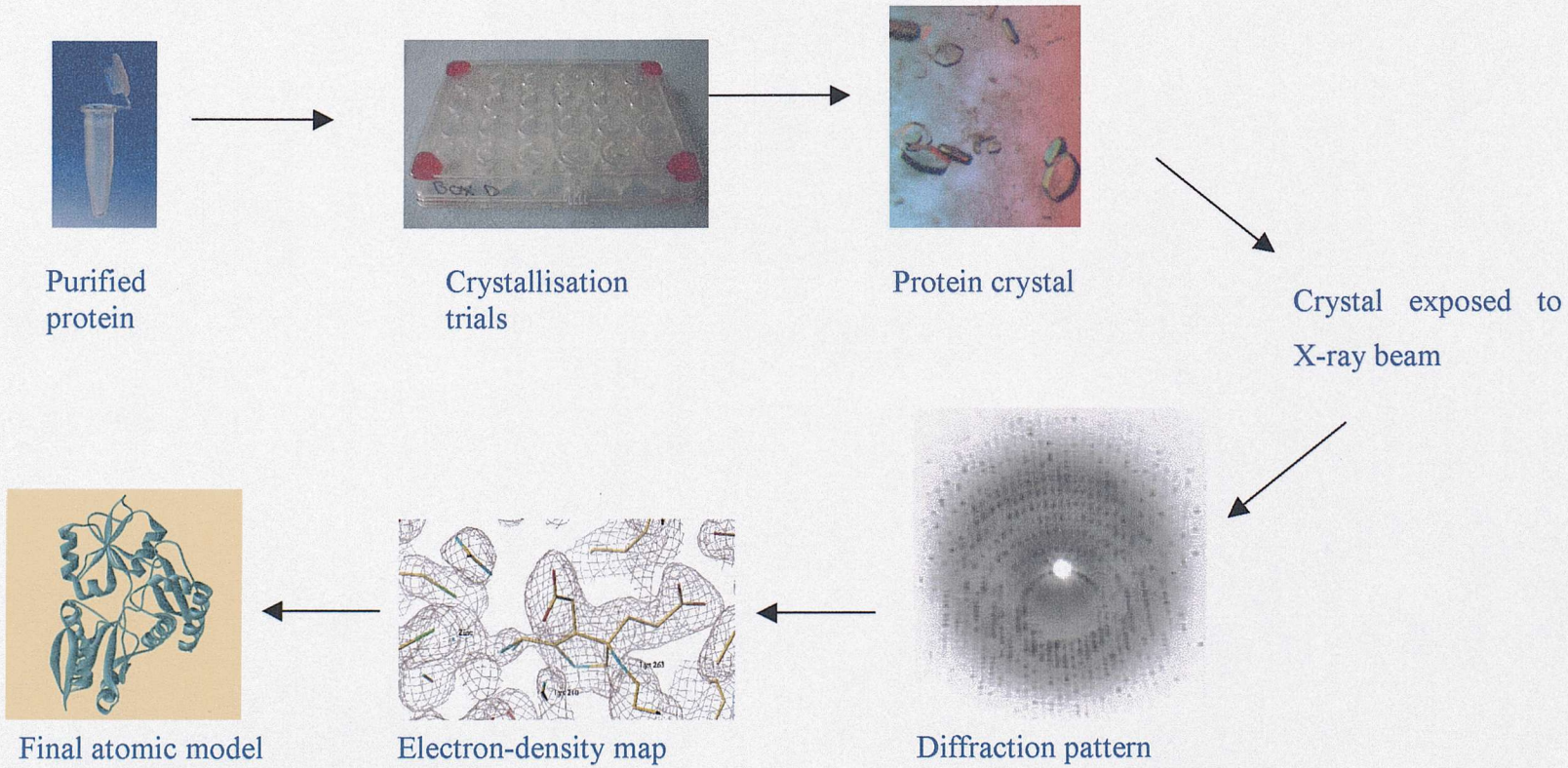

Figure 2.6. An overview of the stages of X-ray crystallography.
The protein is purified to allow initial crystallisation trials. The crystals are exposed to an X-ray beam. Diffraction patterns are processed (determining the intensity of each spot) to provide information about the unit cell dimensions and space group. For each reflection, structure factor amplitudes are combined with estimated phases to calculate an electron density map. The electron density map is then interpreted to allow the molecular structure to be modelled. The structure is then refined to fit the map more accurately adopting a more thermodynamically favoured conformation. Model building and refinement are carried out until the atoms in the structure best fit the data generating the final model.

Chapter Three: Characterisation of human recombinant ALAD and the mutant Phe12Leu.

3.1 Introduction

Purification of human ALAD for characterisation has, in the past, been problematic. Difficulties associated with the purification of human ALAD include the risk of blood-bourne diseases, low yields and the presence of common isoenzymes Lys59 and Asn59 [124, 125]. Production of recombinant human ALAD was thought to be a solution to these problems. This chapter describes the purification of recombinant human ALAD produced by a synthetic gene.

As a native human ALAD cDNA clone was not available, a recombinant human ALAD cDNA was synthesised by Dr M Sarwar (Southampton University). The double stranded coding region of 990 base pairs, encoding the 330 amino acids of human ALAD was constructed from a total of 18 oligonucleotides, 9 primers for each strand. The primers had an overlap of approximately 10 base pairs. Only the codon specifying Pro 3 was changed, from CCC to CCG, as CCC is known to be a weakly expressing Pro codon in *E.coli*. The 5' end of the gene was engineered with an *Nde*I restriction site and the 3' end with a *Bam*HI restriction site. These restriction sites enabled insertion of the cDNA into the plasmid vector for expression in a bacterial host.

Once synthesised, the human ALAD was cloned into the pT7-7 vector (figure 2.1). The vector, with the inserted gene, was transformed into the bacterial strain, BL21 (DE3) and the protein expressed by induction with IPTG. An effective and reproducible purification procedure was developed to provide sufficient quantities of human recombinant ALAD for characterisation and crystallisation. The purification typically yielded 2mg of human recombinant ALAD per litre of *E.coli*.

ALAD is present in great excess in normal cells, thus a partial deficiency of this enzyme is not normally accompanied by clinical symptoms. However, a severely decreased

enzyme activity may occur in the case of inherited ALAD deficiency porphyria (Doss porphyria) [99, 126], in acquired ALAD deficiency produced by lead exposure[127, 128], or in hereditary tyrosinaemia I [101, 129], all of which can cause severe clinical symptoms.

A novel mutation of the ALAD gene in an asymptomatic Swedish infant with erythrocyte ALAD activity at ~12% of normal controls was identified by an ALAD assay for neonatal screening of hereditary tyrosinaemia I. Genomic DNA analysis confirmed that the proband was heterozygous for a Phe12Leu mutation, which was inherited from her father. Akagi *et al*, 1999, overexpressed the mutant cDNA in Chinese hamster ovary (CHO) cells and reported that the mutation encoded a protein with little enzyme activity, and was responsible for the marked ALAD deficiency [55, 126].

Predictions from the human ALAD structure indicate the Phe12Leu mutant enzyme may have been expected to be active as the site of disturbance is on the *N*-terminal arm rather than at the catalytic site of the enzyme (Fig 3.1). Akagi *et al* concluded that their findings probably reflected an abnormal folding of the Phe12Leu protein, since the mutation occurred in the α1 helix of the *N*-terminal arm of the enzyme, which is involved in the extensive quaternary interactions amongst the subunits and postulated that this mutant enzyme was probably unable to form octamers [55].

This chapter describes the purification and characterisation of this mutant and discusses the implications of this mutation in terms of subunit interactions. It was discovered that the mutant enzyme does exist as an octamer and was, in fact, active, but only at a much higher pH.

Hybrid octamers were created from normal ALAD and mutant ALAD monomers to investigate subunit interactions. The unfolding and refolding experiments carried out to find the optimal conditions for this procedure and attempts to separate these hybrids are described in this chapter.

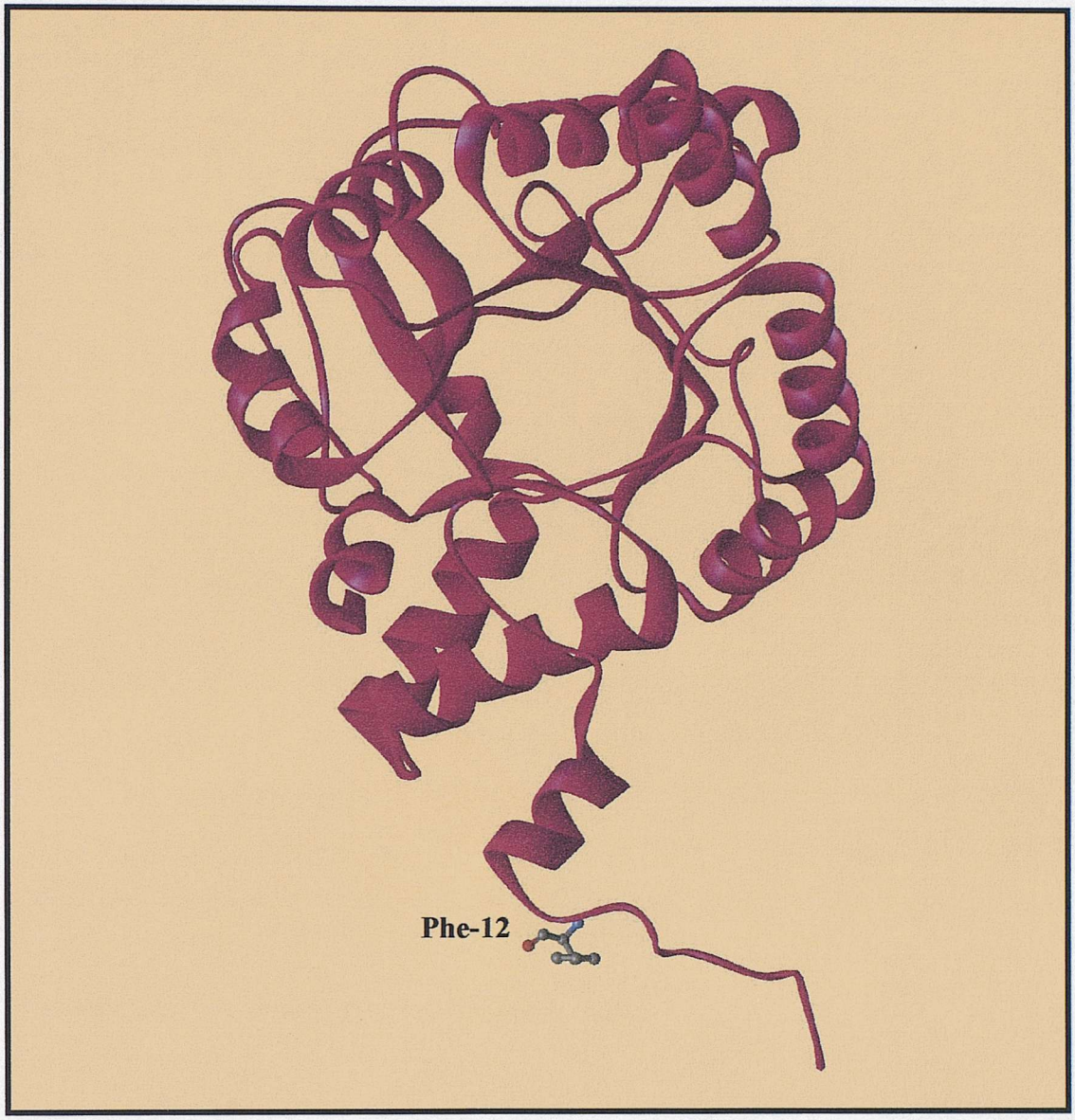

Figure 3.1 Human ALAD monomer showing the position of the residue Phe12. This figure was prepared using WebLab Viewer Lite v3.2 [30].

3.2 Results

3.2.1 Purification of human recombinant ALAD

Initial protein expression studies

A number of colonies harbouring the recombinant pT7-7 plasmids were selected for characterisation by SDS PAGE and activity assays. Cultures were grown for each clone and the cells were sonicated and centrifuged to give supernatant and pellet fractions. SDS PAGE analysis (Fig 3.2) indicated that some of the required protein was insoluble, but there was sufficient enzyme in the soluble fraction to proceed with the purification.

Large-scale (800ml) cultures were grown following the confirmation of soluble protein expression. Bacterial pellets from this large-scale growth could be stored at -20°C, without any significant loss of enzyme activity. In order to characterise and crystallise recombinant human ALAD, an effective and reproducible purification procedure was developed. The human Phe12Leu mutant was also purified in the same way.

Growth of *E.coli* overexpressing human ALAD

Individual colonies of *E.coli* BL21 (DE3) containing the pT7-7 vector expressing ALAD and ampicillin-resistance were grown in 10ml starter cultures of LB media containing ampicillin (100μg/ml) at 37°C overnight. The overnight cultures were each used to inoculate 800ml of LB media containing ampicillin (100μg/ml) in 2L baffled flasks. The flasks were incubated at 37°C, with shaking at 120rpm until the OD_{600}nm was approximately 1. IPTG was then added to a final concentration of 1mM and the cultures were incubated overnight at 25°C. Cells were harvested by centrifugation for 25 minutes at 4,650 x g (5000rpm), using a Beckman centrifuge (JA-21) fitted with a JLA-10.500 rotor, at 4°C. The pellets were used immediately, or were frozen at -20°C.

Sonication

The bacterial pellet from 3.2L of media was resuspended in approximately 80ml of 50mM potassium phosphate buffer, pH 6.8, containing 5mM 2-mercaptoethanol 50μM ZnCl and 100μM PMSF. The resuspended cells were then sonicated on ice for a total of ten cycles, each cycle consisted of 30 seconds sonication with a 45 second cooling period.

Heat treatment

The sonicated cells were placed in a round-bottomed flask and rapidly heated to 60°C in a water-bath with constant swirling; the temperature was maintained for 3 minutes, after which the solution was rapidly cooled by swirling the flask in an ice-water slurry. The heat-treated sample was then ultracentrifuged, using Beckman ultracentrifuge (L7-65), fitted with a TFT-45.94 rotor at 193,750 x g (40,000rpm) for 1 hour, at 4°C. The pellet was discarded and the supernatant was retained.

Ammonium sulphate fractionation

The supernatant was treated with $(NH_4)_2SO_4$ (35% saturation) and the precipitate was collected by centrifugation at 48,000 x g (20,000rpm), using a Beckman centrifuge (JA-21) for 20 minutes, at 4°C. The pellet was discarded and the supernatant was treated with $(NH_4)_2SO_4$ (60% saturation). The precipitate was collected by centrifugation, as before, and the 60% pellet, that contained the enzyme, was resuspended in 2ml of 50mM potassium phosphate buffer, pH 6.8, containing 5mM 2-mercaptoethanol, 50μM ZnCl and 100μM PMSF and the enzyme was dialysed against 10L of the same buffer overnight.

Chromatography on BIO-RAD hydroxyapatite (HTP)

The dialysed enzyme was loaded onto a column of BIO-RAD hydroxyapatite (5.5cm x 10cm) that had been pre-equilibrated with the same buffer used in the previous step. After loading the column it was washed with 1L of the same buffer. A linear gradient

(500ml total; 50mM-300mM potassium phosphate buffer, containing 5mM 2-mercaptoethanol, 50μM ZnCl and 100μM PMSF) was applied to the column and 6ml fractions were collected. The fractions were assayed and purity was judged by SDS-PAGE, before the active fractions were pooled (typically fractions 35-60). A 60% $(NH_4)_2SO_4$ precipitation was carried out on the pooled fractions and the precipitate was collected by centrifugation as before. The pellet was resuspended in 1.5ml of 100mM potassium phosphate buffer, pH6.8 containing 5mM 2-mercaptoethanol, 50μM ZnCl and 100μM PMSF.

Gel filtration chromatography on Bio-Gel A 0.5m

The resuspended pellet from the hydroxyapatite column was applied to a Bio-Gel A 0.5m gel filtration column (3cm x 1m) and the column was developed with 100mM potassium phosphate buffer, pH 6.8, containing 5mM 2-mercaptoethanol and 100μM PMSF. Fractions containing protein were concentrated and assayed for ALAD activity and purity was judged by SDS PAGE, before the fractions were pooled (typically fractions 29-33).

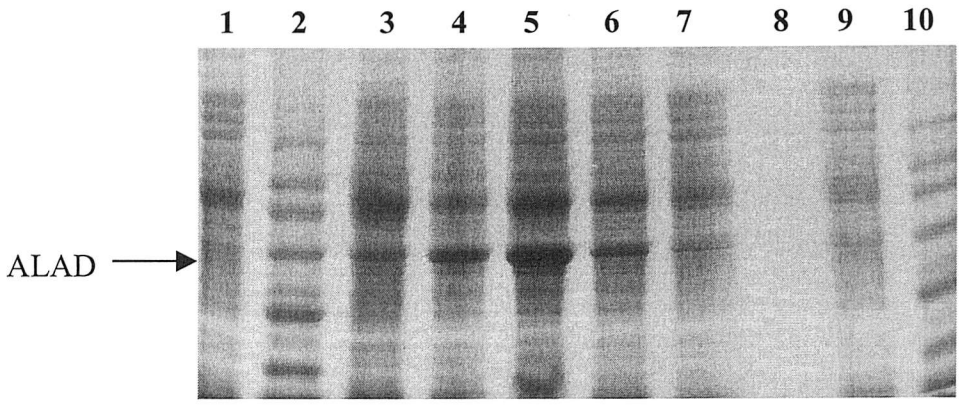

Figure 3.2 Analysis of human recombinant ALAD overexpresion by SDS PAGE.
The effect of temperature and time on the overexpression of human recombinant ALAD was investigated to ascertain the best conditions for overexpression. Incubation for 25°C for 18hrs was chosen as the optimum conditions for overexpression of hrALAD and was used in all subsequent growths.
Lane 1, BL21 DE3 with no plasmid; lane 2, molecular weight marker; lane 3, incubation for 3hrs at 37°C; lane 4, incubation for 18hrs at 25°C; lane 5, incubation for 18hrs at 30°C; lane 6, incubation for 3hrs at 30°C; lane 7, incubation for 3hr at 25°C; lane 8, blank; lane 9, BL21 DE3 with no plasmid and lane 10, molecular weight marker.

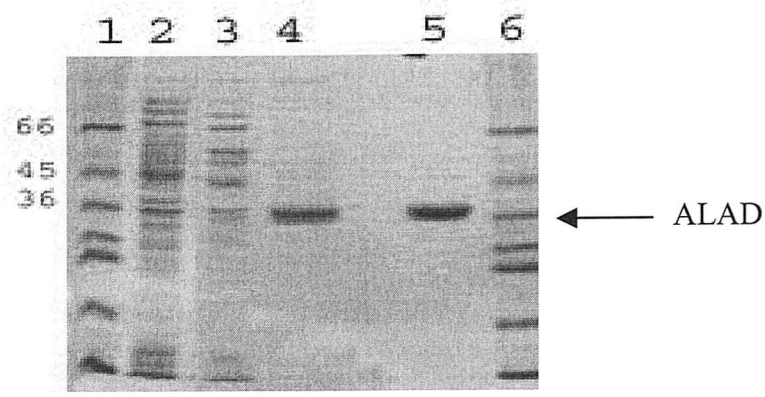

Figure 3.3 Human recombinant ALAD at different stages of purification analysed by SDS PAGE.
Lane 1, Dalton VII Mr marker; lane 2, crude extract; lane 3, after heat treatment; lane 4, after hydroxyapatite column; lane 5, after Biogel gel filtration and lane 6, Dalton VII Mr marker.

Step	Volume (ml)	Protein (mg)	Activity (μMoles/hr)	Specific activity (μMoles/mg/hr)	% Yield
Crude extract	47	897.1	1007.2	1.12	100
After heat treatment	45	114.08	877.4	7.6	87
After hydroxyapatite column and concentration	163	39.9	677.4	16.97	67
After Biogel A.05 gel filtration and concentration	30	7.5	222.8	29.7	22

Table 3.1 The specific activities and yield of the hrALAD at different stages of purification, starting from 4.8L of *E.coli* BL21 DE3.

3.2.2 Phe12Leu mutant ALAD

The Phe12Leu mutant has been studied by another group who expressed the protein in Chinese hamster ovary cells and as a GST-fusion protein [55, 126]. They reported the Phe12Leu mutant to possess 0.5% activity compared to the normal human ALAD. As the amino acid substitution caused by the mutation is located far from the active site [28], Akagi *et al* reasoned the loss of enzyme activity was probably not directly due to a change in the affinity of the enzyme to the substrate. Since the amino acid substitution of Phe to Leu at amino acid residue 12 is located within the *N*-terminal arm, (Fig 3.1) Akagi *et al* suggested this mutation could elicit a stereotactic hindrance in homodimer formation. As the homooctamer is considered the active form of the enzyme it was proposed that the Phe12Leu mutant was unable to form octamers and existed as a lower molecular weight complex, that was inactive. However, this proposal did not explain why the ALAD activity was less than 50%.

The aim of studying this mutant was to investigate the affect that monomers have on each other within the octamer, i.e., is it possible for the mutant monomers to have an inhibitory effect on the normal monomers. The infant had very low ALAD activity despite being heterozygous for the Phe12Leu mutation, which suggested the presence of mutant monomers might affect the activity of the octamer.

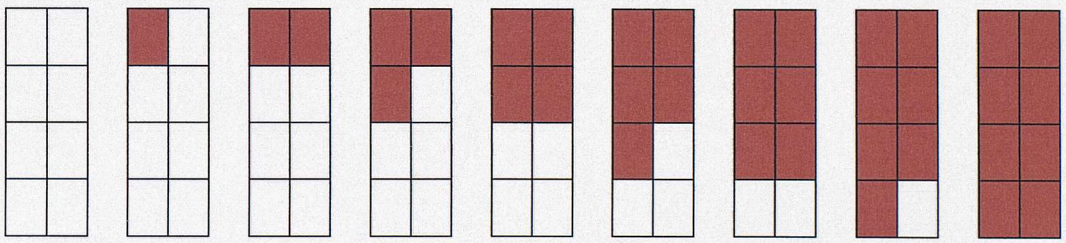

Figure 3.4 Nine possible associations of normal monomers (white boxes) with Phe 12Leu mutant monomers (red boxes).
If all those octamers with one or more mutant monomers present are inactive, and only the octamer with all normal monomers is active there is an 8:1 ratio of inactive to active octamers, which interestingly is approximately 11%, close to that measured for the proband.

As shown in figure 3.4, there are nine possible associations of normal monomers (white boxes) with Phe12Leu mutant monomers (red boxes), assuming that equal amounts of both normal and mutant monomers are formed and both types of monomer form octamers at the same rate. If all those octamers with one or more mutant monomers present are inactive, and only the octamer with all normal monomers is active, this is an 8:1 ratio of inactive to active octamers, which is the equivalent to 11% of normal ALAD activity. This level of activity is very close to that measured for the heterozygote, suggesting that Phe at position 12 may play an important role in interactions between subunits in the octamer.

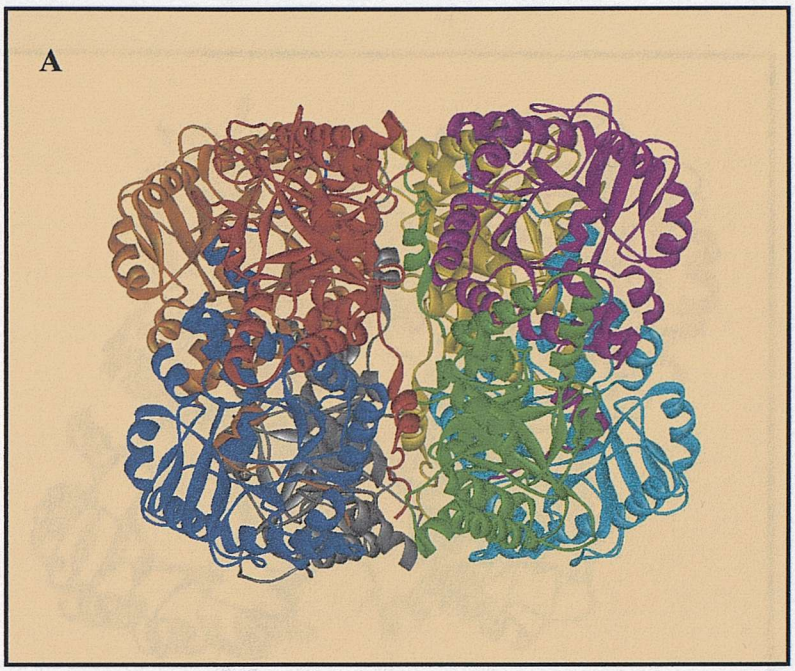

Figure 3.5 Human ALAD octamer.
ALAD is a homo-octameric enzyme, often regarded as a tetramer of dimers. The ALAD monomers (shown here in different colours) wrap their *N*-terminal arms around their dimeric partner and four of these dimers come together to form the octamer.

A.) The ALAD octamer viewed from the side

B.) The ALAD octamer viewed from above.

This figure was prepared using the WebLab Viewer Lite program[30].

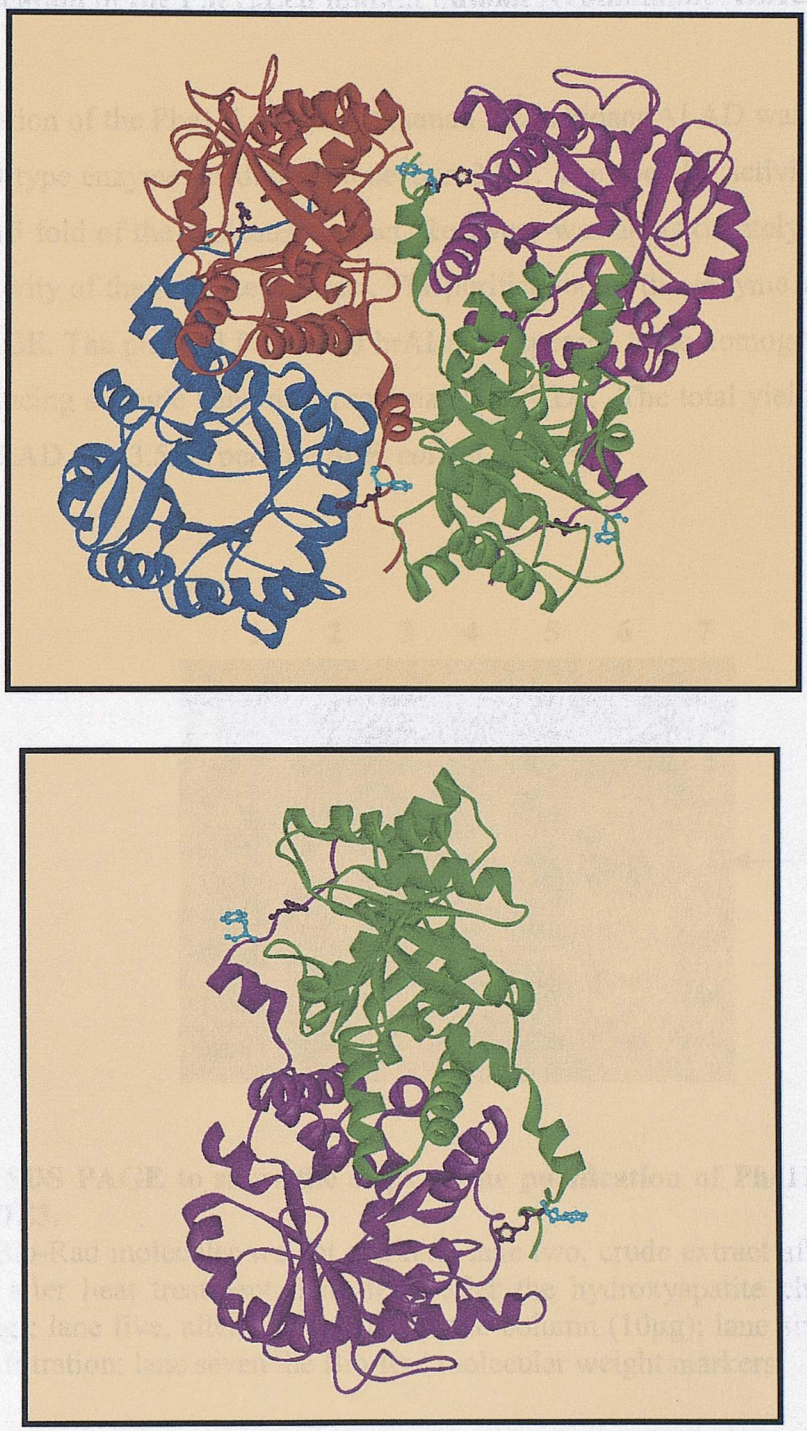

Figure 3.6 Structure of the human ALAD tetramer and dimer showing the positions of His8 and Phe12.
His8 (shown in black) is directed inwards and could interact with the neighbouring monomer within the dimer, whereas Phe12 (shown in light blue) is directed away from the neighbouring monomer and is more likely to interact with the neighbouring dimer. This figure was prepared using the WebLab Viewer program [30].

3.2.3 Purification of the Phe12Leu mutant human recombinant ALAD

The purification of the Phe12Leu mutant human recombinant ALAD was carried out as for the wild type enzyme, as described section 3.2.1. The specific activity at pH 9.0 is more than 15 fold of the sonicated extract. Recovery was approximately 15% based in the total activity of the sonicated extract. The purification of the enzyme was monitored by SDS-PAGE. The purified Phe12Leu hrALAD appeared to be homogenous by SDS-PAGE producing a single band at approximately 35KDa. The total yield of Phe12Leu mutant hrALAD was 3.5mg per litre of *E. coli* BL21 DE3.

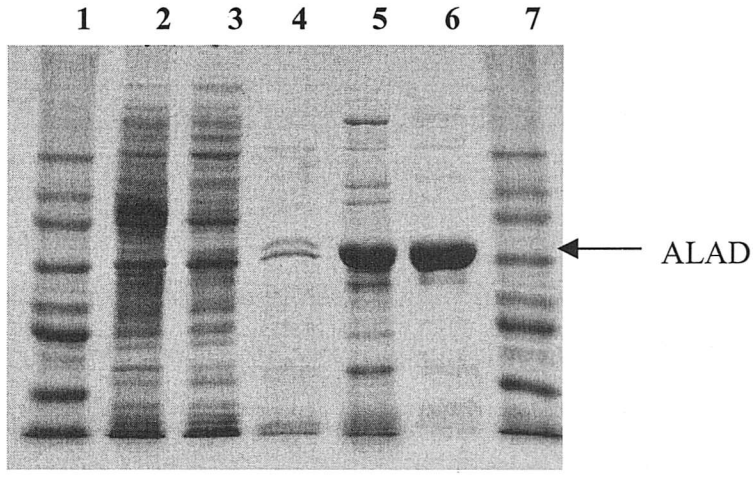

Figure 3.7 SDS PAGE to show the steps in the purification of Phe12Leu from *E. coli* BL21 DE3.
Lane one, Bio-Rad molecular weight markers; lane two, crude extract after sonication; lane three, after heat treatment; lane four, after the hydroxyapatite chromatography column (3μg); lane five, after the hydroxyapatite column (10μg); lane six, after Biogel A 0.5m gel filtration; lane seven the Bio-Rad molecular weight markers.

3.2.4 Comparison of normal hrALAD and Phe12Leu mutant hrALAD.

Polyacrylamide gel electrophoresis of ALAD under non-denaturing conditions, i.e. in the absence of SDS, was carried out to examine potential differences between the normal and mutant enzyme. The mutant Phe12Leu ALAD had a significantly higher mobility compared with the normal ALAD (Fig 3.8), which would suggest that either the mutant has a lower molecular weight or it is less positively charged.

Human ALAD has a Mr of 280 000 and 36 000 for the homo-octamer and for the subunit, respectively. It is thought that mammalian ALAD is active only as the homo-octamer, so if the Phe12Leu cannot form octamers this would explain its lack of catalytic activity. However, the Phe12Leu mutant ALAD had an identical elution volume to the native ALAD from gel filtration, indicating that it also exists as an octamer at pH 6.8, under the conditions used (described in section 3.2.1).

The hrALAD and hrALAD mutant Phe12Leu were found to elute at different salt concentrations from the strong anion exchange column, Mono Q (Fig 3.9). This finding suggests they differ in charge. Intriguingly, the Phe12Leu eluted earlier than the native ALAD from the Mono Q column, suggesting it is less negatively charged, but migrated further on a non-denaturing gel (Fig 3.8), suggesting it is more negatively charged. However, it should be stressed that the pH during non-denaturing PAGE analysis was pH 8.6, whereas, during Mono Q chromatography the pH was 7.5.

The pH optima of the hrALAD was pH 6.8 as described previously for the human enzyme purified from erythrocytes [20]. At pH 6.8 the Phe12Leu mutant has only approximately 1% activity compared to the normal enzyme, however, its activity is increased at higher pH values, with a pH optimum of 8.8, whereas the normal enzyme is virtually inactive at this high pH (Fig 3.10). Therefore, i*n vivo*, the mutant is likely to be essentially inactive.

The effect of heat treatment for 10 minutes prior to enzyme assay revealed that the Phe12Leu mutant had similar thermostability properties compared to the normal

enzyme (Fig 3.11). These findings suggest that the mutant protein has no overt structural abnormality, despite the fact that it has reduced catalytic activity at pH 6.8. Both native and Phe12Leu mutant hrALADs possess remarkable heat stability, a property exploited in their purification.

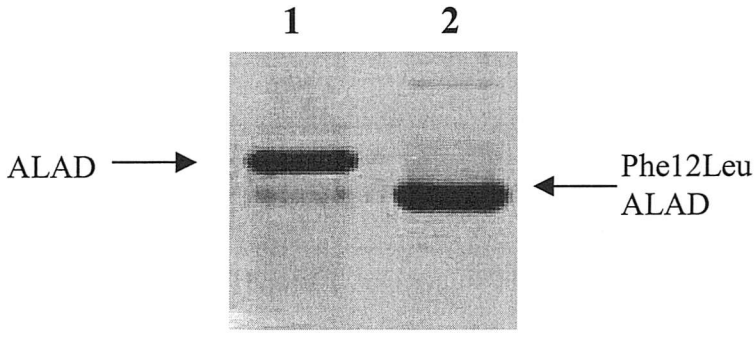

Figure 3.8 Polyacrylamide gel electrophoresis of the native and mutant ALAD protein under non-denaturating conditions.
Lane one, hrALAD and lane two, Phe12Leu mutant hrALAD. The mutation identified in this proband accompanied the loss of ALAD activity, despite the fact that this mutation was located far from the substrate-binding site or the zinc-binding domain of the enzyme. Polyacrylamide gel electrophoresis of ALAD under non-denaturing conditions was carried out to examine potential differences between the mutant and native enzymes. The mutant ALAD Phe12Leu had a significantly higher mobility compared with the native ALAD.

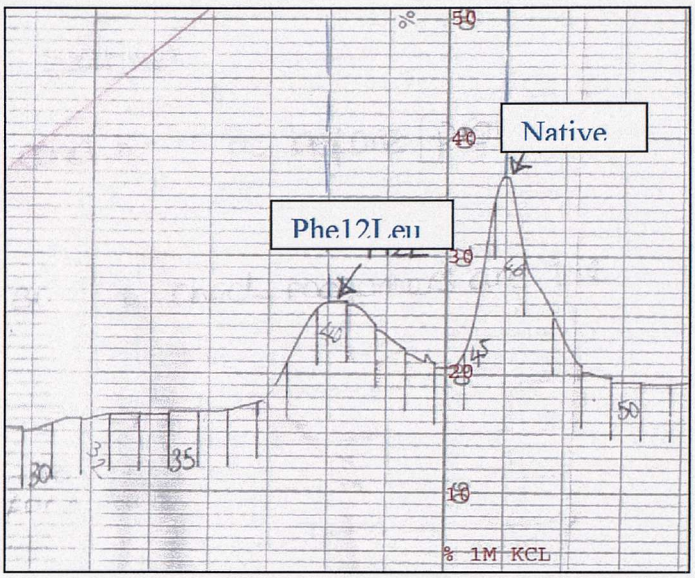

Figure 3.9 Separation of native hrALAD and Phe12Leu mutant hrALAD using a Mono Q column.
It was found that native and Phe12Leu mutant enzymes could be separated by ion-exchange, at pH 7.0. This suggested that the two enzymes differ with respect to charge.

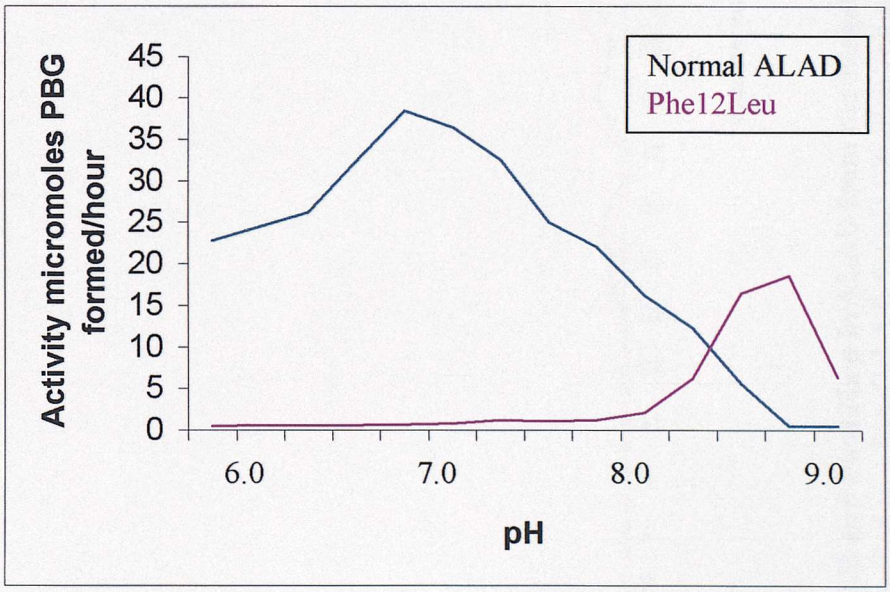

Figure 3.10 pH-dependance of hrALAD and hrALAD Phe12Leu mutant.
Buffers used: 100mM potassium phosphate buffer from pH6.0-6.8; 100mM Tris-HCl from pH 6.8-8.0; 100mM CAPS buffer for pH 9-10. All buffers contained 10mM DTT and 50μM ZnCl. Activity was determined as described in chapter 2, using 10μl of a 1mg/ml enzyme solution, 5mM ALA and 10mins incubation at 37°C. The specific activity of the mutant Phe12Leu, measured at pH 9.0 is approximately half that of the native hrALAD, measured at pH6.8.

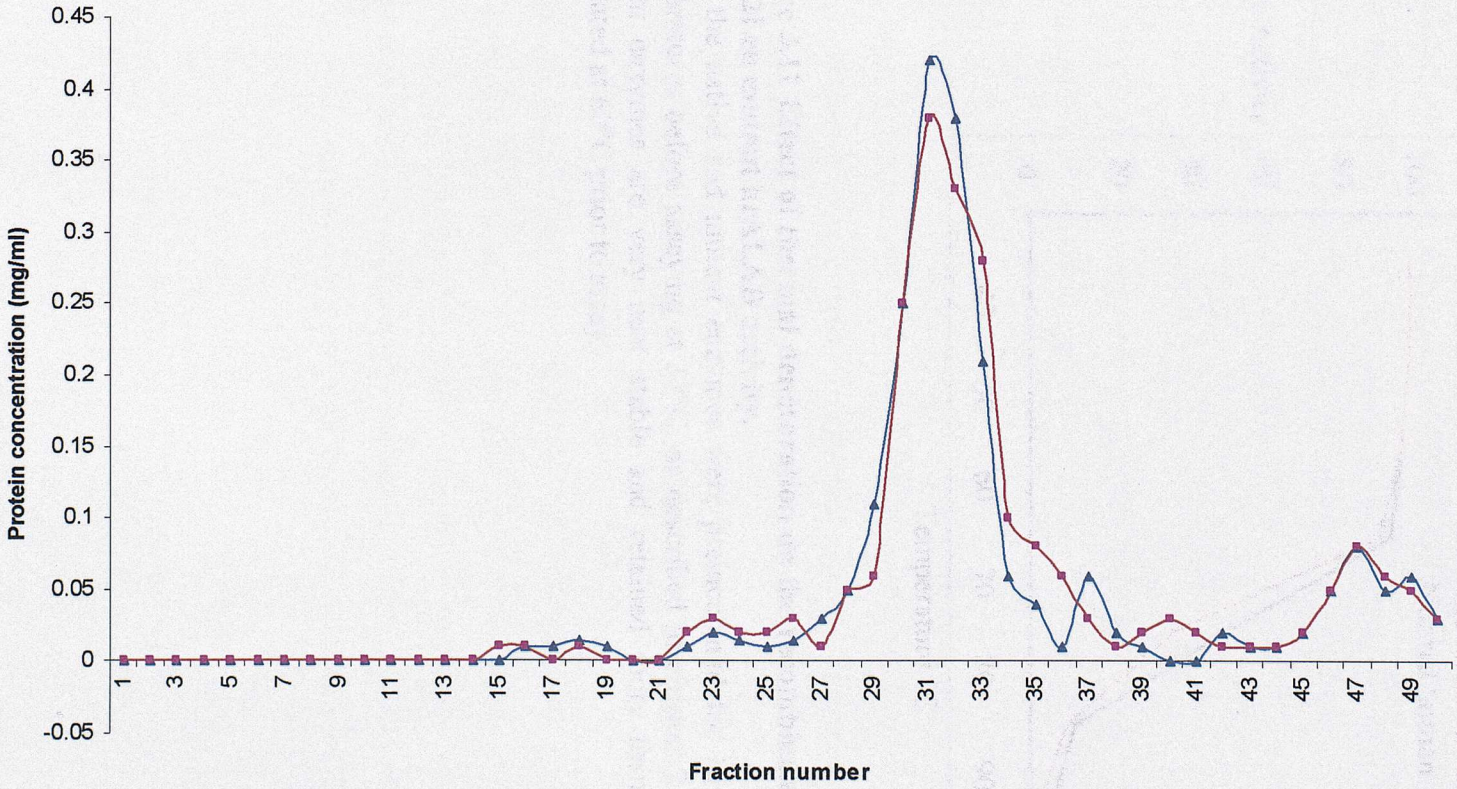

Elution Profile of native hrALAD and Phe12Leu hrALAD from the Biogel A 0.5m gel filtration column.
The enzymes were individually applied to a Bio-Gel A 0.5m gel filtration column (3cm x 1m) and the column was developed with 100mM potassium phosphate buffer, pH 6.8, containing 5mM 2-mercaptoethanol and 100μM PMSF. Fractions (5ml) were collected and those containing protein were assayed for ALAD activity visualised by SDS PAGE. Both native hrALAD and Phe12Leu mutant ALAD typically eluted in fractions 29-33 (145-165ml). The elution profiles of hrALAD and Phe12Leu hrALAD are shown in blue and red, respectively.

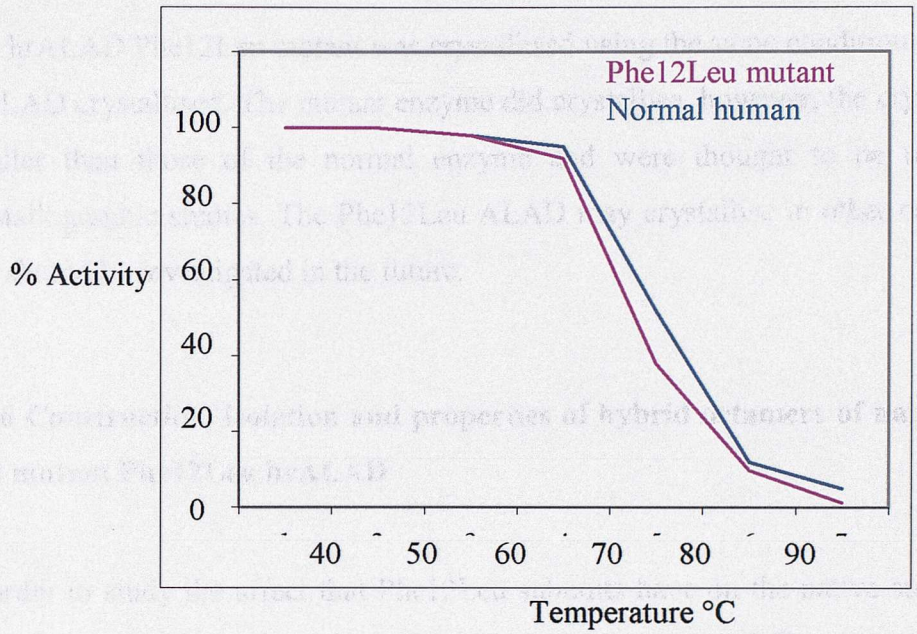

Figure 3.11 Effect of thermal denaturation on the recombinant human ALAD and Phe12Leu mutant hrALAD activity.
Both the native and mutant enzymes were preincubated for 10 mins at a variety of temperatures before assaying at 37°C, as described in chapter 2. Both the native and mutant enzymes are very heat stable and retained more than 90% activity when incubated at 60°C prior to assay.

3.2.5 Crystallisation of the Phe12Leu mutant hrALAD.

The hrALAD Phe12Leu mutant was crystallised using the same conditions in which the hrALAD crystallised. The mutant enzyme did crystallise, however, the crystals were far smaller than those of the normal enzyme and were thought to be unsuitable for crystallographic studies. The Phe12Leu ALAD may crystallise in other conditions and this should be investigated in the future.

3.2.6 Construction, isolation and properties of hybrid octamers of native hrALAD and mutant Phe12Leu hrALAD

In order to study the affect that Phe12Leu subunits have on the native subunits within the octamer, the formation of hybrid octamers was attempted. To create the Phe12Leu mutant and native hybrid octamers, the octamers were dissociated to form monomers and the octamers were reformed in a controlled manner (Fig 3.12).

Normal and Phe12Leu octamers were dissociated in the presence of urea. Normal and Phe12Leu enzymes were mixed together while the urea was slowly removed from solution. It was thought that urea would cause the dissociation of the octamers into monomers and the two types of monomers would than combine to form octamers in a random fashion. Assuming both types of monomer are present and that they recombine to form octamers at the same rate in the human subject, this experiment could mimic the situation of a human heterozygote with the Phe12Leu mutation [55].

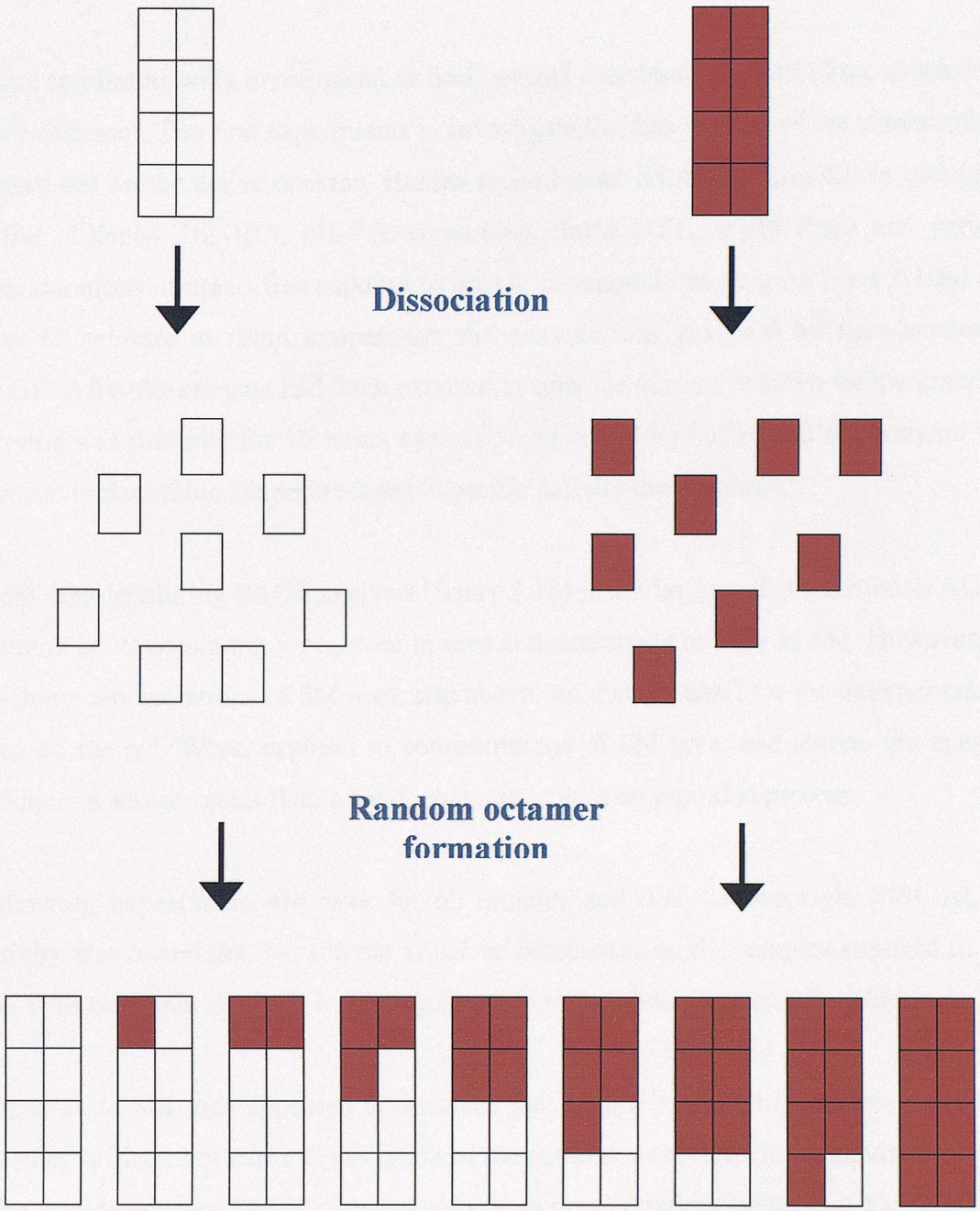

Figure 3.12 Making hybrid octamers of human ALAD and mutant Phe12Leu human ALAD.

Dissociation of octamers into monomers was attempted by exposure to 4.5M urea at room temperature for 60 mins. Native and Phe12Leu mutant enzyme that had been treated with urea were mixed and urea was removed from the solution by dialysis overnight, aiming to form hybrid octamers from native and Phe12Leu monomers.

Phe12Leu hrALAD

Native hrALAD

Unfolding and refolding studies of human recombinant ALAD.

Many conditions were investigated to find optimal conditions for unfolding which were not permanent. The first experiments to investigate the dissociation of the octamer were carried out on the native enzyme. Human recombinant ALAD (1.5mg/ml) in unfolding buffer (100mM Tris-HCl, pH 7.5, containing, 5mM DTT, 50μM ZnCl and varying concentrations of urea.) was exposed to urea at concentrations ranging from 2-10M and after 60 minutes at room temperature the enzyme was analysed by non-denaturing PAGE. After the enzyme had been exposed to urea for 60mins at room temperature the enzyme was dialysed for 16 hours against 5L of refolding buffer and the enzyme was assayed to determine the percentage of specific activity that remained.

From non-denaturing PAGE analysis (figure 3.13) it can be seen that the human ALAD maintained its octameric form, even in urea concentrations as high as 4M. However, on reaching concentrations of 8M urea, and above, no distinct band for the octamer can be seen on the gel. When exposed to concentrations of 8M urea, and above, the enzyme produces a smear, rather than a band, characteristic of an unfolded protein.

Following exposure to 4M urea for 60 minutes and dialysis overnight 80% ALAD activity was recovered. No activity could be detected from the samples exposed to 8M and 10M urea after dialysis, indicating the enzyme had been irreversibly denatured.

Exposure to 8M urea appeared to denature the enzyme irreversibly, whereas 4M urea was not sufficient to cause dissociation of the octamer as no additional bands were seen after non-denaturing PAGE. Subsequently, urea concentrations between 4.5M and 7.0M were investigated (Fig 3.13). Analysis on native PAGE again showed the continued presence of the octameric form of the enzyme, but there are also faint lower bands present indicating lower molecular weight species, possibly tetramers, dimers or monomers (Fig 3.13).

ALA at a final concentration of 5mM was added to the unfolding buffer to see if this would increase the yield of active enzyme after refolding by helping to maintain the monomeric structure, but it had no effect on the recovery of active enzyme.

The final unfolding conditions were as follows: ALAD (1.5mg/ml) was unfolded at room temperature in 4.5M urea in the presence of 5mM 2-mercaptoethanol and 50μM ZnCl for 60 minutes. It was not possible to measure activity over the course of the unfolding period as urea interfered with the assay, but after 60 mins the pattern of unfolding was monitored by non-denaturing PAGE. The unfolded protein was then dialysed against refolding buffer overnight, after which samples were taken for activity assays and non-denaturing PAGE analysis. Enzyme recovery was measured in terms of specific activity, 65% hrALAD activity was recovered and 58% Phe12Leu activity was recovered (measured at pH9.0).

After the optimal conditions for unfolding and refolding had been determined, both the unfolded hrALAD and the unfolded Phe12Leu mutant hrALAD were mixed in equal amounts and then refolded in an attempt to generate hybrid octamers.

Separating hybrid mixtures and determining subunit ratios in the reconstituted hrALAD octamers

Hybrids were detected by non-denaturing PAGE as they can be seen as faint multiple bands on the gel. Phe12Leu is catalytically inactive under these assay conditions so it was assumed that any activity was a result of the native enzyme at pH 6.8. Adding an equal amount of mutant (inactive) enzyme to native enzyme was expected to result in a 50% reduction in specific activity compared to the native enzyme alone. However, after mixing equal amounts of the mutant and normal enzyme the specific activity at pH 6.8 is reduced to less than 20%. The experiments described in this section suggest an inhibitory effect by the mutant monomers. This is an important finding as it could indicate communication exists between subunits in the octamer, where one mutant subunit can suppress the activity of the other subunits. When the hybrid mixture was assayed at pH 9.0 (the pH optima of the mutant) the specific activity of was also reduced to below 20%. As there is no inhibitory affect observed when the two enzymes are simply mixed together omitting the unfolding and refolding steps it was assumed that the hybrid formation accounted for this inhibitory effect.

Yields of hybrids were very low, making studies on individual hybrids very difficult. The recovery of active octameric enzyme was less than 50% after refolding. However,

an inhibitory effect was observed when hybrids were generating supporting the theory there is communication between the subunits.

Successful refolding of ALAD and separation of the hybrid mixture will allow further studies into intersubunit interactions using various mutant forms of ALAD. There may be a more effective way of generating these hybrids, which should be the subject of further studies.

	% Specific activity		% Specific activity after unfolding and refolding		% Specific activity after unfolding, mixing mutant and native enzymes and refolding	
	pH 6.8	pH9.0	pH 6.8	pH9.0	pH 6.8	pH9.0
HrALAD	100	0.5	65	0.4	19.5	*
Phe12Leu	3.1	100	2	58	*	17.2

Table 3.2 The effect on specific activity after unfolding hrALAD and Phe12Leu with urea and refolding the enzymes together in an attempt to form hybrid octamers.
Phe12Leu and hrALAD were unfolded in 4.5M urea, as described in section 3.2.6. After refolding their specific activities were measured and were reduced to approximately 60% at their respective pH optimas. However, when unfolded Phe12Leu and hrALAD were mixed and then refolded the % specific activity recovered was less than 20%.

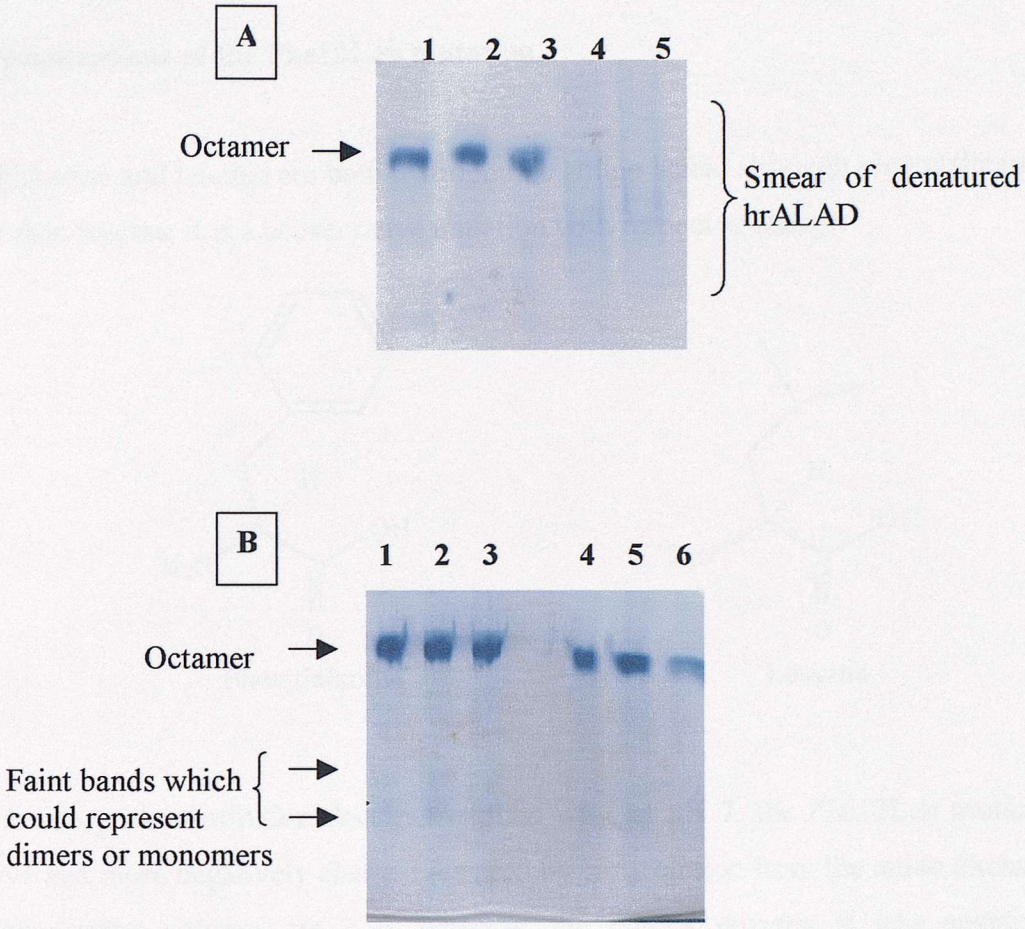

Figure 3.13 Native PAGE analysing human ALAD after exposure to various concentrations of urea.

A.) Lane 1, untreated ALAD, is included as a control, this band is assumed to be ALAD in its octameric form; Lane 2, ALAD which has been exposed to 2M urea for 60 minutes; lane 3, ALAD which has been exposed to 4M urea for 60 minutes; lane 4, ALAD which has been exposed to 8M urea for 60 minutes; lane 5, ALAD which has been exposed to 10M urea for 60 minutes.

The ALAD octamer can be seen as a strong band at lower urea concentrations. As the concentration of urea increases to 8M, and above, the octameric form disappears and is replaced by a smear on the gel, probably due to unfolded ALAD.

B.) Lane 1, ALAD exposed to 4.5M urea for 60 minutes; lane 2, ALAD exposed to 5.0M urea for 60 minutes; lane 3, ALAD exposed to 5.5M urea for 60 minutes; lane 4, ALAD exposed to 6.0M urea for 60 minutes; lane 5, ALAD exposed to 6.5M urea for 60 minutes; lane 6, ALAD exposed to 7.0M urea for 60 minutes.

The higher arrow indicates the band thought to represent the octameric form, the lower arrows indicate two very faint bands that could represent dimers or monomers.

3.2.7 Implications of the Phe12Leu mutation.

Phenylalanine and leucine are both hydrophobic amino acids, although phenylalanine is larger than leucine, it is a conservative mutation with respect to charge.

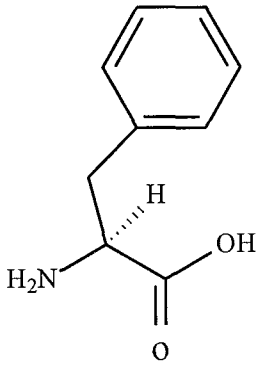

Phenylalanine

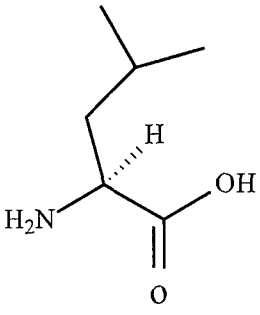

Leucine

This amino acid substitution does not explain why, at pH 7, the Phe12Leu mutant is inactive and more negatively charged (as seen by early elution from the anion exchange chromatography column, fig 3.9), whereas, the mutant enzyme is less negatively charged at pH 8.8 (as seen by non-denaturing PAGE analysis, Fig 3.8) and active. To explain these findings we need to understand the local environment of Phe12Leu.

Phenylalanine-12 is situated on the *N*-terminal arm of the ALAD monomer (Fig 3.6). Other residues nearby include His8, Tyr11 and His13. His8 is a conserved residue in mammalian ALADs and is directed towards the A-site of the active site and adjacent to the zinc-binding site of the other monomer forming the dimer. His8 is directed to residues Tyr224, Met170 and Asp172. The α-carbon of Tyr224, which forms the C-terminal end of the active site, is only 3.8Å away from the aromatic ring of His8. The hydroxyl group of Tyr224 is directed towards Cys132 (one of the residues forming the zinc binding site). His8 also interacts with the side chain of Asp172 of the partnering monomer of the dimer. Asp172 resides in a loop at the C-terminal end of the β6 strand. Met170 forms a hydrogen bond with His8. The positions of His8 and its interactions with residues at the active site suggest it has a role in the activity of human ALAD. It may be possible that mutation of residue 12 from a phenylalanine to a leucine disrupts His8 requiring a higher pH for catalysis to proceed.

In native human ALAD Phe12 is directed in the opposite direction to His8, towards the barrel region of the neighbouring dimer. These contacts appear to be vital for connections between monomers and dimers, although it is not certain they are responsible for communication between subunits.

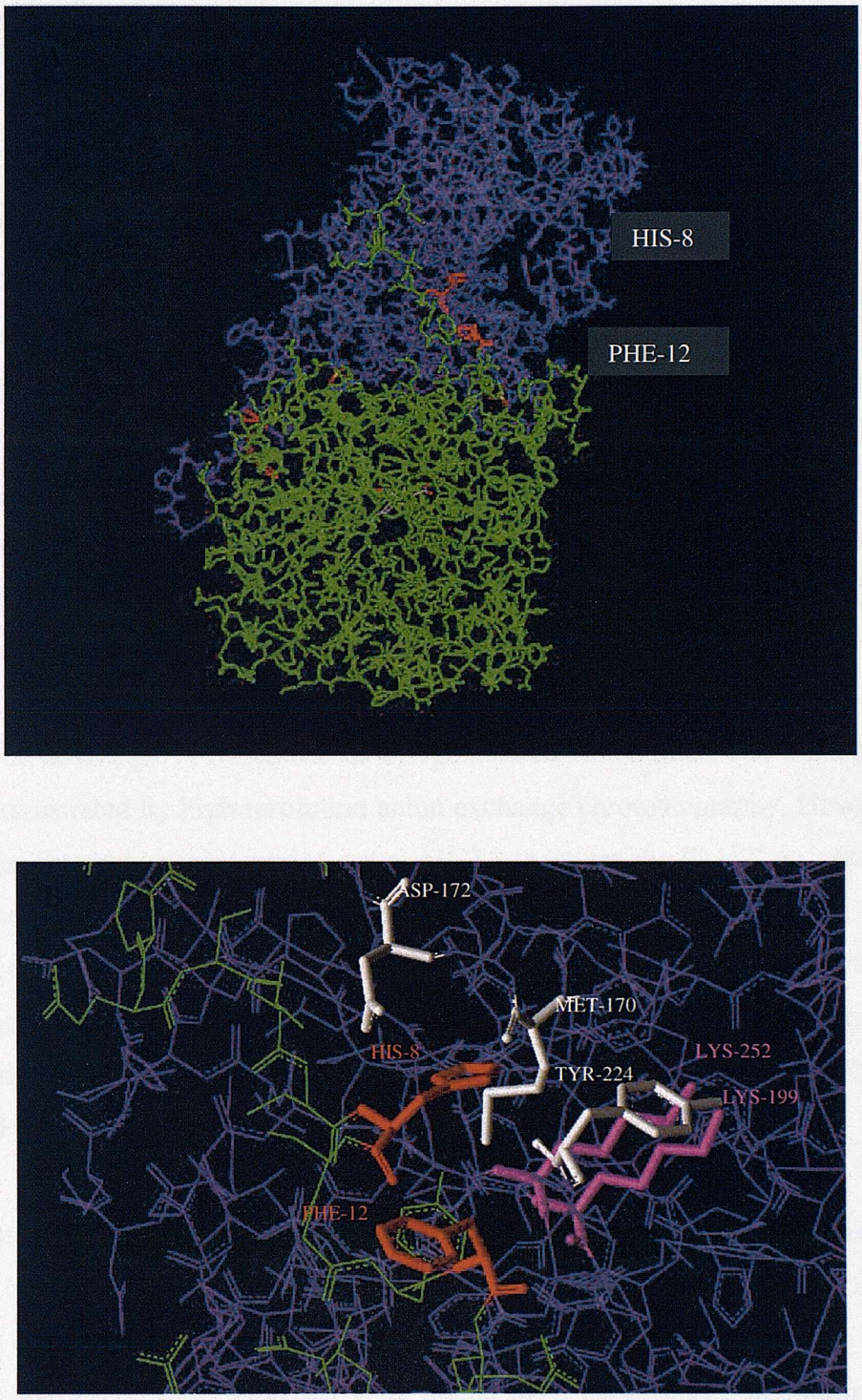

Figure 3.14 Positions of His8 and Phe12 in hrALAD

A) Human ALAD dimer.

B) Positions of His8 and Phe12 in the ALAD dimer.

Monomer A is highlighted in green, Monomer B is highlighted in purple. The *N*-terminal arm of Monomer A is shown wrapped around the barrel of monomer B. His8 and Phe12 of the *N*-terminal arm of monomer A are highlighted in red. His8 points inwards to the barrel and active site of monomer B, whereas Phe12 points away from the barrel, interacting with another dimer. This figure was prepared using WebLab Viewer Lite v3.2 [30].

3.3 Conclusions

Studies on this enzyme have produced interesting results. Importantly, the development of a purification procedure for the human recombinant ALAD enzyme has the advantage of taking less time than the isolation of ALAD from human erythrocytes. The hrALAD protein was produced in less than a week and exhibited a specific activity higher than ALAD purified from erythrocytes [20]. This may be because ALAD isolated from erythrocytes could be up to 120 days old.

The discovery that the Phe12Leu mutant migrates faster when analysed by non-denaturing PAGE is an interesting finding. As the native and mutant enzymes have identical elution profiles from gel filtration chromatography they are presumably both octamers so the different migration on non-denaturing PAGE must be due to a difference in charge. A difference in charge between the normal and mutant ALAD is also demonstrated by high-resolution anion exchange chromatography. However, anion exchange chromatography carried out at pH 7.0 indicates the Phe12Leu mutant ALAD is less negatively charged, whereas the migration on non-denaturing PAGE, carried out at pH 8.6, of Phe12Leu indicates that it is more negatively charged. There is no charge difference between phenyalanine and leucine but the mutation may cause a conformational change, which unmasks a charged group. Histidine 8 is nearby and may affected by this mutation.

Confirming previous reports [20], the optimum pH of the human ALAD was found to be pH 6.8, however, at this pH, the Phe12Leu mutant has only approximately 1% activity compared to the native enzyme (also reported by Akagi *et al* [55]). The mutant enzyme was found to be more active at higher pH values, with a pH optimum of 8.8, whereas the native enzyme is virtually inactive at this high pH. It is intriguing that a mutation on the *N*-terminal arm, far from the active site, is able to affect the pH optimum of this enzyme so profoundly. *In vivo,* the mutant enzyme is expected to be inactive.

Hybrid octamers, composed of native and Phe12Leu monomers, were successfully created and an inhibitory effect was observed. Controls were constructed, in which, the

proteins underwent the unfolding and refolding procedure, without mixing and Phe12Leu and normal enzymes were mixed without the unfolding and refolding steps. Enzyme activity recovery in the controls for both normal and Phe12Leu, after refolding, was approximately 60%, however, after mixing the normal and mutant, prior to refolding, activity recovered was reduced to below 20% when assayed at pH 6.8 (the pH optimum of normal hrALAD) and at pH 8.8 (pH optimum of the Phe12Leu mutant). This result strongly indicates that the mutant monomers are able to have an inhibitory effect on the enzyme. Yields of hybrids were very low, making studies on individual hybrids impossible. The recovery of active octameric enzyme was less than 70% after unfolding by urea. There may be a more effective way of generating these hybrids, which should be the subject of further studies.

Successful refolding of ALAD and separation of the hybrid mixture will allow further studies into intersubunit interactions using various mutant forms of ALAD.

Chapter Four: Discovery of a putative intermediate at the active site of 5-aminolaevulinic acid dehydratase.

4.1 Introduction

The crystal structure of ALAD has been solved from yeast [25], *Escherichia coli* [26, 130], *Pseudomonas aeruginosa [27]* and more recently from human erythrocyte [28] and hrALAD. The crystal structures all reveal ALAD to be a homo-octameric enzyme composed of four dimers. The extended *N*-terminal arm of each monomer closely wraps around its dimeric partner. Despite the fact ALAD is an octamer of approximately 300 kDa, the catalytic and binding residues at each active site are separate for each subunit. However, there is evidence to suggest subunit interactions are essential to catalytic function.

The existing crystal structures have not unequivocally explained the catalytic mechanism, or the structurally and catalytically significant subunit interactions. One uncertainty is the order of bond formation between the two ALA substrate molecules. It is not known if the intersubstrate carbon-carbon bond formation precedes or follows the formation of the intersubstrate carbon-nitrogen bond. Potential intermediate analogues have been characterised with ALAD [40, 131, 132]. The analogues mimic structures that may be intermediates in the mechanism. However, much of the reaction mechanism still remains speculative. The only characterised intermediate in the ALAD catalysed reaction is a Schiff base formed between the keto group of P-side ALA and the amino group of an invariant lysine residue [38].

Crystallography studies on ALAD purified from human erythrocytes [28], strongly indicated the presence of a ligand at half the active sites of the octamer. At first this was suggested to be the product PBG, as reported earlier by Jaffe with experiments on the *E.coli* and bovine ALAD [133], suggesting human ALAD possesses half site reactivity. However, work described in this chapter contradicts this as PBG cannot be detected, raising the possibility that it may be a genuine intermediate seen at the active site in the

crystal structure. This is an important discovery as it could provide further information about the catalytic mechanism of ALAD. A number of experiments, were carried out to detect either the presence of PBG or intermediates, bound to the enzyme, including, mass spectrometry and enzyme assays designed to liberate any bound molecules from the active site.

Crystals of recombinant human ALAD (hrALAD) were obtained for two reasons. Firstly, in an attempt to identify the ligand at the active site and secondly, to clarify areas of the enzyme, that were not well ordered in the initial human erythrocyte ALAD crystal structure. Recently, a structure of the yeast ALAD has been solved which has a very similar ligand at its active site [134]. This chapter describes attempts to identify this ligand and explain its presence at the active site.

4.2 Results

4.2.1 Reaction of hrALAD with Ehrlich's reagent

To detect PBG at the active site of hrALAD, the enzyme was tested for reaction with Ehrlich's reagent, which should produce a pink coloured adduct with pyrroles such as PBG [121] (figure 4.1). However, the enzyme-ligand complex was found to be unreactive with Ehrlich's, which suggests that the ligand is not a pyrrole, i.e. it has no free α-position to react with the aldehyde of the Ehrlich's reagent (figure 4.1).

The hrALAD was incubated in a variety of conditions designed to liberate the ligand from the active site of the enzyme. The hrALAD was incubated in 100mM Tris-HCl, pH6.8 with 5mM DTT and 50μM Zn at 37°C for 10 minutes before an equal volume of Ehrlich's reagent was added to test for the presence of PBG, however the Ehrlich's test was negative. Ehrlich's reagent contains acid, which is expected to denature the enzyme, despite this no PBG was detected, suggesting the ligand at the active site was not PBG, or that the PBG remained tightly buried in the enzyme, and was not accessible to the reagent.

Similar experiments were carried with various variations, as detailed in the left-hand column of table 4.1, to encourage the enzyme to liberate the ligand as PBG. The incubation was carried out at a higher pH (8.8) and EDTA was added to the enzyme in another incubation, intending to strip zinc from the enzyme and trigger the release of the ligand. After incubation in these conditions, Ehrlich's reagent was added, but no positive reaction was detected. A positive reaction with Ehrlich's reagent was only seen when the substrate ALA was added to the incubation.

As the possibility of PBG at the active of human ALAD was excluded by its negative reaction with Ehrlich's reagent, it was considered the ligand seen at the active site could be a reaction intermediate. NMR studies on ALAD by Jaffe *et al* had previously detected an unknown pyrrole-like compound, which was not PBG. It was proposed to be a derivative of PBG, which had been modified by a contaminating protein [135, 136].

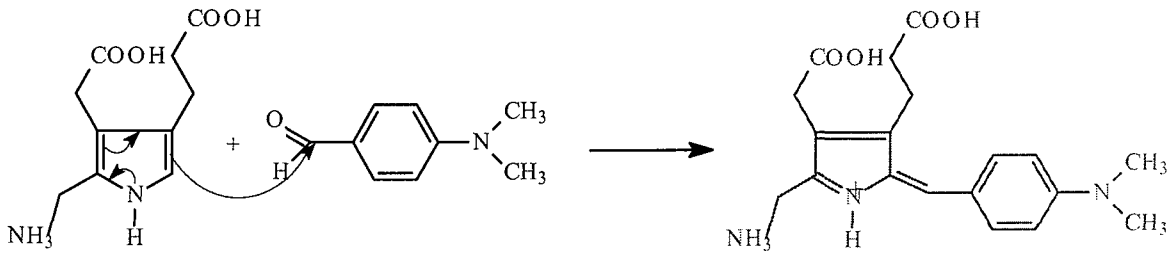

Figure 4.1 Ehrlich's reaction with PBG.
The aldehyde group of the 4-dimethylaminobenzaldehyde is attacked by the α-carbon of the pyrrole ring.

HrALAD incubation conditions	Reaction with Ehrlich's reagent
1) Substrate, ALA , (5mM) added	Positive
3) pH 6.8	Negative
4) pH 8.8	Negative
5) 100μM Zn and 10mM DTT	Negative
6) 1mM EDTA	Negative

Table 4.1 Results of experiments to detect any pyrrole at the active site of ALAD.
The human ALAD was incubated in the following conditions: 100mM Tris-HCl with 5mM DTT and 50μM Zn at 37°C, with variations detailed in the left-hand column. After incubation in these conditions, Ehrlich's reagent was added. A positive reaction with Ehrlich's reagent was only seen when ALA was added to the incubation. Despite a number of pH variations and the presence of EDTA no reaction with Ehrlich's was detected.

4.2.2 The use of time-of-flight (TOF) mass spectrometry for the analysis of hrALAD under denaturing and non-denaturing conditions

Purified human recombinant ALAD was diluted to 1 pmol/ul with acetonitrile-water (1:1) containing 0.1% formic acid. It is generally accepted that under these conditions the protein is highly unfolded. Figure 4.2B shows a multiply charged envelope from m/z 800-2000. Upon deconvolution with Maximum Entropy 1 the major species has a mass of 36292Da (Figure 4.2A), as compared to the expected value of 36295Da (average mass from the primary sequence) for the human ALAD monomer. It can be observed from both spectra that the sample is free from any major contaminants. It also indicates that no small molecules can be detected bound to ALAD under denaturing conditions.

Purified hrALAD was buffer exchanged into 10 mM aqueous ammonium acetate, pH 6.4, and sent to Dr Iain Campuzano at Micromass UK, Warrington, Cheshire, for analysis of hrALAD under non-denaturing conditions. It can be observed immediately that infusing the hrALAD sample into the mass spectrometer in 10 mM aqueous ammonium acetate pH 6.4 (as opposed to 50% acetonitrile, 0.1% formic acid), produces a completely different mass spectrum (Figure 4.3B). The multiply charged species are far fewer and much further up the m/z scale. Upon infusion of Human ALAD in 50% organic solution, the multiple charge distribution is present in the range m/z 800-2000 (Figure 4.2B). Infusion of hrALAD in 100% aqueous solution gives a multiple charge distribution in the range of m/z 7000-11000. The six multiply charged species centred around m/z 7500 (m/z 7112.3, 7292.6, 7479.6, 7678.9, 7888.5, 8116.7 with charge states +41, +40, +39, +38, +37, +36 respectively) when deconvoluted produce a mass of 291579.3 Da (Figure 4.3A). This mass is consistent with the mass of the active octameric structure.

There are a number of particularly interesting points that can be taken from this single spectrum (Figure 4.3). The multiply charged species that represent the octamer are very dominant in the spectra, suggesting that the octameric structure is very stable and can survive the transition from solution to gas phase. The absence of the dimeric hrALAD structure in the mass spectra (Figure 4.3) is consistent with data already observed by

crystallography. This observation confirms the hrALAD octamer is indeed a very stable structure and that no equilibrium between the octamer and dimer structures are observed by mass spectrometry.

The calculated mass of the hrALAD octameric structure is 290360 Da. The mass obtained by mass spectrometry is 291579.3 Da. The difference is 1219.3 Da or 0.4 %. This difference could be due to the presence of substrates and/or chelated metal ions that are known to participate in the catalysis, within the active site of hrALAD (table 4.2). The observed larger mass (Figure 4.3), and broad multiply charged peaks in the spectrum, could also be due to extensive small molecule adducting of the protein molecule under the conditions used, therefore, leading to a higher observed mass.

If it is to be assumed that the electrospray spectrum and conditions used within the mass spectrometer reflect the abundance of the species in solution, then the spectrum shown in Figure 4.3 reveals that the octamer is the most stable protein assembly in 10 mM ammonium acetate, pH 6.4.

A

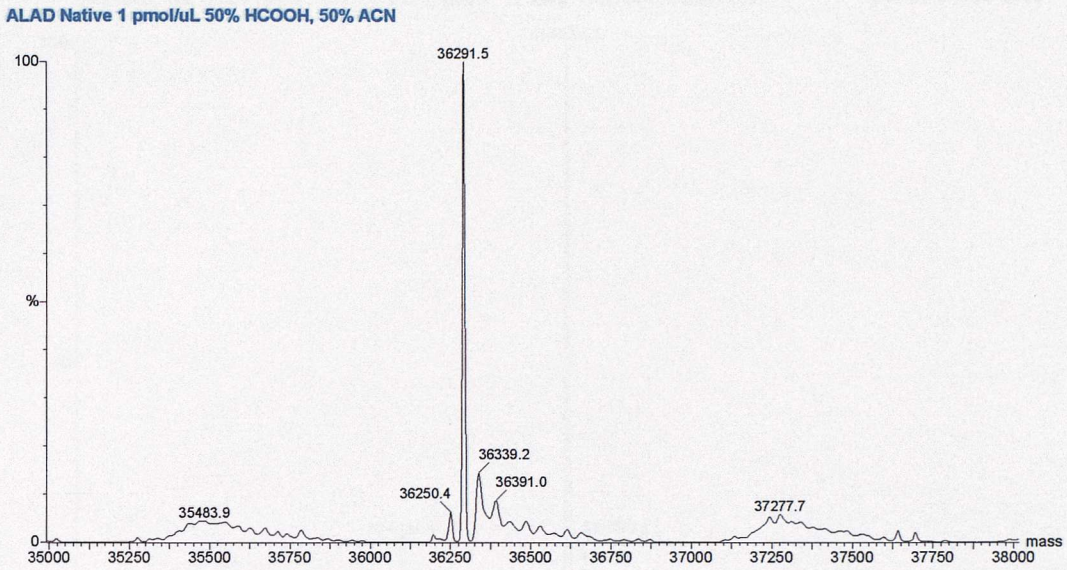

B

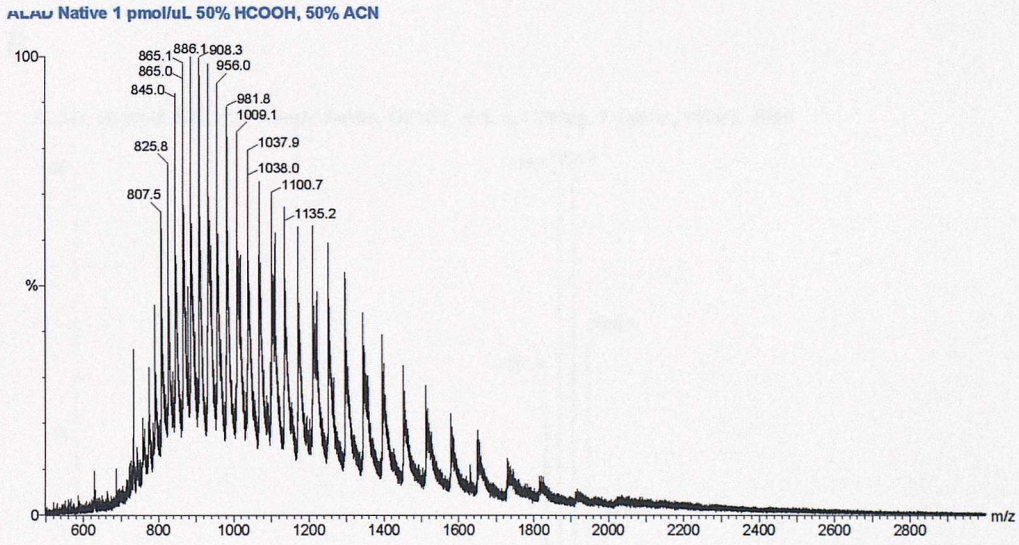

Figure 4.2 QToF-MS Electrospray mass spectra of hrALAD in acetonitrile-water (1:1), including 0.1% formic acid.

A.) Maximum entropy 1 deconvoluted spectra of hrALAD, indicating the presence of the monomer as the major species at 36291.5 Da close to the expected value of 36295 Da predicted from the primary sequence.

B.) Raw Data

A

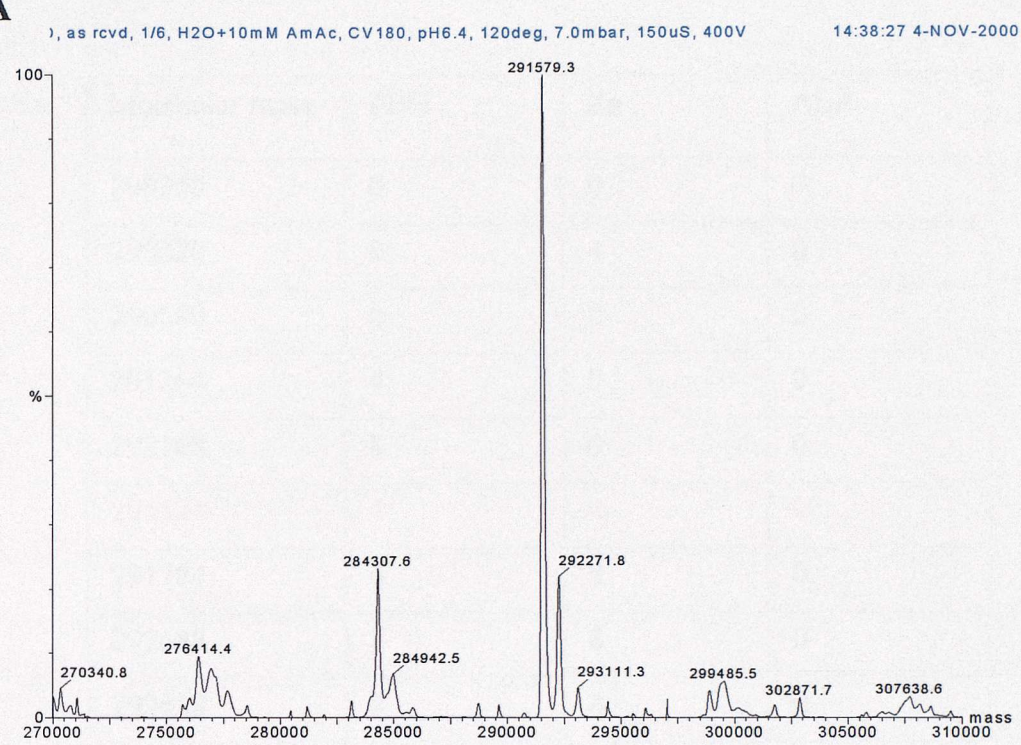

B

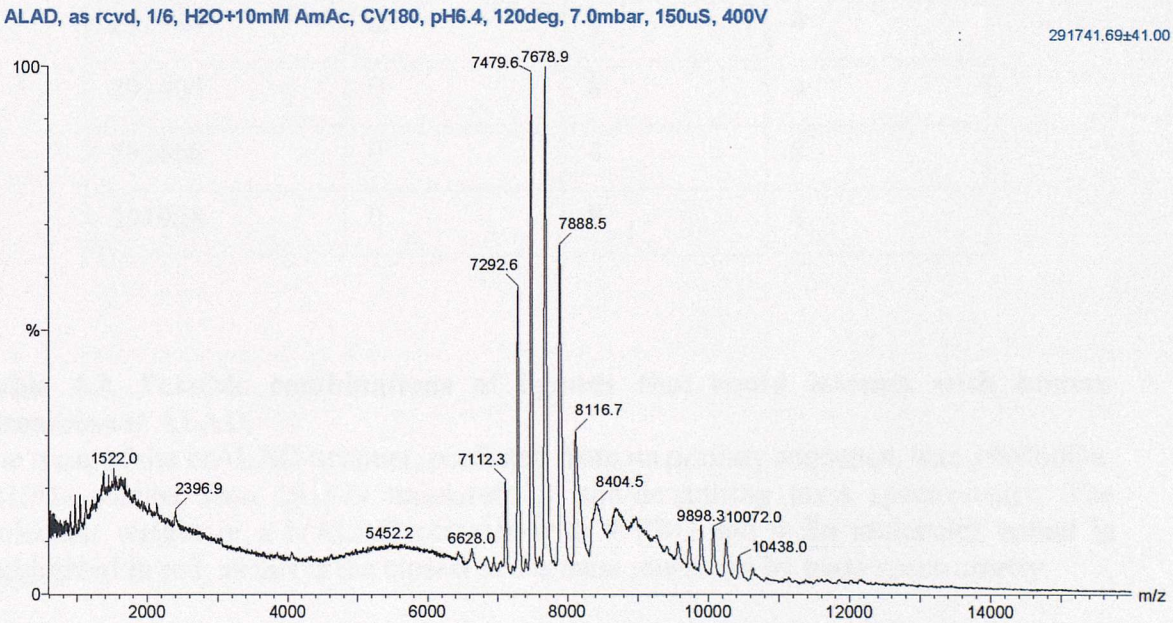

Figure 4.3 LCT-MS Electrospray mass spectra of hrALAD in 10 mM aqueous ammonium acetate, pH 7.0.

(Kindly measured by Dr Iain Campuzano (Micromass UK).

A.) Maximum entropy 1 deconvoluted spectra of native hrALAD, indicating the presence of the octamer as the major species at 291,579Da. The expected value of the octamer was 290,360Da, predicted from the primary sequence, as the measured mass was 1219Da greater than expected this indicate the presence of molecules associated with octamer.

B.) Raw data.

Molecular mass	PBG	Zn	ALA
290360	0	0	0
290620	0	4	0
290880	0	8	0
291264	4	0	0
292168	8	0	0
291524	4	4	0
291784	4	8	0
292688	8	8	0
292428	8	4	0
290884	0	0	4
291408	0	0	8
291144	0	4	4
291404	0	8	4
291668	0	4	8
291928	0	8	8

Table 4.2. Possible combinations of ligands that could interact with human recombinant ALAD.
The mass of the hrALAD octamer, predicted from its primary sequence, was 290360Da, 1219Da smaller than 291579 measured by non-denaturing mass spectrometry. The molecular weight of a hrALAD octamer with 4 PBG and 4 Zn molecules bound is highlighted in red, as this is the closest to the mass measured by mass spectrometry.

4.2.3 Experiments to determine the origin of the ligand seen at the active site of hrALAD.

Several experiments were performed to determine the origin of the molecule found at the active site of the crystallised hrALAD. Tests with Ehrlich's reagent revealed the ligand at the active site was not, as first thought, PBG despite its similarity in structure as seen by X-ray crystallography. The experiments described in the section were carried out in collaboration with James Youell, a fellow postgraduate.

To determine that the ligand at the active site was derived from the substrate, ALA, a series of experiments were performed utilising ^{14}C-ALA. The ^{14}C-ALA used had a specific activity of 51.5mCi/mmol. Labelled ALA (10nmoles, 515nCi) was diluted with unlabelled ALA (600nmoles) and added to 1mg of hrALAD (30nmoles of subunit) in 100mM Tris-HCl, pH 7.0, containing, 50 μM Zn and 5mM DTT, followed by incubation for 5 minutes at 37°C. The enzyme mixture was loaded onto a Pharmacia PD10 column and eluted with 100mM Tris-HCl, pH 7.0, containing, 50μM Zn and 5mM DTT. The eluant was collected in fractions of approximately 0.5ml. The enzyme activity, PBG concentration, protein concentration and carbon-14 counts were measured and recorded for each fraction (figure 4.4 A). The carbon-14 content was measured, after dilution with scintillation fluid, by a Beckman LS6500 counter.

It was immediately apparent that most of the carbon-14 label eluted in the later fractions indicative of small molecules (figure 4.4A). It is most likely that the labelled ALA was converted into PBG during the incubation and the product and enzyme were separated on the PD10 column. The enzyme eluted first due to size and was detected by activity assays and protein assays (see chapter 2 for experimental detail). The product (PBG), now labelled with carbon-14, was also detected in fractions using Ehrlich's reagent (figure 4.6).

It was of great interest to note that some of the carbon-14 label remained associated with the enzyme after the gel filtration (PD10 column). This indicates the molecule seen at the active site in the X-ray crystallographic structure of hrALAD is derived from the substrate ALA, as proposed. The stoichiometry of ALA:hrALAD was calculated and

each monomer of hrALAD appeared to be associated with two molecules of ALA. This is strong evidence of the presence of an intermediate at the active site of the enzyme and importantly, the enzyme was shown to be active with activity assays of each fraction.

4.2.4 Stoichiometry of ALA binding to hrALAD.

The ALA (10nmoles) labelled with carbon-14 was used as a radioactive tracer in 600nmoles of unlabelled ALA. ALA (10nmoles) with a specific activity of 51.5mCi/mmol ALA contained 515.5nCi (1133000dpm) of ^{14}C radioactivity. The radioactivity associated with the hrALAD, after elution from the PD10 column, was measured. Accounting for dilution, 1mg of hrALAD (30nmoles of subunit) was found to associate with equivalent to 59.57nmoles of ALA. As 30nmoles of enzyme is associated with approximately 60nmoles of ALA this indicates each subunit of enzyme binds 2 molecules of ALA.
($1\mu Ci = 2.2x10^6$ dpm)

4.2.5 Turnover of the putative intermediate.

Enzyme containing the label from the previous experiment (300μg; 10nmoles) was incubated with excess unlabelled ALA (600nmoles), with the aim of replacing the labelled molecule at the active site, demonstrating it was subject to turnover. As can be seen in figure 4.4B, most of the carbon-14 label eluted much later than the enzyme, indicating that the molecule had been prompted to dissociate from the enzyme by the presence of fresh unlabelled substrate. A small amount approximately 3.5% remained associated with the enzyme the rest of the label eluted in the later fractions, which tested positive for PBG with Ehrlich's reagent. This indicates the putative intermediate is subject to turnover in the presence of the substrate ALA and is a true intermediate.

To determine the radiolabelled ALA was not just non-specifically associated with the hrALAD, and could only be removed from the enzyme in the presence of fresh substrate, a control experiment was performed. The labelled hrALAD from the first experiment was again loaded onto a PD10 column and eluted with buffer. The label was detected in the fractions containing enzyme, which indicates the radiolabel remains

bound to the enzyme during gel filtration and is only liberated in the presence of fresh substrate.

4.2.6 Effect of laevulinic acid and PBG on the turnover of the putative intermediate

As it had been established the substrate, ALA, induced the release of the molecule at the active site, the ability of other molecules to induce turnover was investigated. Laevulinc acid is a substrate analogue of ALA and is a potent inhibitor of ALAD. It was thought that laevulinic acid would bind to the active site causing the putative intermediate to turnover and be released as labelled PBG. Enzyme containing the label from the previous experiment (approximately 250μg; 10nmoles) was incubated with excess unlabelled laevulinic acid (600nmoles) (figure 4.5A) or excess PBG (300nmoles) (figure 4.5B) for 1hr at 37°C, with the aim of replacing the labelled molecule at the active site, demonstrating it was subject to turnover. Both laevulinic acid and PBG caused the enzyme to release the bound labelled molecule, leaving only a small amount of label associated with the enzyme (8% of the label remained bound to the enzyme after incubation with laevulinic acid, whereas 10% of the label remained bound to the enzyme after incubation with PBG).

It is likely that the presence of ALA, laevulinic acid or PBG would induce the enzyme to complete the catalytic cycle liberating labelled PBG. However, the small amount of PBG liberated from the enzyme, after incubation with laevulinic acid, would be too dilute to be detected using Ehrlich's reagent so it is not certain the radioactive labelled molecule is PBG. It could be detected using HPLC, and an Ehrlich's test could be carried out on the concentrated fractions as a final confirmation.

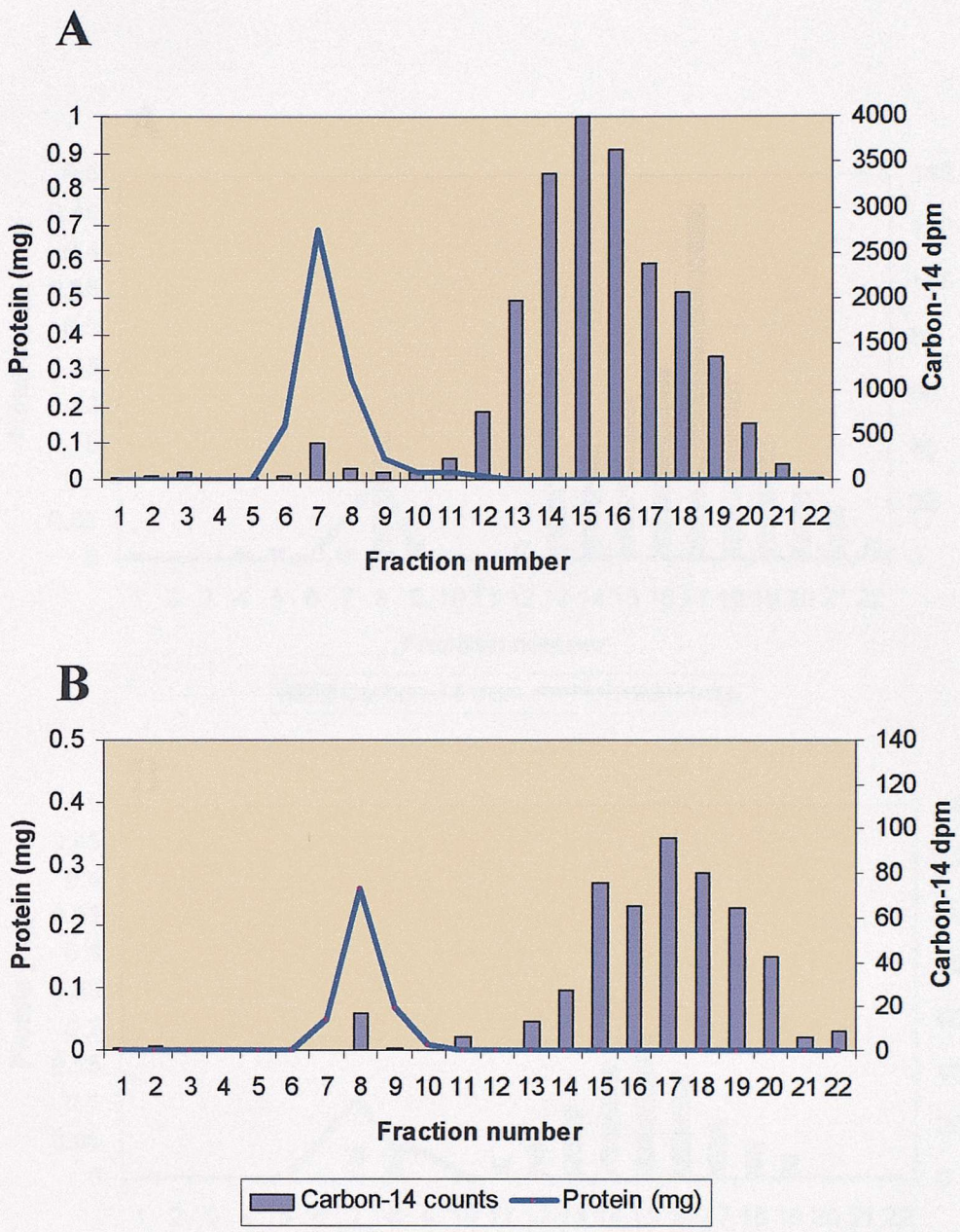

Figure 4.4 Graph to show association of hrALAD with radiolabelled ALA, under different conditions.

A.) Graph showing the elution from PD10 column after the hrALAD had been incubated with labelled tracer. The larger molecules elute earlier during gel filtration, the enzyme elutes in fractions 6-9. The smaller product PBG, which is labelled with carbon-14, elutes later in fractions 12-20. It is of great interest to note that some carbon-14 label remains associated with the enzyme, indicating some ALA or intermediate derived from ALA remains bound to the enzyme.

B.) Graph displaying the elution from the PD-10 column after the hrALAD from the previous experiment had been incubated with unlabelled ALA in an attempt to remove the radioactive label from the enzyme. It can clearly be seen that most of the radioactive label has been displaced from the enzyme and although a residual amount remains bound, perhaps indicating how strongly ALAD binds to the molecule at the active site.

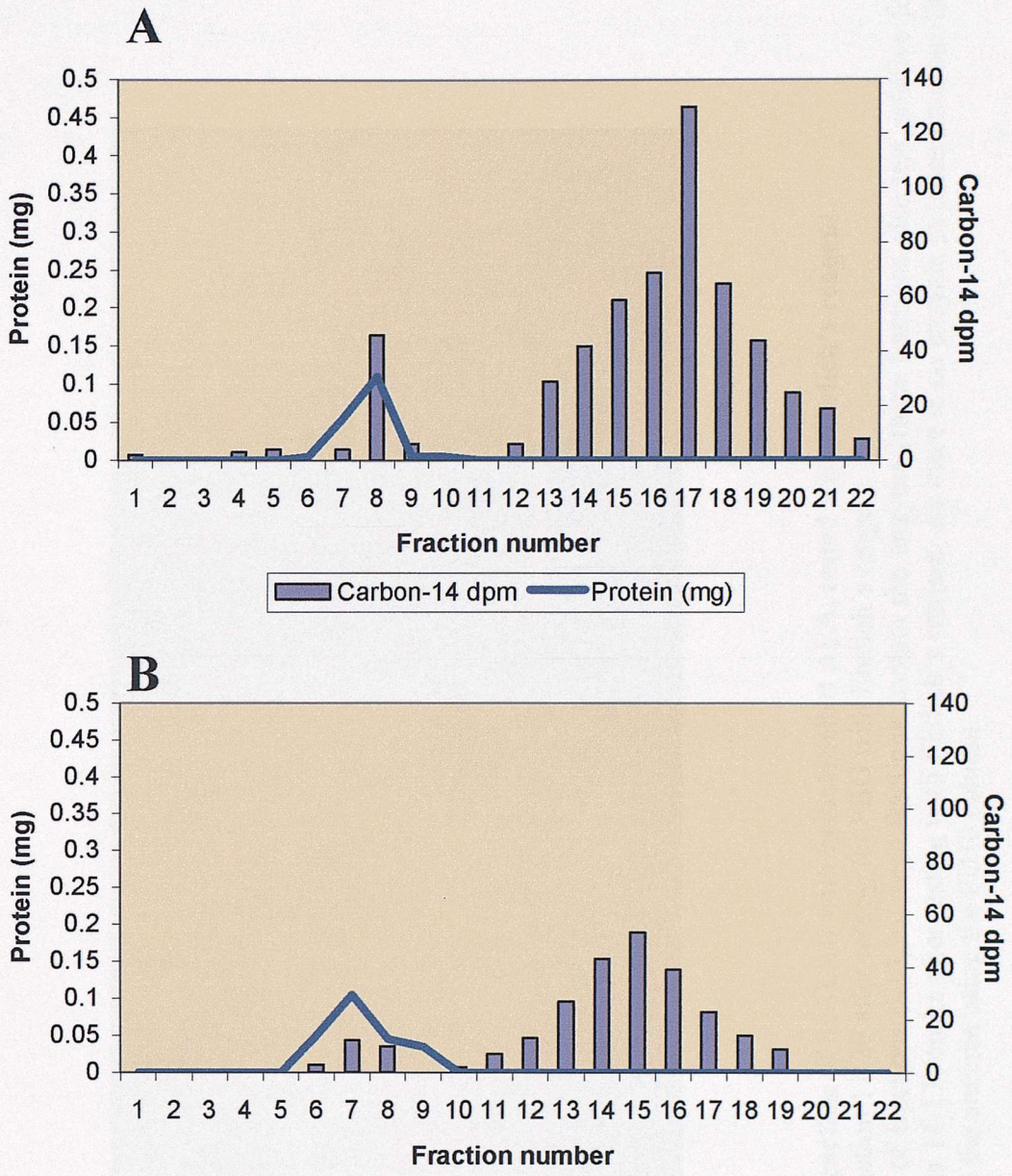

Figure 4.5 Graphs to show the association of radiolabelled ALA with hrALAD after incubation with laevulinic acid and PBG.

A.) Graph showing the elution from PD10 column after the hrALAD containing the labelled ^{14}C-ALA was incubated with laevulnic acid. The larger molecules elute earlier during gel filtration, the enzyme elutes in fractions 6-9. The majority of the label is eluted later, in fractions 12-22, indicating that laevulinic acid is causing the release of the labelled molecule from the enzyme. It is of great interest to note that slightly more some carbon-14 label remains associated with the enzyme, than detected when ALA is used (figure 4.4B) This indicates that laevlunic acid is able to induce the release of labelled molecules but not as efficiently as ALA.

B.) Graph showing the elution from PD10 column after the hrALAD containing the labelled ^{14}C-ALA was incubated with PBG. Incubation with the product PBG has a similar effect to incubation with laevulinc acid. It causes the release of most of the label from the enzyme, but not as efficiently as ALA.

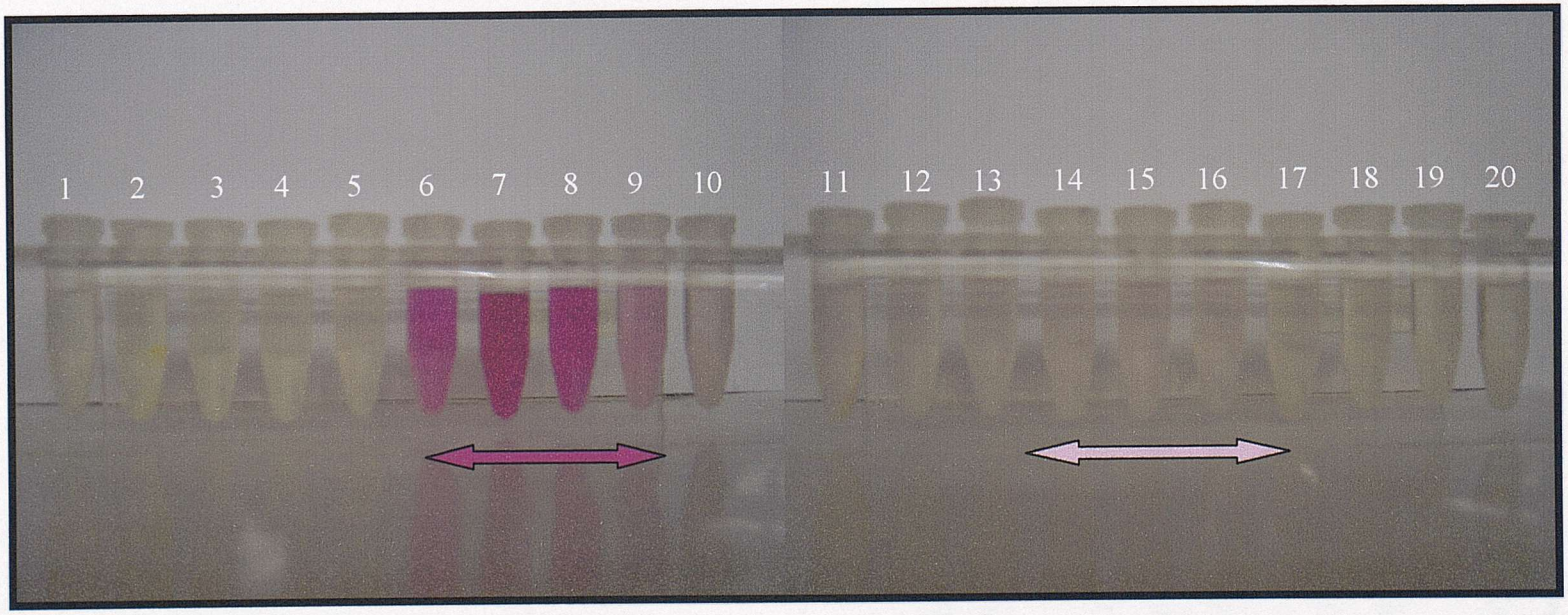

Figure 4.6 Eluant of the PD10 column, after reaction of hrALAD with radiolabelled ALA, tested with Ehrlich's reagent.
Fractions 1-10 after ALAD activity assay and fraction 11-20 after testing for PBG with Ehrlich's reagent.
The intense pink colour is seen after the assay of fractions 6-10, as these fractions contain the enzyme (these fractions also test positive for protein). The lighter pink colouration of fractions 14-17 results after testing with Ehrlich's reagent. As there is no enzyme in these fractions the colour must result from PBG was separated from the enzyme using the PD10 column.

4.2.7 Crystallisation and preliminary X-ray studies on human recombinant ALAD

The hrALAD was crystallised in an attempt to provide a clearer image of the interactions at the active site of ALAD with the putative intermediate.

ALAD at approximately 10mg/ml was used for a crystal screen based on the same crystallisation conditions employed for the ALAD purified from human erythrocytes [28], described in chapter 2. Crystals were grown in 0.1M Mes buffer, containing ammonium sulphate and dioxane. The effect of the pH of the 0.1M Mes buffer on crystal growth was investigated using 3 different pH values, pH 6.2, 6.4 and 6.8. The concentration of ammonium sulphate was varied from 1.0M to 1.6M. The dioxane concentration was also varied at 0%, 1%, 5% or 10% (Figure 4.7A). The hrALAD crystal used for crystallographic studies was a very large plate-shaped crystal, almost 1mm in length, similar to the crystal shown in figure 4.7B. The structure was solved by Dr Peter Erskine (Southampton University).

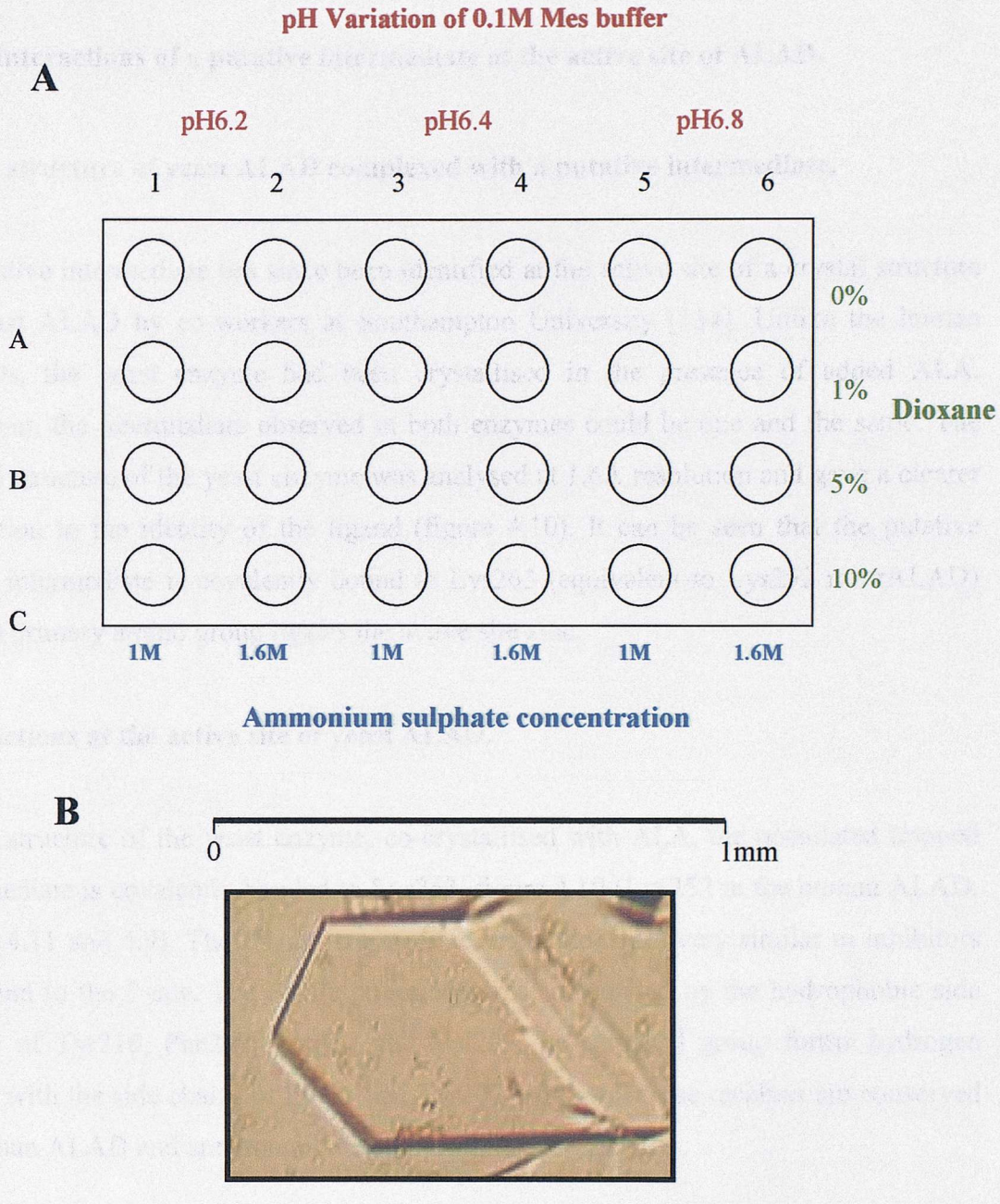

Figure 4.7 Crystal screen for human recombinant ALAD.

A.) Crystal screen used to crystallise hrALAD. Crystals were grown in 0.1M Mes buffer, containing ammonium sulphate and dioxane. The effect of the pH of the 0.1M Mes buffer on crystal growth was investigated using 3 different pH values, pH 6.2, 6.4 and 6.8. The concentration of ammonium sulphate was varied from 1.0M to 1.6M. The dioxane concentration was also varied at 0%, 1%, 5% or 10%. The protein concentration used was 10 mg/ml.

B.) HrALAD crystal similar to the one used for X-ray diffraction. The crystal used for X-ray diffraction studies was grown in 0.1M Mes buffer, containing 1.6M ammonium sulphate and 1% dioxane at a protein concentration of 10mg/ml.

4.2.8 Interactions of a putative intermediate at the active site of ALAD.

X-ray structure of yeast ALAD complexed with a putative intermediate.

A putative intermediate has since been identified at the active site of a crystal structure of yeast ALAD by co-workers at Southampton University [134]. Unlike the human ALADs, the yeast enzyme had been crystallised in the presence of added ALA. However, the intermediate observed in both enzymes could be one and the same. The crystal structure of the yeast enzyme was analysed at 1.6Å resolution and gave a clearer indication to the identity of the ligand (figure 4.10). It can be seen that the putative cyclic intermediate is covalently bound to Lys263 (equivalent to Lys252 in hrALAD) and its primary amino group ligates the active site zinc.

Interactions at the active site of yeast ALAD.

In the structure of the yeast enzyme, co-crystallised with ALA, the postulated trapped intermediate is covalently bonded to Lys263, figure 4.10 (Lys252 in the human ALAD, figure 4.11 and 4.9). The P-side intermediate interactions are very similar to inhibitors that bind to the P-site. The P-side intermediate is surrounded by the hydrophobic side chains of Tyr216, Phe219, Tyr287 and Val289. Its carboxyl group forms hydrogen bonds with the side chains of Phe89 and Tyr207 [134]. All these residues are conserved in human ALAD and are thought to act in a similar fashion.

The A-site is formed by the enzymes zinc ion and a number of invariant residues such as, Arg220, Arg232 and Gln236. The arginine side chains were found to interact with the A-side carboxyl (this was also seen in the 4,7 dioxosebacic acid-ALAD complex, which occupies the A and P sites [41].

4.2.9 Implications for the catalytic mechanism

Despite various available crystal structures, including some with substrate analogues bound to the active site [25, 26, 40, 42, 131, 137] the mechanism is still relatively uncharacterised. The synthesis of PBG requires the formation of a C-C bond and a C-N bond between the substrate molecules, but it is not known which occurs first.

The structure of a putative intermediate from the yeast and human enzyme suggests the A-side ALA is in contact with a zinc bound hydroxide, a strongly basic group, which could act on the C-3 of the A-side ALA. The recently proposed double schiff base mechanism [42] would assist in the deprotonation of the C-3 carbon atom, yielding an enamine (Figure 4.8). This could lead to nucleophillic attack of the enamine in the A-site on the C-4 of P-side ALA, forming the C-C bond. The intersubstrate C-N bond would then be able to form which would yield the putative intermediate found in the crystal structures, indicated by a star in figure 4.8.

The C-N bond is unlikely to occur first as this would imply the schiff base formed between Lys199 and A-site ALA would serve no catalytic role other than to hold the A-side ALA in the correct orientation.

The stability of this ligand is remarkable. The human enzyme was subjected to multiple steps of heat treatment, dialysis and chromatography and the ligand remained at the active site. This indicates a conformational change may be needed to complete the final steps of catalysis and release PBG. It is possible that the structure of the ligand at the active site is only seen due to the crystallisation conditions, and exists differently in solution. It is important to note that the crystallisation conditions did not adversely affect the activity of the enzyme, the re-dissolved human ALAD crystals had the same specific activity as human enzyme left at room temperature for two weeks (the length of crystallisation). This indicates the ligand seen at the active site does not adversely affect the activity of the enzyme.

The question to why the enzyme has such a ligand attached to the active site and does not simply complete the catalysis remains unanswered, but the presence of substrate may trigger the release of PBG.

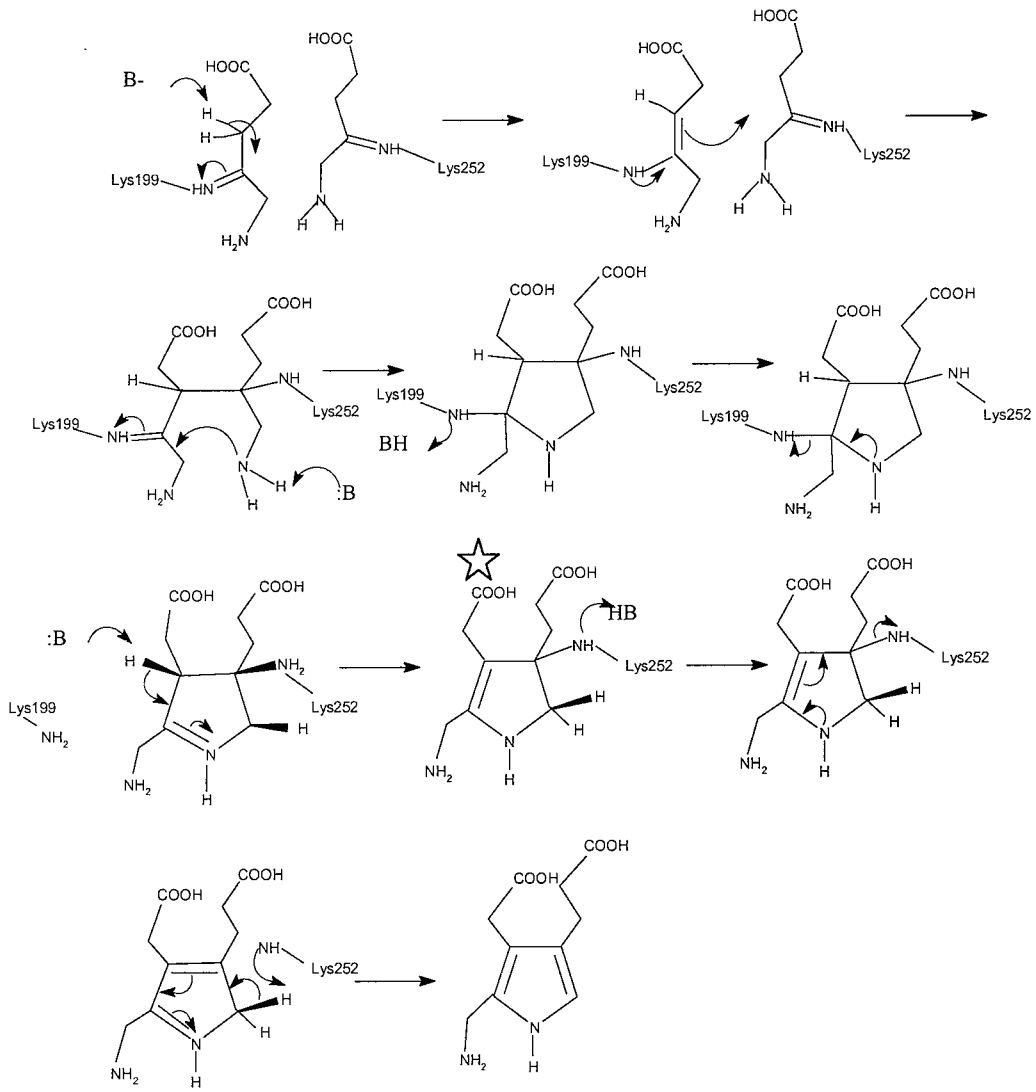

Figure 4.8 A possible mechanism for ALAD.
Two Schiff bases form between Lys252 and Lys199. The Schiff base formed with Lys199 may allow proton abstraction at the C-3 position of A-side ALA, which could lead to nucleophillic attack on the P-side ALA forming the C-C bond linking the two substrates. The C-N bond would then form followed by the loss of the second deprotonation of the A-site substrate to yield the putative intermediate found in the crystallised enzymes. It its though that the final steps of catalysis may require conformational changes of the enzyme. The putative intermediate is labelled with a star (☆). Adapted from Erskine *et al*, [134].

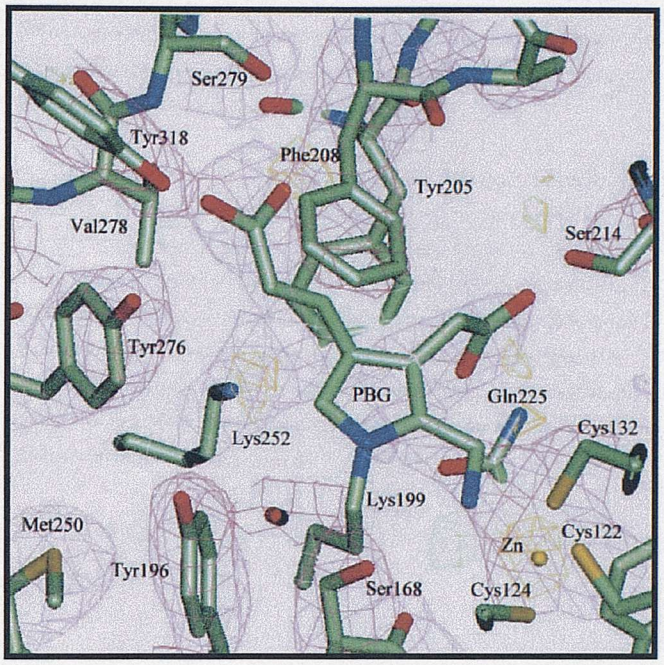

Figure 4.9 Active site of human ALAD from the crystal stucture of ALAD purified from human erythrocytes.
PBG was modelled to fit the electron density in the active site [32].

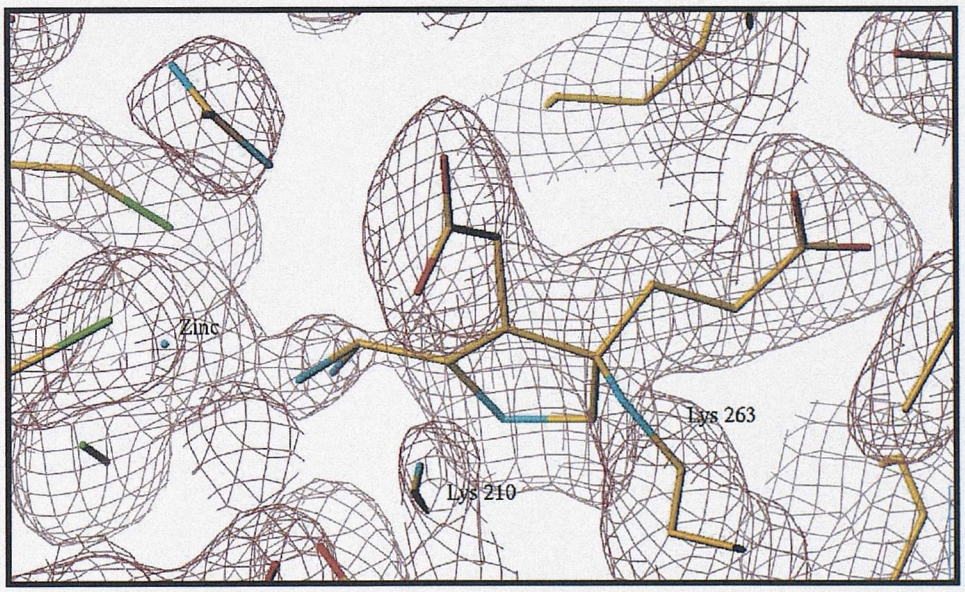

Figure 4.10 The electron density map of the putative intermediate covalently bound to the Lys263 of yeast ALAD at 1.6Å resolution.
The P-site is on the right-hand side and the A-site is formed by residues on the left-hand side, including the zinc ion. The other invariant lysine is in the foreground to the left of Lys263 but has been omitted for clarity. Image provided by J. B. Cooper, Southampton University.

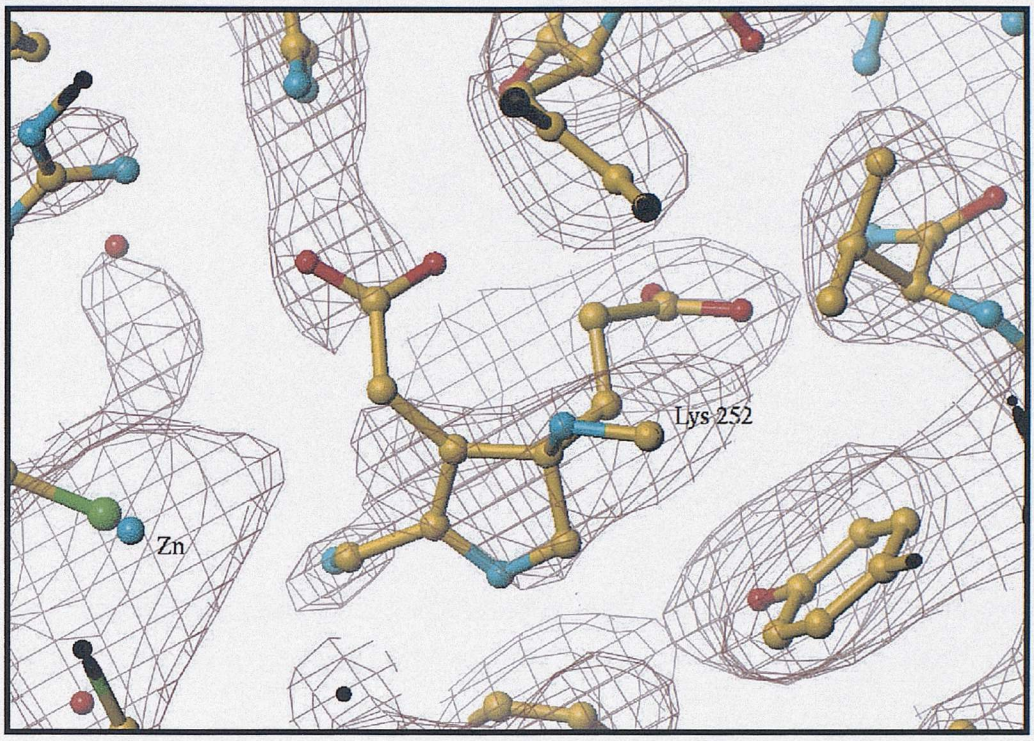

Figure 4.11 The electron density map of the putative intermediate covalently bound to the Lys252 of hrALAD at 2.8Å resolution.
The P-site is on the right-hand side and the A-site is formed by residues on the left-hand side, including the zinc ion. The other invariant lysine is in the foreground to the left of Lys-252 but has been omitted for clarity. Image provided by Dr. Peter Erskine, Southampton University.

4.3 Conclusions

A putative intermediate was first observed at the active site of human ALAD, crystallised after purification from erythrocytes, by N. Mills-Davis a fellow postgraduate. PBG was modelled into the density at the active site, as the molecule was at first thought to be the product bound to half the active sites [28]. It was previously reported from NMR studies, on bovine and *E.coli* ALAD, that product was tightly bound to the enzyme [135, 138]. On this basis N. Mills-Davis suggested mammalian ALADs possessed half site reactivity [28].

To confirm, using biochemical experiments, that PBG was at the active site of hrALAD, hrALAD was tested for reaction with Ehrlich's reagent, which should produce a pink coloured adduct (see figure 4.1) with pyrroles such as PBG [121]. However, the enzyme-ligand complex did not react with Ehrlich's reagent, which shows that the ligand is not a pyrrole, i.e. it does not contain a free α-position to react with the aldehyde of the Ehrlich's reagent. Different conditions were investigated in an attempt to liberate any PBG product from the enzyme, including, incubation at range of pH values and incubation with EDTA (table 4.1).

As the possibility that PBG was bound at the active site of human ALAD was excluded by its inactivity with Ehrlich's reagent, the possibility that the ligand was an intermediate in the catalytic mechanism was considered. NMR studies on ALAD by Jaffe *et al* had previously detected an unknown pyrrole-like compound, which was not PBG. It was proposed to be a derivative of PBG, which had been modified by a contaminating protein [136].

In order to obtain more information about the nature of the ligand bound to hrALAD mass spectrometry was carried out to see if it was possible to detect the presence of a specific ligand bound to human ALAD. Mass spectrometry in the presence of formic acid and acetonitrile only indicated the mass of the enzyme alone, suggesting that if the ligand is covalently attached to the enzyme, the bond is acid-labile. HrALAD was subjected to non-denaturing mass spectrometry, i.e. in the absence of solvent and acid, by Dr. I. Campuzano (Micromass UK). At pH 6.4 hrALAD was found to have a

molecular mass close to that expected if the enzyme had 4 PBG and 4 Zn bound to the enzyme (table 4.2).

The crystallisation of human ALAD was repeated with hrALAD in an attempt to achieve a higher resolution structure, which would provide a clearer indication to the identity of the ligand at the active site. The hrALAD protein was isolated in less than a week and had a specific activity 2-fold higher than ALAD purified from erythrocytes (some molecules of ALAD from erythrocytes could be up to 120 days old) [32].

Although the hrALAD was only solved to 2.8Å (the same resolution as the erythrocyte ALAD [32]) and did not provide a higher resolution picture of the active site, some residues were apparent in the hrALAD structure, that were disordered in the erythrocyte ALAD structure. More importantly, convincing electron density for the active site ligand was seen in four out of the eight active sites, as seen in the native erythrocyte ALAD structure. This is an interesting finding as it suggests the human ALAD is half site reactive, as proposed previously [28]. PBG can be modelled into the electron density at the active site, however, reaction of hrALAD with Ehrlich's reagent produced a negative result. If the molecule at the active site was a reaction intermediate, this could provide an explanation for these findings. It is possible that the electron density at the active site is due to an advanced reaction intermediate, similar to PBG. The fact that the enzyme is Ehrlich's reagent negative provides very strong evidence for the presence of a reaction intermediate.

Recently, such a putative intermediate has been identified at the active site of a crystal structure of yeast ALAD [134]. Unlike the human ALADs, the yeast enzyme had been crystallised in the presence of ALA. However, it is likely to be the same intermediate observed in both enzymes. The crystal structure of the yeast enzyme was analysed at 1.6Å resolution and gives a far clearer indication to the identity of the ligand. It can be seen that the putative cyclic intermediate is covalently bound to Lys263 and its primary amino group ligates the active site zinc (Figure 4.10).

Interestingly, the hrALAD was not incubated with ALA during crystallisation, yet still showed electron density at the active site. Presumably the putative intermediate remains tightly bound to the active site of the ALAD throughout multiple purification steps,

including heat treatment, dialysis and two chromatography steps, indicating that the intermediate is stable during purification.

There is a great deal of evidence to suggest mammalian ALADs are half site reactive and it is clear the mechanisms controlling half site reactivity are complicated. The crystal structure of hrALAD has four out of eight active sites occupied by the ligand, non-denaturing mass spectrometry also indicates the presence of 4 ligands (with the same molecular mass as PBG) bound to hrALAD. However, the radiochemical experiments with labelled ALA indicate the equivalent of 16 molecules of ALA bound to every octamer, this may be due to the high levels of ALA in the incubation, as ALA was not added during crystallisation or mass spectrometry. The levels of ALA *in vivo* are tightly regulated and the concentration of ALA in the radiochemical experiments are far high than the concentration of ALA *in vivo.*

Despite crystal structures of human ALAD the structural basis for half site reactivity remains unclear, although a number of residues have been identified that may play an integral role. The identification of an intermediate at the active site of ALAD is of great interest. Although many structures of ALADs are known there are many aspects of the catalytic mechanism that remain unresolved. The identification of a reaction intermediate provides information on interactions at the active site and assists in predicting a possible reaction mechanism.

Chapter five: Characterisation and crystallisation of recombinant human PBGDs

5.1 Introduction

Porphobilinogen deaminase (PBGD) was described by Bogorad in 1958 [139] and has since been isolated from a variety of sources including human [60, 61], and *Rhodobacter sphaeroides* [59].

Human porphobilinogen deaminase is encoded by a single gene of 10kb, encompassing 15 exons [65, 107], located on chromosome 11. The gene contains two promoters and is differentially transcribed and spliced in a tissue-specific manner to give ubiquitous (houskeeping) and erythroid mRNAs [80]. The ubiquitous isoenzyme, specified by exon 1 and exons 3-15, has 361 amino acids whereas the erythroid isoenzyme, specified by exons 2-15 is smaller with 344 amino acids (figure 5.1). The ubiquitous isoenzyme has a M_r of 39,330 and includes an *N*-terminal extension that is 17 amino acids longer than the erythroid enzyme, M_r of 37,699.

The X-ray structure of porphobilinogen deaminase was first determined in 1992 using the *E. coli* enzyme [66] and subsequently refined to a resolution of 1.76Å [71]. The three-dimensional structure has vastly increased our understanding of how the enzyme is folded and how it accommodates the dipyrromethane cofactor.

When the primary amino acid sequences for human and *E. coli* porphobilinogen deaminases are aligned, 46% of the residues are identical but over 60% are similar in nature. This allowed the construction of a molecular model for the human enzyme [140].

Despite the broad similarities between the *E. coli* and human deaminases, there are a few differences between the enzymes that make it essential to determine the X-ray structure of both human deaminases. One such difference between the *E.coli* and the human enzymes is an insertion of 29 amino acids in domain 3 in the human enzyme. In

addition, the ubiquitous human enzyme has an *N*-terminal sequence of 15 extra amino acids compared with the *E. coli* deaminase. There are also a few residues which when mutated are thought to cause acute intermittent porphyria (AIP) in humans, but are not conserved in *E.coli*, which make it difficult to predict the precise effects of human mutations that lead to AIP, using the model based on the *E.coli* enzyme.

Studies on the heterogeneity of purified recombinant human ubiquitous PBGD are presented in this chapter. The heterogeneity of PBGD purified from human erythrocytes has been noted previously [60, 61]. Both erythroid and ubiquitous isoenzymes were found to produce two bands when analysed by non-denaturing PAGE. HruPBGD was found to separate on a strong anion exchange (Mono Q) column into two separate active forms described in this thesis as A and B. The A and B forms of hruPBGD had similar properties and appeared homogenous by SDS-PAGE. Both forms of deaminase were found to elute as a single peak from gel filtration and after separation both species were found to have a specific activity of 2.1 μmol/mg/hr and pH optima of 8.2.

Initially it was postulated that this heterogeneity could be attributed to an enzyme-substrate (ES) intermediate, which would have an altered electrophoretic mobility. However, subsequent investigations described in this chapter suggest this postulation is incorrect. Additionally, the determination of a 1Da difference between the two species by mass spectrometry suggested the heterogeneity was not due to an ES intermediate as the substrate molecules are covalently bound to the enzyme and would be detectable by mass spectrometry.

This chapter describes unsuccessful attempts to interconvert the two deaminase species, using heat, hydroxylamine and enzyme turnover, and also details the attempts to identify the molecular difference between species A and B from peptides generated from V8 protease and tryptic digestion, using reverse phase high performance liquid chromatography and mass spectrometry.

This chapter also details attempts to obtain crystals of the ubiquitous and erythroid enzymes for determination of their X-ray structures. Both isoenzymes were purified and

crystallised. However, only crystals of the erythroid isoenzyme were of diffractable quality.

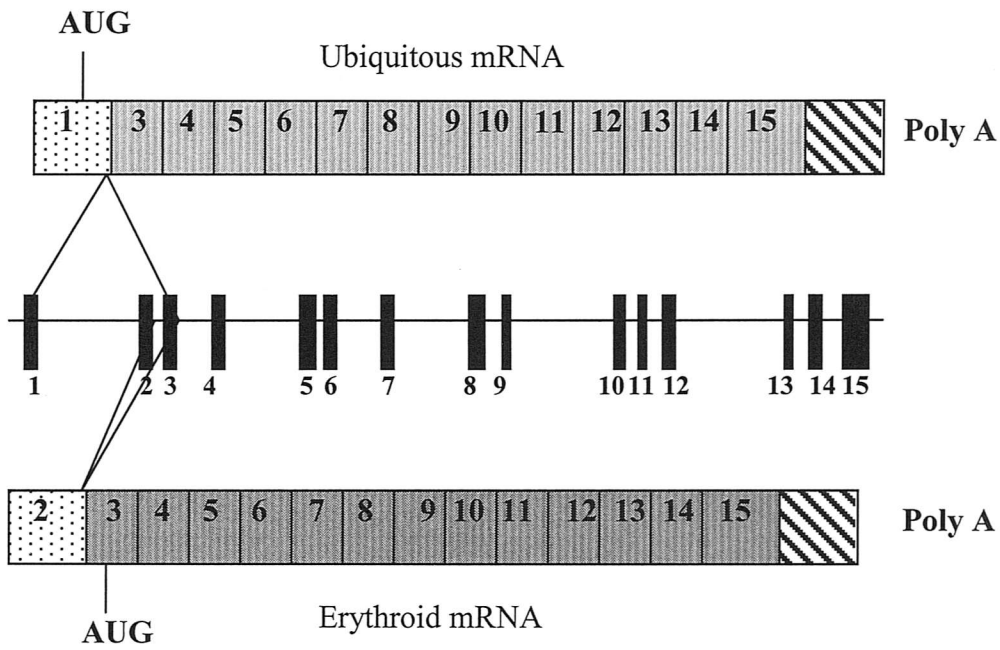

Figure 5.1 Genomic organisation of the human porphobilinogen deaminase gene and alternative splicing of the ubiquitous (housekeeping) and erythroid specific transcripts.
Adapted from Deybach and Puy 1995 [141].

5.2 Results.

5.2.1 Purification of human recombinant ubiquitous PBGD (hruPBGD).

The purification of hruPBGD is summarised in table 5.1 and is described in detail in chapter 2. The specific activity is more than 13 fold of the sonicated extract. Recovery was approximately 16% based on the total activity of the sonicated extract. The purification of the enzyme was monitored by SDS-PAGE. The purified hruPBGD appeared to be "homogenous" by SDS-PAGE producing a single band at approximately 45kDa (figure 5.2).

Step	Volume (ml)	Total protein (mg)	Total activity μmoles/hr	Specific Activity μmoles/mg/hr	% Yield
After sonication	90	1637.4	255.4	0.16	100
After heat treatment and ultracentrifuge	86	303.2	203.8	0.67	80
After DEAE ion exchange	190	45.1	78.5	1.7	31
Concentrated fractions after G-75	8	19.6	41.3	2.1	16

Table 5.1 The specific activities and yield of the hruPBGD at different stages of purification, starting from 2.4L of *E.coli*.

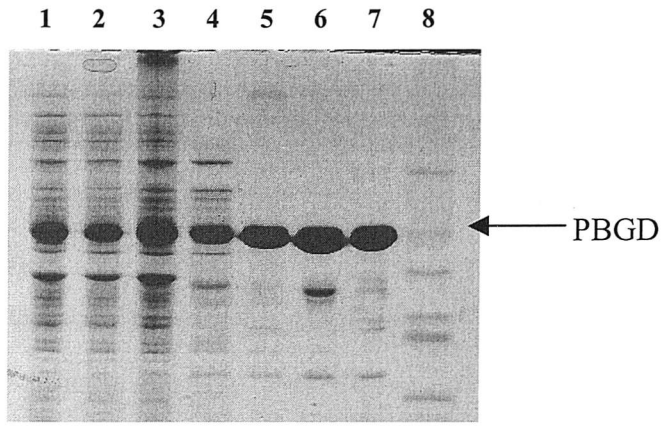

Figure 5.2 SDS-PAGE of samples taken from each stage of the hruPBGD enzyme purification.
Lane 1, resuspended cells; lane 2, sonicated extract; lane 3, heat treated extract; lane 4, supernatant after heat treatment and ultracentrifugation; lane 5, after DEAE-sephacryl column; lane 6/7, after gel filtration and lane 8, Dalton VII protein standards.

5.2.2 Purification of human recombinant erythroid PBGD (hrePBGD)

The purification of hrePBGD is summarised in table 5.2 and is described in detail in chapter 2. The specific activity is more than 15 fold of the sonicated extract. Recovery was approximately 20% based on the total activity of the sonicated extract. The purification of the enzyme was monitored by SDS-PAGE. The purified hrePBGD appeared to be "homogenous" by SDS-PAGE producing a single band at approximately 45KDa (figure 5.3).

Step	Volume (ml)	Total protein (mg)	Total activity µmoles/hr	Specific Activity µmoles/mg/hr	% Yield
After sonication	101	1351.3	225.4	0.168	100%
After heat treatment	94	259.4	192.9	0.744	86%
After DEAE ion exchange	180	36.4	77.22	2.12	34%
After G-75	8	18	45.92	2.55	20%

Table 5.2 The specific activities and yield of the hrePBGD at different stages of purification, starting from 2.4L of *E.coli*.

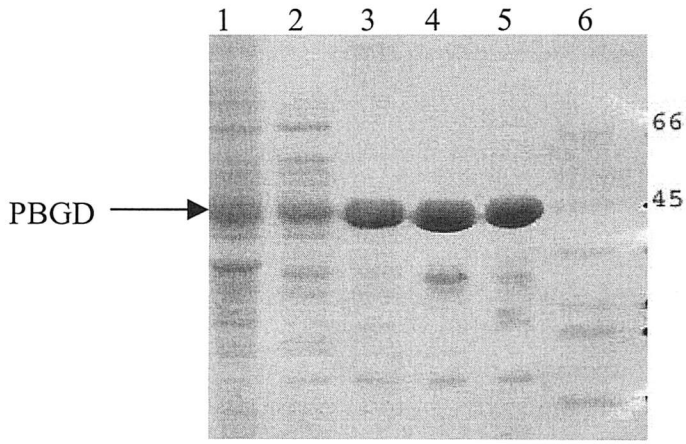

Figure 5.3 SDS PAGE analysis of stages in the purification of erythroid PBGD.
Lane 1, crude extract after sonication; lane 2, sample after heat treatment; lane 3, sample after the DEAE ion exchange column (5µg); lane 4, sample after the DEAE ion exchange column (10µg); lane 5, EPBGD after gel filtration and lane 6, Dalton VII marker.

5.2.3 Electrospray mass spectrometry (ESMS) of recombinant human porphobilinogen deaminase

Mass spectra for the human ubiquitous and erythroid PBGD were obtained by electrospray mass spectrometry using a Quattro II mass spectrometer (Fisons Instruments). Optimal spectra were produced for native protein by mixing 50µl of enzyme at 0.2mg/ml with 50µl 50% acetonitrile/ 50% H_2O/ 1% formic acid.

Previous *N*-terminal sequencing showed that the *N*-terminal methionine of recombinant human ubiquitous PBGD is clipped [142] and this was confirmed by ESMS analysis.

The spectra obtained for native ubiquitous and erythroid porphobilinogen deaminase (Figures 5.4, 5.5) agrees with the theoretical molecular masses (Table 5.3) confirming the identity of the enzymes. As expected, the cofactor, which is covalently bound to Cys261, remains bound during ESMS. Enzyme-substrate intermediates can also be visualised using this technique [143, 144].

	Mr from cDNA sequence	Expected mass (+ DPM cofactor = 420.4 mass units)	Actual mass by ESI-MS
Erythroid PBGD	37,699	38,120	38,118.8
Ubiquitous PBGD	39,330	39,751	39,615.2

Table 5.3 Table of the expected mass of hrePBGD and hruPBGD compared with the actual values achieved by electrospray ionisation mass spectrometry (ESMS). The dipyrromethane (DPM) cofactor remains bound to both the hrePBGD and the hruPBGD during mass spectrometry. It is also apparent that the *N*-terminal methionine of the hruPBGD is clipped, whereas the methionine at the *N*-terminal of the hrePBGD remains intact.

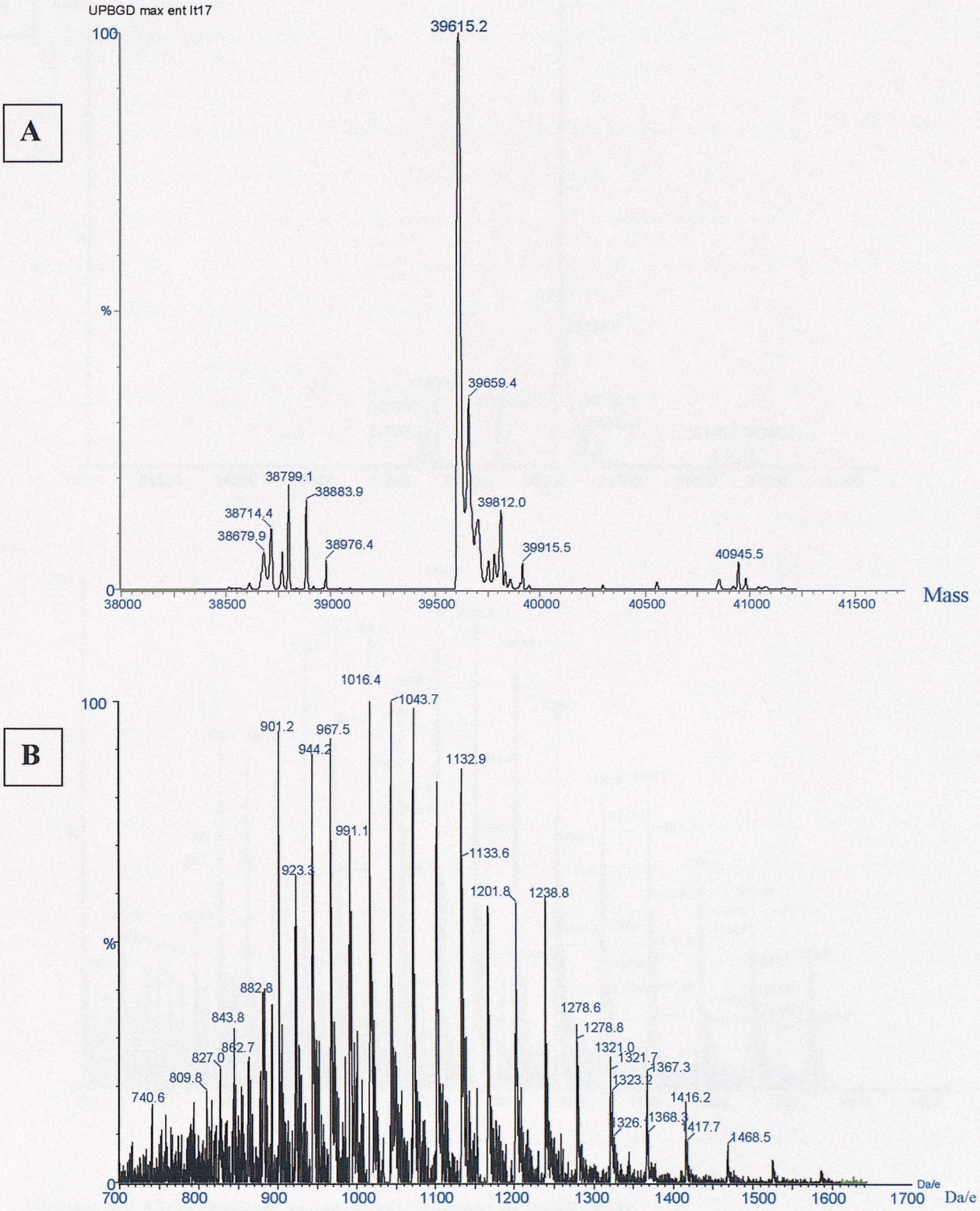

Figure 5.4 Electrospray mass spectrometry of hruPBGD

A) Maximum entropy. The Mr of 39,615 is close to the expected value of 39,620 Da the Mr expected from the primary sequence minus the mass of the *N*-terminal methionine and plus the molecular weight of the bound dipyrromethane cofactor.

B) Raw subtracted data.

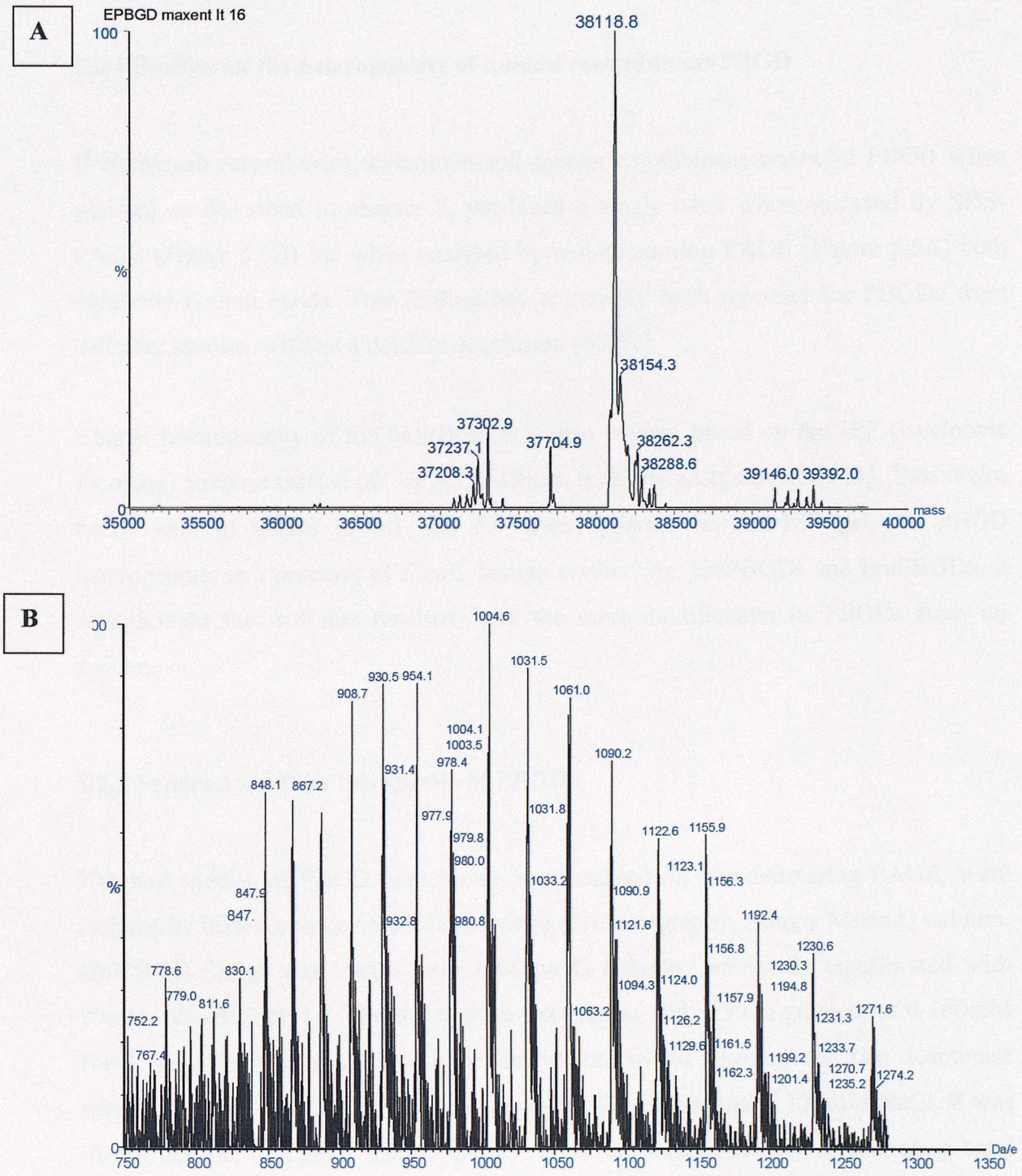

Figure 5.5 Electrospray mass spectrometry of hrePBGD.

A) Maximum entropy spectra. The main peak at 38,118.8 is close to the expected value of 38,120 Da the Mr expected from the primary sequence plus the molecular weight of the bound dipyrromethane cofactor.

B) Raw subtracted data.

5.2.4 Studies on the heterogeneity of human recombinant PBGD

Both human recombinant ubiquitous and human recombinant erythroid PBGD when purified as described in chapter 2, produced a single band when analysed by SDS-PAGE (Figure 5.6B) but when analysed by non-denaturing PAGE (Figure 5.6A) both exhibited double bands. This finding has previously been reported for PBGDs from different species, without a definite conclusion [60-62].

Charge heterogeneity of the hruPBGD was also evident based on the IEF (isoelectric focusing) analysis carried out by A. Al-Dbass, a fellow postgraduate [145]. Two major bands with pI values of 6.1 and 5.9 were apparent on the IEF gel. As PBGD heterogeneity is a property of *E.coli*, human erythrocyte, hrePBGDs and hruPBGDs, it was thought the isoforms resulted from the same modification in PBGDs from all species.

5.2.5 Separation of the two species of PBGD

The two species of PBGD, which can be visualised on non-denaturing PAGE, were isolated by high-resolution anionic exchange chromatography, using a Mono Q column. HruPBGD (2mg) was loaded onto a Mono Q column, previously equilibrated with 20mM Tris-HCl, pH7.5. The two species were eluted with a 50ml gradient of 0-160mM NaCl. Two distinct peaks elute from the column, which represent the two deaminase species (figure 5.7), the first peak eluted at 110mM, the second at 125mM NaCl. It was shown that the first peak, named species A, corresponds to the slower migrating band on native page and the second peak, named species B, eluted slightly later corresponds to the faster migrating band (figure 5.7 and 5.8). This indicated the lower, faster migrating, band is the more negatively charged of the two species.

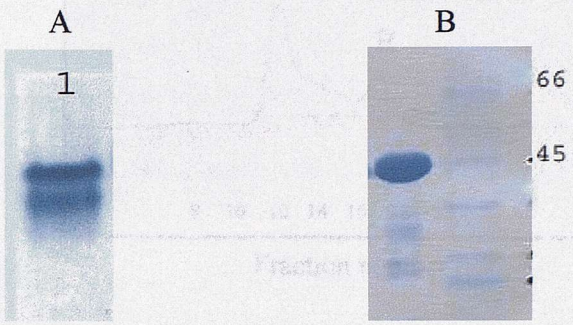

Figure 5.6 Polyacrylamide gel electrophoresis of hruPBGD

A) Non-denaturing PAGE analysis of hruPBGD,

B) SDS-PAGE analysis of hruPBGD.

A double band can clearly seen after analysis by non-denaturing PAGE, whereas, after SDS-PAGE the enzyme appears homogeneous.

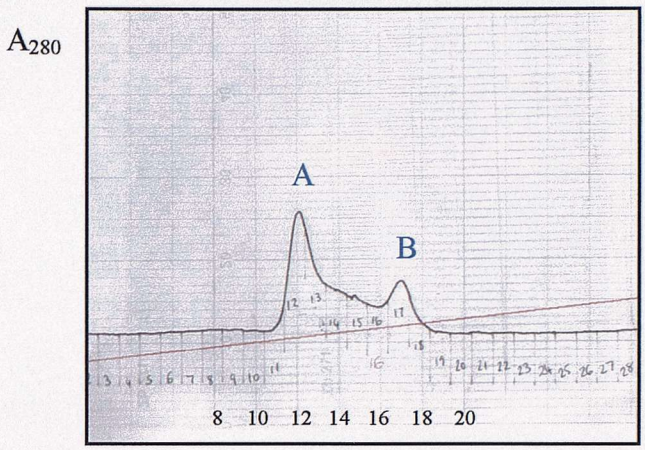

Figure 5.7 The elution profile of native ubiquitous hruPBGD from the high-resolution anion exchange chromatography column, HR5/5 Mono Q column attached to an f.p.l.c system, in an attempt to separate the heterogeneous deaminase enzyme.

The enzyme was loaded onto a pre equilibriated Mono Q column using 20mM Tris-HCl buffer, pH 7.5, then eluted at 110mM NaCl using a 50ml gradient 0-160mM NaCl. Two peaks were observed for the native ubiquitous PBGD in fractions 12-18 where the volume of each fraction was 0.5ml. The black line is absorbance at 280nm and the red line is the salt gradient.

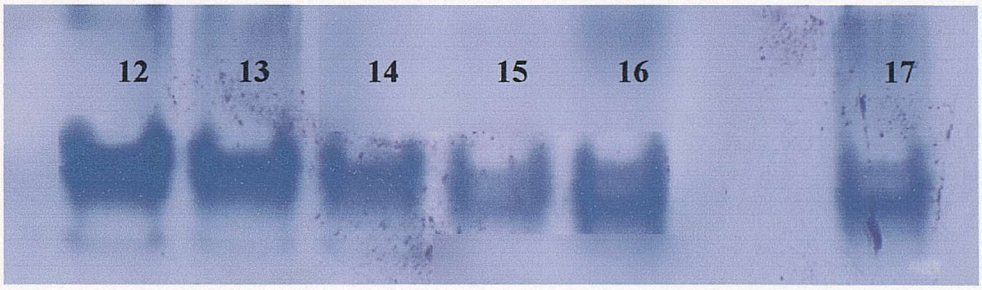

Figure 5.8 Non denaturing PAGE analysis to show the elution of native ubiquitous PBGD from a pharmacia f.p.l.c HR 5/5 Mono Q chromatography column.

Lanes are labelled with their corresponding fraction number (see figure 5.7). The protein species (A), which produces the higher band, elutes earlier from the Mono Q column, indicating it is less negatively charged than the protein species (B) eluting later, which corresponds to the lower band on the gel.

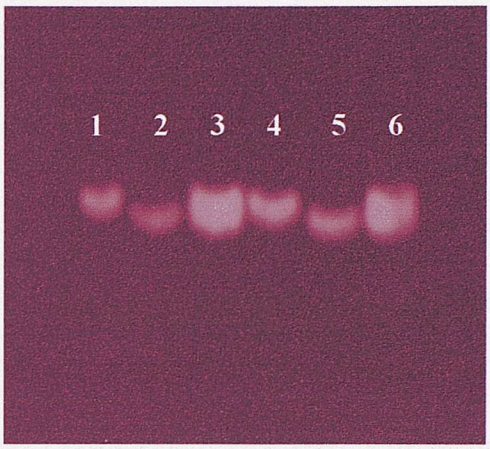

Figure 5.9 Non denaturing PAGE analysis to show the unseparated native ubiquitous PBGD and the two separated species which were subjected to an in-gel assay for PBGD activity.

Track one, protein from the first peak eluted from the Mono Q column (5μg); track two, protein from the second peak (5μg); track three, hruPBGD before separation (5μg); track four, protein from the first peak eluted from the monoQ column (10μg); track five, protein from the second peak (10μg) and track six, hruPBGD before separation. The in-gel assay was carried out as described in chapter 2. The pink fluorescence from the porphyrins formed in the assay was visualised using an uv transilluminator.

5.2.6 Characterisation of the two species of PBGD

Once isolated the two species were both assayed and their specific activities were found to be very similar.

Species A	Species B
2.11	2.06

Table 5.4. Specific activities (μmol uroporphyrin I formed/mg/hr) of the hruPBGD species.

The pH optima of both species A and B were found to be pH 8.2, this indicates the activity of species A and B had not been adversely affected.

Nanospray mass spectrometry

The electrospray ionisation mass spectrometry (ESI-MS) performed on a mixture of species A and B did not detect any molecular weight difference between the two species, a more sensitive technique, Nanospray mass spectrometry, was used to analyse both species. Nanospray mass spectrometry was carried out by Paul Skipp (Southampton University). The Nanospray mass spectrometry data indicated a difference of only 1 amu between the species, although it is not certain that the machine could distinguish such a small difference. However, this is important evidence that species B is not an enzyme substrate intermediate, as a substrate molecule would be covalently bound and detected by mass spectrometry. Clearly the difference between A and B is very subtle.

5.2.7 Attempts to interconvert the two hruPBGD species.

The possibility existed that A and B were conformers of the enzyme. The following experiments were carried out in an attempt to interconvert the two species after they had been separated. The species were not found to be interconvertable *in vitro*, i.e. once

separated species A could not revert to species B or *vice versa*. The experiments described below therefore, suggest that the double band seen by non-denaturing PAGE represents two independent species of porphobilinogen deaminase.

Heat treatment

As heat treatment is a step in the purification of PBGD, it was important to examine the effect of heat on species A and B. The crude extract and the heat-treated extract were analysed by non denaturing PAGE, rather than staining the gels with Coomassie brilliant blue, the enzyme was subjected to an 'in-gel' assay (Chapter 2). The PBGD bands could then be visualised using a u.v. transilluminator. Two bands were visible before and after the heat treatment step, indicating the two species existed in the crude extract and the heat treatment did not generate the two species.

The effect of heat on the individual species after they had been purified was also examined. Heat treatment at different temperatures (37°C and 60°C) and for different time periods (1hr, 2hr and 3hr), failed to generate species B from species A or *vice-versa*.

pH

The effect of pH on species A and B was examined. Sonication was carried out at different pHs (pH 6.8, pH 7.4, pH 8.2) and the crude extracts were subjected to non-denaturing PAGE and an in-gel assay, as described in chapter 2. The double band was seen in all cases, indicating the two species were not generated by exposure to a slightly alkaline pH during purification.

Hydroxylamine

Treatment with hydroxylamine, an ammonia analogue, will cause the liberation of PBG when added to PBGD substrate intermediates. The addition of hydroxylamine did not affect the distribution of bands on non-denaturing PAGE, indicating the second band

cannot be an enzyme substrate intermediate, confirming earlier work by mass spectrometry.

Treatment with the crude extract of *E.coli*

The possibility that an endogenous *E.coli* enzyme was acting on the enzyme either during its overexpression or purification was considered. Both separated forms of deaminase were incubated with crude extract of sonicated BL21 (DE3) in an attempt to regenerate the two species, the mixture was analysed by non-denaturing PAGE and subjected to an "in-gel" assay. Incubation with the crude extract of *E.coli* was found to have no affect on either species, as both A and B remained as single bands on the gel. Therefore, *E.coli* enzymes under these conditions did not regenerate both species from either band. The fact that Anderson and Desnick [61] had previously observed two forms of PBGD purified from human erythrocytes means that the production of these two enzyme species is not due to overexpression in *E.coli.*

Effect of aging on PBGD isoforms

The effect of aging on isoforms A and B was investigated by analysing enzyme which had either been: freshly purified; freeze dried and stored for a month at -20°C; stored at 4°C for one week or room temperature for 2 days. In all cases the enzyme was stored in 20mM Tris-HCl, pH 8.2, containing 5mM DTT, except the freeze-dried sample. The enzyme samples were then subjected to non-denaturing PAGE and activity assays, using the freshly purified enzyme as a control. PBGD that had been freeze-dried did not loose any activity, enzyme stored at 4°C for one week lost less than 10% activity as compared to the freshly purified enzyme and enzyme stored at room temperature for 2 days only retained 40% activity compared to the freshly purified enzyme. All PBGD samples produced an identical migration pattern on non-denaturing PAGE to the freshly purified PBGD, although PBGD that had been left at room temperature for two days produced more smearing on the gel, indicating proteolytic breakdown. The intensities of the two bands did not alter during aging, indicating the difference between the two isoforms cannot be attributed to any aging process.

Effect of turnover on the isoforms of PBGD

Mutants with lower activities were found to have a much higher percentage of A, the higher band (such as Arg167Gln) (figure 5.13). This could mean that the ratio of the two bands is dependent on turnover, however, it may require several turnovers to see this effect.

To investigate this, 2.5nmoles of both species (50μg) were incubated with 200nmoles of PBG for 30 minutes to complete a number of turnovers. After incubation and gel filtration with a Pharmacia PD10 column, to remove any product, both species were analysed by native PAGE, however, the distribution of the two bands on the gel did not alter, indicating that turnover during assay conditions did not interconvert or alter the proportion of the two species.

The above experiments indicate the two deaminase species are not interconvertable under the conditions investigated so it is reasonable to suggest there is a definite molecular difference between species A and B. Deamidation is the only modification known to decrease the charge of a protein with only a one mass increase per modification.

5.2.8 Possible deamidation sites in human recombinant PBGD

The difference between the two species of deaminase could be due to deamidation during bacterial growth, where an amide group of either glutamine or asparagine has been replaced with a carboxyl group. This modification of a single amino acid could account for the charge difference and mass difference, asparagine and aspartate: 114.11 and 115.09 and glutamine and glutamate: 128.14 and 129.12. (values apply to amino acids in proteins).

It is also possible for non-enzymic deamidation of amino acids to occur in proteins. Many reviews on deamidation of proteins are available [146, 147] and computer programs [148], which predict possible sites of deamidation are also available. For proteins in which deamidation has been established and the site determined, glycine is the most common neighbouring residue [146]. If the neighbouring residue is small like glycine, the residue to be deamidated will be more accessible and the polypeptide chain will be more flexible. Asparagine or glutamine residues followed by a hydrophobic amino acid with a bulky side chain are not commonly deamidated as the side chain may limit the accessibility of the reactive nitrogen anion to the asparagines side chain amide. Neighbouring serine and threonine also increase the rate of deamidation. Deamidation will occur more readily if the asparagines or glutamines flanking regions are solvent accessible and reside within a flexible region of the protein. The crystal structure and the primary sequence of hruPBGD were used to predict possible deamidation sites.

There are 10 asparagine and 19 glutamine residues in human erythroid PBGD. As the double band is seen in both erythroid and ubiquitous PBGD the first 17 residues of ubiquitous PBGD were discounted as possible deamidation sites. The double band on non-denaturing PAGE is also seen when analysing the *E.coli* enzyme so the deamidation site can be tentatively narrowed down further to residues conserved in both human and *E.coli*. There are only 2 asparagines and 3 glutamines found in both human deaminase and *E.coli* deaminases.

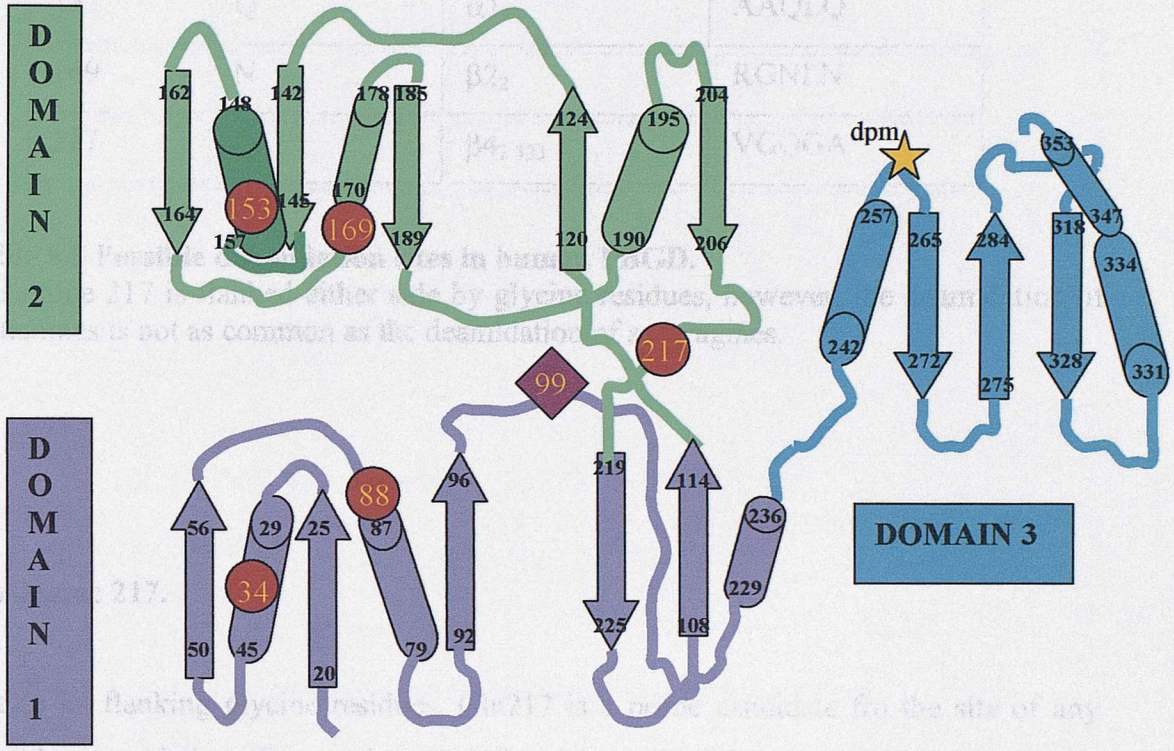

Figure 5.10 Possible deamidation sites highlighted as red circles on a secondary structure model of human PBGD.

Active site aspartate-99 is indicated by ◆

The dipyrromethane cofactor, which binds to Cysteine 262 is indicated by ☆

Position	Amino acid	Secondary structure	Flanking sequence
34	Q	$\alpha 1_1$	RIQTD
88	N	$\alpha 2_1$	EKNEV
153	Q	$\alpha 1_2$	AAQLQ
169	N	$\beta 2_2$	RGNLN
217	Q	$\beta 4_{2\ 333}$	VGQGA

Table 5.5 Possible deamidation sites in human PBGD.
Glutamine 217 is flanked either side by glycine residues, however, the deamidation of glutamines is not as common as the deamidation of asparagines.

Glutamine 217.

Due to its flanking glycine residues, Gln217 is a prime candidate fro the site of any possible deamidation. The residue Gln217 in human PBGD is in a polar environment, on a hinge region at the rear of the active site cleft, see figure 5.12 A and B, where some movement with adjoining residues could lead to a catalytic hydrolysis by other nearby groups. This would have to be a very slow reaction, otherwise this residue would be completely converted to the glutamate form.

Gln217 (198 in *E.coli*) is conserved and the crystal structures of the human and *E.coli* enzymes indicate its importance, where it forms hydrogen bonds to the side chains of invariant Asp106, Lys98 and Arginine131 and contributes to the hydrogen-bonding network around the cofactor.

Species	214			217			220
1.Human	A	V	G	Q	G	A	L
2. E.coli	A	V	G	Q	G	A	V
3.Euglena gracilis	A	A	G	Q	G	A	L
4. Rat	A	V	G	Q	G	A	L
5. Mouse	A	V	G	Q	G	A	L
6.Bacillus substillis	A	V	G	Q	G	A	L
7. Pea	A	V	A	Q	G	A	I

Table 5.6 Sequence alignment around Gln217.
This region is very conserved throughout all known PBGD sequences. The numbering refers to hruPBGD all other sequences are topologically related.

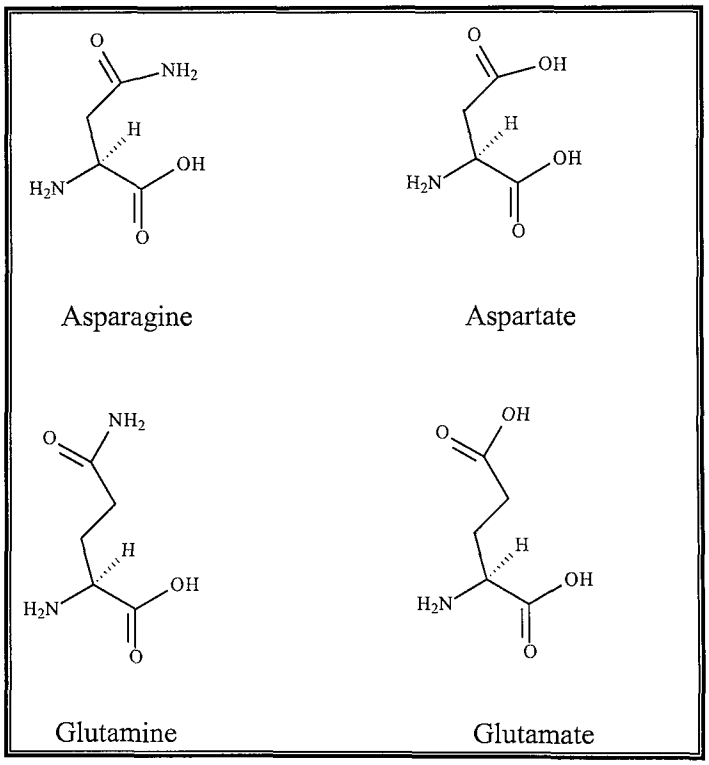

Figure 5.11 Structures of asparagine, aspartate, glutamine and glutamate.

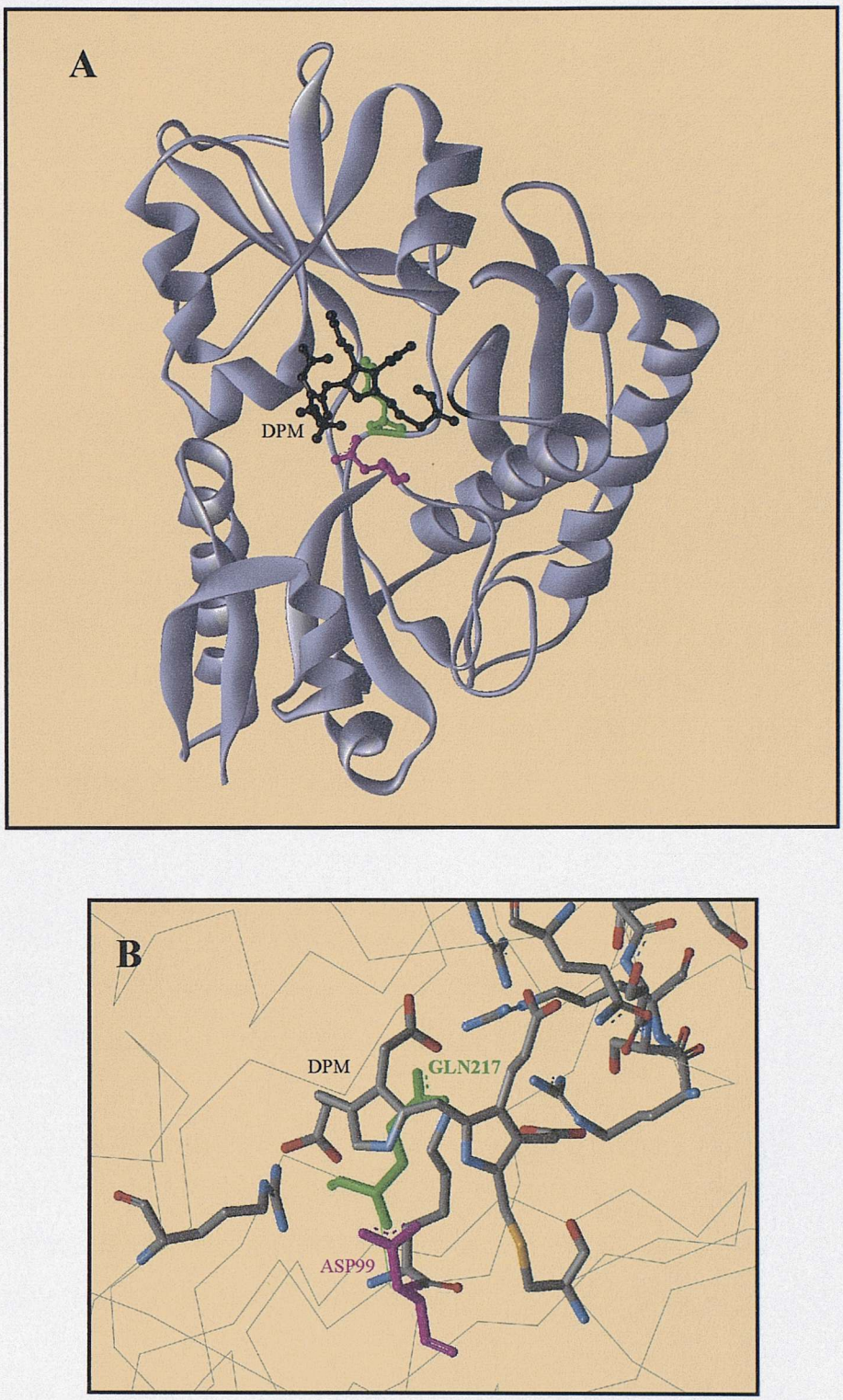

Figure 5.12. The position of Glutamine 217 in human PBGD.

A. The position of Glutamine 217 in human PBGD.

B. A close up view of Glutamine 217 in human PBGD.

Glutamine 217 is highlighted in green, the active site aspartate is highlighted in pink and the DPM cofactor can be seen to link via a thioether linkage to domain III. Glutamine is positioned in a flexible region of the molecule, behind the cofactor and behind the active site Lysine98. This figure was prepared using the program WebLab Viewer [30].

5.2.9 Predicting deamidation rates using a computational method.

Robinson and Robinson have described a method of predicting potential deamidation sites (http://www.deamidation.org). However, this program can only be used to predict the deamidation rates of Asparagine (Asn) residues. The sequence-controlled Asn deamidation rates of most of the 400 possible near-neighbour combinations in pentapeptide models have been measured [149] and these rates and the 3D structures of proteins with well characterized deamidations have been combined to produce a computation method that predicts the deamidation rates of most Asn residues for which the 3D structure is known [148]. This method is said to be more than 95% reliable in predicting relative deamidation rates of Asn residues within a protein. This computer program was used to predict the possible deamidation of asparagine residues in *E.coli* PBGD (1PDA) whose 3D structure had been deposited in the Brookhaven protein databank (http://www.rcsb.org/pdb)[31]. This program required the primary sequence and the 3-D structure of the enzyme (table 5.7).

The deamidation coefficients (C_D) of each Asn in the protein are calculated according to an equation, which accounts for the primary sequence and 3-D structure of the enzyme. The C_D value can then be used to indicate how likely the residue is to be deamidated. Asparagines with the lowest C_D values are the most unstable.

Using this computer prediction method a *C*-terminal asparagine was indicated to be very susceptible to deamidation. However, this is not conserved in the human enzyme. The conserved asparagines are Asn4, Asn73 and Asn151 (4, 88 and 169 human numbering) and their deamidation coefficients are 33.1, 4,783.1 and 26.4, respectively.

Unfortunately deamidation of glutamine residues cannot yet be predicted using this computer program.

Primary sequence	C_D
Asp-Asn-4-Val	33.169
Glu-Asn73-Arg	4,783.098
Ser-Asn111-Asn	4.885
Asn-Asn112-Tyr	15.999
Gly-Asn151-Val	26.366
Asp-Asn161-Gly	0.918
Leu-Asn220-His	33.929
Met-Asn235-Thr	136.987
Leu-Asn296-Asn	324.183
Asn-Asn297-Gly	1.998
Tyr-Asn308-Gly	0.017

Table 5.7 Table of the deamidation coefficients (C_D) of the asparagine residues in *E.coli* PBGD.
Using the pdb file for the *E.coli* PBGD (1PDA) [31] the deamidation prediction method was used (http://www.deamidation.org) [148]. The conserved asparagines are highlighted in red. The lower the deamidation coefficient the more likely the asparagine is to be deamidated. The predicted half-life, in days, for the amide is 100 times the C_D.

5.2.10 Protease digestion and peptide mapping of hruPBGD

As described previously, analysis by non-denaturing PAGE and strong anion exchange chromatography has revealed two major isoforms of human recombinant PBGD (A and B) and the two isoforms may arise due to deamidation. MALDI-TOF and electrospray ionization mass spectrometry were used to characterise the isoforms A and B in an attempt to detect differences between them.

It is a difficult undertaking to characterise directly by ESMS the nature of variants resulting from a single site modification of an amino acid in a 40kDa protein, due to limits in mass resolution. Cleavage of the protein into smaller fragments using a protease was therefore carried out in an attempt to identify possible sites of modification.

Peptide mapping by chromatographic methods

Reverse phase chromatography using a C18 column, with a gradient of acetonitrile was used to separate peptides from the proteolytic digests of species A and B. The elution profiles of the digests of species A and B were compared to identify any alterations, such as a shift in retention time or new or missing signals indicating modified peptides. The V8 digest did produce peptides of interest, which were collected and mass spectrometry was attempted. The V8 peptides were found to fly very poorly on the mass spectrometer so a tryptic digest was performed. No difference could be seen in the elution profiles of both A and B so the tryptic peptides were subjected to on line HPLC/MS analysis.

V8 protease digestion and analysis of resulting peptides using HPLC

Endoproteinase, Glu-C *Staphylococcus aureus*, V8 purchased from Sigma™ was used to digest species A and B of hruPBGD (100μg), at a ratio of protease: deaminase 1:20. The digestion was carried out in Tris-HCl buffer, pH 7.8, containing 10% acetonitrile as recommended by Sigma™. Digestion was carried out at room temperature overnight. Peptides produced by V8 protease were analysed by reverse phase HPLC. An aliquot

(20μg) was separated on a C18 column (0.3 × 250 mm, C18-PM, LC-Packings). Using a 0-100% acetonitrile gradient in water, both with 0.05%TFA, over 100 min, with a flow rate of 0.5ml/min. Peptide elution was monitored at 214nm (figure 5.14).

If a glutamine is deamidated in one of the PBGD isoforms and not the other, V8 protease digestion was expected to give rise to different patterns of peptide products for each isoform. Since, V8 protease cleaves protein at glutamates, any species with glutamine in that position would not be cleaved, but a species with glutamate would be cleaved.

Intriguingly, despite the same conditions used in the digestion of isoforms A and B, the digestion of isoform A was more complete. The peak representing the undigested protein is far larger for isoform B than A, suggesting A is digested more easily than B. This indicates a conformational difference may exist which makes the isoform B less susceptible to digestion than isoform A.

Minor differences seen between the elution profiles of A and B from the HPLC were promising but attempts to identify these peptides by mass spectrometry could not be carried out.

Tryptic digestion

Proteomics sequencing grade trypsin purchased from Sigma™ was used to digest species A and B of hruPBGD at a ratio of 1:20. The trypsin was reconstituted with 1mM HCl to a concentration of 1mg/ml. The protein to be digested (100μg) was dissolved in 100mM ammonium bicarbonate buffer, pH 8.5, with 10% acetonitrile, to a concentration of 1mg/ml, as recommended by Sigma™. The trypsin was added to the enzyme solution in a ratio of 1:20. Digestion was carried out at 37°C for 18hrs. Peptides produced by tryptic digestion were analysed by reverse phase HPLC. An aliquot (20μg) was separated on a C18 column (0.3 × 250 mm, C18-PM, LC-Packings). Using a 0-100% acetonitrile gradient in water, both with 0.05%TFA, over 100 min, with a flow rate of 0.5ml/min. Peptide elution was monitored at 214nm (figure 5.15). It was

apparent, as with the V8 digest, that isoform B was less readily digested and that lower concentration of peptides were produced as a result (figure 5.15).

On-line HPLC/MS analysis of tryptic digests

On-line HPLC/MS analysis of tryptic digests of the PBGD was carried out by Paul Skipp (Southampton University). As the peptides eluted from the C18 column they were sampled for mass spectrometry. The on-line HPLC/MS provided a method for screening tryptic peptides of the protein against the theoretical peptides (based on the cDNA sequence). By detecting peptides that do not match the mass of any theoretical peptides it is possible to detect sites that may have undergone post-translational modification. The individual peptides were characterised by their molecular mass.

The expected peptide containing Gln217 was seen in the analysis of the tryptic digest of isoform A, but was not detected in isoform B. However, no mass could be seen 1Da greater in the digest from isoform B, since the digestion of isoform B was less complete. The possibility that the low concentrations of peptides from B was hindering the identification of the peptide 1Da greater was considered and in an attempt to concentrate peptides from B a yellow colour was produced, which did not occur when concentrating A. Therefore, deamidation of Gln217 was not conclusive.

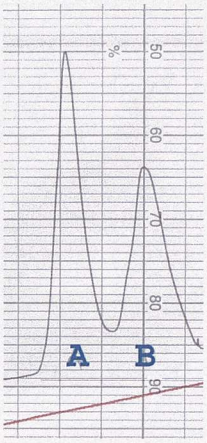

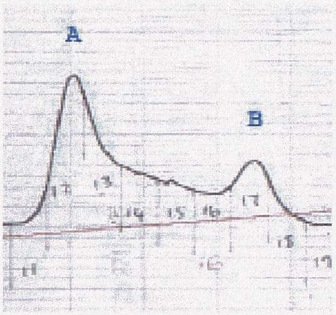

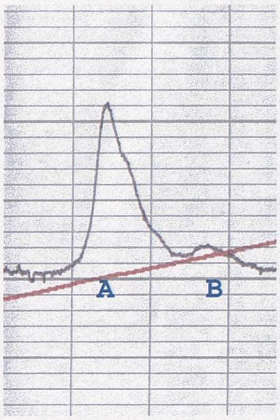

A. Lys210Glu B Native C. Arg167Trp

Figure 5.13. Elution profiles of native hruPBGD and two mutant hruPBGD showing the separation of the two deaminase species labelled A and B.
Elution A is the Lys210Glu hruPBGD variant, elution B is the native hruPBGD and elution C is the Arg167Trp mutant hru PBGD. Interestingly, the mutant Lys210Glu, which is more active than the native enzyme, has a larger peak B than the native enzyme, whereas the much less active mutant Arg167Trp has a smaller peak B than the native enzyme. This could suggest the presence of this second species is related to enzyme turnover.

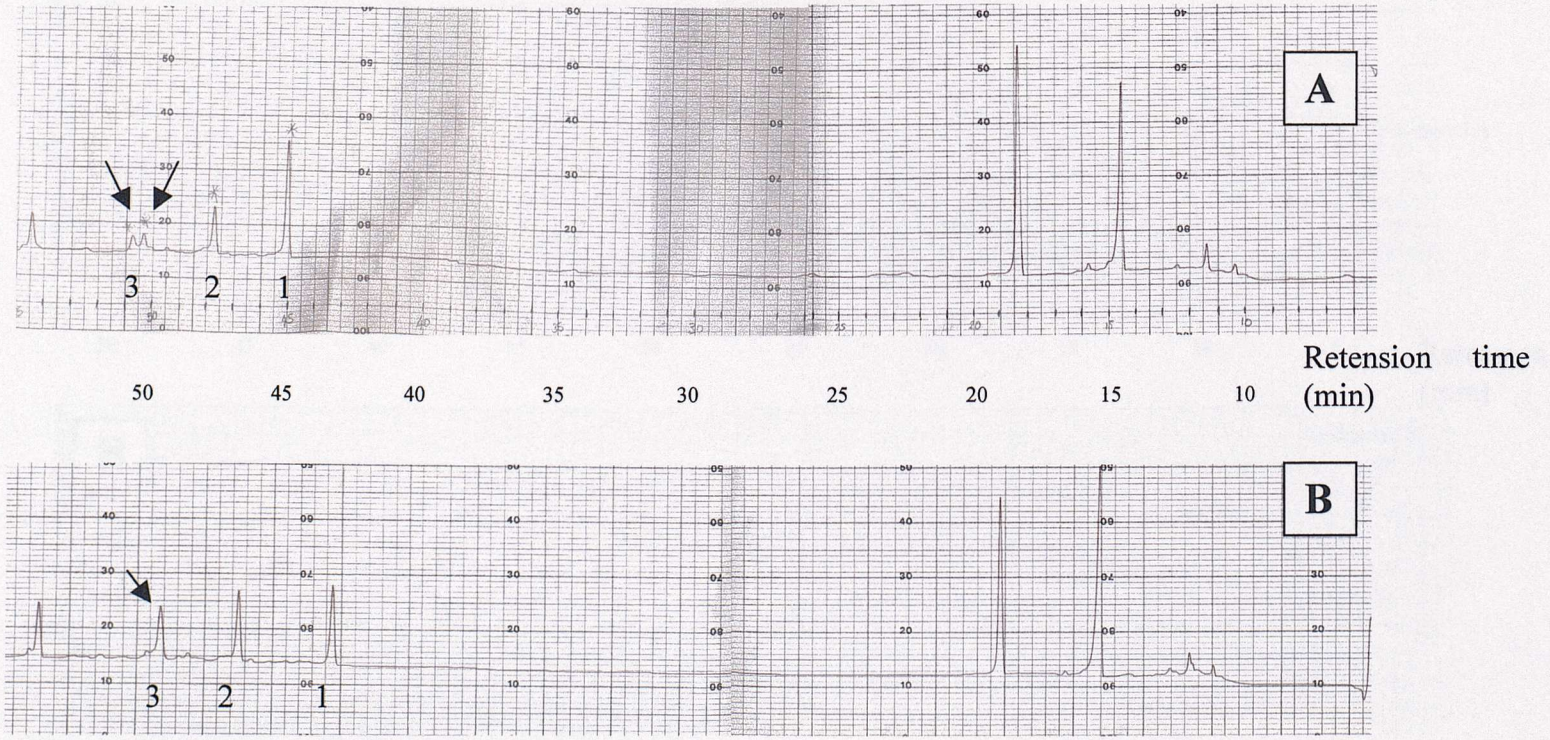

Figure 5.14. HPLC elution of peptides from the V8 digestions of species A and B of hruPBGD.

A.) HPLC elution of peptides produced by the V8 digestion of species A.

B.) HPLC elution of peptides produced by the V8 digestion of species B.

Species A and B were digested with V8 protease and the resulting peptides were separated by H.P.L.C. A C18 column with a 0-50% acetonitrile gradient was used to elute the peptides over 100 minutes at a flow rate of 0.5ml/min. The elution profiles of A and B were similar apart from the peaks numbered. Peak one is larger than peak two in the digest of A, whereas both peaks are of similar size in digest B. The arrows indicate peaks that differ when the elution profiles of both species A and B are compared. Interestingly, peak 3 is a single peak in the digest of species B, whereas, there are two peaks in the same position in the elution profile of species A.

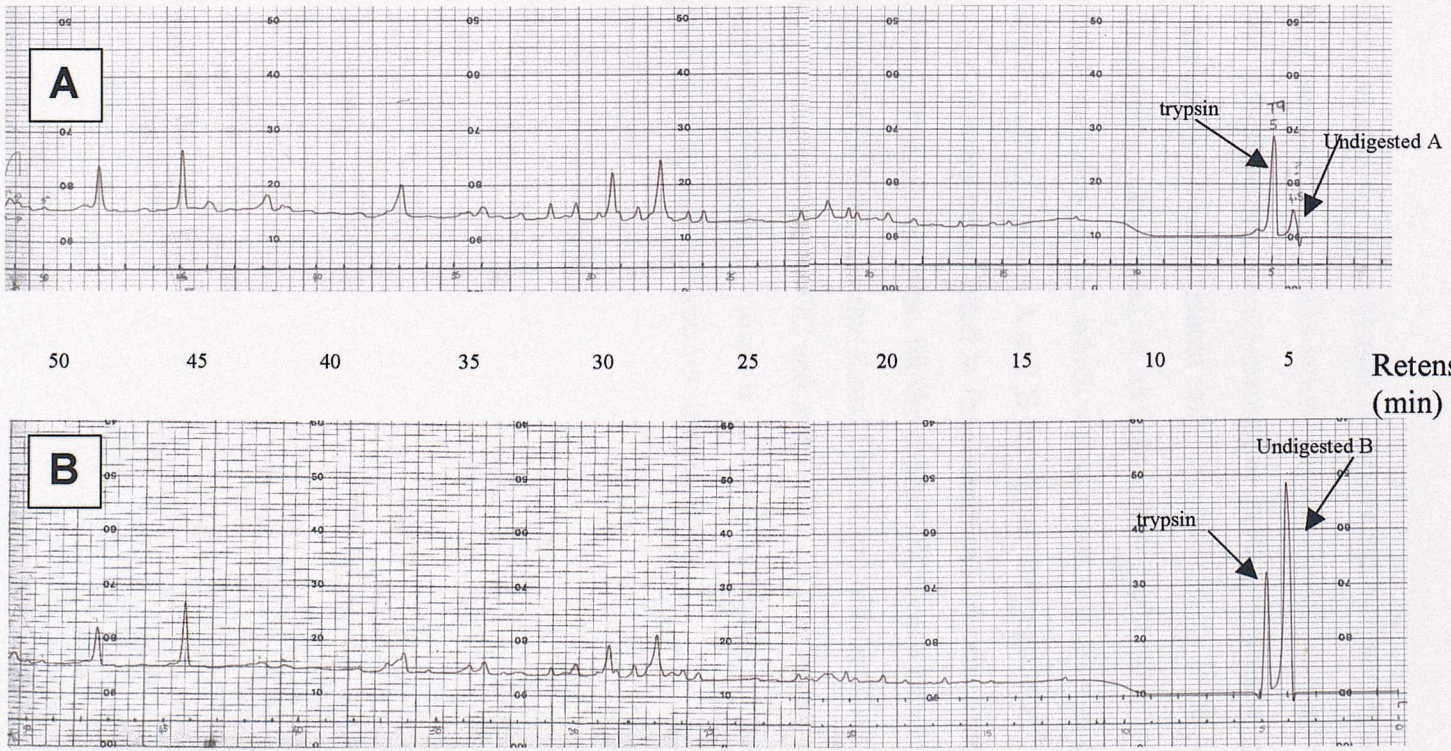

Figure 5.15. HPLC elution of peptides from the tryptic digestion of species A and species B of hruPBGD.

A.) HPLC elution of peptides from the tryptic digestion of species B.

B.) HPLC elution of peptides from the tryptic digestion of species B.

Species A and B were digested with trypsin and the resulting peptides were separated by H.P.L.C. A C18 column with a 0-50% acetonitrile gradient was used to elute the peptides over 100 minutes at a flow rate of 0.5ml/min. It can be clearly seen that species B is far more resistant to digestion than species A. The elution profiles of A and B were remarkably similar but were subjected to mass spectrometry as it is possible that different peptides may coelute.

Deamidation of an *N*-terminal asparagine residue to aspartate.

The *N*-terminal tryptic peptide (MSGNGNAAATAEENSPK) with an expected monoisotopic mass of 1647.7 was not detected as the N-terminal methionine had been clipped. The expected mass for this peptide without the methionine residue was 1516.6, however, the peptide detected had a mass 1 Da greater (1517.6) than the expected mass. This indicates deamidation may have occurred in the *N*-terminal region.

The potential for deamidation is influenced by the primary sequence and residues are most susceptible to deamidation when followed by a glycine. According to the cDNA sequence there are three asparagines in this *N*-terminal peptide, however only one is deamidated. The deamidated residue is most likely to be Asn4 as the subsequent residue is a glycine. One effect of an Asn→Asp conversion would be in an increase in the overall negative charge, which would result in further migration during electrophoresis. However, both species A and B contained the peptide at 1517.6, indicating both species A and B were deamidated at the *N*-terminus. As the deamidation was detected in both species it cannot account for the charge difference between species A and B. Both the erythroid isoform and the E.coli PBGD are also produce double bands when analysed by non-denaturing PAGE and as the first 17 residues of the ubiquitous enzyme are not conserved, suggesting there is another modification elsewhere in the enzyme, which generates the A and B species of deaminase.

5.2.11 Crystallisation and preliminary X-ray studies on human recombinant PBGD isoenzymes

Crystallisation conditions for the ubiquitous isoenzyme were initially determined by fellow postgraduates, J. Mosley and A. Al-Dbass [142, 145]. Optimisation of these conditions was carried out, by varying pH and precipitant concentrations around the original conditions, achieving rectangular plate shaped crystals of the erythroid and ubiquitous isoenzyme with dimensions of 100x50x40 microns.

Erythroid PBGD crystals of diffractable quality were grown at a protein concentration of 5mg/mL in 50mM sodium citrate, pH 5.6, containing, 1.25M lithium sulphate, 0.6M ammonium sulphate, 5% v/v ethylene glycol, 0.5% v/v dioxane and 5mM DTT (figure 5.16).

The hanging drop method was used as described in chapter 2. Each well was filled with nitrogen gas to prevent oxidation and crystals were grown in the dark.

Crystals were harvested after one week and immersed in a cryoprotectant containing 15% w/v glycerol in the mother liquor, before freezing the crystals in liquid ethane and liquid nitrogen. Using these crystals the structure of hrePBGD was solved to 3Å resolution, by Dr Darren Thompson, using the Arg167Gln mutant for molecular replacement. There are still areas of the structure that are incomplete. It is possible that the crystallisation of species A and B, separately, may provide crystals that diffract at a higher resolution.

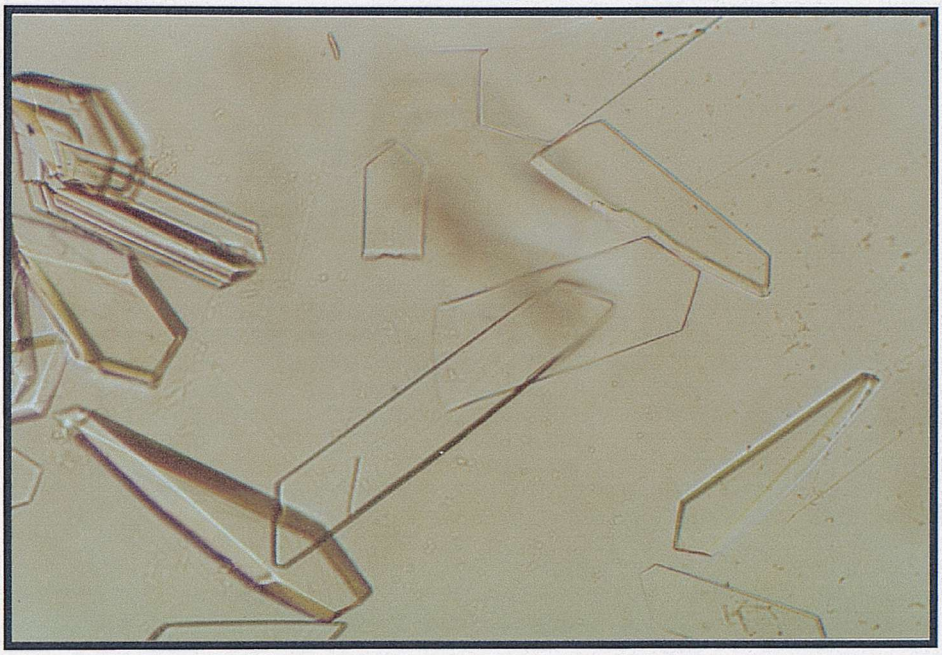

Figure 5.16. Human erythroid porphobilinogen deaminase crystals.
Crystallisation of human erythroid PBGD was carried out at a concentration of 5 mg/mL in 1.25M lithium sulphate, 0.6M ammonium sulphate, 50mM sodium citrate, pH 5.6, 5mM DTT, 0.5 % v/v dioxane and 15% v/v ethylene glycol, at room temperature, in the dark.

5.3 Conclusions.

The heterogeneity of PBGD has been observed previously with enzyme purified from many sources including hruPBGD and hrePBGD. Despite the fact this observation was first made over twenty years ago, no explanation that fits all the experimental findings has been proposed. As human recombinant PBGD could be a candidate for enzyme replacement therapy in the treatment of AIP heterogeneity of PBGD is an important consideration for protein drug development. The impact of modifications such as deamidation on protein structure and function, could result in decreased efficacy and increased immunogenicity.

The aim of the first part of this chapter was to identify the difference between the observed isoforms of hruPBGD. It seems likely that the presence of these two species results from a post-translational modification, such as deamidation. This would explain both the charge difference and the 1amu difference between the two deaminase species.

The isoforms of hruPBGD were resolved by Mono Q f.p.l.c and found to be homogeneous in size and no difference in enzyme activity was detected *in vitro*. Despite numerous attempts, isoforms A and B were not found to be interconvertable *in vitro*. The effect of pH, temperature, enzyme turnover were all investigated but did not induce isoform A to convert to isoform B or *vice versa*.

To determine a potential cause of charge heterogeneity of the PBGD, the charge isoforms were digested by V8 protease or trypsin and the resulting peptides were analysed by an HPLC-based method. Differences in the elution profiles of the peptides from the proteolytic digests of isoforms A and B from RP-HPLC were detected and the tryptic digest was subjected to LC-MS to identify points of difference between isoforms A and B. Deamidation of an asparagine was identified in the *N*-terminal peptide of the hruPBGD, however, this deamidation was seen in both isoforms so could not be the cause of heterogeneity. The peptide CMYAVGQGALGVEVR incorporating Gln217 was detected in the digest from isoform A but it was not detected in the digest of isoform B, however, the corresponding peptide with a mass 1Da greater

(CMYAVGEGALGVEVR) was also absent, so there was no conclusive evidence of deamidation at this position. Isoform A was found to be notably more susceptible to digestion by both V8 protease and trypsin, than isoform B, which indicated a resistance to proteolysis possibly due to a difference in conformation between the two isoforms.

Recent interest in the field of proteomics has provided many resources for protein analysis, which could be exploited in the future to solve this elusive problem. Site-directed mutagenesis of hruPBGD would be valuable in determining once and for all whether this residue is partially deamidated in human PBGD causing the presence of isoforms A and B. If this single glutamine residue is responsible for the charge heterogeneity of human PBGD its replacement with glutamate should result in a single species. However, if Gln217 is essential for protein folding then it may be difficult to express and isolate the Glu217 variant.

The X-ray crystallography model of hrePBGD is complete in all but two sections and further crystallisation and refinement of the structure is needed. The crystallisation of the separated A and B isoforms of hrPBGD may result in structures at higher resolution.

Chapter six: Studies on recombinant human ubiquitous PBGD (hruPBGD) mutants.

6.1 Introduction

Acute intermittent porphyria (AIP) is an autosomal dominant disorder caused by the partial deficiency of porphobilinogen deaminase (PBGD), the third of eight enzymes in the haem biosynthetic pathway. The disease is characterised by symptoms such as, muscular weakness and psychiatric symptoms that are usually triggered by exogenous factors. The aim of this chapter has been to study mutants of the hruPBGD and examine the molecular and functional consequences of these mutations.

The first mutation in the PBGD gene, associated with AIP, was reported in 1989 [150] and there are now close to 300 known mutations affecting the human PBGD gene [82]. This chapter describes work on the following human recombinant ubiquitous PBGD mutants: Lys210Glu; Asp99Glu; Asp99Gly; Arg167Gln and Arg167Trp.

One of the first published cDNA sequences of human ubiquitous PBGD reported a lysine at position 210 [65] and the cDNA used throughout this project has a lysine at 210. However, subsequent publications reported a glutamate at position at 210 [151]. To investigate the possible effect of a glutamate at 210 on the ubiquitous PBGD the Lys210Glu mutant was generated by Dr M. Sarwar, Southampton University. Analysis of this enzyme determined it had the slightly higher specific activity than the native enzyme and the mutation appeared to have no adverse effect on the enzymes function or stability.

In human PBGD Asp99 is a key catalytic residue, situated in the active site and corresponds to Asp84 in *E. coli*. From X-ray crystallographic structures and previous site directed mutagenesis in *E. coli* [69]. Asp99 is predicted to play crucial roles in catalysis including protonation of the leaving group ammonia, stabilization of the developing charges on the pyrrole rings during condensation and final deprotonation of the α-proton of the pyrrole ring.

To investigate the importance of this residue in the human enzyme, site directed mutagenesis was carried out by Dr. M. Sarwar, (Southampton University) creating both Asp99Glu and Asp99Gly mutants. When Asp99 was mutated to glycine the activity of the enzyme was reduced to zero, supporting the idea that this acidic group participates in the catalytic cycle. When this aspartate residue was mutated to glutamate, an addition of a single methylene group, resulted in a severely impaired enzyme with an activity of less than 0.5% of the wild type.

When expressed in *E.coli* it appeared that both aspartate mutants Asp99Glu and Asp99Gly, had a polypyrrolic cofactor attached to the enzyme. Further evidence presented in this chapter suggested the aspartate mutants existed as stable ES_2 complexes. As these mutants were thought to be stable analogues of ES_2 complexes crystallographic studies were attempted to determine the position of the two extra pyrrole rings in the enzyme.

Porphobilinogen deaminase catalyses a novel polymerisation reaction that involves the addition of four porphobilinogen molecules in a stepwise fashion through intermediate complexes ES, ES_2, ES_3 and ES_4. The X-ray structure of the enzyme indicates that a single substrate binding site is used for each addition of PBG. This indicates conformational changes in the vicinity of the active site cleft must occur as the protein adjusts to accommodate the growing polypyrrole chain.

Arginine167 in human PBGD is thought to play a role in stabilising the escalating negative charge as pyrrole rings are added during catalysis. Arg167Gln is a known human mutation [152]. The patient with this mutation, had decreased erythrocyte PBGD activity and increased urinary PBG. Interestingly, Arg167Gln, was shown to form stable ES complexes to which antibodies bind much more actively than they do to the native human enzyme [152], this reinforces the theory that a conformational change occurs during catalysis. The crystal structure of Arg167Gln mutant hruPBGD is known, Abeer Al-dBass, a fellow postgraduate, in collaboration with F. Mohammed purified and crystallised the Arg167Gln mutant and solved its crystal structure to 2.65Å [84, 145]. Arg167Trp is also a known human mutation, which accumulates enzyme substrate intermediate complexes [153].

This chapter describes the isolation of these enzyme substrate intermediates using high-resolution anion exchange chromatography, and attempts to obtain crystals of diffractable quality of the enzyme substrate complexes in an attempt to increase our understanding of the tetrapyrrole assembly process.

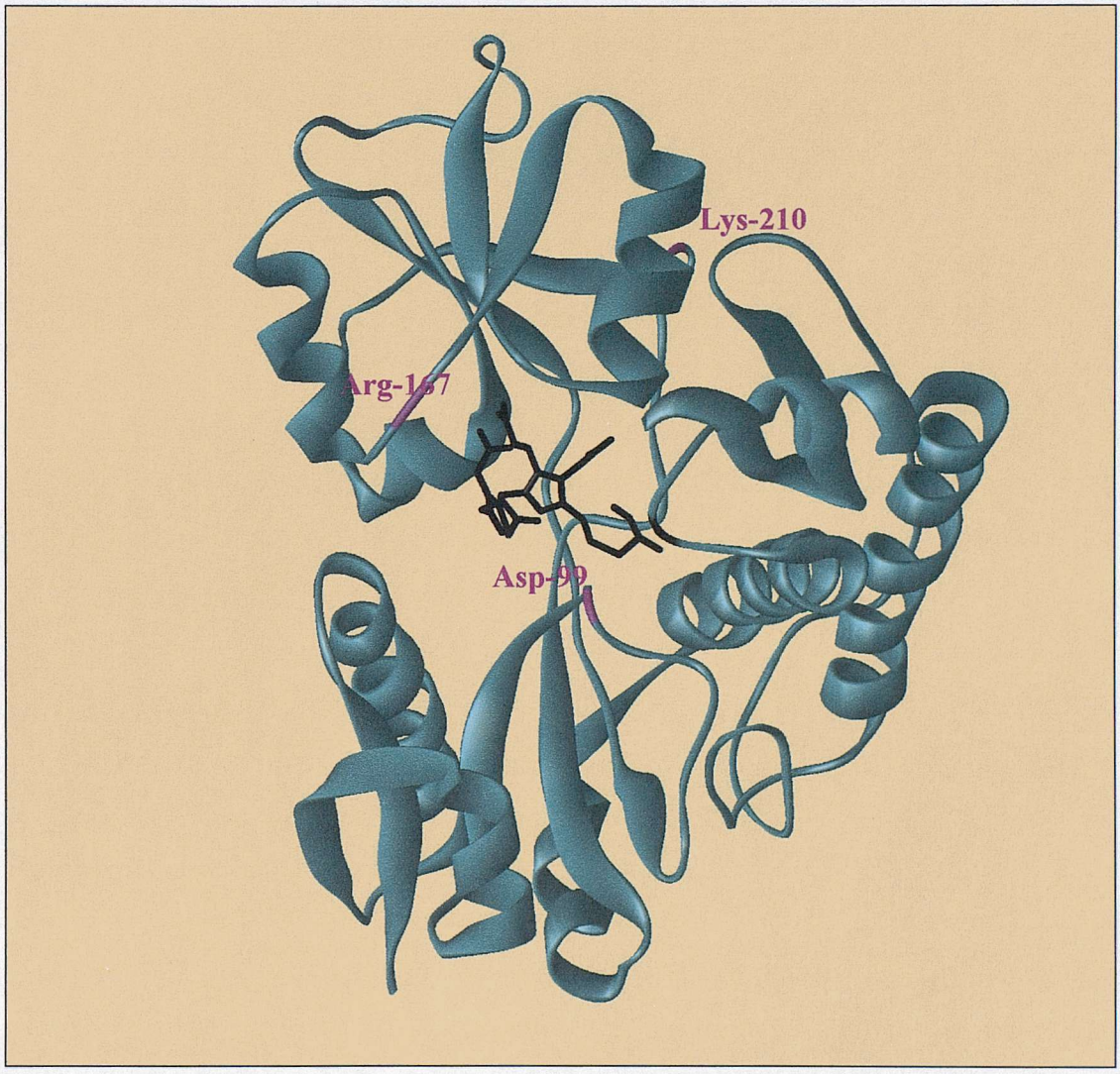

Figure 6.1 Model of human recombinant PBGD with positions of the residues discussed in this chapter highlighted in pink.
This figure was prepared using WebLab Viewer v3.2 [30].

6.2 Results

6.2.1 Expression, characterization and purification of Lys210Glu.

In the original published nucleotide sequence of human ubiquitous PBGD the residue at 210 is reported to be a lysine [65], however, in subsequent published nucleotide sequences, it is reported to be a glutamate [151]. In this research project, cDNA used in the overexpression of the human porphobilinogen deaminase encodes a lysine at position 210 in the primary sequence. Site-directed mutagenesis was employed to produce glutamate at this position so the protein could be compared with the enzyme with a lysine at 210.

Purification of Lys210Glu was carried out exactly as described for the hruPBGD chapter 2. After each step of purification, the enzyme was assayed and analysed by SDS-PAGE. The purification is shown in table 6.2 and the SDS-PAGE at stages of the purification in figure 6.3. The specific activity for the Glu210 and Lys210 are compared in table 6.2. The Glu210 is slightly more active in the conditions of the assay, than Lys210, with a specific activity approximately 10% greater.

Lys210 is situated on a loop region linking domains 1 and 2 (figure 6.2). The fact that the dramatic substitution of a lysine for a glutamate does not have a greater effect on activity is surprising. In other mammalian PBGDs the residue is a glutamate, but is not completely conserved in other species and is an isoleucine in *E.coli* PBGD.

When analysed by non-denaturing PAGE the Glu210 enzyme migrated as a double band, as seen for Lys210. As expected the Glu210 enzyme migrated slightly further than Lys210 due to its additional negative charges.

Analysis by Mono Q anion exchange indicated the presence of two isoforms for both Glu210 and Lys210. Interestingly, Glu210 appears to have a greater amount of the second isoform (B), than Lys210 (chapter five, figure 5.13). The reason for this is not clear.

A substitution of Glu209Lys has been reported as a natural mutation causing AIP, with a CRIM –ve phenotype. This demonstrates how the same mutation in the previous residue at position 209 has a profound effect on enzyme function, compared to the relatively minor effect of Lys210Glu.

	207	208	209	210	211	212	213
Human	H	P	E	K	C	M	Y
E.coli	P	P	E	I	S	L	.
Euglena gracilis	D	P	N	V	M	C	.
Rat	H	P	E	E	C	M	Y
Mouse	H	P	E	E	C	M	Y
Bacillus substillis	E	P	E	R	C	L	.
Pea	S	I	D	D	M	L	.

Table 6.1 Alignment of the primary sequences of PBGD in the region of residue 210.
In this thesis cDNA encoding a lysine at position 210 was used, as reported in the original published sequence for human PBGD. Subsequent sequences published encode a glutamate at 210, which is conserved in mammalian PBGDs. The numbering applies to hruPBGD, other sequences are topologically related.

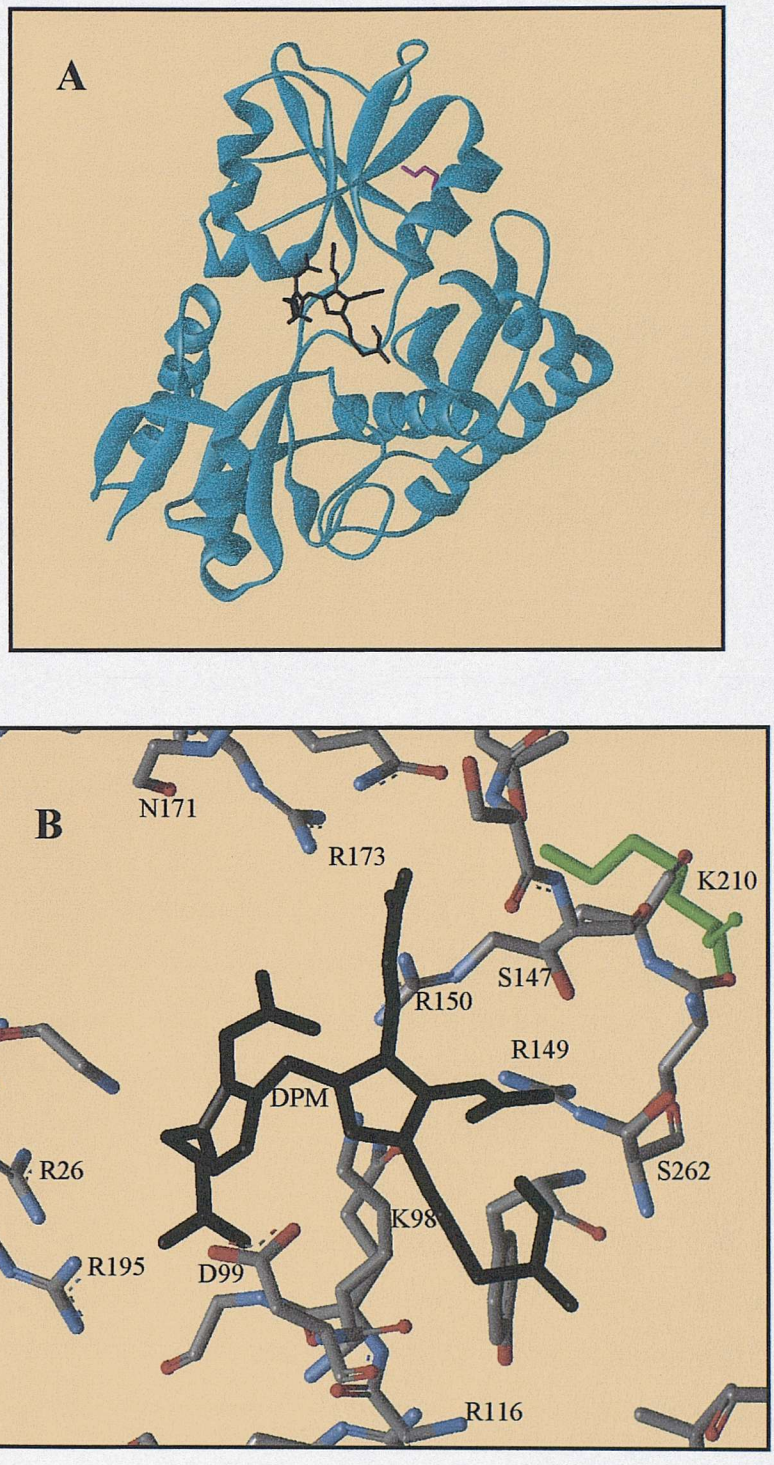

Figure 6.2 Position of Lys210 in hruPBGD

A) Position of Lys210, highlighted in pink on a model of the active site of human porphobilinogen deaminase.

B) Close up view of Lysine 210, highlighted in green, with the DPM cofactor, in black, at the active site.

This figure was prepared using WebLab Viewer Lite v3.20©[30].

6.2.2 Expression, characterization and purification of hruPBGD mutants Asp99Glu and Asp99Gly

This section describes the results of substituting aspartate-99 with glutamate and glycine. Asp99 is an active site residue, which had previously been shown to have great importance in PBGD activity by site-directed mutagenesis of Asp84 in *E.coli* [69]. Asp84 is situated on a β-sheet strand deep in the catalytic cleft, with the carboxyl group close to the nitrogen atoms of cofactor rings, C1 and C2, [66, 68]. The X-ray structures of both the human ubiquitous Arg167Gln mutant and the native human erythroid PBGD confirm the same positioning of the aspartate in the human enzyme. The aspartate is located in a highly conserved region, and is within hydrogen bonding distance (3Å) of the dipyrromethane cofactor [66].

Asp99 is thought to play multiple roles in catalysis including: protonation of the leaving group; stabilizing the negative charge on the pyrrole rings during condensation and final deprotonation of the α-proton of the pyrrole ring.

Asp99Gly is a natural mutation found in an AIP patient [106]. The proband did not experience an acute AIP attack until she was 37. During the attack, the proband excreted port-wine coloured urine with very high levels of urinary ALA and PBG and her erythrocyte PBGD activity was 16nkat/l (58pkat/gHb). The same mutation was found in both her children [106].

Asp99Glu has not been associated with AIP to date. This mutant was studied as the mutation Asp99Glu causes no charge difference and glutamate is only slightly larger than aspartate, yet the equivalent mutation in *E.coli* PBGD has a dramatic effect on activity [69]. The human PBGD mutant was expected to have similar properties.

Step	Volume (ml)	Total Protein (mg)	Total Activity (μmoles/hr)	Specific activity (μmoles/mg/hr)	% Yield
Crude extract	60	1110	177.6	0.16	100
After heat treatment	58	269	164	0.61	92
After DEAE column	120	22	40	1.82	22
After G-75 gel filtration and concentration	30	15	31.5	2.12	18

Table 6.2 The specific activities and yield of the hruPBGD Lys210Glu at different stages of purification, starting from 2.4L of *E.coli*.

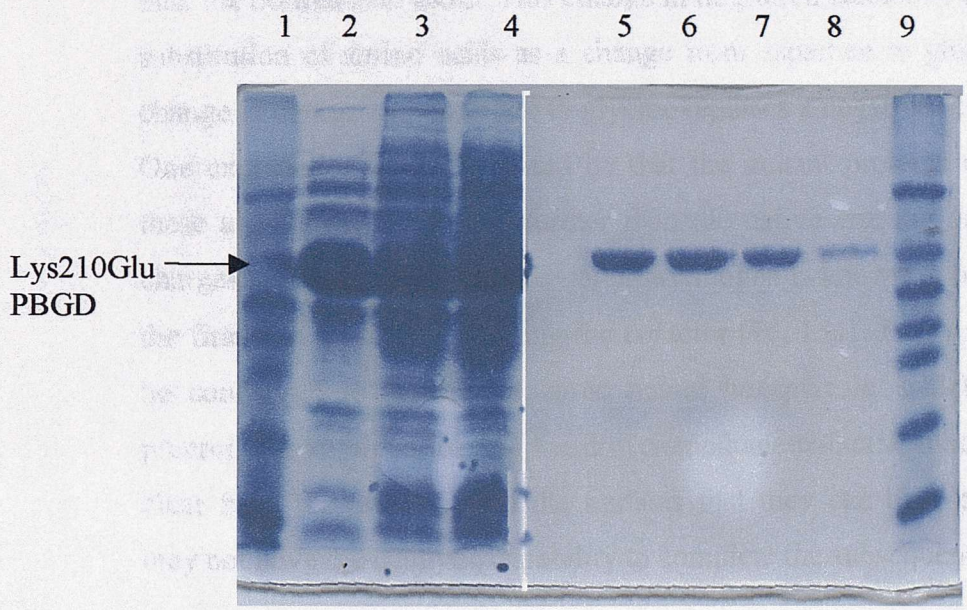

Figure 6.3 SDS PAGE gels showing the steps in the purification of Lys210Glu human recombinant ubiquitous PBGD.

A.) Lane one, Bio-Rad molecular weight marker; lane two Lys210Glu after heat treatment; lane three and four, crude extract before heat treatment; lane five and six, Lys210Glu human recombinant ubiquitous PBGD elution from the DEAE column; lane seven and eight, Lys210Glu elution from G-75 column and lane nine, Bio-Rad molecular weight marker.

6.2.3 General properties of the aspartate mutants

Both mutant proteins were purified using the method described in chapter 2. The purity of the mutants was established by analysing them by SDS-PAGE. Both mutants ran as a single band when analysed by SDS-PAGE, equivalent to 42,000Da, migrating to the same position as the normal PBGD enzyme (figure 6.7). During their purification both Asp99Glu and Asp99Gly were found to require a slightly higher concentration of salt to elute from DEAE ion exchange column. The mutants were eluted with 100mM KCl, whereas, the normal human PBGD eluted with 70mM KCl.

When analysed by non-denaturing PAGE (Figure 6.10) the aspartate mutant proteins appeared to have folded correctly. The apoenzyme migrates as a smear on non-denaturing PAGE, indicating it is not properly folded. This suggests both mutants contain the dipyrromethane cofactor. Both Asp99Glu and Asp99Gly migrated further than the normal hruPBGD. This change in migration cannot be explained directly by the substitution of amino acids as a change from aspartate to glutamate results in no net change in charge and aspartate to glycine replaces a negative residue with a neutral one. One explanation could be could be that the mutant proteins exist as ES_2 complexes, these are known to migrate further than the native enzyme due to the extra negative charges. This is feasible, as preuroporphyrinogen is known to bind to the apoenzyme as the first step towards generating the cofactor [76, 154]. Two further PBG units need to be condensed to form an enzyme bound hexapyrrole, which allows the release of preuroporphyrinogen leaving the dipyrromethane cofactor attached to the enzyme. It is clear from the properties of the mutants that they can bind preuroporphyrinogen but may not have the catalytic capability to complete the subsequent steps.

The mutants were purified and their specific activities were compared to that of the normal enzyme. The glutamate mutant showed a specific activity of 0.012μmol/mg/hr, less than 1% of the normal enzyme. The glycine mutant was catalytically inactive under the assay conditions used (chapter 2).

Although only a conservative mutation, addition of a single carbon to the alkyl chain on the acidic side chain of the mutant hruPBGD Asp99Glu has a profound effect on activity. This dramatic effect on deaminase activity is also seen for the *E.coli* Asp84Glu mutant PBGD. This result suggests Asp99 is involved in catalysis and even the addition of a single carbon to the alkyl chain on the acidic side chain can dramatically affect activity.

The heat stability of these mutants was investigated by heating the mutant enzymes to 60°C for 10mins then analysing them by non-denaturing PAGE, where they displayed unchanged migration patterns, indicating these mutations did not affect their thermostablity.

The mutant proteins were applied to a Mono Q HR5/5 strong anion exchange column attached to a Pharmacia f.p.l.c system and their elution profiles were compared to normal hruPBGD. HruPBGD elutes from the column at 110mM salt and the mutants eluted later, Asp99Gly at 140mM and Asp99Glu at 145mM. Interestingly, using the same conditions the ES_2 complex of hruPBGD elutes at 145mM salt.

When freeze-dried both aspartate mutants were light pink in colour, compared to the colourless native hruPBGD, which suggest the mutants are more susceptible to oxidation than the normal hruPBGD.

Pyrrolic intermediates can be released from PBGD by treatment with bases related to the product ammonia, such as NH_2OH [72]. The reaction with hydroxylamine is the reverse of the deamination reaction and is thought to be catalysed by Asp99. Hydroxylamine (NH_2OH) was incubated with the aspartate mutants and samples were analysed by non-denaturing PAGE, to determine if any products or intermediates had been released (figure 6.9). The mutants were found to have unchanged migration patterns when analysed by non-denaturing PAGE, suggesting either the conformation of the mutants did not allow release of pyrroles, or that Asp99 is needed for the reverse reaction as predicted.

Both mutant proteins were incubated with 5M equivalent PBG at 37°C for 10 minutes before analysing by non-denaturing PAGE at 4°C. Additional bands, which migrate further toward the anode can be seen for Asp99Glu, which indicates it is able to incorporate PBG molecules, but this is far slower than with normal hruPBGD. This raises the possibility of crystallising enzyme-substrate intermediates. The Asp84Glu mutant *E.coli* PBGD been crystallised previously however the resolution of the extra pyrrole rings was not clear [68].

Arabidopsis thaliana	SMKDVPT
Chlorobium vibrioformes	SLKDVPT
Escherichia coli	SMKDVPV
Euglena gracilis	STKDVPM
Pseudomonas aeruginosa	SMKDVPM
Saccharomyces cerevisiae	SLKDMPT
Rattus norvegicus	SLKDVPT
Homosapiens	SLKDLPT

Figure 6.4 Alignment of the primary sequences of PBGD in the region of the catalytic aspartate group.
The active site aspartate is highlighted in red. The proline residue is one of two, which prevents helix formation in part of domain 1, positioning the conserved aspartate next to the cofactor.

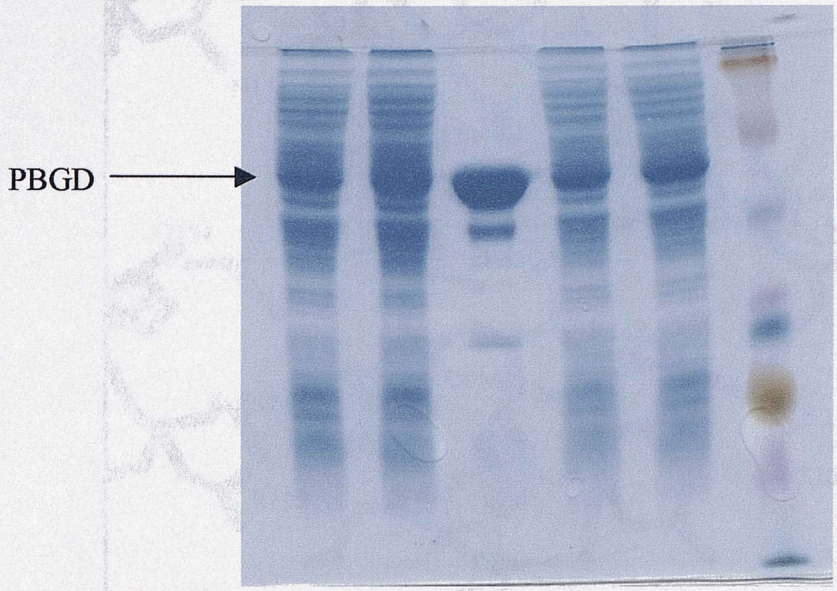

Figure 6.5 SDS PAGE analysis of Asp99Glu and Asp99Gly overexpression and thermostability.

Lane one, crude extract of Asp99Glu; lane two, crude extract of Asp99Gly; lane 3, native ubiquitous enzyme; lane four, Asp99Glu after heat treatment (60°C, for 5 minutes); lane five, Asp99Gly after heat treatment (60°C, for 5 minutes and lane six, molecular weight marker (multimark).

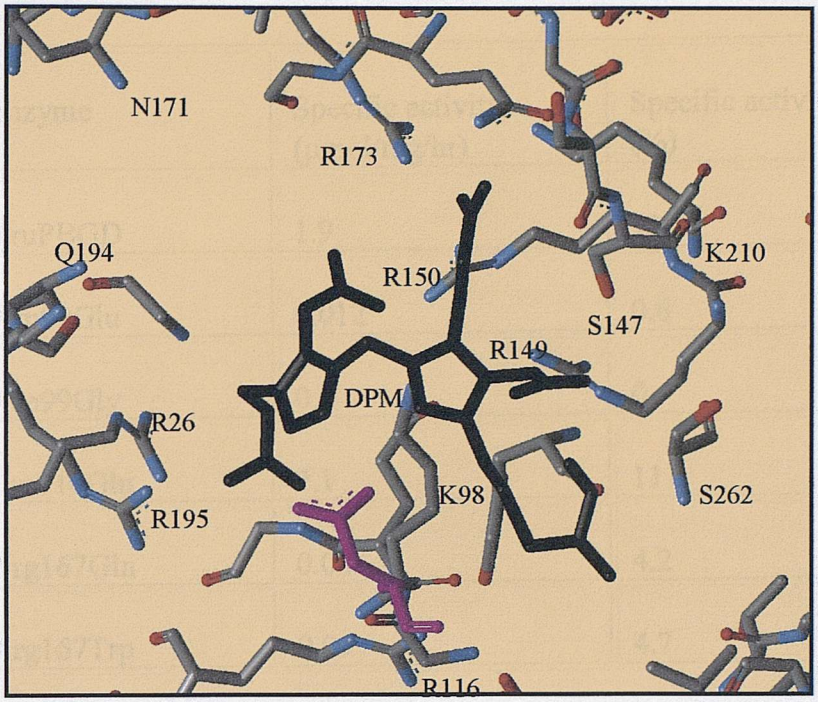

Figure 6.6 Model of the active site cleft region of human PBGD, with active site aspartate-99 highlighted in pink.
The dipyrromethane (dpm) cofactor is shown in black. This figure was prepared using the WebLab Viewer Lite program v3.2 [30].

Enzyme	Specific activity (μmol/mg/hr)	Specific activity (%)
HruPBGD	1.9	100
Asp99Glu	0.012	0.6
Asp99Gly	0	0
Lys210Glu	2.1	111
Arg167Gln	0.08	4.2
Arg167Trp	0.09	4.7

Table 6.3. Comparison of the specific activities of normal hruPBGD and hrePBGD with mutant hruPBGDs.
Assays were carried out at pH8.2 and units are μmol of product formed per mg of protein per hour.

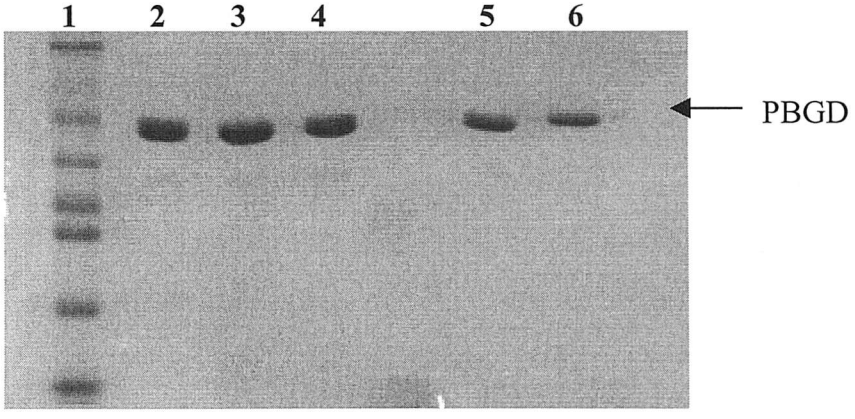

Figure 6.7 SDS-PAGE of purified and mutant human ubiquitous PBGDs.
Lane one, molecular weight marker (Dalton VII); lane two, normal human ubiquitous PBGD; lane three, Arg167Trp mutant human ubiquitous PBGD; lane four, Arg167Gln mutant human ubiquitous PBGD; lane five, Asp99Glu mutant human ubiquitous PBGD and lane six, Asp99Gly mutant human ubiquitous PBGD.

6.2.4 Reaction with modified Ehrlich's reagent to check for the presence of a dipyrromethane cofactor of the hruPBGD Asp99Glu mutant, compared to the native enzyme.

All deaminases require the dipyrromethane cofactor, which as having a free pyrrole α position, reacts with Ehrlich's reagent [73]. The reaction of Ehrlich's reagent with the holoenzyme initially produces an intense purple colour at λmax=565nm, as a result of the reaction between Ehrlich's reagent and the free α-position of the pyrrole of the dipyrromethane cofactor. During a period of 10 minutes, the colour changes to orange with an λmax=495nm, due to the formation of a conjugated dipyrromethene (figure 2.4).

Ehrlich's reagent was added to the native enzyme and both mutant enzymes, Asp99Glu and Asp99Gly, as described in chapter 2, and the reaction was measured using a spectrophotometer over a range of 400 nm to 650nm. Spectra were recorded after the addition of Ehrlich's reagent (within 1 minute) and again after 15 minutes (figure 6.8).

Unlike the native human deaminase the mutant Asp99Glu and Asp99Gly enzymes form a peak at 495nm even before 1 min has elapsed and the peak at 565nm was not observed. The spectral profiles are more indicative of a reaction of a bilane rather than a dipyrromethane (as judged by the immediate appearance of a maximum at 495nm). The spectrum of an ES_2 complex, an enzyme bound bilane, treated with Ehrlich's reagent is similar to that of a dipyrromethane except that it occurs ten times faster [155]. This suggests the Asp99Glu and Asp99Gly exist as the enzyme substrate intermediate complex ES_2.

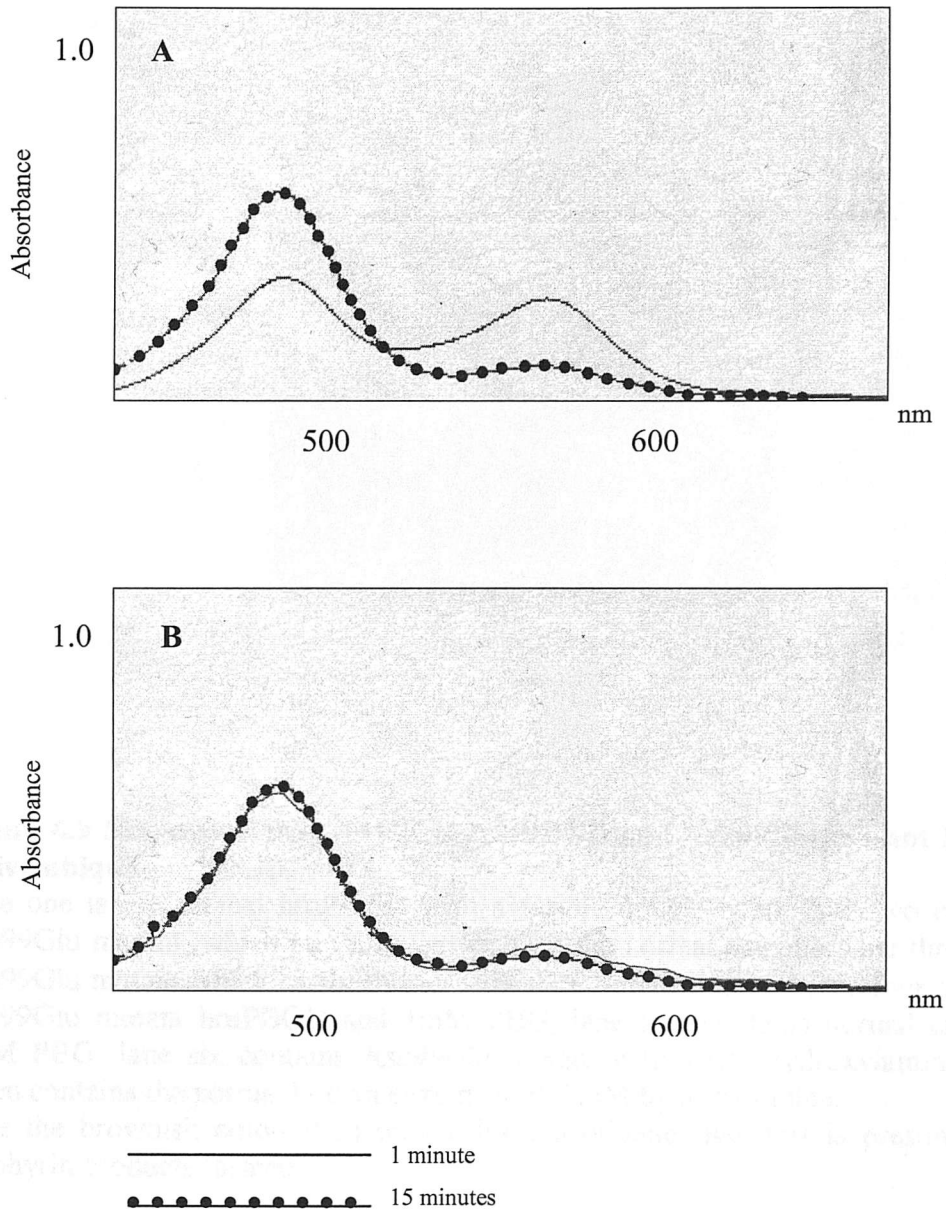

Figure 6.8 Spectra of hruPBGD and hruPBGD Asp99Glu mutant after reaction with modified Ehrlich's reagent.

A) Spectra of hruPBGD after reaction with modified Ehrlich's reagent.
B) Spectra of hruPBGD Asp99Glu mutant after reaction with modified Ehrlich's reagent.

Spectra were recorded after the reaction was performed using a u.v.-vis spectrophotometer over a range of 400-650nm, immediately after and 15 minutes after the reaction was performed. In the case of this mutant, in contrast to the native enzyme, no difference in spectra can be seen between the two time intervals.

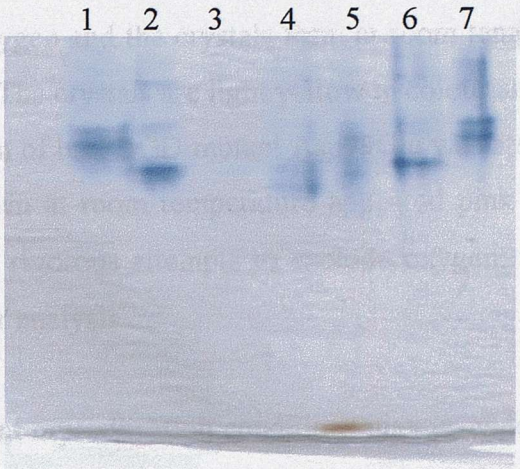

Figure 6.9 Non-denaturing PAGE of hruPBGD and Asp99Glu mutant PBGD and native ubiquitous PBGD.

Lane one is the normal hruPBGD with a visible double band; lane two contains the Asp99Glu mutant, which migrates further than the normal enzyme; lane three contains Asp99Glu mutant which has been heated at 65°C for 30 minutes; lane four contains the Asp99Glu mutant hruPBGD and 1mM PBG; lane five contains normal enzyme and 1mM PBG; lane six contains Asp99Glu mutant with 1mM hydroxylamine and lane seven contains the normal human enzyme with 1mM hydroxylamine.

Note the brownish colouration on the bottom of lane five, this is presumably from porphyrin products formed.

6.2.5 Crystallisation of Asp99Glu.

The crystallisation of human PBGD requires the presence of DTT and N_2 in the crystal tray wells, to exclude oxygen and the crystals form at room temperature in the absence of light (section 5.2.11). The crystals are light yellow in colour and are formed after two weeks. The crystallisation of hrePBGD mutant Asp99Glu was attempted in very similar conditions. Crystals grown at room temperature appeared pink in colour, presumably due to oxidation despite rigorous attempts to exclude oxygen. Crystals grown at 4°C were too small for further analysis.

It is possible that different crystallisation conditions may provide better quality crystals as the presence of substrate is thought to change the conformation of the enzyme, explaining the mutants inability to crystallise as well as the normal enzyme in these conditions.

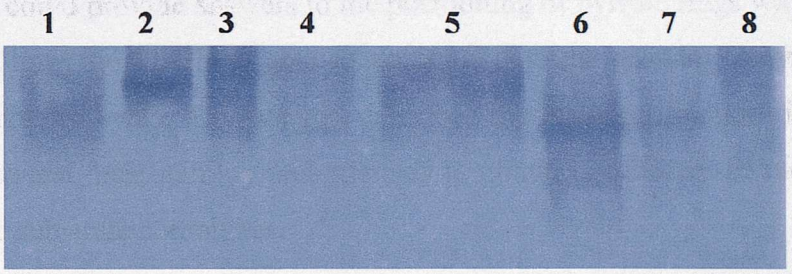

Figure 6.10 Non-denaturing PAGE to compare hruPBGD and various hruPBGD mutants.
Lane 1, hrePBGD; lane 2, Lys210Glu hruPBGD; lane 3, hruPBGD; lane 4, blank; lane 5, Arg167Trp mutant hruPBGD; lane 6, Asp99Glu hruPBGD; lane 7, Asp99Gly hruPBGD and lane eight, hruPBGD.

6.2.6 Expression, characterisation and purification of hruPBGD Arg167Gln and Arg167Trp mutants.

Arginine 167 is an invariant residue, which corresponds to Arg149 in *E.coli*. Natural mutations from human patients with AIP have been identified at Arg167 with arginine substituted by a glutamine residue [152] or by a tryptophan residue [153]. Site directed mutagenesis was used to investigate the importance of Arg149 in *E.coli*, were the arginine was mutated to histidine [81] and also with the arginine mutated to leucine [156].

A. Al-Dbass, F. Mohammed and R. Gill purified, crystallized and solved the crystal structure of the Arg167Gln mutant hruPBGD, which was the first human PBGD structure to be solved [84]. A. Al-Dbass characterized both Arg167Gln and Arg167Trp and found, after mixing with substrate, they both accumulated stable enzyme substrate complexes, which were visualized using non-denaturing PAGE [145]. The possible exploitation of the Arg167 mutants in the elucidation of the tetrapyrrole assembly process was immediately apparent. The crystal structures of enzyme substrate intermediates could provide answers to the positioning of pyrrole rings within the active site cleft and how the PBGD is able to accommodate the growing polypyrrole chain during the catalytic cycle. This section describes the isolation of these intermediates, experiments to test their stability and attempts to obtain crystals of diffractable quality of the enzyme substrate complexes.

The Arg167Gln mutant and Arg167Trp mutants were isolated to 90% purity using the same method as the normal hruPBGD, as described in chapter 2.

6.2.7. Formation of enzyme substrate complexes by Arg167Gln and Arg167Trp and normal hruPBGDs

Porphobilinogen deaminase (PBGD) catalyses the polymerisation of four molecules of PBG to give a chain of six pyrroles in length attached to the enzyme (including the dpm cofactor). The addition of the four substrate molecules occurs in a stepwise fashion via the enzyme substrate intermediate complexes ES, ES_2, ES_3, ES_4, after which the product, preuroporphyrinogen, is released. PBGD isolated from *E.coli, R.sphaeroides* and human erythrocytes have all been shown to form enzyme substrate complexes [61, 77, 157, 158].

The enzyme substrate intermediate complexes can be visualized using high-resolution anion exchange chromatography, using a Mono Q column attached to a Pharmacia f.p.l.c [62] (figure 6.12) and by non-denaturing PAGE analysis [61] (figure 6.11) (see chapter 2 for experimental details).

As discussed in chapter five, the purified hruPBGD separates into two species during high resolution anion exchange chromatography, referred to as species A and species B in this thesis. When species A and B are mixed with PBG separately and analysed by Mono Q f.p.l.c they both produce a similar elution profile, however, the peaks in the elution profile of species B are shifted to the right, that is they require a higher salt concentration to elute. Species A and its ES complexes elute slightly earlier than species B and its ES complexes; this means that when species A and B are analysed together some peaks overlap. Both arginine mutants were found to share this property and contained both species A and B. To avoid cross-contamination the experiments described in the following section used only species A of hruPBGD and the mutants.

Site directed mutagenesis studies on conserved arginine residues in *E.coli* PBGD, lining the active site cleft, indicate arginines play a vital role in stabilizing the escalating negative charge as substrate molecules are incorporated and are thought to aid in the translocation of the pyrrole chain [81].

Enzyme		Salt concentration required for elution (mM)
Species A	E	110
Species A	ES	125
Species A	ES_2	145
Species A	ES_3	160
Species B	E	125
Species B	ES	140
Species B	ES_2	160
Species B	ES_3	175

Table 6.4 The concentration of salt (NaCl) required to elute species A and B of hruPBGD and their enzyme substrate intermediate complexes from the Mono Q column.

6.2.8 The accumulation of enzyme substrate intermediates in hruPBGD and hruPBGD mutants Arg167Gln and Arg167Trp visualized by non-denaturing PAGE.

Incubation of Arg167Gln, Arg167Trp mutants and normal hruPBGD with PBG (1:10 molar ratio) at 37°C for 2 minutes, generates enzyme substrate (ES) complexes. The enzymes and their substrate complexes were detected using non-denaturing PAGE and the bands were visualized by staining with Coomassie brilliant blue. The ES complexes migrate through the non-denaturing gels with different migration depending on the charge of the complex. As additional acetate and propionate groups of the substrate are bound to the enzyme, ES, ES_2, ES_3, ES_4 are formed, each with a higher negative charge and mobility on the gel than its predecessor. From figure 6.11 it can be seen that the enzyme substrate intermediate complexes of Arg167Gln are far more stable than normal hruPBGD, and ES complexes were still present after 2hrs incubation at 37°C, unlike

intermediates of the normal hruPBGD which completely disappear before 5 mins has elapsed as they turnover to give free enzyme.

The accumulation of enzyme substrate intermediate complexes by Arg167Gln and Arg167Trp human mutants PBGDs strongly suggests the arginine residue is important in the translocation process, which had previously been proposed by similar experiments with the *E.coli* Arg149 mutant PBGD [81].

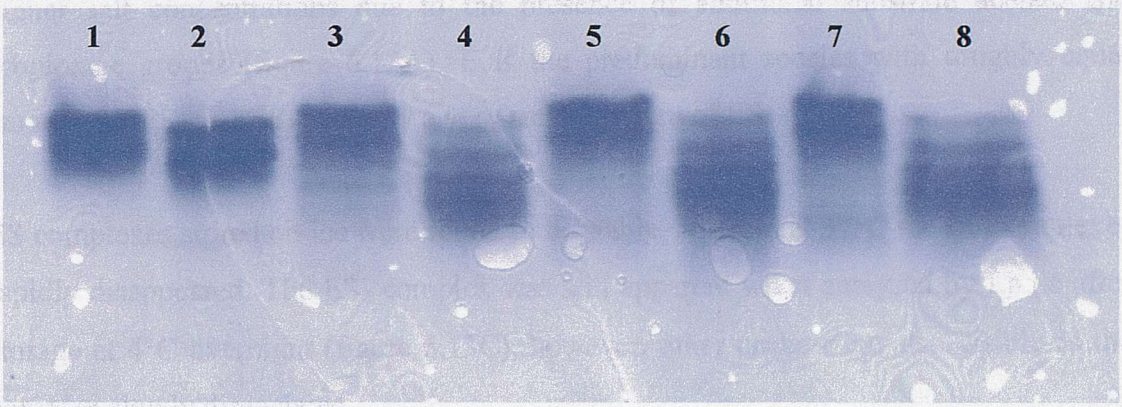

Figure 6.11 Non-denaturing PAGE analysis of the enzyme substrate intermediates formed by hruPBGD and the hruPBGD mutant Arg167Gln, illustrating the mutant intermediates are far more stable than those formed by the normal enzyme.

Lane one, hruPBGD; lane two, hruPBGD mutant Arg167Gln; lane three, hruPBGD after incubation for with PBG for 3 minutes; lane four, hruPBGD mutant Arg167Gln after incubation with PBG for 3 minutes; lane five, hruPBGD after incubation with PBG for 30 minutes; lane six, hruPBGD mutant Arg167Gln after incubation with PBG for 30 minutes; lane seven, hruPBGD after incubation with PBG for 2 hours and lane eight, hruPBGD mutant Arg167Gln after incubation with PBG for 2 hours. (All incubations were carried out at 37°C).

6.2.9 The accumulation of enzyme substrate intermediates in hruPBGD and hruPBGD mutants Arg167Gln and Arg167Trp visualized by Mono Q f.p.l.c

Normal hruPBGD

When purified hruPBGD, species A, isolated by f.p.l.c was mixed with 10 molar equivalents of PBG and analysed by Mono Q anion exchange chromatography four peaks were observed in the elution profile, corresponding to the enzyme alone (E), enzyme with one substrate molecule bound (ES), enzyme with two substrate molecules bound (ES_2), and enzyme with three molecules of substrate bound (ES_3). The normal hruPBGD elutes at a salt concentration of 110mM, whereas the ES complexes elute at higher salt concentrations due to the presence of additional substrate acetate and propionate groups (figure 6.13A). E is the predominant species with roughly equal amounts of ES_2 and ES_3 and only a very small amount of ES.

ES complexes stored on ice were found to be stable, whereas at 37°C the ES complexes rapidly disappeared. The ES_2 complex was still apparent when analysed by f.p.l.c after storage at 4°C overnight (figure 6.13C), however, other peaks were also visible as the complex slowly dissociated.

Arg167Gln mutant hruPBGD

Purified Arg167Gln PBGD, species A, was mixed with 10 molar equivalents of PBG producing four peaks when analysed by f.p.l.c (figure 6.13D). The elution profile was very different to that of the normal enzyme with far more ES complexes than seen for the normal enzyme and less free enzyme. The Arg167Gln mutant and its ES complexes eluted slightly later from the Mono Q column than the normal enzyme due to the loss of positive charge with arginine substituted for tryptophan.

The ES complexes of the Arg167Gln mutant were far more stable than the ES complexes of the normal enzyme. Figure 6.13C shows the ES_2 complex of the normal enzyme has begun to dissociate after incubation at 4°C overnight, whereas, the ES_2

complex of Arg167Gln dissociates very little over 4 days at 4°C (figure 6.13F). This is an important finding as it indicates the ES_2 complex of Arg167Gln is stable enough to attempt crystallography studies at 4°C.

Arg167Trp mutant hruPBGD

Purified Arg167Trp hruPBGD, species A, was mixed with 10 molar equivalents of PBG, which, when analysed by f.p.l.c was found to have a very similar elution profile to the ES complexes of Arg167Gln (figure 6.12 and 6.13D). However, its ES_2 complex was found to be less stable than that of Arg167Gln, so the Arg167Gln ES_2 complex was used for crystallisation trials.

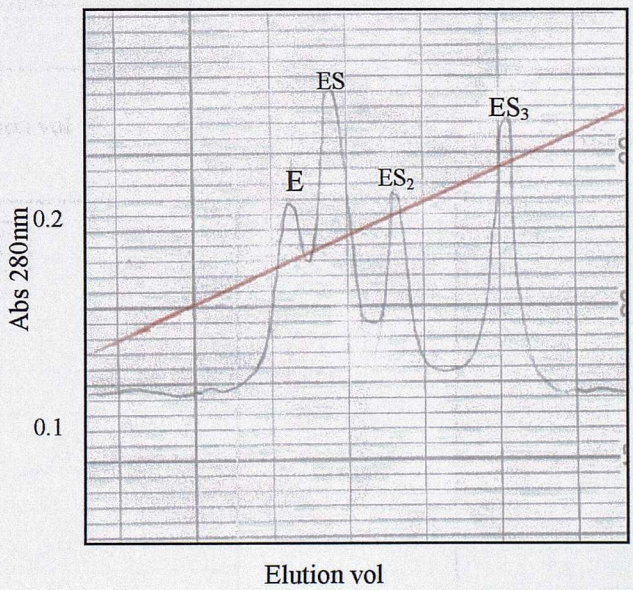

Figure 6.12 Isolation and identification of enzyme substrate complexes of Arg167Trp by high resolution ion-exchange chromatography.
The red line is the salt gradient and the black line is absorbance at 280nm.

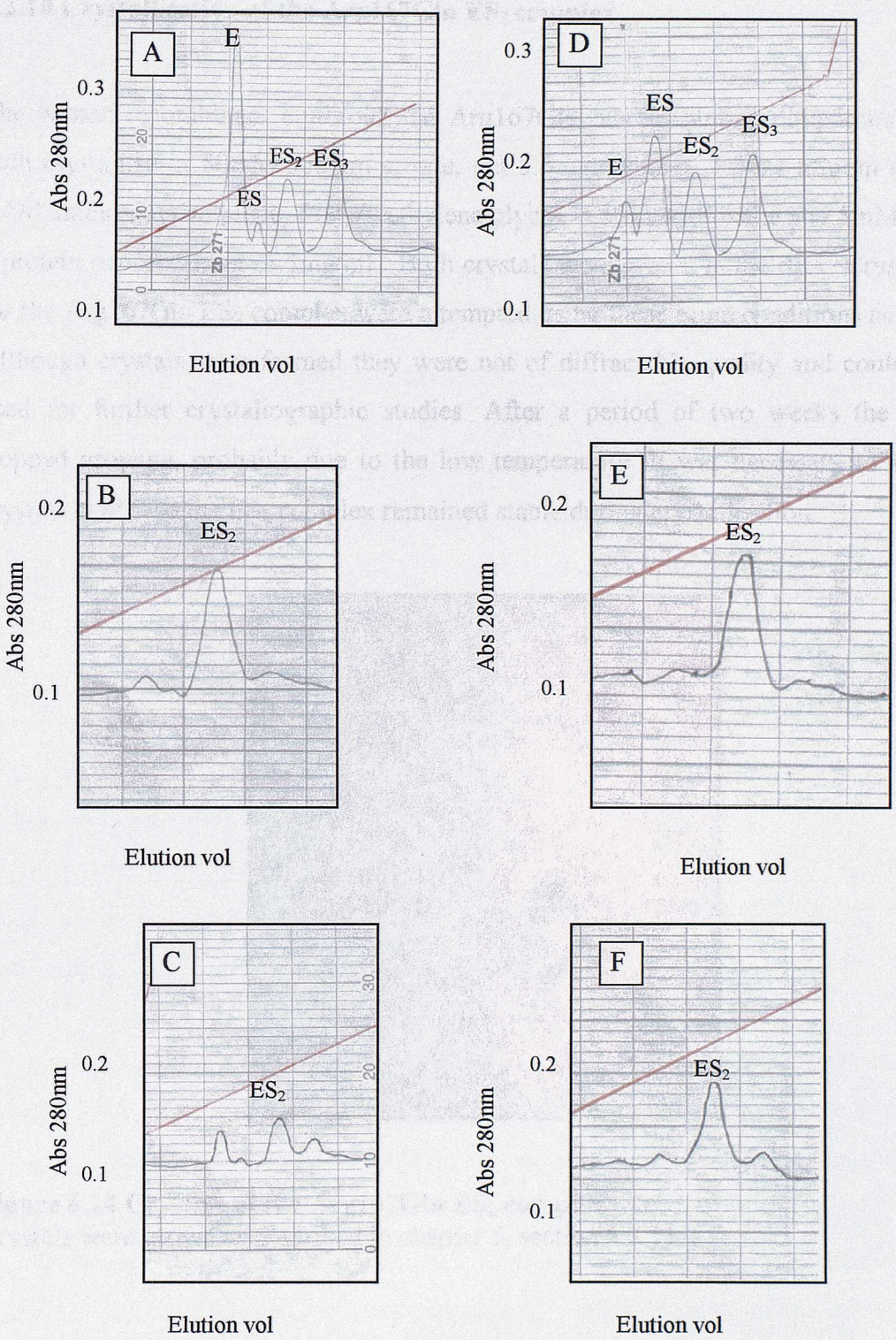

Figure 6.13 Isolation and identification of enzyme: substrate complexes by high resolution ion-exchange chromatography.

Red line is the salt gradient and the black line is absorbance at 280nm.

A) Normal hruPBGD with PBG; B) Purified normal hruPBGD ES_2; C) Purified normal hruPBGD ES_2 after incubation at 4°C overnight; D) Arg167Gln with PBG; E) Purified Arg167Gln ES_2 and F) Arg167Gln ES_2 after incubation at 4°C for four days.

6.2.10 Crystallisation of the Arg167Gln ES_2 complex

The human recombinant erythroid and Arg167Gln mutant human ubiquitous PBGDs both crystallise in 50mM sodium citrate, pH 5.6, containing, 1.25M lithium sulphate, 0.6M ammonium sulphate, 5% v/v ethylene glycol, 0.5% v/v dioxane and 5mM DTT at a protein concentration of 5mg/mL. Both crystals were grown in the dark. Crystal trials for the Arg167Gln ES_2 complex were attempted using these same conditions as a guide. Although crystals were formed they were not of diffractable quality and could not be used for further crystallographic studies. After a period of two weeks the crystals stopped growing, probably due to the low temperature. It was necessary to keep the crystals at 4°C so the ES_2 complex remained stable during crystallisation.

Figure 6.14 Crystals of the Arg167Gln ES_2 complex.
Crystals were grown as described in chapter 5, section 5.2.11.

6.3 Conclusions.

A difference in the published nucleotide sequences of human ubiquitous PBGD was noted, in one publication the residue at 210 was a lysine, in others it was a glutamate. All previous research described in this thesis and carried out by this research group at Southampton University used the hruPBGD with a lysine residue at position 210 in the primary sequence. The Lys210Glu mutant was purified and characterised to assess the effect this substitution has on deaminase function.

The Lys210Glu mutant hruPBGD was found to possess the same heat stability as the normal enzyme and could be purified using the same method. The Lys210Glu mutant had a slightly higher specific activity, 110%, compared to the normal enzyme. Both Lys210Glu and the normal enzyme produce the same characteristic double band when analysed by non-denaturing PAGE. Interestingly, Lys210Glu had a higher percentage of the lower band than the normal enzyme. This mutation did not compromise the function of the PBGD and could be a polymorphism, that is, both Lys210 and Glu210 may be present in the population.

Two deaminase mutants Asp99Glu and Asp99Gly were purified and were found to be heat- stable, indicating they were not apoenzymes.

Asp99Glu is a conservative mutation, as glutamate possesses the same charge as aspartate, but is one carbon unit longer. However, this conservative mutation produced a dramatic effect on the activity of PBGD, the activity of the mutant was less than 0.5% of that of the normal hruPBGD. The extra length of the side chain may put the carboxyl group in an unfavourable position for catalysis. This implies aspartate99 has an extremely important role in catalysis and even a subtle change can have a profound effect on activity.

Asp99Gly is a natural AIP mutation and the mutant was found to have no activity under the assay conditions. The Asp99Gly mutation is located in exon 7 and involves the substitution of the vital catalytic aspartate residue for an amino acid incapable of

participating in catalysis. As anticipated the resulting protein is devoid of catalytic activity.

Preliminary results suggest that the aspartate mutants form stable ES_2 complexes, due to their later elution from anion-exchange columns, their increased migration when analysed by non-denaturing PAGE and their very rapid reaction with Erhlich's reagent. As PBGD is known to derive its cofactor from preuroporphyrinogen it is clear that the Asp99Gly mutant is able to bind preuroporphyrinogen but cannot complete the next step of catalysis, whereas, the Asp99Glu can proceed with the reaction but at a very slow rate. Analysis by mass spectrometry could confirm the aspartate mutants exist as ES_2; unfortunately, the mutants did not 'fly' well on the mass spectrometer.

Arginine and aspartate mutants were crystallised, as a crystal structure of an ES_2 intermediate complex would provide important information on how the enzyme is able to accommodate the growing polypyrrole chain. Arg167Gln and Arg167Trp were found to produce enzyme substrate intermediate complexes, which are far more stable than those produced by the normal enzyme. Crystals of ES_2 intermediates complexes were generated, although they were not of diffractable quality. Further adjustment of the crystallisation conditions may yield more suitable crystals.

References

1. Jordan PM (editor), Neuberger A and Van Deenen L (general editors), *The biosynthesis of tetrpyrroles.* New comprehensive biochemistry.Vol. **19**. ISBN 0 444 89285 0, Elsevier, 1991.
2. Chadwick D and Ackrill K (editors), *The biosynthesis of the tetrapyrrole pigments*. Ciba Foundation symposium **180**. ISBN 0 471 93947 1, John Wiley and sons Ltd, 1994.
3. Stamford NP, Crouzet J, Cameron B, Alanine AI, Pitt AR, Yeliseev AA and Battersby AR, Biosynthesis of vitamin B12: the preparative multi-enzyme synthesis of precorrin-3A and 20-methylsirohydrochlorin (a 2,7,20-trimethylisobacteriochlorin). *Biochem J* **313 (Pt 1):** 335-42, 1996.
4. Shoolingin-Jordan PM, Structure and mechanism of enzymes involved in the assembly of the tetrapyrrole macrocycle. *Biochem Soc Trans* **26**(3)**:** 326-36, 1998.
5. Ferreira GC, Heme biosynthesis: biochemistry, molecular biology, and relationship to disease. *J Bioenerg Biomembr* **27**(2)**:** 147-50, 1995.
6. Shoolingin-Jordan PM, Cheung, KM, Biosynthesis of haem. *Comprehensive natural products chemistry*, Kelly JW, (editor), series edited by Barton SD, Nakanishi, K and Mth-Cohn, O. Vol. **4**: 66-108, Elsevier, 1999.
7. Beale SI, Gough SP and Granick S, Biosynthesis of delta-aminolevulinic acid from the intact carbon skeleton of glutamic acid in greening barley. *Proc Natl Acad Sci U S A* **72**(7)**:** 2719-23, 1975.
8. Shemin D and Russel CS, 5-aminolevulinic acid, its role in the biosynthesis of porphyrins and purines. *J Am Chem Soc* **76:** 4873, 1953.
9. Hunter GA and Ferreira GC, Lysine-313 of 5-aminolevulinate synthase acts as a general base during formation of the quinonoid reaction intermediates. *Biochemistry* **38**(12)**:** 3711-8, 1999.
10. Bishop DF, Henderson AS and Astrin KH, Human delta-aminolevulinate synthase: assignment of the housekeeping gene to 3p21 and the erythroid-specific gene to the X chromosome. *Genomics* **7**(2)**:** 207-14, 1990.

11. May BK, Bhasker CR, Bawden MJ and Cox TC, Molecular regulation of 5-aminolevulinate synthase. Diseases related to heme biosynthesis. *Mol Biol Med* **7**(5): 405-21, 1990.

12. Kramer MF, Gunaratne P and Ferreira GC, Transcriptional regulation of the murine erythroid-specific 5-aminolevulinate synthase gene. *Gene* **247**(1-2): 153-66, 2000.

13. Goodfellow BJ, Dias JS, Ferreira GC, Henklein P, Wray V and Macedo AL, The solution structure and heme binding of the presequence of murine 5-aminolevulinate synthase. *FEBS Lett* **505**(2): 325-31, 2001.

14. Tishler PV, The effect of therapeutic drugs and other pharmacologic agents on activity of porphobilinogen deaminase, the enzyme that is deficient in intermittent acute porphyria. *Life Sci* **65**(2): 207-14, 1999.

15. Bottomley SS, May BK, Cox TC, Cotter PD and Bishop DF, Molecular defects of erythroid 5-aminolevulinate synthase in X-linked sideroblastic anemia. *J Bioenerg Biomembr* **27**(2): 161-8, 1995.

16. Furuyama K and Sassa S, Multiple mechanisms for hereditary sideroblastic anemia. *Cell Mol Biol (Noisy-le-grand)* **48**(1): 5-10, 2002.

17. Doss M, von Tiepermann R and Schneider J, Acute hepatic porphyria syndrome with porphobilinogen synthase defect. *Int J Biochem* **12**(5-6): 823-6, 1980.

18. Wilson EL, Burger PE and Dowdle EB, Beef-liver 5-aminolevulinic acid dehydratase. Purification and properties. *Eur J Biochem* **29**(3): 563-71, 1972.

19. Schmid R and Shemin, D, The Enzymatic Formation of Porphobilinogen From δ-Aminolevulinic Acid and Its Conversion To Protoporphyrin. *J Am Chem Soc* **77**: 506-507, 1955.

20. Gibbs PN, Chaudhry AG and Jordan PM, Purification and properties of 5-aminolaevulinate dehydratase from human erythrocytes. *Biochem J* **230**(1): 25-34, 1985.

21. Nandi DL and Shemin D, 5-Aminolevulinic acid dehydratase of Rhodopseudomonas capsulata. *Arch Biochem Biophys* **158**(1): 305-11, 1973.

22. Liedgens W, Grutzmann R and Schneider HA, Highly efficient purificaton of the labile plant enzyme 5-aminolevulinate dehydratase (EC 4.2.1.24) by means of monoclonal antibodies. *Z Naturforsch [C]* **35**(11-12): 958-62, 1980.

23. Sato S and Wilson RJ, The genome of Plasmodium falciparum encodes an active delta-aminolevulinic acid dehydratase. *Curr Genet* **40**(6): 391-8, 2002.

24. Spencer P and Jordan PM, Purification and characterization of 5-aminolaevulinic acid dehydratase from Escherichia coli and a study of the reactive thiols at the metal-binding domain. *Biochem J* **290 (Pt 1):** 279-87, 1993.

25. Erskine PT, Senior N, Awan S, Lambert R, Lewis G, Tickle IJ, Sarwar M, Spencer P, Thomas P, Warren MJ, Shoolingin-Jordan PM, Wood SP and Cooper JB, X-ray structure of 5-aminolaevulinate dehydratase, a hybrid aldolase. *Nat Struct Biol* **4**(12): 1025-31, 1997.

26. Erskine PT, Norton E, Cooper JB, Lambert R, Coker A, Lewis G, Spencer P, Sarwar M, Wood SP, Warren MJ and Shoolingin-Jordan PM, X-ray structure of 5-aminolevulinic acid dehydratase from Escherichia coli complexed with the inhibitor levulinic acid at 2.0 A resolution. *Biochemistry* **38**(14): 4266-76, 1999.

27. Frankenberg N, Erskine PT, Cooper JB, Shoolingin-Jordan PM, Jahn D and Heinz DW, High resolution crystal structure of a Mg2+-dependent porphobilinogen synthase. *J Mol Biol* **289**(3): 591-602, 1999.

28. Mills Davis N, Crystal structure of human ALAD purified from erythrocytes. Personal communication.

29. Wu WH, Shemin D, Richards KE and Williams RC, The quaternary structure of delta-aminolevulinic acid dehydratase from bovine liver. *Proc Natl Acad Sci U S A* **71**(5): 1767-70, 1974.

30. www.accelrys.com/viewer/index/html, WebLab Viewer Lite v3.2. Molecular Simulations Inc., 1998.

31. www.rcsb.org/pdb, Brookhaven Protein Databank (pdb).

32. Mills Davis N, Crystal structure of human ALAD purified from erythrocytes. *PhD thesis*. Southampton University, Southampton, 2000.

33. Corpet F, Multiple sequence alignment with hierarchical clustering. *Nucleic Acids Res* **16**(22): 1081-10890, 1988.

34. Nandi DL and Shemin D, Delta-aminolevulinic acid dehydratase of Rhodopseudomonas spheroides. 3. Mechanism of porphobilinogen synthesis. *J Biol Chem* **243**(6): 1236-42, 1968.

35. Jordan PM and Seehra JS, 13C NMR as a probe for the study of enzyme-catalysed reactions: mechanism of action of 5-aminolevulinic acid dehydratase. *FEBS Lett* **114**(2): 283-6, 1980.

36. Jordan PM and Gibbs PN, Mechanism of action of 5-aminolaevulinate dehydratase from human erythrocytes. *Biochem J* **227**(3): 1015-20, 1985.

37. Spencer P and Jordan PM, Characterization of the two 5-aminolaevulinic acid binding sites, the A- and P-sites, of 5-aminolaevulinic acid dehydratase from Escherichia coli. *Biochem J* **305 (Pt 1):** 151-8, 1995.

38. Gibbs PN and Jordan PM, Identification of lysine at the active site of human 5-aminolaevulinate dehydratase. *Biochem J* **236**(2): 447-51, 1986.

39. Shoolingin-Jordan PM, Spencer P, Sarwar M, Erskine PE, Cheung KM, Cooper JB and Norton EB, 5-Aminolaevulinic acid dehydratase: metals, mutants and mechanism. *Biochem Soc Trans* **30**(4): 584-90, 2002.

40. Kervinen J, Jaffe EK, Stauffer F, Neier R, Wlodawer A and Zdanov A, Mechanistic basis for suicide inactivation of porphobilinogen synthase by 4,7-dioxosebacic acid, an inhibitor that shows dramatic species selectivity. *Biochemistry* **40**(28): 8227-36, 2001.

41. Erskine PT, Coates L, Newbold R, Brindley AA, Stauffer F, Wood SP, Warren MJ, Cooper JB, Shoolingin-Jordan PM and Neier R, The X-ray structure of yeast 5-aminolaevulinic acid dehydratase complexed with two diacid inhibitors. *FEBS Lett* **503**(2-3): 196-200, 2001.

42. Frere F, Schubert WD, Stauffer F, Frankenberg N, Neier R, Jahn D and Heinz DW, Structure of porphobilinogen synthase from Pseudomonas aeruginosa in complex with 5-fluorolevulinic acid suggests a double Schiff base mechanism. *J Mol Biol* **320**(2): 237-47, 2002.

43. Jaffe EK, The porphobilinogen synthase family of metalloenzymes. *Acta Crystallogr D Biol Crystallogr* **56 (Pt 2):** 115-28, 2000.

44. Jaffe EK, Investigations on the metal switch region of human porphobilinogen synthase. *J Biol Inorg Chem* **8**(1-2): 176-84, 2003.

45. Jaffe EK, Ali S, Mitchell LW, Taylor KM, Volin M and Markham GD, Characterization of the role of the stimulatory magnesium of Escherichia coli porphobilinogen synthase. *Biochemistry* **34**(1): 244-51, 1995.

46. Nandi DL, Baker-Cohen KF and Shemin D, Delta-aminolevulinic acid dehydratase of Rhodopseudomonas spheroides. *J Biol Chem* **243**(6): 1224-30, 1968.

47. Gibbs PN, Gore MG and Jordan PM, Investigation of the effect of metal ions on the reactivity of thiol groups in human 5-aminolaevulinate dehydratase. *Biochem J* **225**(3): 573-80, 1985.

48. Jordan PM and Seehra JS, Purification of porphobilinogen synthase from bovine liver. *Methods Enzymol* **123:** 427-34, 1986.

49. Petrucci R, Leonardi A and Battistuzzi G, The genetic polymorphism of delta-aminolevulinate dehydrase in Italy. *Hum Genet* **60**(3): 289-90, 1982.

50. Beyersmann D and Cox M, Affinity labelling of 5-aminolevulinic acid dehydratase with 2-bromo-3-(5-imidazolyl)propionic acid. *Biochim Biophys Acta* **788**(2): 162-6, 1984.

51. Wetmur JG, Influence of the common human delta-aminolevulinate dehydratase polymorphism on lead body burden. *Environ Health Perspect* **102 Suppl 3:** 215-9, 1994.

52. Akagi R, Nishitani C, Harigae H, Horie Y, Garbaczewski L, Hassoun A, Mercelis R, Verstraeten L and Sassa S, Molecular analysis of delta-aminolevulinate dehydratase deficiency in a patient with an unusual late-onset porphyria. *Blood* **96**(10): 3618-23, 2000.

53. Ishida N, Fujita H, Fukuda Y, Noguchi T, Doss M, Kappas A and Sassa S, Cloning and expression of the defective genes from a patient with delta-aminolevulinate dehydratase porphyria. *J Clin Invest* **89**(5): 1431-7, 1992.

54. Plewinska M, Thunell S, Holmberg L, Wetmur JG and Desnick RJ, delta-Aminolevulinate dehydratase deficient porphyria: identification of the molecular lesions in a severely affected homozygote. *Am J Hum Genet* **49**(1): 167-74, 1991.

55. Akagi R, Yasui Y, Harper P and Sassa S, A novel mutation of delta-aminolaevulinate dehydratase in a healthy child with 12% erythrocyte enzyme activity. *Br J Haematol* **106**(4): 931-7, 1999.

56. Akagi R, Shimizu R, Furuyama K, Doss MO and Sassa S, Novel molecular defects of the delta-aminolevulinate dehydratase gene in a patient with inherited acute hepatic porphyria. *Hepatology* **31**(3): 704-8, 2000.

57. Rechsteiner M, Hoffman, L. and Dubiel, W., *J Biol Chem* **268:** 6065, 1993.

58. Guo GG, Gu M and Etlinger JD, 240-kDa proteasome inhibitor (CF-2) is identical to delta-aminolevulinic acid dehydratase. *J Biol Chem* **269**(17)**:** 12399-402, 1994.

59. Jordan PM and Shemin D, Purification and properties of uroporphyrinogen I synthetase from Rhodopseudomonas spheroides. *J Biol Chem* **248**(3)**:** 1019-24, 1973.

60. Miyagi K, Kaneshima M, Kawakami J, Nakada F, Petryka ZJ and Watson CJ, Uroporphyrinogen I synthase from human erythrocytes: separation, purification, and properties of isoenzymes. *Proc Natl Acad Sci U S A* **76**(12)**:** 6172-6, 1979.

61. Anderson PM and Desnick RJ, Purification and properties of uroporphyrinogen I synthase from human erythrocytes. Identification of stable enzyme-substrate intermediates. *J Biol Chem* **255**(5)**:** 1993-9, 1980.

62. Jordan PM, Thomas SD and Warren MJ, Purification, crystallization and properties of porphobilinogen deaminase from a recombinant strain of Escherichia coli K12. *Biochem J* **254**(2)**:** 427-35, 1988.

63. Mazzetti MB and Tomio JM, Characterization of porphobilinogen deaminase from rat liver. *Biochim Biophys Acta* **957**(1)**:** 97-104, 1988.

64. Spano AJ and Timko MP, Isolation, characterization and partial amino acid sequence of a chloroplast-localized porphobilinogen deaminase from pea (*Pisum sativum*). *Biochim Biophys Acta* **1076**(1)**:** 29-36, 1991.

65. Grandchamp B, De Verneuil H, Beaumont C, Chretien S, Walter O and Nordmann Y, Tissue-specific expression of porphobilinogen deaminase. Two isoenzymes from a single gene. *Eur J Biochem* **162**(1)**:** 105-10, 1987.

66. Louie GV, Brownlie PD, Lambert R, Cooper JB, Blundell TL, Wood SP, Warren MJ, Woodcock SC and Jordan PM, Structure of porphobilinogen deaminase reveals a flexible multidomain polymerase with a single catalytic site. *Nature* **359**(6390)**:** 33-9, 1992.

67. Scott AI, Clemens KR, Stolowich NJ, Santander PJ, Gonzalez MD and Roessner CA, Reconstitution of apo-porphobilinogen deaminase: structural changes induced by cofactor binding. *FEBS Lett* **242**(2)**:** 319-24, 1989.

68. Lambert R, Brownlie PD, Woodcock SC, Louie GV, Cooper JC, Warren MJ, Jordan PM, Blundell TL and Wood SP, Structural studies on porphobilinogen deaminase. *Ciba Found Symp* **180:** 97-104; discussion 105-10, 1994.

69. Woodcock SC and Jordan PM, Evidence for participation of aspartate-84 as a catalytic group at the active site of porphobilinogen deaminase obtained by site-directed mutagenesis of the hemC gene from Escherichia coli. *Biochemistry* **33**(9)**:** 2688-95, 1994.

70. Warren MJ, Gul S, Aplin RT, Scott AI, Roessner CA, O'Grady P and Shoolingin-Jordan PM, Evidence for conformational changes in Escherichia coli porphobilinogen deaminase during stepwise pyrrole chain elongation monitored by increased reactivity of cysteine-134 to alkylation by N-ethylmaleimide. *Biochemistry* **34**(35)**:** 11288-95, 1995.

71. Louie GV, Brownlie PD, Lambert R, Cooper JB, Blundell TL, Wood SP, Malashkevich VN, Hadener A, Warren MJ and Shoolingin-Jordan PM, The three-dimensional structure of Escherichia coli porphobilinogen deaminase at 1.76-A resolution. *Proteins* **25**(1)**:** 48-78, 1996.

72. Plusec J and Bogorad L, A dipyrrylmethane intermediate in the enzymic synthesis of uroporphyrinogen. *Biochemistry* **9:** 4736-4743, 1970.

73. Jordan PM and Warren MJ, Evidence for a dipyrromethane cofactor at the catalytic site of E. coli porphobilinogen deaminase. *FEBS Lett* **225**(1-2)**:** 87-92, 1987.

74. Miller AD, Hart GJ, Packman LC and Battersby AR, Evidence that the pyrromethane cofactor of hydroxymethylbilane synthase (porphobilinogen deaminase) is bound to the protein through the sulphur atom of cysteine-242. *Biochem J* **254**(3)**:** 915-8, 1988.

75. Scott AI, Roessner CA, Stolowich NJ, Karuso P, Williams HJ, Grant SK, Gonzalez MD and Hoshino T, Site-directed mutagenesis and high-resolution NMR spectroscopy of the active site of porphobilinogen deaminase. *Biochemistry* **27**(21)**:** 7984-90, 1988.

76. Shoolingin-Jordan PM, Warren MJ and Awan SJ, Discovery that the assembly of the dipyrromethane cofactor of porphobilinogen deaminase holoenzyme proceeds initially by the reaction of preuroporphyrinogen with the apoenzyme. *Biochem J* **316 (Pt 2):** 373-6, 1996.

77. Warren MJ and Jordan PM, Investigation into the nature of substrate binding to the dipyrromethane cofactor of Escherichia coli porphobilinogen deaminase. *Biochemistry* **27**(25): 9020-30, 1988.

78. Jordan PM and Seehra JS, The biosynthesis of uroporphyrinogen III: order of assembly of the four porphobilinogen molecules in the formation of the tetrapyrrole ring. *FEBS Lett* **104**(2): 364-6, 1979.

79. Alefounder PR, Abell C and Battersby AR, The sequence of hemC, hemD and two additional E. coli genes. *Nucleic Acids Res* **16**(20): 9871, 1988.

80. Chretien S, Dubart A, Beaupain D, Raich N, Grandchamp B, Rosa J, Goossens M and Romeo PH, Alternative transcription and splicing of the human porphobilinogen deaminase gene result either in tissue-specific or in housekeeping expression. *Proc Natl Acad Sci U S A* **85**(1): 6-10, 1988.

81. Jordan PM and Woodcock SC, Mutagenesis of arginine residues in the catalytic cleft of Escherichia coli porphobilinogen deaminase that affects dipyrromethane cofactor assembly and tetrapyrrole chain initiation and elongation. *Biochem J* **280 (Pt 2)**: 445-9, 1991.

82. Cappellini MD, Martinez di Montemuros F, Di Pierro E and Fiorelli G, Hematologically important mutations: acute intermittent porphyria. *Blood Cells Mol Dis* **28**(1): 5-12, 2002.

83. Desnick RJ, Ostasiewicz LT, Tishler PA and Mustajoki P, Acute intermittent porphyria: characterization of a novel mutation in the structural gene for porphobilinogen deaminase. Demonstration of noncatalytic enzyme intermediates stabilized by bound substrate. *J Clin Invest* **76**(2): 865-74, 1985.

84. Mohammad F, Structural Studies on porphobilinogen deaminase. *PhD thesis*. Southampton University, 2001.

85. Fritsch C, Lang K, Bolsen K, Lehmann P and Ruzicka T, Congenital erythropoietic porphyria. *Skin Pharmacol Appl Skin Physiol* **11**(6): 347-57, 1998.

86. Stamford NP, Capretta A and Battersby AR, Expression, purification and characterisation of the product from the Bacillus subtilis hemD gene, uroporphyrinogen III synthase. *Eur J Biochem* **231**(1): 236-41, 1995.

87. Tsai SF, Bishop DF and Desnick RJ, Purification and properties of uroporphyrinogen III synthase from human erythrocytes. *J Biol Chem* **262**(3): 1268-73, 1987.

88. Jordan PM, Mgbeje BI, Alwan AF and Thomas SD, Nucleotide sequence of hemD, the second gene in the hem operon of Escherichia coli K-12. *Nucleic Acids Res* **15**(24): 10583, 1987.

89. Mathews MA, Schubert HL, Whitby FG, Alexander KJ, Schadick K, Bergonia HA, Phillips JD and Hill CP, Crystal structure of human uroporphyrinogen III synthase. *Embo J* **20**(21): 5832-9, 2001.

90. Jordan PM, Highlights in haem biosynthesis. *Curr Opin Struct Biol* **4**(6): 902-11, 1994.

91. Macalpine I and Hunter R, The "insanity" of King George 3d: a classic case of porphyria. *Br Med J* **5479:** 65-71, 1966.

92. Warren MJ, Jay M, Hunt DM, Elder GH and Rohl JC, The maddening business of King George III and porphyria. *Trends Biochem Sci* **21**(6): 229-34, 1996.

93. Sassa S, The porphyrias. *Photodermatol Photoimmunol Photomed* **18**(2): 56-67, 2002.

94. Waldenstrom J, The porphyrias as inborn errors of metabolism. *Am J Med* **22**, 1957.

95. Watson CJaS, S., Simple test for urinary porphobilinogen. *Proc Soc Exp Biol Med* **47:** 393-394, 1941.

96. Watson CJ, Pierach CA, Bossenmaier I and Cardinal R, Postulated deficiency of hepatic heme and repair by hematin infusions in the "inducible" hepatic porphyrias. *Proc Natl Acad Sci U S A* **74**(5): 2118-20, 1977.

97. Watson CJ, Pierach CA, Bossenmaier I and Cardinal R, Use of hematin in the acute attack of the "inducible" hepatic prophyrias. *Adv Intern Med* **23:** 265-86, 1978.

98. Granick S, The induction in vitro of the synthesis of delta-aminolevulinic acid synthetase in chemical porphyria: a response to certain drugs, sex hormones, and foreign chemicals. *J Biol Chem* **241**(6): 1359-75, 1966.

99. Doss M, von Tiepermann R, Schneider J and Schmid H, New type of hepatic porphyria with porphobilinogen synthase defect and intermittent acute clinical manifestation. *Klin Wochenschr* **57**(20): 1123-7, 1979.

100. Sassa S, ALAD porphyria. *Semin Liver Dis* **18**(1): 95-101, 1998.

101. Schierbeek H, Beukeveld GJ, van Faassen H, van Spronsen FJ, Bijsterveld K, Venekamp-Hoolsema EE, Wolthers BG and Smit GP, Hereditary tyrosinaemia type I: a long-term study of the relationship between the urinary excretions of succinylacetone and delta-aminolevulinic acid. *J Inherit Metab Dis* **16**(6): 1034-40, 1993.

102. Brennan MJ and Cantrill RC, Delta-aminolaevulinic acid is a potent agonist for GABA autoreceptors. *Nature* **280**(5722): 514-5, 1979.

103. Meyer UA, Schuurmans MM and Lindberg RL, Acute porphyrias: pathogenesis of neurological manifestations. *Semin Liver Dis* **18**(1): 43-52, 1998.

104. Meyer UA, Strand LJ, Doss M, Rees AC and Marver HS, Intermittent acute porphyria--demonstration of a genetic defect in porphobilinogen metabolism. *N Engl J Med* **286**(24): 1277-82, 1972.

105. Grandchamp B, Acute intermittent porphyria. *Semin Liver Dis* **18**(1): 17-24, 1998.

106. Floderus Y, Shoolingin-Jordan PM and Harper P, Acute intermittent porphyria in Sweden. Molecular, functional and clinical consequences of some new mutations found in the porphobilinogen deaminase gene. *Clin Genet* **62**(4): 288-97, 2002.

107. Raich N, Romeo PH, Dubart A, Beaupain D, Cohen-Solal M and Goossens M, Molecular cloning and complete primary sequence of human erythrocyte porphobilinogen deaminase. *Nucleic Acids Res* **14**(15): 5955-68, 1986.

108. Namba H, Narahara K, Tsuji K, Yokoyama Y and Seino Y, Assignment of human porphobilinogen deaminase to 11q24.1----q24.2 by in situ hybridization and gene dosage studies. *Cytogenet Cell Genet* **57**(2-3): 105-8, 1991.

109. Desnick RJ and Astrin KH, Congenital erythropoietic porphyria: advances in pathogenesis and treatment. *Br J Haematol* **117**(4): 779-95, 2002.

110. Martasek P, Hereditary coproporphyria. *Semin Liver Dis* **18**(1): 25-32, 1998.

111. Kirsch RE, Meissner PN and Hift RJ, Variegate porphyria. *Semin Liver Dis* **18**(1): 33-41, 1998.

112. Cox TM, Erythropoietic protoporphyria. *J Inherit Metab Dis* **20**(2): 258-69, 1997.

113. Kauppinen R, Management of the acute porphyrias. *Photodermatol Photoimmunol Photomed* **14**(2): 48-51, 1998.

114. Batlle AM, Bustos NL, Stella AM, Wider EA, Conti HA and Mendez A, Enzyme replacement therapy in porphyrias--IV. First successful human clinical trial of delta-aminolevulinate dehydratase-loaded erythrocyte ghosts. *Int J Biochem* **15**(10): 1261-5, 1983.

115. de Verneuil H, Ged C, Boulechfar S and Moreau-Gaudry F, Porphyrias: animal models and prospects for cellular and gene therapy. *J Bioenerg Biomembr* **27**(2): 239-48, 1995.

116. Pawliuk R, Bachelot T, Wise RJ, Mathews-Roth MM and Leboulch P, Long-term cure of the photosensitivity of murine erythropoietic protoporphyria by preselective gene therapy. *Nat Med* **5**(7): 768-73, 1999.

117. Studier FW, Rosenberg, A. H., Dunn J.J. and Dubendorff, J. W., The use of T7 RNA polymerase to direct expression of cloned genes. *Methods in Enzymology* **185:** 60-89, 1990.

118. Yanisch-Perron C, Vierra J. and Messing, J., Improved M13 phage cloning vectors and host strains: nucleotide sequences of the M13mp18 and PUC19 vectors. *Gene* **33**(1): 103-19, 1985.

119. Tabor S, *Current protocols in Mol Biol.* Greene publishing and Wiley-Interscience, New York, 1990.

120. Bradford MM, A rapid and sensitive method for the quantitation of microgram quantities of protein utilizing the principle of protein-dye binding. *Anal Biochem* **72:** 248-54, 1976.

121. Mauzerall D and Granick S, The occurrence and determination of delta-aminolevulinic acid and porphobilinogen in urine. *J Biol Chem* **219:** 435-436, 1956.

122. Laemmli UK, Cleavage of structural proteins during the assembly of the head of bacteriophage T4. *Nature* **227**(259): 680-5, 1970.

123. McPherson A, Crystallisation of proteins from polyethylene glycol. *J Biol Chem* **251**(20): 6300-6303, 1976.

124. Wetmur JG, Bishop DF, Cantelmo C and Desnick RJ, Human delta-aminolevulinate dehydratase: nucleotide sequence of a full-length cDNA clone. *Proc Natl Acad Sci U S A* **83**(20): 7703-7, 1986.

125. Wetmur JG, Kaya AH, Plewinska M and Desnick RJ, Molecular characterization of the human delta-aminolevulinate dehydratase 2 (ALAD2) allele: implications for molecular screening of individuals for genetic susceptibility to lead poisoning. *Am J Hum Genet* **49**(4): 757-63, 1991.

126. Maruno M, Furuyama K, Akagi R, Horie Y, Meguro K, Garbaczewski L, Chiorazzi N, Doss MO, Hassoun A, Mercelis R, Verstraeten L, Harper P, Floderus Y, Thunell S and Sassa S, Highly heterogeneous nature of delta-aminolevulinate dehydratase (ALAD) deficiencies in ALAD porphyria. *Blood* **97**(10): 2972-8, 2001.

127. Sakai T, Biomarkers of lead exposure. *Ind Health* **38**(2): 127-42, 2000.

128. Dyer J, Garrick DP, Inglis A and Pye IF, Plumboporphyria (ALAD deficiency) in a lead worker: a scenario for potential diagnostic confusion. *Br J Ind Med* **50**(12): 1119-21, 1993.

129. Holme E and Lindstedt S, Neonatal screen for hereditary tyrosinaemia type I. *Lancet* **340**(8823): 850, 1992.

130. Erskine PT, Senior N, Maignan S, Cooper J, Lambert R, Lewis G, Spencer P, Awan S, Warren M, Tickle IJ, Thomas P, Wood SP and Shoolingin-Jordan PM, Crystallization of 5-aminolaevulinic acid dehydratase from Escherichia coli and Saccharomyces cerevisiae and preliminary X-ray characterization of the crystals. *Protein Sci* **6**(8): 1774-6, 1997.

131. Erskine PT, Newbold R, Brindley AA, Wood SP, Shoolingin-Jordan PM, Warren MJ and Cooper JB, The x-ray structure of yeast 5-aminolaevulinic acid dehydratase complexed with substrate and three inhibitors. *J Mol Biol* **312**(1): 133-41, 2001.

132. Jarret C, Stauffer F, Henz ME, Marty M, Luond RM, Bobalova J, Schurmann P and Neier R, Inhibition of Escherichia coli porphobilinogen synthase using analogs of postulated intermediates. *Chem Biol* **7**(3): 185-96, 2000.

133. Mitchell LW and Jaffe EK, Porphobilinogen synthase from Escherichia coli is a Zn(II) metalloenzyme stimulated by Mg(II). *Arch Biochem Biophys* **300**(1): 169-77, 1993.

134. Erskine P., Coates, L., Butler, D., Brindley, A., Youell, Y., Warren, M., Jordan, P.M., Wood, S. and Cooper, J., The discovery of a putative intermediate at the active site of ALA dehydratase. *Eur J Biochem*, 2003 In Press.

135. Jaffe EK, Markham GD and Rajagopalan JS, 15N and 13C NMR studies of ligands bound to the 280,000-dalton protein porphobilinogen synthase elucidate the structures of enzyme-bound product and a Schiff base intermediate. *Biochemistry* **29**(36): 8345-50, 1990.

136. Mitchell LW, Volin M, Martins J and Jaffe EK, Mechanistic implications of mutations to the active site lysine of porphobilinogen synthase. *J Biol Chem* **276**(2): 1538-44, 2001.

137. Erskine PT, Newbold R, Roper J, Coker A, Warren MJ, Shoolingin-Jordan PM, Wood SP and Cooper JB, The Schiff base complex of yeast 5-aminolaevulinic acid dehydratase with laevulinic acid. *Protein Sci* **8**(6): 1250-6, 1999.

138. Jaffe EK and Markham GD, 13C NMR studies of porphobilinogen synthase: observation of intermediates bound to a 280,000-dalton protein. *Biochemistry* **26**(14): 4258-64, 1987.

139. Bogorad L, The enzymatic synthesis of porphyrins from porphobilinogen I. Uroporphyrinogen I. *J Biol Chem* **233:** 501-509, 1958.

140. Wood S, Lambert, R., and Jordan, P. M., Molecular basis of acute intermittent porphyria. *Molecular medicine today* **1**(5): 232-239, 1995.

141. Deybach JC and Puy H, Porphobilinogen deaminase gene structure and molecular defects. *J Bioenerg Biomembr* **27**(2): 197-205, 1995.

142. Moseley J, Studies on human porphobilinogen deaminase. In: *PhD thesis*. University of Southampton, 2002.

143. Aplin RT, Baldwin, J. E., Pichon, C., Rossener, C. A., Scott, A. I., Schofield, C. J., Stolowich, N.J. and Warren, M.J., Observation of bound intermediates in the biosynthesis of preuroporphyrinogen by porphobilinogen deaminase. *Bioorg and Med Chem Letts* **1:** 503-507, 1991.

144. McNeill LA, Studies on the self-assembly and catalytic mechanism of porphobilinogen deaminase. *PhD thesis*. Southampton University, 1999.

145. Al Dbass A, Studies on porphobilinogen deaminase. *PhD thesis*. University of Southampton, 2001.

146. Robinson NE, and Robinson, AB, Prediction of protein deamidation rates from primary and three-dimensional structure. *Proc Natl Acad Sci U S A* **98:** 4367-4372, 2001.

147. Robinson NE, Protein Deamidation. *Proc Natl Acad Sci U S A*:, 2002.

148. www.deamidation.org, Prediction of protein deamidation rates from primary and three-dimensional protein structure. Robinson, N and Robinson, A. B, 2001.

149. Meinwald YC, Stimson, E. R. and Scheraga, H. A., *Int J Pept Protein Res* **28:** 79, 1986.

150. Grandchamp B, Picat C, de Rooij F, Beaumont C, Wilson P, Deybach JC and Nordmann Y, A point mutation G----A in exon 12 of the porphobilinogen deaminase gene results in exon skipping and is responsible for acute intermittent porphyria. *Nucleic Acids Res* **17**(16)**:** 6637-49, 1989.

151. Yoo HW, Warner CA, Chen CH and Desnick RJ, Hydroxymethylbilane synthase: complete genomic sequence and amplifiable polymorphisms in the human gene. *Genomics* **15**(1)**:** 21-9, 1993.

152. Delfau MH, Picat C, de Rooij FW, Hamer K, Bogard M, Wilson JH, Deybach JC, Nordmann Y and Grandchamp B, Two different point G to A mutations in exon 10 of the porphobilinogen deaminase gene are responsible for acute intermittent porphyria. *J Clin Invest* **86**(5)**:** 1511-6, 1990.

153. Gu XF, de Rooij F, Voortman G, Te Velde K, Nordmann Y and Grandchamp B, High frequency of mutations in exon 10 of the porphobilinogen deaminase gene in patients with a CRIM-positive subtype of acute intermittent porphyria. *Am J Hum Genet* **51**(3)**:** 660-5, 1992.

154. Awan SJ, Siligardi G, Warren MJ and Shoolingin-Jordan PM, Discovery of a novel mechanism for cofactor assembly by Escherichia coli porphobilinogen deaminase. *Biochem Soc Trans* **25**(1)**:** 79S, 1997.

155. Radmer R, and Bogorad, L, A tetrapyrrole intermediate in the enzymic synthesis of uroporphyrinogen. *Biochemistry* **11:** 904-910, 1972.

156. Lander M, Pitt AR, Alefounder PR, Bardy D, Abell C and Battersby AR, Studies on the mechanism of hydroxymethylbilane synthase concerning the role of arginine residues in substrate binding. *Biochem J* **275 (Pt 2):** 447-52, 1991.

157. Berry A, Jordan PM and Seehra JS, The isolation and characterization of catalytically competent porphobilinogen deaminase-intermediate complexes. *FEBS Lett* **129**(2)**:** 220-4, 1981.

158. Jordan PM and Berry A, Mechanism of action of porphobilinogen deaminase. The participation of stable enzyme substrate covalent intermediates between

porphobilinogen and the porphobilinogen deaminase from Rhodopseudomonas spheroides. *Biochem J* **195**(1): 177-81, 1981.